The University Of Sheffield.

Investigations on the Microbiology of the Stratosphere and Other Habitats in Relation to the Theory of Panspermia

By:

Tareq Lafta Salman Omairi

A Thesis submitted in partial fulfilment of the requirements for the Degree of Doctor of Philosophy

The University of Sheffield
Faculty of Science
Department of Molecular Biology and Biotechnology

2017

To Sabreen

DECLARATION

This work has not been submitted in substance for any other degree or award at this or any other university or place of learning, nor is being submitted concurrently in candidature for any degree or other award.

Signed …… (candidate) Date …….

STATEMENT 1

This thesis is being submitted in partial fulfillment of the requirements for the degree of PhD.

Signed …… (candidate) Date …….

STATEMENT 2

This thesis is the result of my own independent work/investigation, except where otherwise stated. Other sources are acknowledged by explicit references. The views expressed are my own.

Signed …… (candidate) Date …….

STATEMENT 3

I hereby give consent for my thesis, if accepted, to be available for photocopying and for interlibrary loan, and for the title and summary to be made available to outside organisations.

Signed …… (candidate) Date …….

STATEMENT 4: BAR ON ACCESS APPROVED

I hereby give consent for my thesis, if accepted, to be available for photocopying and for interlibrary loans after expiry of a bar on access approved by the Academic Standards & Quality Committee.

Signed …… (candidate) Date …….

Acknowledgements

I wish to express my grateful thanks to my supervisor, Prof. Milton Wainwright, for his invaluable guidance, advice, and supervision during the course of this project.

I am also extremely grateful to Dr. Jim Gilmour and Dr. Dave Kelly for their help and enlightening discussions.

I also want to thank Dr. Kurt Konhauser, for enabling me to spend the time in his lab at the University of Alberta, and for the valuable discussions and suggestions he shared with me. The Worldwide Universities Network (WUN) is also to be thanked for providing me the funds to do the visit and make this collaboration a reality.

Special thanks also goes to Alex Baker and Chris Rose for their tremendous help with the various equipment and apparatus used during this study. Thanks are also due to Chris Hill for his help in obtaining electronic microscope images. Many thanks also goes to all the staff and colleagues in our G10 lab for supporting me throughout the time of doing this study. Dr. Paul Heath and Dr. Afsanah Maleki-Dezaji are also thanked for their help on the next-generation sequencing analysis of our samples.

Special thanks also goes to the Higher Committee of Education Development in Iraq (HCED), and Soran University, for providing financial support to make this project a reality.

Finally, I wish to thank my family for their support; my wife, Sabreen, for her understanding, encouragement, and patience during the time of my study, and my daughters, Angie and Helda, for providing inspiration to push through and overcome obstacles arising throughout the project. I want also to thank my parents for their continuous support and inspiring me to be where I am today.

Summary

The theory of Panspermia suggests that life was brought to Earth from an external source in space. The theory can be further divided into a) Neopanspermia, the view that life continues to arrive from space to Earth, b) Pathospermia, the idea that pathogenic organisms arrive from space and c) Cometary Panspermia which specifies that extraterrestrial organisms originate from comets. This main aim of this study was providing evidence in support of Neopanspermia. Six stratospheric balloon launches were carried out in order to sample the stratosphere for microbial cells (biological entities, BE). Analysis of isolates was achieved using Scanning Electron Microscopy (SEM), Energy Dispersive X-Ray Spectroscopy (EDAX), and Molecular techniques, to help determine the biological nature of any isolates and their origin. SEM and EDAX showed that, while most of the isolated material was inorganic cosmic dust, a few were biological in nature, although generally not recognizable as known terrestrial organisms. Some of the BEs were larger than the theoretical 5 micron limit for the transfer of a particle from Earth to the sampling heights, thereby suggesting a non- terrestrial origin. This was confirmed by the lack of similar sized (i.e. exceeding 5 micron) known terrestrial organisms such as pollen, grass shards, and fungal spores. There is clearly no sieve present in the atmosphere that would allow the isolated BEs to be elevated to the stratosphere from Earth while holding back known biological forms. It was therefore concluded that the large biological entities we isolated from the stratosphere are incoming to Earth from space and continually impact the Earth. Single cell amplification and identification also showed the presence of DNA and revealed a diverse population of known microorganisms distinct from the isolated biological entities.

The ability of microbes to regain viability from ancient samples was also assessed by the isolation of bacteria from amber and halite rocks, thereby providing evidence that these organisms can survive after an extended period of millions of years, a finding which is of potential relevance to the transfer of microbes in the process of panspermia.

Three meteorite types were also examined for biosignatures using SEM and EDAX techniques, two showed microfossil formations which can provide evidence for the theory of cometary panspermia.

Evaluation of microbial survivability in the presence of exposure to ultraviolet C when embedded in ice was evaluated, as was the potential shielding by the presence of solid inorganic particles. It was also demonstrated, that the use of visible light generated by UV from fluorescence can provide energy for Cyanobacteria, which might have been the first microbes to inhabit our planet. Showing that life can survive in such conditions without the need of a protective atmosphere made up of oxygen that is necessary to form the protective ozone layer, this may explain how the first microbes were introduced to earth in the panspermia theory.

Publications arising from this study:

- **Omairi, T**., and Wainwright, M. A Fluorescent Mineral Shield: Protection and energy source for photosynthetic microbes against harmful ultraviolet radiations. AbReCon2015 Astrobiology Conference/ August 21-23rd/ University of Peradeniya- Sri Lanka. (Conference paper).
- **Omairi, T.,** and Wainwright, M. (2015). Fluorescent minerals–A potential source of UV protection and visible light for the growth of green algae and cyanobacteria in extreme cosmic environments. *Life Sciences in Space Research*, 6, 87-91.
- Wainwright, M., Rose, C. E., Baker, A. J., Wickramasinghe, N. C., and **Omairi, T**. (2015). Biological Entities Isolated from Two Stratosphere Launches-Continued Evidence for a Space Origin. *Journal of Astrobiology & Outreach*, 3(129), 2332-2519.
- Wainwright, M., Wickramasinghe, N. C., Harris, M., and **Omairi, T**. (2015). Masses Staining Positive for DNA-Isolated from the Stratosphere at a Height of 41 km. *Journal of Astrobiology & Outreach*, 3(130), 2332-2519.
- **Omairi, T**., and Wainwright, M. (2014). Studies on Astrobiology with Particular Reference to Cometary Panspermia. The 14th European workshop on astrobiology, European Astrobiology Network Association/ EANA 14/Edinburgh/ UK. (Poster and Presentation).
- Wainwright, M., Rose, C. E., **Omairi, T**., Baker, A. J., Wickramasinghe, C., and Alshammari, F. (2014). A Presumptive Fossilized Bacterial Biofilm Occurring in a Commercially Sourced Mars Meteorite. *Journal of Astrobiology & Outreach*, 2(114), 2332-2519.

Table of Contents

1 Chapter 1: History of the Panspermia Theory 2

1.1 Changes to the Panspermia concept and its introduction as a scientific theory 2

1.2 The “new Abiogenesis theory” 3

1.3 Emergence of the modern theory of panspermia 6

1.3.1 Cometary Panspermia 7

2 Chapter 2: Sampling the Stratosphere 11

2.1 Introduction 11

2.2 Earth’s Biosphere 12

2.2.1 The Atmosphere 12

2.2.2 Microbial presence in the atmosphere 16

2.3 Previous studies to sample the upper stratosphere 16

2.4 Materials and methods 27

2.4.1 Launch of stratospheric balloons with samplers 27

2.4.2 Identification and sequencing of DNA from single cells on the stubs 31

2.4.3 Control Flights 36

2.5 Results and Discussion 37

2.5.1 Findings from the first sampling flight 37

2.5.2 Findings from the second sampling flight 48

2.5.3 Findings from the third sampling flight 49

2.5.4 Findings from the Fourth Stratospheric Flight 55

2.5.5 Findings from the Fifth Stratospheric Flight 60

2.5.6 Findings from the Sixth sampling flight 85

2.6 The argument for a space origin for the stratospheric findings 92

3 Chapter3: Lithopanspermia - Microbial survival in terrestrial samples, terrestrial rocks, amber and halite. 97

3.1 Introduction 97

3.2 Microbial transfer through space within rocks 97

3.3 Long-term preservation of bacteria in various samples 99

3.4 Predicting the long-term survival for nucleic acids 101

3.5 Materials and Methods 103
3.5.1 Isolation of Microbes from Baltic Amber samples 103
3.5.2 Isolation of microbes from terrestrial rock samples 109
3.5.3 Isolation of microbes from halite crystals 110
3.6 Results 114
3.6.1 Growth from the Amber and the terrestrial rock samples 114
3.6.2 Growth from the halite mineral samples 116
3.7 Discussion 119
4 Chapter 4: Indications of the presence of microbial fossils in recovered meteorite samples. 125
4.1 Introduction 125
4.2 Meteorites, transporters of the building blocks of life 125
4.2.1 Biosignatures in the ALH84001 meteorite 126
4.2.2 Microfossils in meteorites 130
4.3 Materials and methods 135
4.3.1 Northwest Africa 4925 meteorite sample: 135
4.3.2 The Polonnaruwa meteorite sample 137
4.3.3 The Carancas meteorite samples 138
4.4 Results and Discussion 143
4.4.1 Analysis of the Northwest Africa 4925 meteorite 143
4.4.2 Analysis of the Polonnaruwa meteorite 151
4.4.3 Analysis of the Carancas meteorite 156
5 Chapter 5: Microbial Survivability Under Exposure to UV in Extreme Cosmic Conditions 164
5.1 Introduction 164
5.2 Microbial survival during the stages of panspermia interplanetary travel 165
5.3 Composition of Asteroids, Comets and Meteoroids 167
5.4 Cosmic radiation in the universe 167
5.5 Relevance of microbial resistance against cosmic UV to the panspermia theory 168
5.5.1 Microbial embedment and UV penetration of ice 170
5.6 Exploiting UV as an in indirect energy source for microbes 172
5.6.1 Light conversion within fluorescent minerals 173
5.7 Materials and Methods 176

5.7.1 Resistance of bacteria to UV radiation in pristine ice 176
5.7.2 Resistance to Ultraviolet Radiation in Ice and Charcoal Mixture 178
5.7.3 Resistance to Ultraviolet Radiation in Ice and Fumed Silica Mixture 179
5.7.4 Methods for investigating the use of UV light as an indirect microbial energy source 180
5.8 Results 185
5.8.1 CFU count of microbes exposed to Ultraviolet radiation in pristine ice, and ice mixed with nanoparticles 185
5.8.2 The use of visible light generated from fluorescence by UV for photosynthesis 201
5.9 Discussion 210
5.9.1 Microbial resistance to UV in ice or water 210
5.9.2 UV as an indirect energy source for Cyanobacteria 215
6 Chapter Six: General Discussion 219
References 224
7 APPENDICES 247
Appendix A 247
Appendix B 260
Appendix C 262
Appendix D 265

List of Figures

Figure 1-1 The Miller and Urey experiment 5
Figure 2-1: The Average Temperature Profile of Earth's Atmosphere:..... 15
Figure 2-2: Dual layered gel block, produced for the Tanpopo mission..... 18
Figure 2-3: Particles stained by the Live/Dead BacLight Bacterial Viability Kit:20
Figure 2-4: Particle masses isolated from the Indian stratospheric mission 21
Figure 2-5: Fragment of a diatom frustule, collected form the stratosphere. ... 22
Figure 2-6: An aggregate of small entities isolated from the stratosphere..... 23
Figure 2-7: Large flask-shaped biological entity isolated from the stratosphere 24
Figure 2-8: Relatively large BE recovered on one of the stratospheric SEM stubs..... 25
Figure 2-9: BEs on a SEM stub from the first stratospheric sampling mission 26
Figure 2-10: The samples drawer, which was automatically opened and closed in the stratosphere:..... 29
Figure 2-11: A polished copper slide being examined under the microscope . 30
Figure 2-12: The workflow of the genome analysis 32
Figure 2-13: SEM images of Earth-related biological material found on outside of sampler 38
Figure 2-14: Impact craters on the sampling stubs..... 39
Figure 2-15: Examples of cosmic dust and other inorganic particles collected from the stratosphere 40
Figure 2-16: Large, mucus-based biological entity isolated between 22-27km 41
Figure 2-17: EDAX analysis for one of the filaments shown in Figure 2-16..... 42
Figure 2-18: Large biofilm covered BE that impacted the SEM stub at speed 43
Figure 2-19: A complex biological entity that was isolated from the stratosphere 44
Figure 2-20: Amorphous particle recovered from the first stratosphere-sampling mission 45
Figure 2-21: SEM images for the Large Spherical Object (LSO)..... 46
Figure 2-22: Detailed SEM image for the LSO prior to dislodging it from the impacting site 47
Figure 2-23: Close-up SEM image for a section of the LSO..... 48
Figure 2-24: A gossamer-like particle recovered from the third stratospheric sampling trip..... 50
Figure 2-25: A bell-shaped BE recovered from the stratosphere 51
Figure 2-26: A star-shaped BE recovered from the stratosphere 52
Figure 2-27: Large clump of particles captured on one of the stubs from the third mission 53
Figure 2-28: Three inorganic particles recovered from the stratosphere 54
Figure 2-29: Three inorganic particles recovered from the upper stratosphere above Reykjavik – Iceland..... 56
Figure 2-30: Shows scattered inorganic particles on one of the copper slides 57

Figure 2-31: Four cosmic dust particles collected from the fourth stratospheric launch..... 59
Figure 2-32: An SEM image for a large-complex entity which was recovered from the fifth stratospheric launch 61
Figure 2-33: A large stratospheric masses sampled from the fifth launch..... 64
Figure 2-34: SEM image for one of the entities recovered from the fifth stratospheric flight 67
Figure 2-35: SEM of two masses recovered from the fourth stratospheric flight 69
Figure 2-36: SEM image for an amorphous entity recovered from the fourth launch..... 71
Figure 2-37: SEM image of relatively small particle close to the TEL limit in size 73
Figure 2-38: Negative image of an ethidium bromide-stained 1% agarose gel of the REPLI-g® Single Cell products 75
Figure 2-39: Negative image of an ethidium bromide-stained 1% agarose gel 76
Figure 2-40: Total sequence count, grouped by species name, for sample 1 of the seven non-axenic DNA samples: 80
Figure 2-41: : Total sequence count, grouped by species name, for sample 2 of the seven non-axenic DNA samples: 80
Figure 2-42 : Total sequence count, grouped by species name, for sample 3 of the seven non-axenic DNA samples: 81
Figure 2-43: Total sequence count from sample 4 of the seven non-axenic DNA samples:..... 81
Figure 2-44: : Total sequence count, grouped by species name, for sample 5 of the seven non axenic DNA samples:..... 82
Figure 2-45: : Total sequence count, grouped by species name, for sample 6 of the seven non-axenic DNA samples: 82
Figure 2-46: Total sequence count, grouped by species name, for sample 7 of the seven non-axenic DNA samples: 83
Figure 2-47: A collapsed particle that impacted the SEM at speed 86
Figure 2-48: Extremely close similarity in EDAX reading between three different regions 87
Figure 2-49: A complex entity which appears to be surrounded by a biofilm formation 89
Figure 2-50: An SEM for an entity recovered from the sixth stratospheric flight 90
Figure 2-51: An SEM for a large particle, comprising mainly of silicon..... 91
Figure 2-52: Image of the SEM analysis for volcanic dust..... 92
Figure 2-53: Small bacterial cells isolated from the stratosphere by Yang *et al.* (2008a)..... 95
Figure 3-1: The amber samples selected for the attempted microbial isolation 104
Figure 3-2: The sterile samples breakage apparatus 105

Figure 3-3: A Google aerial image showing the collection sites of the rock samples 110
Figure 3-4: Sequence of rocks associated with salt deposits in Kansas 111
Figure 3-5: Some fluid inclusions in the halite salt crystals 112
Figure 3-6: DNA bands visualized on Agarose gel for microbes within terrestrial rocks 117
Figure 3-7: Successful DNA amplification by PCR in which the products are demonstrated on a 1% (w/v) agarose gel 118
Figure 4-1: False-colour backscatter electron microscopy image for the surface of one of the chips of the ALH84001 meteorite 127
Figure 4-2: Two SEM images for sections of the ALH84001 meteorite 128
Figure 4-3: An SEM image for a section of the lunar meteorite QUE 94281 . 130
Figure 4-4: Nanobes isolated from Rainbow hydrothermal vents 131
Figure 4-5: SEM image of an Acritarch 132
Figure 4-6: Some of the microfossils recovered from the CI1 meteorites 133
Figure 4-7: An SEM for a diatom fragment 134
Figure 4-8: A section of the inner surface of the Polonnaruwa meteorite 134
Figure 4-9: One of the recovered Carancas meteorite samples 139
Figure 4-10: An SEM image for the analysed meteorite sample 144
Figure 4-11: Presumptive bacterial biofilm within the freshly cut Northwest Africa 4925 meteorite 145
Figure 4-12: SEM images showing details of the many presumptive bacteria-like forms 146
Figure 4-13: Two almost identical EDAX readings for different regions within the same sample 147
Figure 4-14: An SEM of filaments observed on the surface of a fragment of the Mars meteorite 149
Figure 4-15: Results for the EDAX analysis for the fiber bundle 150
Figure 4-16: SEM image for a section of the Polonnaruwa meteorite, EDAX signatures for two locations is shown 152
Figure 4-17: SEM and EDAX data for a large microfossil, identified within the Polonnaruwa meteorite 154
Figure 4-18: A view of a section of the Polonnaruwa meteorite showing a large spherical hollow structure 155
Figure 4-19: Oxygen isotopic composition data 156
Figure 4-20: SEM section from the Carancas meteorite particles 158
Figure 4-21: SEM images for sections of the Carancas samples showing ovoid and rod-shaped formations 159
Figure 4-22: An SEM image for a section of the Carancas meteorite 160
Figure 5-1: Hypothetical scenarios were the UV from a young star is absorbed by fluorescent rocks present on a planet’s surface 175
Figure 5-2: Two rocks composed of fluorite, calcite and pyrite 181
Figure 5-3: One of the rocks placed inside the incubator in front of a UV type-A lamp 182

Figure 5-4: Controls for Water and Ice (CFU) count after spreading on Nutrient agar for the ten bacterial samples. 186
Figure 5-5: Plate (CFU) count for *Bacillus subtilis*, in the charcoal experiment. 188
Figure 5-6: Plate (CFU) count for *Bacillus sphaericus*, in the charcoal experiment. 189
Figure 5-7: Plate (CFU) count for *Bacillus thuringiensis*, in the charcoal experiment. 190
Figure 5-8: Plate (CFU) count for *Bacillus licheniformis*, in the charcoal experiment. 191
Figure 5-9: Plate (CFU) count for *Rhizobium radiobacter*, in the charcoal experiment. 192
Figure 5-10: Plate (CFU) count for *Salmonella typhi*, in the charcoal experiment. 193
Figure 5-11: Plate (CFU) count for *Bacillus subtilis*, in the fumed Silica experiment. 194
Figure 5-12: Plate (CFU) count for *Bacillus sphaericus*, in the fumed Silica experiment 195
Figure 5-13: Plate (CFU) count for *Bacillus thuringiensis*, in the fumed Silica experiment. 196
Figure 5-14: Plate (CFU) count for *Bacillus licheniformis*, in the fumed silica experiment. 197
Figure 5-15: Plate (CFU) count for *Rhizobium radiobacter*, in the fumed silica experiment. 198
Figure 5-16: Plate (CFU) count for *Salmonella typhi*, in the fumed silica experiment. 199
Figure 5-17: Five *Rhizobium radiobacter* plates containing fumed Silica 200
Figure 5-18: Mixed culture of *Dunaliella* and *Chlorella* under the light microscope 201
Figure 5-19: culture of *N. commune* under the light microscope 203
Figure 5-20: Growth measured by OD to estimate cellular density for the four sample types of *N. commune* 205
Figure 5-21: Growth measured by OD to estimate cellular density for the four sample types of *S. elongate* 206
Figure 5-22: Growth measured by OD to estimate cellular density for the four sample types of the algal mixed culture (*Chlorella* and *Dunaliella*) 207
Figure 5-23: Chlorophyll measurement of the four sample types for *N. commune* 208
Figure 5-24: Chlorophyll measurement of the four sample types for *S. elongates* 209
Figure 5-25: Chlorophyll measurement of the four sample types for the algal species (*Chlorella* and *Dunaliella*) 210
Figure 5-26: Morphological changes in growth of bacteria on the plates..... 214

List of Tables:

Table 2-1: Average composition of the atmosphere up to an altitude of 25 km13
Table 2-2: The elemental composition of the neodymium magnets alloys 60
Table 2-3: Elemental results from EDAX for the A-D regions outlined in Figure 2-32. 63
Table 2-4: Elemental results from EDAX for the A-C regions outlined in Figure 2-33 65
Table 2-5: The elemental composition for the entity shown in Figure 2-34. 68
Table 2-6: The elemental composition for the entity shown in Figure 2-35. 70
Table 2-7: The elemental composition for the amorphous entity shown in Figure 2-36. 72
Table 2-8: The elemental composition revealed EDAX analysis of the small particle shown in Figure 2-37. 74
Table 3-1: PCR reaction mixture (Weisburg *et al.*, 1991) 108
Table 3-2: The nucleotide sequences of the two primers used for 16S rRNA PCR..... 108
Table 3-3: Growth results of the rock samples after and before breaking, and the DNA sequencing results. 115
Table 3-4: List of some of the surface sterilization protocols evaluated, with the washing steps employed for each 122
Table 5-1: Plates distribution used for each bacterial species for the UV C resistance in pristine ice and water. 177
Table 5-2: Plates used for each bacterium species in the charcoal experiment. 179
Table 5-3: Plates used for each bacterium species in the fumed silica experiment. 180

CHAPTER 1

1 Chapter 1: History of the Panspermia Theory

1.1 Changes to the Panspermia concept and its introduction as a scientific theory

The suggestion that life exists beyond our planet is not a new one; many ancient cultures believed that other stars and planets, observable from Earth harbour a variety of living and even spiritual entities (Clark, 1959, Oppenheim, 1977). Panspermia, or "Seeds everywhere" in Greek (Luisi, 2006), was initially suggested by the philosopher Anaxagoras about 2500 years ago, who stated that living organisms are taken in by the universe, and once conditions are favourable they will settle on a planet and replicate. It was, however, Aristotelian belief that life could arise spontaneously that dominated the scientific literature up into the 19th century and the idea that everyday living organisms can be spontaneously created from inanimate dead matter was widely received as a logical explanation for the origin of life. During the 17th into the 19th century, many researchers tried to disprove the spontaneous generation theory, including, Francesco Redi in 1668, John Needham in 1745, Joseph Priestley in 1803, and Charles. C. De la Tour and Theodor Schwan in 1873 (Levine and Evers, 2000). One researcher, in particular, De Maillet, described in his book, The Telliamed (1748) his theory of how life is distributed around the cosmos by special seeds, which he believed brought life for the first time to our Earth (Wainwright and Alshammari, 2010).

Louis Pasteur appeared to settle the spontaneous generation debate once and for all in 1859. By using specially designed swan-neck flasks that contained boiled meat broth, he was able to demonstrate the connection between airborne bacterial spores and what was previously thought to be a spontaneous creation of life in the culture. With this final blow to the spontaneous generation theory, the scientific community accepted the principle that all life comes from life (Schwartz, 2001). However, this finding led to another question, namely, where did life come from? This question shifted interest back to the idea of Panspermia.

Lord Kelvin was probably the first to present the idea of panspermia in a serious scientific manner (in 1871), during his Presidential Address to the British Association for the Advancement of Science. He stated:

"…Hence, and because we all confidently believe that there are at present, and have been from time immemorial, many worlds of life besides our own, we must regard it as probable in the highest degree that there are countless seed-bearing meteoritic stones moving about through space. If at the present instant no life existed upon the Earth, one such stone falling upon it might, by what we blindly call natural causes, lead to its becoming covered with vegetation."(Napier, 2004).

In a brief paper, Arrhenius (1903), gathered all the previous ideas on panspermia into one explicit astronomical context and then expanded these ideas in his book " Worlds in the Making" (1908), pointing to the fact that some microbes can survive a wide range of hostile conditions, including exposure to near zero degrees Kelvin. He suggested that microbes or other similar small particles such as spores can use the momentum from the radiation pressure of starlight to travel at the speed of lights into other habitable worlds across the universe. Although this principle is correct theoretically, there are two major objections to it; firstly, microbes must be less than 1.5 μm in diameter in order to be propelled by light, even though many microbes can meet this requirement, the second hurdle is presented by the presence in space of harmful cosmic rays and ultraviolet radiations. As a result, in order for microbes to survive panspermic-transfer, they would need to be protected by some sort of shielding material, such as rocks, which is not possible within the suggested size limit for radiation pressure-based transfer (Becquerel, 1924, Shklovskii and Sagan, 1966).

1.2 The "new Abiogenesis theory"

Due to the criticisms to radiopanspermia, and because few extremophiles were known at that time; it was presumed that microbes would never be able to survive the extremes of space, a view which led most scientists to reject Arrhenius's theory in favour of the "primordial soup theory". Working independently, both Alexander Oparin (1924) and John Haldane (1929)

proposed what is best described as the modified version of the Abiogenesis theory; they explained that early life on Earth must have developed in a chemically reducing atmosphere and, with the help of various energy forms such as lighting or ultraviolet light, various simple organic compounds were produced (i.e. monomers). These molecules then must, it is suggested, have come together as a soup in aqueous environments, such as deep-sea vents and shorelines. This would be followed by further complicated reactions leading to the synthesis of complex organic polymers; these may later have acquired lipid membranes thereby creating the first cells which eventually led to the formation of life.

Inspired by the primordial soup theory, Stanley Miller and Harold Urey tried to simulate what they thought at the time to be the conditions present on the early Earth (Miller, 1953). Essentially, they used an array of connected sterile flasks containing water, methane, ammonia, and hydrogen, representing their ideas on the early Earth's atmosphere and ocean. Lightning was also simulated using a pair of electrodes, in which water vapour was allowed to pass through in a continuous cycle of heating and cooling. After two weeks, the circulation liquid became coloured pink and when analysed it was shown to contain a mixture of more than 20 amino acids (Figure 1-1). This was, and continues to be, considered a ground-breaking experiment, in that it showed that various organic compounds, including amino acids and other macromolecules (which could act as potential building blocks) can be synthesized abiotically in nature. However, later, strong evidence showed that early Earth atmosphere might have been different from what Miller imagined (mainly in relation to the debate about the hydrogen content in the upper early atmosphere (Tian *et al.*, 2005)). Many researchers have modified the Miller-Urey experiment and have synthesized a vast array of other organic compounds. However, the synthesis of monomers, by itself is not enough to explain how the more complex blocks for life were assembled, and more importantly, how proto-life forms achieved the ability to replicate; it soon became evident therefore that far more complex mechanisms must be involved in the origin of life.

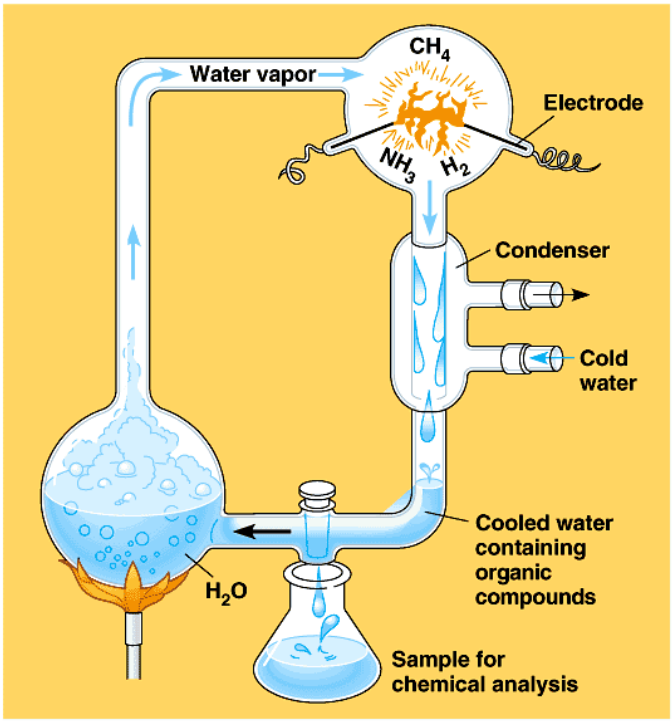

Figure 1-1 The Miller and Urey experiment

Showing that several organic compounds can be formed by non-biological processes by simulating what was thought to represent the conditions of Earth's early atmosphere (Figure: Pearson Education. Inc.).

The first early self-replicating molecule is highly unlikely to be DNA, simply because the double-stranded nature of it seems extremely complicated, and its synthesis relies heavily on proteins and RNA; because of this problem, the so-called “RNA world hypothesis has been suggested. RNA is simpler than DNA, yet it can still retain heredity information and act as a chemical catalyst for copying; according to this hypothesis then life eventually evolved and moved on from RNA to use DNA (Nirenberg, 1963, Warner *et al.*, 1963).

The alternative “Clay World” hypothesis was first proposed in (1966), it suggested that life has evolved through natural selection from inorganic clay systems, such as silicate crystals which might have acted as a non-organic replication medium for the slow development of complex organic molecules and eventually living cells (Cairns-Smith, 1982). Numerous other hypotheses have been suggested to explain the origin of life, but they all remain

speculative and lack any substantial evidence. One idea suggested by Woese (1979) proposed that life first originated in a droplet phase rather than in aqueous or solid environments, because prebiotic Earth possibly lacked water surfaces, thus early Earth might have evolved on conditions similar to those found on present-day Venus. Another idea speculates that life might have originated during the melting of the ice-caps as a result of a meteorite impact (3.6- 4.0) billion years ago (Bada *et al.*, 1994). None of the above mentioned theories and speculations have provided us with a definitive explanation of how life could have originate *de novo* on Earth, thereby leaving open the possibility that such a transformation never in fact occurred and that life on Earth originated from elsewhere, i.e. the theory of panspermia.

1.3 Emergence of the modern theory of panspermia

Following the Miller-Urey experiments, most scientists believed that the question of the origin of life on Earth would soon be solved with the solution being simply based on chemical theory. However, as stated above, many years have now passed since the appearance of Oparin and Haldane's theory and still, no conclusive proof has been provided to show that life can originate from non-living matter, a fact which has led to a resurgence of interest in the panspermia theory.

In order to solve the problems of long space transit time and exposure to cosmic radiations during panspermia, Francis Crick and Leslie Orgel proposed the so-called "Directed Panspermia Theory" (1973). This view is based on the suggestion that some unknown intelligent extraterrestrials spread life to planets, throughout the cosmos, including Earth. This theory is impossible to prove unless we were to find the object that delivered the directed-life sample, or we were to somehow obtain some information from extraterrestrial sources concerning its veracity. As a result, although not implausible, this idea can be regarded as being unscientific, and it is unlikely that it would have been entertained had it been suggested by less eminent scientists.

Perhaps the most interesting aspect about Crick's speculations is a) his observation that molybdenum, which is needed for enzymic reactions in living

organisms, is rarely found on Earth and b) his argument that if a single extraterrestrial organism was intentionally inoculated into Earth and then cloned and evolved into other life forms, it would provide a good explanation for why the genetic code is universal in all Earth's life forms; of course the same argument applies to the possibility that a single cell randomly arrived at Earth from space, i.e. non–Directed Panspermia.

1.3.1 Cometary Panspermia

The modern version of non-directed panspermia theory is credited to Sir Fred Hoyle and Chandra Wickramasinghe; their theory has been termed Cometary Panspermia.

According to cometary panspermia, when new star systems were still in the formation process, comets were also forged by the condensation of interstellar dust, this interstellar matter also contained a small percentage of viable microbes, which came from old comets formed during a previous cycle. These bacteria, it is suggested, were incorporated into the new comets where they remain protected from the harmful external environment; the inner core also provided a warm, watery environment for the multiplication of the microbes, which have access to all necessary nutrients (including molybdenum). A small percentage of living entities are likely to escape from the newly formed comets to return to space and thereby maintain a constant number of panspermic organisms. As new comets usually are formed in the outer, colder regions of the star systems, only a small percentage of these seeded comets will migrate internally towards the warmer planets, ending up in seeding them with microbes and life. The cycle will then be repeated again each time a new star system is formed.

After Hoyle and Wickramasinghe proposed their theory, a surge of new ideas and research emerged including a search for the presence of living or dead microbes within recovered pieces of meteorites, as well as in the upper regions of the atmosphere. A large number of meteorites have now been examined for evidence of fossilised microbes within them (McKay *et al.*, 1996, Hoover *et al.*, 1998, Wallis *et al.*, 2013, Wickramasinghe *et al.*, 2013c, Wainwright *et al.*, 2014, Lee *et al.*, 2017). In addition, several attempts have

also made to search for biological signatures in stratospheric and interplanetary dust particles (IDP) (Wainwright *et al.*, 2004, Yang *et al.*, 2008b, Wainwright *et al.*, 2013d).

Cometary panspermia also helped to generate a number of new terms which relate to the distribution of microbes throughout the cosmos, including Lithopanspermia (to describe microbes embedded within rocks), Archipanspermia (microbes distributed inside artificial rocks e.g. cement and bricks, created by intelligent species), and Neopanspermia (the continuing seeding of life to earth up until this moment) (Alharbi *et al.*, 2011). Calculations by Worth *et al*., (2013) have shown that not only is the interplanetary exchange of material containing life plausible, but also Earth, and similar planets can receive a significant rate of re-impacting rocks within the first million years following ejection. This means that planets which have been completely, or partially, sterilised by large impact events could have been re-seeded again by the return of their own microbes contained within ejected rocks.

It has recently been claimed that data received from the recent successful Rosetta mission, including the high-resolution images of Comet 67P/Churyumov–Gerasimenko 2, also appear to be compatible with the panspermia theory (Wickramasinghe *et al.*, 2015). According to Wallis *et al.,* (2009) in comets that are sufficiently large, a significant fraction of its interior volume could have remained for millions of years in a liquid state, because of the radioactive heating occurring during its early history. Therefore, microorganisms (methanogens and chemotrophs) that might have existed before the formation of the comets within the solar system could, it is claimed, have undergone extensive replication, and prior to the comet being frozen completely, it could have been effectively colonised. Wickramasinghe *et al*., (2015) suggest that for Comet 67P/Churyumov–Gerasimenko 2, the Rosetta images for refrozen seas and lakes and the indications for the earlier outgassing activity on the comet, all points to the action of microbes. The same study suggests that, while microbes still needed sufficient liquid water during the earlier comet colonisation-period, they can later inhabit cracks within the surface of the comet, in ice and sub-crystal snow, especially if those extremophile microbes possess anti-freeze salts and biopolymers.

A recent focused effort from a major space agency to investigate the panspermia theory, has been instigated by the Japanese Space Agency (JAXA), with the Tanpopo mission (Yano *et al.*, 2015). Low-density silica aerogel blocks were sent in 2015 to the International Space Station (ISS), and are currently exposed on the ISS Kibo exposed facility, with the hope that the gel will capture in-falling particles that might contain microbes. Subsequent analysis and findings would have a major impact on the panspermia research, and, if positive, will provide a strong evidence for the results of the work undertaken in the present study.

The news of the recent discovery of seven Earth-sized planets, around a single star in the TRAPPIST-1 system, by NASA's Spitzer Space Telescope, with three of the planets firmly placed in the habitable zone (Gillon *et al.*, 2017), also comes in support of the panspermia theory. Lingam and Loeb (2017) used a model for estimating the probability of panspermia occurring between the planets of the newly discovered system, compared to the Earth-to-Mars case, and found that panspermia, in the former is potentially orders of magnitude more likely to happen than in the latter. Another study also reached a similar conclusion, showed the possibility of lithopanspermia to take place in the habitable zone of TRAPPIST-1 within relatively short timescales; thus showing that about ten percent of the ejected planetary material from one planet of the system reaches the next within 102 years, therefore indicating it to be four to five times faster than in our solar system (Krijt *et al.*, 2017).

CHAPTER 2

2 Chapter 2: Sampling the Stratosphere

2.1 Introduction

Hoyle and Wickramasinghe's modern version of the panspermia theory (cometary panspermia) states that microbes can arrive at Earth carried within meteorites and comets (Hoyle and Wickramasinghe, 1981a). Neopanspermia is a continuation of this theory explaining that if microbes arrived at certain time in the past to deliver the first life to Earth from space, then there is no reason why this process cannot continue today. Life may therefore still be arriving in the stream of cosmic dust and meteorites being continually brought to Earth (Wainwright, 2003). The obvious way in which to investigate this possibility is to capture microbes as they are incoming to Earth. Such capture needs to be achieved at a height to which we can be confident that life forms from Earth would not reach under normal conditions. As a result, it would appear best to try to capture any incoming organism from deep in space; however, this approach is hindered by the fact that because space lacks an atmosphere, any incoming material (unless an aerogel-type material is employed) would be smashed beyond identification. (Tabata *et al.*, 2011). The stratosphere is likely to be the most suited region from which to sample such incoming biological material if it exists (Wainwright, 2008), therefore providing an alternative frontier to investigate the panspermia theory. Many attempts have been made to sample the stratosphere with varying degrees of success and scepticism about the obtained results (Smith *et al.*, 2010). One of the methods involved sending balloons into the stratosphere, which carried various types of samples that can capture microbes for subsequent analysis (Wainwright *et al.*, 2004, Yang *et al.*, 2008b, Smith *et al.*, 2014, Wainwright *et al.*, 2015a).

In this Chapter, work carried out on sampling of the stratosphere for living entities will be discussed in relation to the possible extra-terrestrial origin of any isolates.

2.2 Earth's Biosphere

The biosphere is the region of a planet that contains life. Earth is at present the only planet known to contain a biosphere and this can be divided into three sections: the lithosphere, followed by the hydrosphere and the atmosphere; secondary, smaller regions also exist e.g. the cryosphere and the anthrosphere. The biosphere is a complex system which results from the global interactions of all of these regions (Smil, 2003).

The biosphere is not isolated but continuously exchanges both matter and energy with the non–biosphere thereby enabling the biochemical cycling of elements on a global scale (Vernadsky, 1998). It also should be noted that Earth is not a closed system and that outer space and Earth exchange materials and energy; the fact that Earth's biosphere relies on our sun is undeniable. Meteorites, comets and cosmic dust all contribute to the input of complex organic compounds to Earth, including amino acids and nucelobases "i.e. the so-called "building blocks of life" (Kvenvolden *et al.*, 1970, Engel and Macko, 1997, Ciesla and Sandford, 2012). Rough calculations suggest that Earth receives an average amount of about 40 tonnes per year of meteors and interplanetary dust, most of which burns up in before it reaches Earth's surface (Leinert and Grün, 1990). Clearly then, the Earth was always, and continues to be, an open system which is exposed to the cosmos.

2.2.1 The Atmosphere

Earth's atmosphere is made up of the layer of gases that surrounds the planet; these gases are maintained by Earth and not stripped into space by solar winds due to two factors, namely the Earth's magnetic field, and the planet's gravity. Undoubtedly, the atmosphere of any planet plays an essential role in determining what life forms can exist on it. The suitable conditions for life on Earth are regulated by a fine delicate balance between the gases of the atmosphere. Carbon dioxide for example helps to create the greenhouse effect which keeps the Earth warm enough to sustain life; if the CO_2 concentration was higher however, the greenhouse effect would prove

harmful for life forms living on its surface. The Ozone layer in the stratosphere helps to absorb harmful radiations that otherwise would have been lethal for most of terrestrial organisms, including humans. As can be seen from Table 2-1 Dry air in the atmosphere is made up predominantly of nitrogen (78.08%) and oxygen (20.95%), with the rest made mostly of argon, CO_2 and other gases (Wayne, 1991, Pidwirny, 2006).

Table 2-1: Average composition of the atmosphere up to an altitude of 25 km

The percentage of the chemical components within the troposphere and the lower stratosphere (Pidwirny, 2006).

Gas Name	Chemical Formula	Percent Volume
Nitrogen	N_2	78.08%
Oxygen	O_2	20.95%
***Water**	H2O	0 to 4%
Argon	Ar	0.93%
***Carbon Dioxide**	CO_2	0.0360%
Neon	Ne	0.0018%
Helium	He	0.0005%
***Methane**	CH_4	0.00017%
Hydrogen	H_2	0.00005%
***Nitrous Oxide**	N_2O	0.00003%
***Ozone**	O_3	0.000004%

* Variable gases

Planet Earth’s atmosphere can be divided into four main parts, starting from the lowest region; the troposphere, stratosphere, mesosphere, and the thermosphere (Brasseur and Solomon, 2006).

The lowest one, the troposphere starts from the Earth's surface and extends to an average of 12 Km. The maximum height for the troposphere at the equator is 17 Km while on the poles it extends to only 9 Km. This region is warmest at the bottom and drops with height to about −60 °C at the top; it is the densest layer of the atmosphere since it holds about 80% of all the air mass. Since it contains most of the water vapour ; Earth’s weather changes take place within this layer (Wayne, 1991).

The stratosphere can extend to an altitude of 55 km above the surface and is separated from the troposphere by the tropopause. Unlike the troposphere, the temperature in the stratosphere eventually increases with height to an average of 0°C at the highest point of the layer (Figure 2-1), this is because this layer contains Ozone (O_3), made from the combining of O and O_2, which absorbs ultraviolet radiation energy coming from the sun. Since there is very little water vapour in the stratosphere, rarely do clouds form in it (Brasseur and Solomon, 2006). On top of the stratosphere is the stratopause, a barrier that separates it from the mesosphere. Since the stratosphere is suited above the compressed troposphere, air density is about 10^3 times less on the top of the stratosphere than at sea level, due to this; highest altitudes for aircrafts and balloons can be achieved within the stratosphere (Hartmann *et al.*, 2001, Wainwright *et al.*, 2006).

The mesosphere is the third layer of the atmosphere and starts at about 50 km above sea level and extends to 80-85 km in the mesopause. It is also the coldest layer with a temperature average of about −85 °C, temperature is the lowest in the base of the mesosphere at around 0°C and keeps dropping until it reaches below -100°C in the mesopause (Brasseur and Solomon, 2006, Sullivan, 2013).

The final main layer is the thermosphere, which stretches from the mesopause, up into thermopause at a height of 500-1000 km; as the name suggests the temperature in this region increases with height up to as high

as 1500°C (Figure 2-1); this is because the molecules within it are at an extremely low density. The thermosphere also contains the ionosphere in its lower part. The exosphere comes after the thermosphere, separating it from outer space; no meteorological phenomena occur within this region (Smil, 2003).

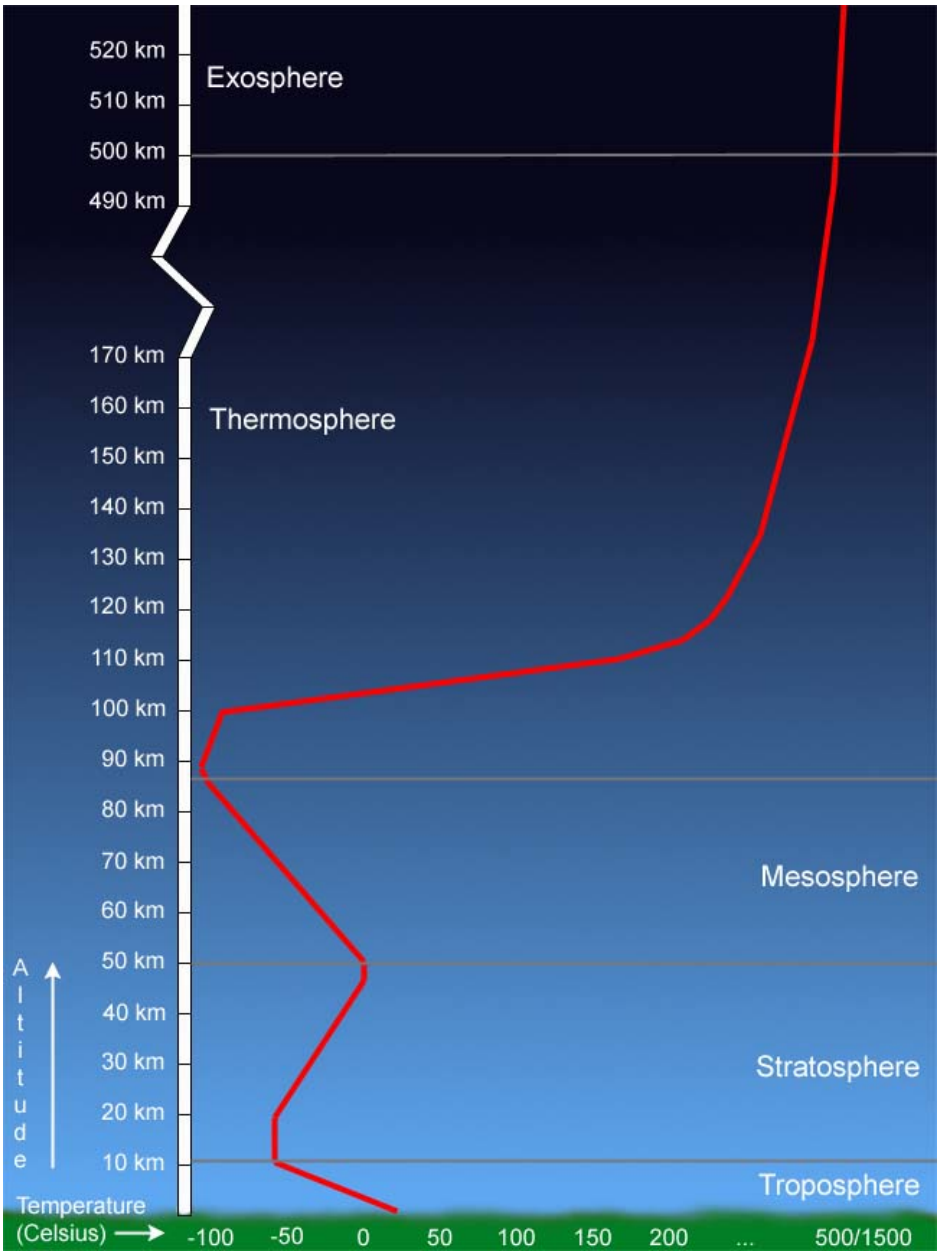

Figure 2-1: The Average Temperature Profile of Earth's Atmosphere:

Showing the vertical variations in temperature within the atmosphere (Sullivan, 2013)

2.2.2 Microbial presence in the atmosphere

As was previously stated, the troposphere is the region in which most of the weather changes occur and these are generally concentrated within the boundary layer, typically extending to 2 km above the Earth's surface. This results in heavy mixing of the air with all types of particles small enough to be elevated, such as dust, smoke, aerosols and clumps of all manner of microbial life of both terrestrial and marine origin (Kellogg and Griffin, 2006). Modern human practices also contribute to the microbial flora of the air, e.g. factories, waste-water treatment, and agricultural techniques which might help in generating bioaerosols (Smith, 2013). It has also been shown that the flora of the lower atmosphere is not passive; Bauer (2002) also showed that microbes, mainly bacteria can act as nuclei for cloud and ice formation.

Numerous challenges exist when sampling the stratosphere since the density of gases and bioaerosols decrease with height, so in order to collect a sufficient biomass a relatively large volume of air needs to be sampled. Maintaining samples free of contamination is another major problem (Smith, 2013). Even with the emergence of molecular methods, mainly PCR for microbial identification, it is still very challenging to identify microbes in any recovered samples mainly because they occur in extremely low numbers. Also, the use of gold coating on SEM samples makes identification using molecular techniques almost impossible (Wainwright *et al.*, 2013c).

2.3 Previous studies to sample the upper stratosphere

Many techniques exist to evaluate the existence and nature of airborne microbes found above the troposphere, while none can serve as the ultimate method, the results from each helps us to form a more complete picture of the Earth's biosphere. The most cost effective and simplest method of determining the biotic and abiotic input to Earth is to sample snow and hail as it reaches the Earth's surface; certain microbes have special proteins within their cell membranes that raise the freezing point of water, which can

lead to the formation of selective rain (DeLeon-Rodriguez *et al.*, 2013). Microbes either can act as condensation nuclei, or get caught within the precipitation particles as it forms within the clouds. Christner (2008) reported positive results from collecting snow and hail samples. However several limitations exist for this method; contamination is always a risk since falling precipitation can pick up microbes from any height, also, ice nucleation and precipitate formation mainly occur in the troposphere (Wayne, 1991). High altitude particles can also be sampled using high flying aircraft, as proposed early by Timmons (1966) to use a sampler mounted on the aircraft with a filter. Since then, subsequent attempts did not deviate much from the original mechanism for collection (Yang *et al.*, 2009, DeLeon-Rodriguez *et al.*, 2013)

Sounding rockets, which can reach any heights, can also be used, but they suffer from high cost and engineering challenges in regards to the sampler attachment and functioning, and the limited exposure time. Soviet Scientists made the first attempt to collect microbes using rockets which reached an altitude of 77 km from where they obtained bacteria and fungi (Imshenetsky *et al.*, 1978) ; these results are still however, questioned by some researchers (Smith, 2013).

Perhaps being the only time that a major space agency has taken an interest in the panspermia theory, the Japanese space agency (JAXA) launched the “Tanpopo mission” back in May 2015, which is an orbital astrobiological study used to investigate the transfer of microbes between planets throughout space. The Tanpopo mission is currently utilizing the exposed facility located on the exterior part of the Japanese unit of the International Space Station (ISS), and it is operating under the same principle of our stratospheric collection effort; which is the passive collection of infalling particles on its collection stage, later to be analysed in the lab after the samples are brought back to Earth. The only main difference is being that in the Tanpopo mission, the sample acquisition time will be a year, and the collection stage will have blocks of “low-density aerogels” (Figure 2-2) mounted on it in order to collect the incoming micrometeorites and other

particles. After retrieval, the samples will be examined to determine the size and velocity of the infalling particles, and determine their mineralogical and biological characteristics (Kawaguchi *et al.*, 2013a, Yano *et al.*, 2015, Kawaguchi *et al.*, 2016).

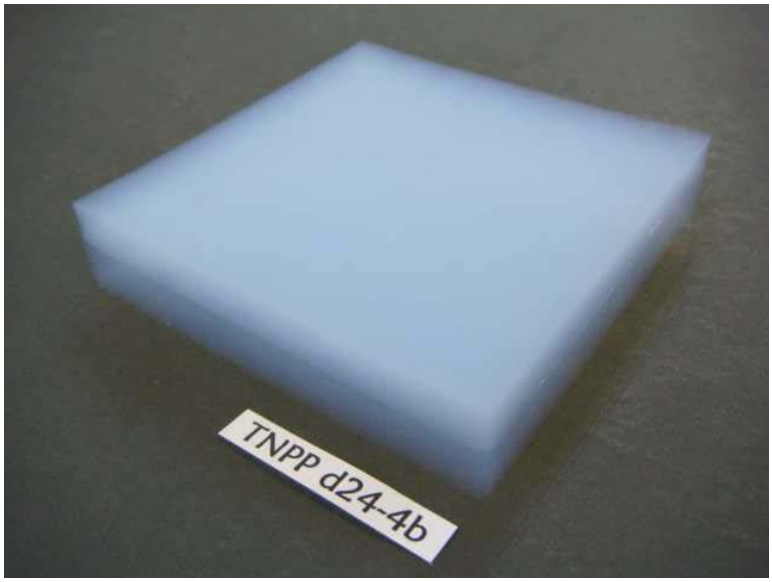

Figure 2-2: Dual layered gel block, produced for the Tanpopo mission

density is 0.01 g/cm3 and 0.03 g/cm3 surface and base layers respectively (Tabata *et al.*, 2011).

Balloon launches (for microbial sampling) provides a suitable, cost effective, contamination free sampling method, with a relatively good sampling exposure time. This method provides an opportunity to sample heights previously used methods cannot reach, excluding rockets, the highest record is currently at 53 km (Yamagami *et al.*, 2004). Balloons generally come at a relatively low cost and are easier to operate and control. Those used for scientific purposes are made from a thin layer of polyethylene, and filled with Helium in order to float. The sampler is hanged below it, with the size and shape of it depending on the balloon design. The height and the floating time (time the balloon spent at its maximum height) is dependent on the type and size of the balloon.

On August 2014, a large balloon was launched from New Mexico, USA, as part of NASA's programme to investigate Exposing Microorganisms in the Stratosphere (E-MIST). Aluminium coupons were used to hold *Bacillus pumilus* SAFR-032 spores, which were deposited on the surface of it. Conclusive results from this launch showed that although exposure of microbes on the coupons to flight conditions at 37.6 km for four hours did reduce the number of viable spores, there were a relatively few spores which survived the stratospheric exposure (Smith and Team, 2015). This provides strong evidence that some microbes can resist the extreme conditions of the upper stratosphere, and suggest that such microbes play a significant role in the evolution of early life on Earth and similar planets. As Khodadad *et al.* (2017) explains, based on E-MIST results ""It is therefore plausible that bacteria enduring radiation-rich environments (e.g., Earth's upper atmosphere, interplanetary space, or the surface of Mars) may be pushed in evolutionarily consequential directions".

One of the most relevant balloon launches which are directly related to our work was the Indian balloon mission; On the 21st of January 2001, a balloon was launched from the National Scientific Balloon Facility of the Tata Institute of Fundamental Research at the city of Hyderabad, India (Harris *et al.*, 2002). The aim of the mission was to sample the stratosphere for microbes using a cryosampler carried under the balloon that collected air samples from a height of 20-41 km. After the balloon came down, analysis of the results showed clear evidence of microbial living cells, clumps of viable cells were reported from all altitudes within the launch. Although the initial analysis for the samples only reported, viable, but non-culturable microbes, further analysis and microbial isolation and incubation attempts by Wainwright *et al.* (2003) yielded positive growth on some on the agar media; Two bacterial species (*Bacillus simplex and Staphylococcus pasteuri*) were recovered from the cultured plates, in addition to one fungal species, *Engyodontium album*. Viable staining technique was also used for some of the findings from the Indian balloon launch, which revealed positive results for living bacterial cells (Figure 2-3).

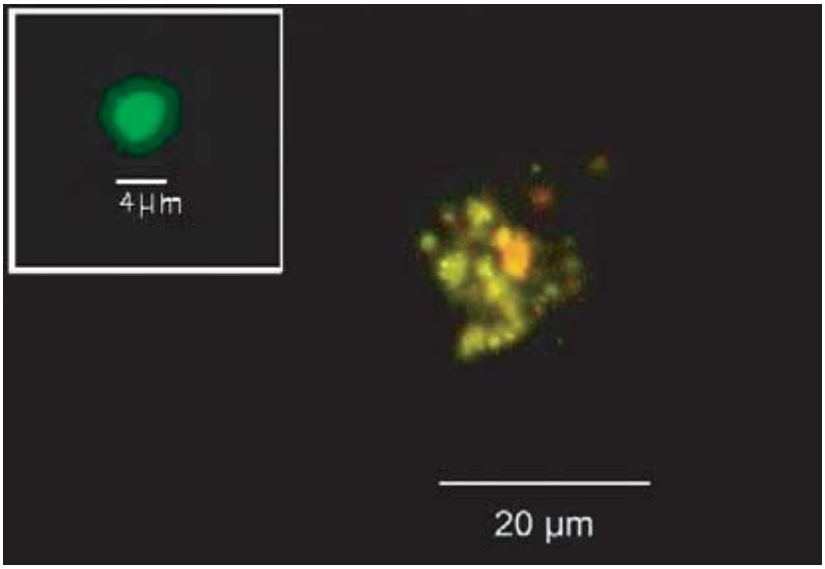

Figure 2-3: Particles stained by the Live/Dead BacLight Bacterial Viability Kit:

showing living bacteria (red: dead, Green: living) which were found on membranes exposed to the stratospheric air from the Indian balloon mission (Wainwright *et al.*, 2004).

Although not published at the time, there were also large clumps of material (10-30 um) isolated from the same Indian stratospheric mission, and deposited on the micropore filters used throughout the work, those were treated at the time with DAPI and $DIOC_6$ stains, later, the samples were observed with an epifluorecence microscope (Figure 2-4). Our team recently re-examined the unpublished data from the mission and interpreted them in light of the new evidence from our UK stratospheric launches (Wainwright *et al.*, 2015b).

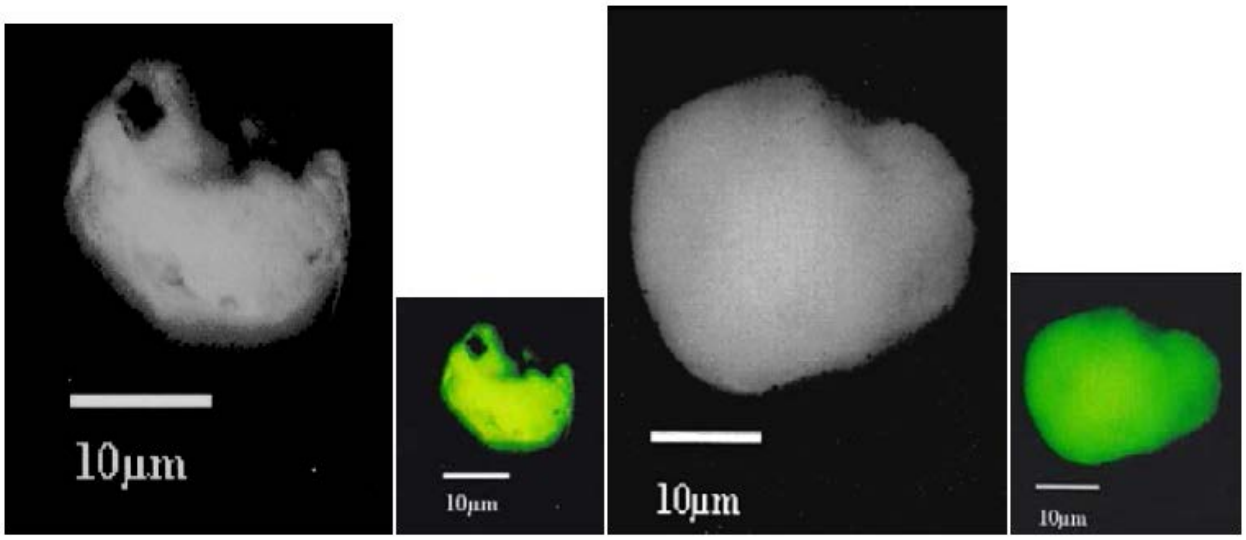

Figure 2-4: Particle masses isolated from the Indian stratospheric mission stained with DAPI, and showing positive result confirming the biological nature of it (Wainwright *et al.*, 2015b).

The Indian balloon mission of 2001, successful as it was, had a relatively high budget, the alternative was to use small balloons, which contained another collection method that did not require the uplift of the heavy cryosampling equipment (Wainwright *et al.*, 2015a).

The above discussion included mention of relatively recent attempts to use large helium-filled balloons to study the microbiology of the stratosphere in order to determine if microbes occur in this region, and if so, whether or not they originate from space (rather than coming up from Earth), i.e. the work represents an attempt to demonstrate the validity of the theory of Panspermia. The following section will discuss the use of weather balloons and a simple non-crysosampler based sampler. While these are cheaper than cryosamplers to make and launch, the balloons are incapable of reaching the heights achieved by large balloons, and sample at around 27-30Km as opposed to 41km for cryosamplers. The aim of the work described here was to sample the stratosphere for microorganisms, or other biological entities, which presumptively arrive to Earth from space. In the case of the first weather balloon launch (details in 2.4.1) the samples were initially analysed with SEM without the use of EDAX. This was conducted before our

study; Numerous organic and inorganic particles were recovered from the first stratospheric launch, SEM analysis showed many to be inorganic cosmic dust particles, while others had morphologies and an organic composition suggestive of them being biological entities. It is notable that some of the cosmic dust particles seen here are similar to the ones collected during the Indian balloon mission at a height of 41 km (Wainwright, 2008). One of the entities, which is clearly biological since it highly resembles a part of a familiar terrestrial organism is shown in Figure 2-5. Although it clearly appears to be incomplete and broken, it bears obvious resemblance to the *Nitzschia* species of diatoms; it appears however, to lack a protoplast. Whether it reached the stratosphere in this state as a fragmented diatom frustule, or had a viable protoplast inside an intact frustule is unclear and will be further commented upon below.

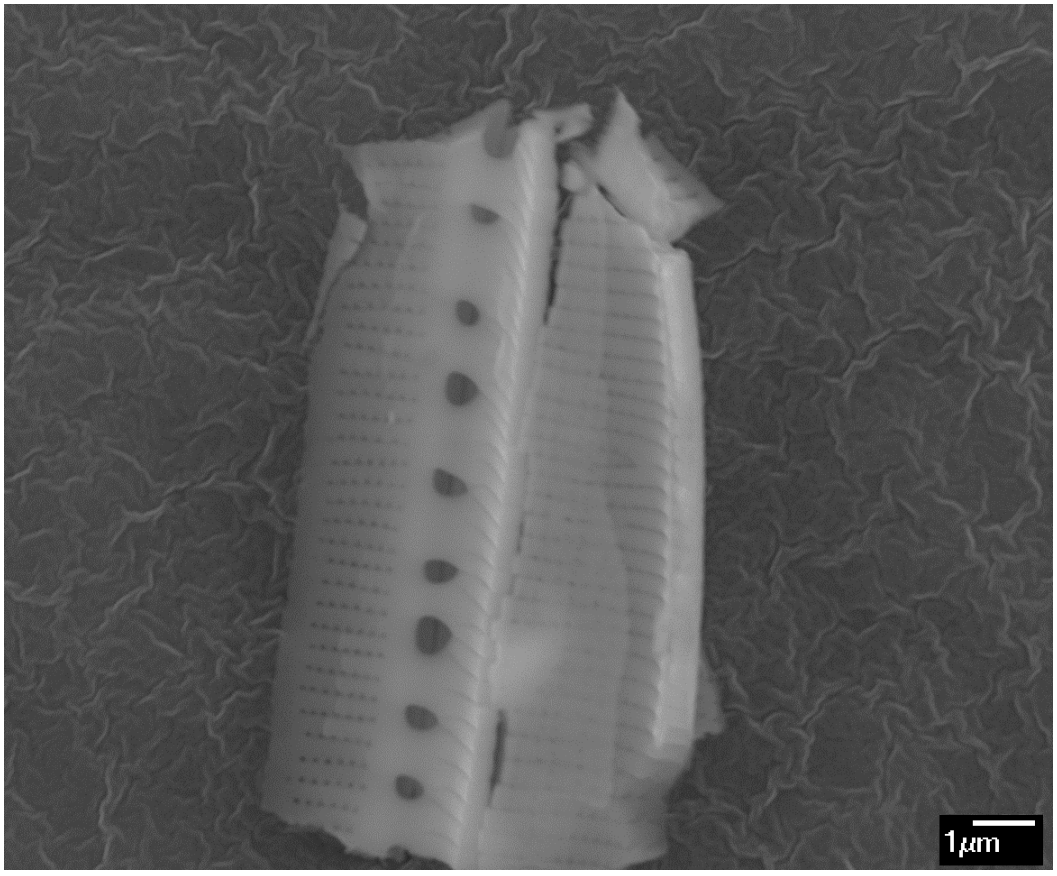

Figure 2-5: Fragment of a diatom frustule, collected form the stratosphere.

Observed on a stub from the first stratospheric sampling flight, results were obtained by Wainwright *et al.* (2013d)

Figure 2-6 shows what appears to be a clumped group of particles isolated from the stratosphere, which looks similar to ordinary bacterial clump, with the difference that the cells are extremely small (~100nm), i.e. smaller than "normal" bacteria. These nano-entities should not be immediately dismissed as being non-biological, especially taking into account their uniform appearance, the pattern of their aggregation, and the signs of "budding" demonstrated by some of them, all are familiar features shared by many bacteria (Wainwright *et al.*, 2013c).

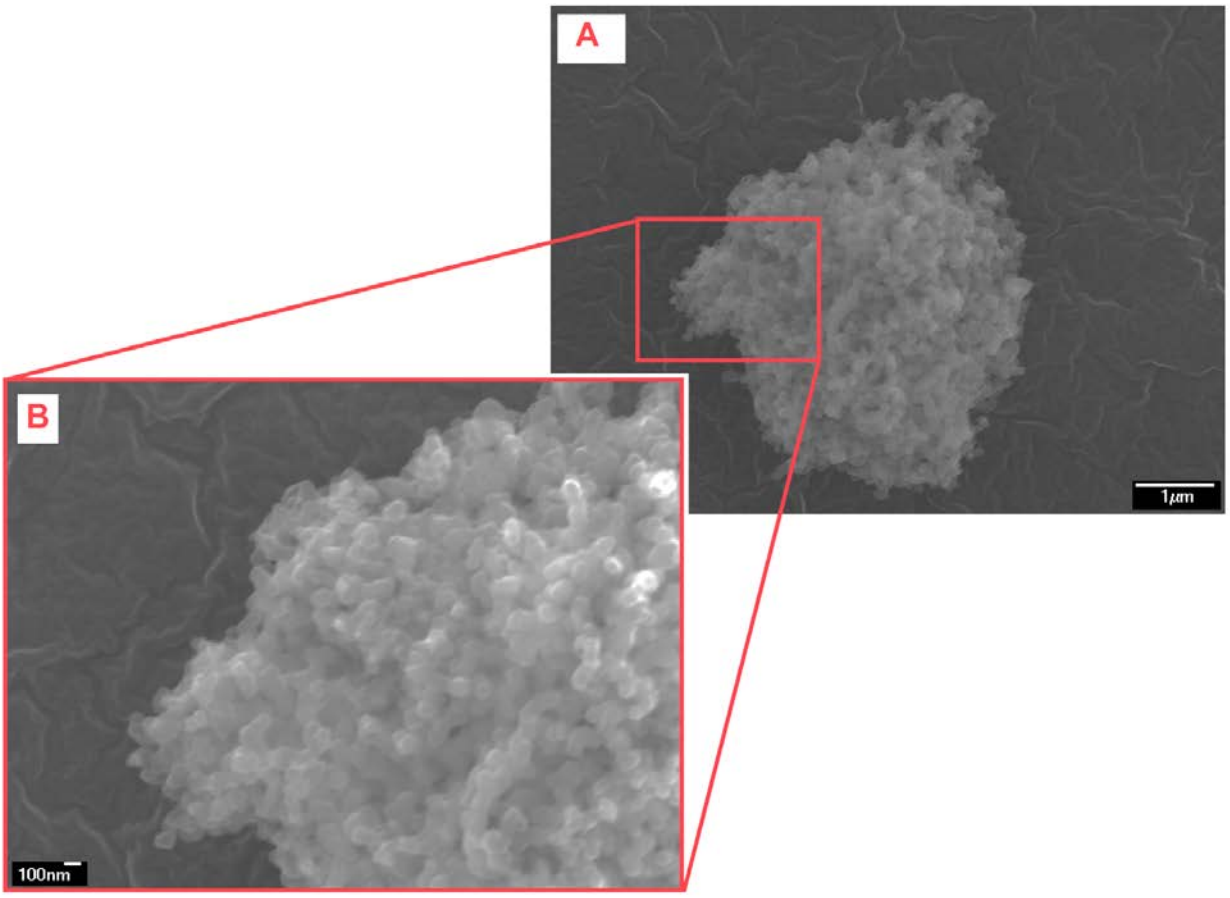

Figure 2-6: An aggregate of small entities isolated from the stratosphere

A: a possible clump of putative organisms (possibly nanobacteria) sampled from the stratosphere. B: a detailed SEM image for the same clump, clearly showing "budding".

It is possible however, that the clump shown in Figure 2-6 is not biological, since minute inorganic particles can also create similar, clumping morphologies. The large individual BE shown in Figure 2-7 on the other hand is readily interpreted as being biological due to its unique shape, bilateral symmetry, as well as complexity. Showing what appears to be a flask-shaped object that has collapsed upon impact on the surface of the stub. Despite its biological nature, it does not appear to be bacterial, and more likely to belong to an organism analogous to algae or protozoa. This entity is not a pollen grain or an obvious angiosperm component; we are also currently unable to allocate it to a known living terrestrial organism, or known fossil (Wainwright *et al.*, 2013c).

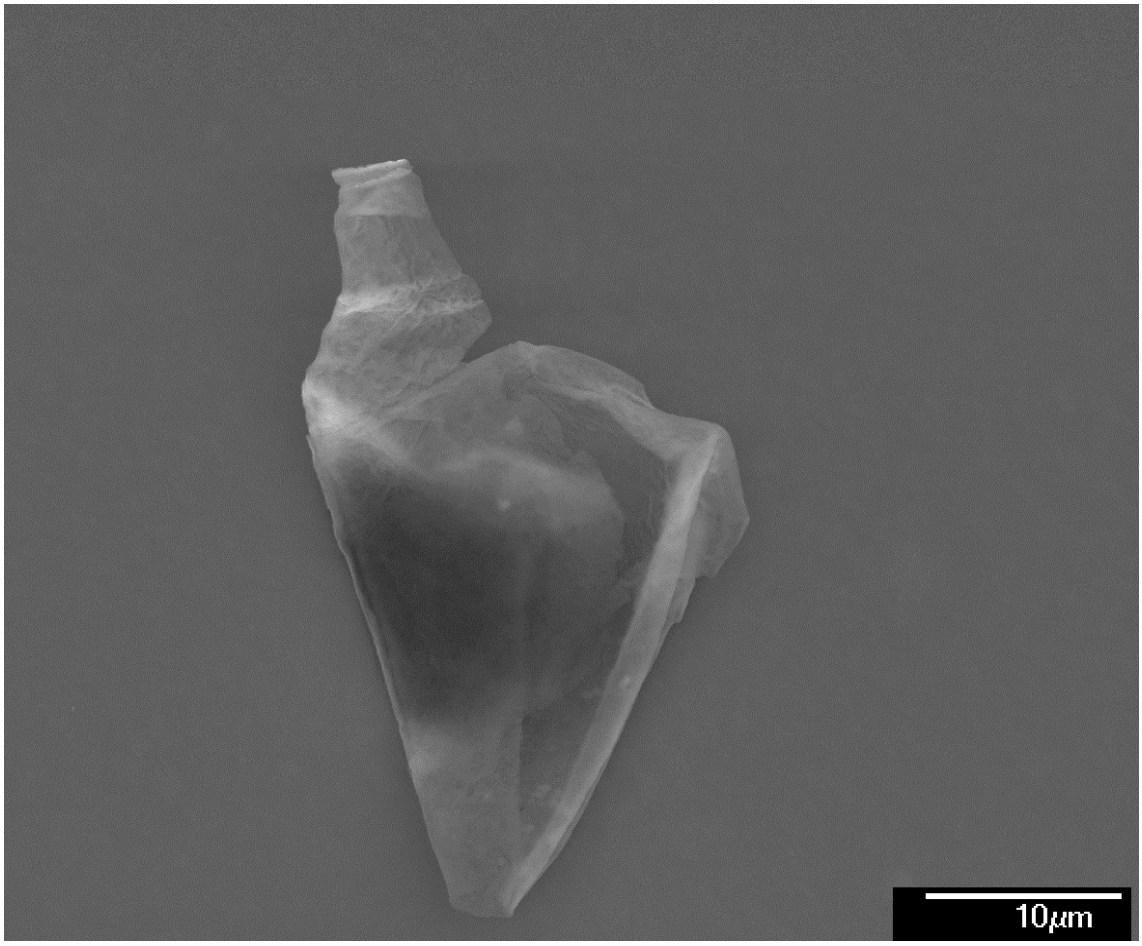

Figure 2-7: Large flask-shaped biological entity isolated from the stratosphere

Showing a collapsed appearance suggesting it to have deformed upon impact on the SEM stub or due to EM imaging (Wainwright *et al.*, 2013c).

Another large BE is shown in Figure 2-8. It has a clear structure and shows bilateral symmetry, morphology suggests it being organic. Its large size makes it unlikely to be a prokaryote, but instead is closer in appearance to an algae or a protozoan (Wainwright *et al.*, 2013c).

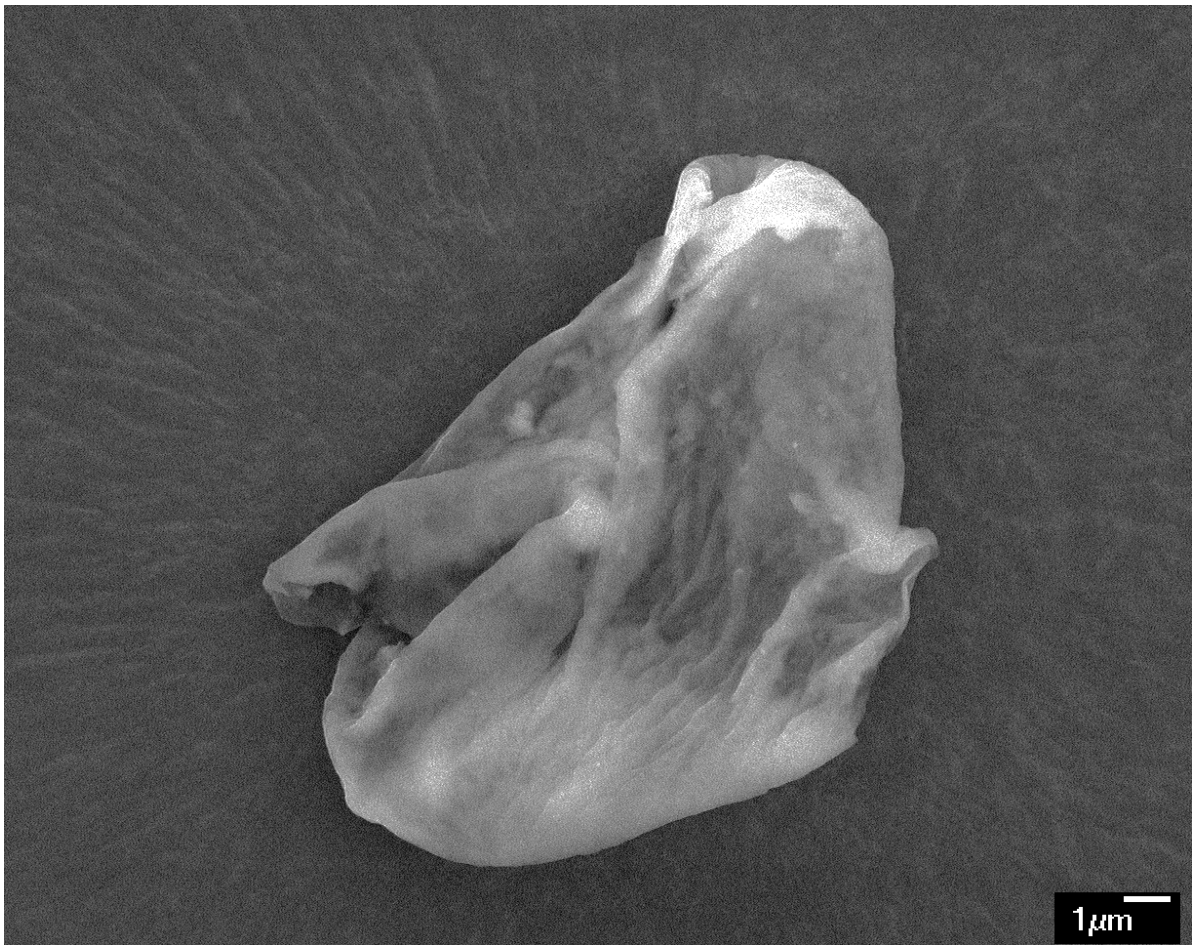

Figure 2-8: Relatively large BE recovered on one of the stratospheric SEM stubs

(Wainwright *et al.*, 2013c).

A group of BEs are shown in Figure 2-9, comprising four distinct structures, which are clearly not amorphous cosmic dust particles.

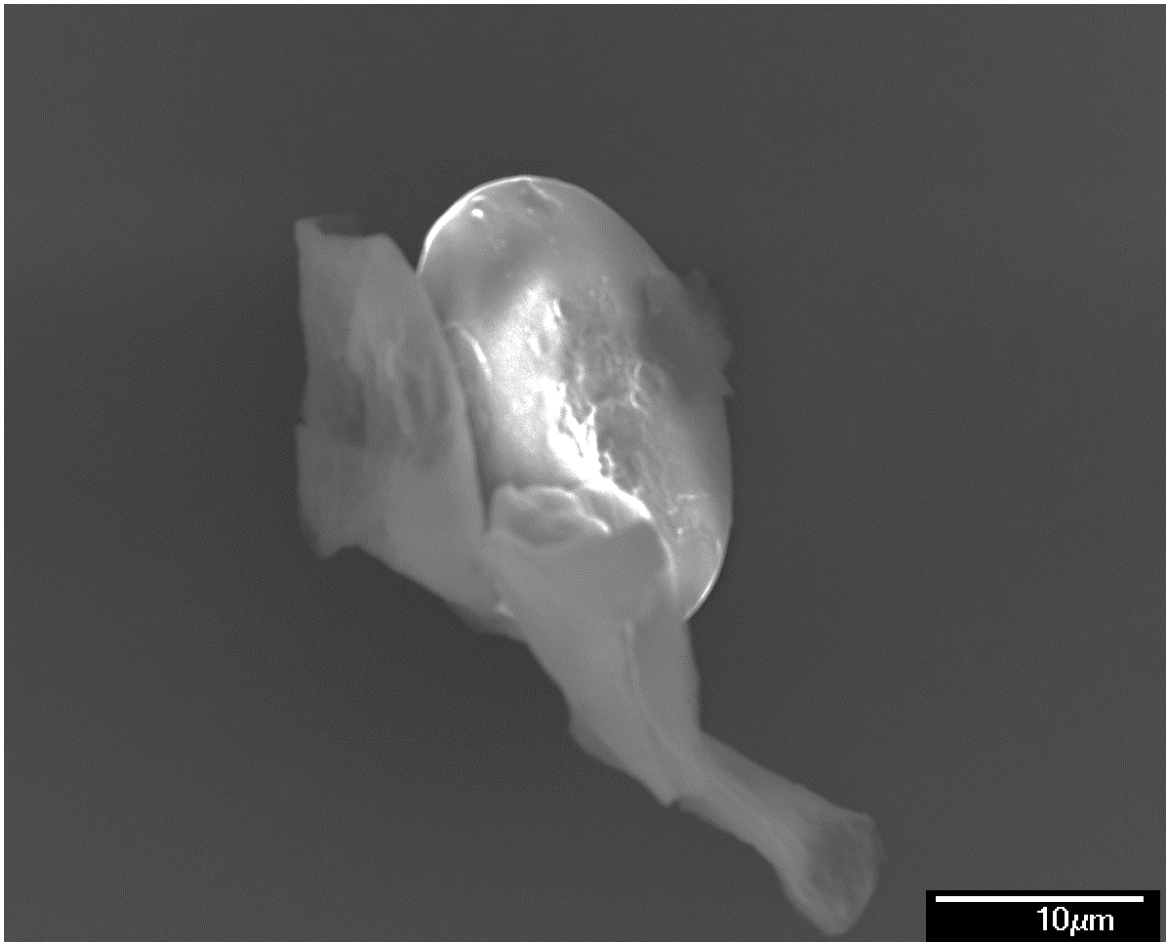

Figure 2-9: BEs on a SEM stub from the first stratospheric sampling mission

(whether these structures are part of a complete organism or are individuals is not clear) (Wainwright *et al.*, 2013c).

Unfortunately, EDAX was not available during the examination of the above shown BEs, so it was impossible to conduct elemental analysis, as was done with subsequent samples. However, these entities do appear distinguishably different from non-biological particles captured during the same flight, as shown later in Figure 2-15.

2.4 Materials and methods

2.4.1 Launch of stratospheric balloons with samplers

Six successful stratospheric sampling launches using helium-filled balloons were conducted during the period between 2013 and 2015. The same procedures and techniques were used for the uplifting and retrieval of the sampler, unless stated otherwise. The first balloon was launched in July 2013 from Chester, Cheshire and landed near Wakefield, West Yorkshire. The second sampling balloon, launched in August 2014, was released from Ashbourne, Derbyshire and landed at Sturston, Derbyshire. The sampling drawer opened between 22- 27km for 17 minutes during the first and second flight. On January 2015, the third balloon launched from Ashbourne, Derbyshire and landed at Sturston, Derbyshire, the sampling drawer opening time was between 23-25km. The fourth launch was carried out in Iceland, and was therefore the first to be made outside of the UK, it was conducted on the 24th of March 2015, from an area to the east of Reykjavik (coordinates 64.312117, -20.145208), and it landed at 63.932935, -22.109618; the flight duration lasted 145 minutes with a maximum altitude of 31 km (the sampling drawer opened from 22 km to 25 km). The fifth launch was performed from Sheffield – UK, on the 9th of August 2015, and retrieved near March (East of Peterborough), it reached an altitude of 32.8 km and the sample acquisition window was between 22 km to 25 km. The sixth launch was performed on December 2015 in the United States, launched from the Death Valley National Park (36.610791, -117.086220), and landed 30 km to the east of Goldfield town in Nevada. The maximum altitude was 34km, with a sample acquisition window between 24-28 km.

A video camera was attached to the sampler box on all of the launches to monitor the opening and closing of the sampling drawer in addition to recording the view of the Earth from the stratosphere. The sampler also contained a black box, which recorded various data such as GPS position

and altitude, internal and external temperature, humidity, air pressure, acceleration (multi directional), magnetometry, all of which were analysed and interpreted following the sampler's retrieval. A locator (SIM based positioning system) was also included, which enabled the box to be located soon after its return to Earth.

After release, as the balloon keeps ascending, it exits the troposphere layer and the tropopause boundary, entering into the stratosphere, where the low pressure caused the thinning and expanding of the balloon's elastic material, eventually leading to it to burst, this caused the box to descend at speed, and trigger the deployment of a parachute causing the box to slow down to the re-entry speed, and return safely to Earth. Later, the box was retrieved using the installed locator, and a preliminary eye-examination is performed on the box to make sure it was not damaged or breached due to a strong impact. If the box was intact, it was sent to the lab for analysis to take place. Samples were zip-lock sealed and the sample chamber remained unopened until it was delivered to a clean room.

The sampling box, made primarily from Styrofoam, had a build-in drawer mechanism (a modified standard CD tray) that could be automatically opened and closed at the desired altitude by pre-programing the data before the launch. This drawer, shown in Figure 2-10, carried sterile SEM stubs which collected the incoming particulate material substances which fell onto it. The sampling apparatus was shielded from the possible downfall of particulate matter from the balloon itself by means of a cover. Before the launch, the sampling drawer was scrupulously cleaned, air-blasted, and swabbed with 70% alcohol to ensure no remaining contaminants were present.

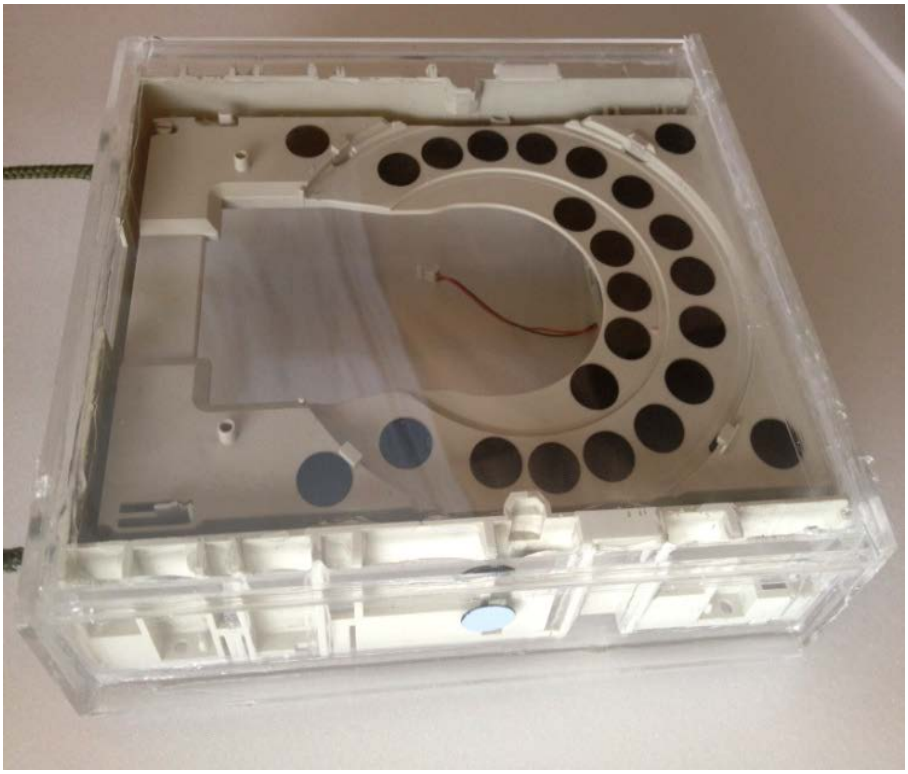

Figure 2-10: The samples drawer, which was automatically opened and closed in the stratosphere:

Showing scanning electron microscope stubs onto which stratospheric particles were directly deposited.

Scanning electron stubs (adhesive carbon tabs, sometimes referred to as Leit tabs - Agar Scientific) were placed in rows inside the drawer, as shown in Figure 2-10, with the top surface, initially covered by a protective grey tape layer, facing upwards. As a result, when the drawer was opened during flight, the stubs captured any infalling matter. The protective grey layer on the stubs was removed moments before launch under sterile conditions using sterilised tweezers to minimise contamination. The only launch in which SEM stubs were not used was the fourth one launched from Iceland. In this case, copper stubs were used instead of the carbon stubs, prepared by first setting pure copper blanks in Konduktomet Phenolic compound (20-3375-016) and wet ground using a ‘Bueler Automet 250’ for 2 minutes with a

pile coarseness of 120 microns, using a touch force of 20N, a head speed of 50 RPM and a platen speed of 240 RPM. Later, the copper samples were polished using a 0.5 micron diamond polishing slurry for 4 minutes; using a 20N touch force, head speed of 50 RPM and a platen speed of 140 RPM. The polishing process was repeated using a 0.25 micron diamond solution. To further remove the remaining diamond particles, samples were ultrasonicated in distilled water for 3x1 minute. Samples were then gold coated using an Emscope SC-500 gold sputter coater with deposition duration of 2 minutes at 15 milli-amps. Figure 2-11 show one of the polished copper samples prior to their use for stratospheric balloon launches.

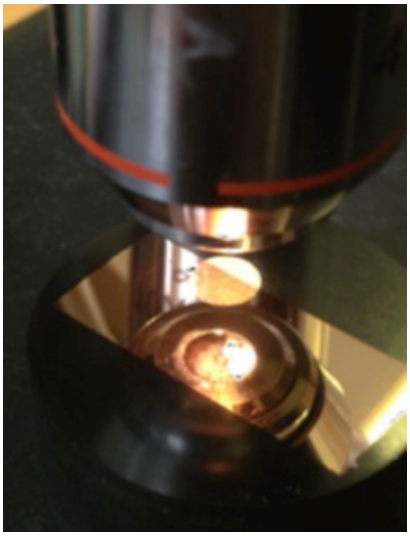

Figure 2-11: A polished copper slide being examined under the microscope

Similar ones were polished, cleaned, and sterilized in preparation for the Reykjavik sampling mission.

In the fifth launch, although carbon Leit tabs were used as with most of the other launches, however, they were fixed by their base using a neodymium magnet, these were cylindrical in shape, 8mm in diameter and 4mm in length. Each had one carbon stub fixed on its upper surface. The magnets were pre-cleaned, and autoclaved in the same way of all the other equipment in other launches. Despite this, as an extra-precautionary step,

no metal instruments were brought into contact with, or close proximity to the magnets at any point during processing.

Another major change, introduced for the first time in the fifth launch was the use of direct DNA amplification of any possible biological substances on the stubs. More details are given in section 2.4.2.

The exposed carbon stubs were fixed to sterile aluminium stubs (32x10mm) for SEM analysis. Then, the samples were sputter-coated with gold for 30 seconds at 30 mA in order to prepare them for the subsequent SEM and EDAX examination (JEOL 6500F).

2.4.2 Identification and sequencing of DNA from single cells on the stubs

As mentioned above, the fifth launch included the introduction of a new technique for the detection and sequencing of DNA, the workflow of this project followed the typical chronological steps of any standard genome assembly project, whatever its size (Earl *et al.*, 2011) (Figure 2-12).

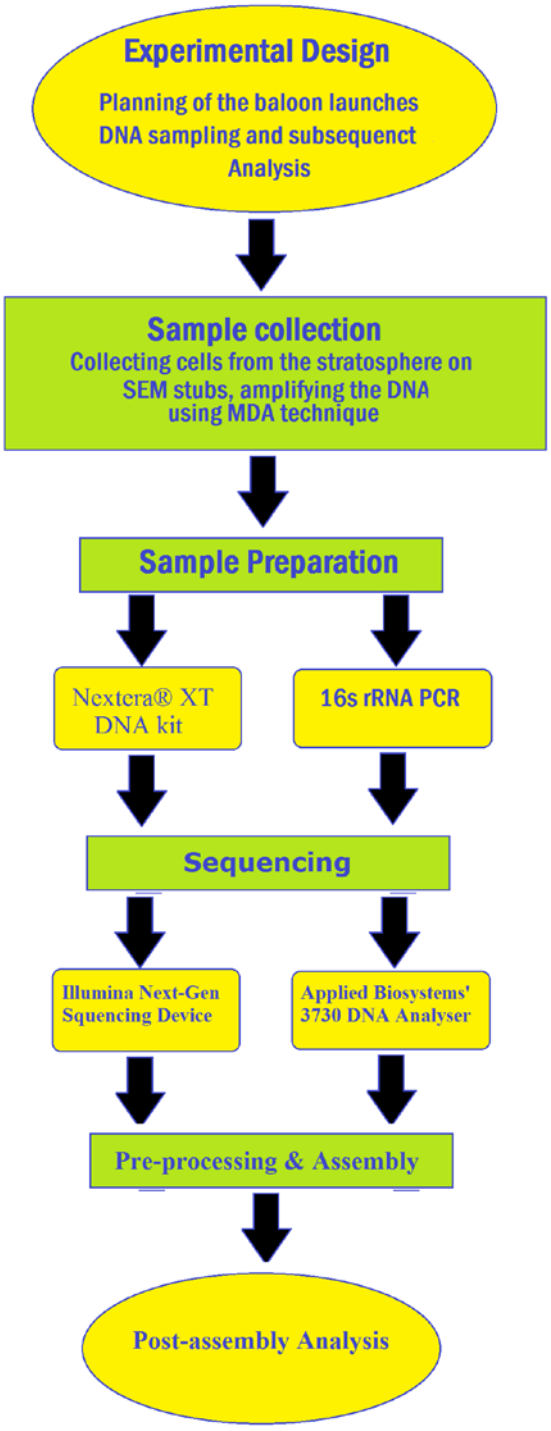

Figure 2-12: The workflow of the genome analysis

Conducted for the fifth stratospheric launch, in which the samples were prepared and sequencing using two methods.

This process involved the amplification and detection of DNA from minute samples (the cells on the stubs) using REPLI-g® Single Cell Kit. The products from the kit were ran on agarose gels to confirm the presence of DNA; any samples showing positive presence of bands were selected for 16S rRNA PCR identification, if no positive results were revealed, the samples were sent to be directly sequenced after preparation using an Illumina next generation sequencer, located at the Sheffield Institute for Translational Neuroscience (SITraN), followed by *De Novo* Assembly and BLAST. More details are outlined below.

2.4.2.1 Sample's DNA amplification

Although earlier launches employed SEM and EDAX when analysing samples, the latest launch also utilized an additional technique. Firstly, the stubs were covered with 200 µl of 10% (v/v) sterile Poly (vinyl alcohol) (PVA), and left to dry for 24 hours. The stubs were then covered individually with PVA, one sterile stub was also covered with PVA to act as a negative control. Sterile tweezers and a scalpel were next used to peel the forming PVA layer, and transfer it to a 1.5 snap-cap tube containing 0.5 ml DW. The sample was then briefly vortexed and centrifuged at 10000 rpm for 5 minutes, before discarding the supernatant by pipetting, leaving a small amount of liquid (no more than 2 µl) in the tube; twenty-four tubes were used at this step with one of them being the control containing the sterile stub.

Then, REPLI-g® Single Cell Kit was used. This uses the Phi 29 polymerase enzyme for whole genome amplification (WGA) of single or limited number of cells, using Multiple Displacement Amplification (MDA) (Dean *et al.*, 2002). This kit provides a highly uniform DNA amplification for the whole genome. Using the MDA technology, which initiates the isothermal genome amplification utilizing Phi 29 polymerase, a unique enzyme that replicates up to 100 kb without being separated away from the genomic DNA template. High yields of DNA product can be recovered from a broad range of mammalian and bacterial cells using the MDA technology in the presence of exonuclease- resistant primers (Hosono *et al.*, 2003). The procedure for

amplifying DNA from single cells or limited samples is explained in detail in the REPLI-g® Single Cell Handbook. Essentially, first stage cell lysis and DNA denaturation is achieved by first adding the denaturation solution mix. A neutralization buffer is then added to stop the denaturation process. Then, a buffer and DNA polymerase-containing master mix is added, which initiates an isothermal amplification reaction for 8 hours at 30^0C inside a thermocycler. Finally, the reaction is stopped by raising the temperature to 65^0C for three minutes, which ended up with the amplified DNA, ready for other downstream applications.

In order to confirm the presence of DNA within the samples, 5 µl from each sample was used for electrophoresis on 1% agarose gel in a 1× Tris-acetate-EDTA buffer (200 V, 1h); ethidium bromide staining was used. Samples which failed to show positive DNA bands when viewed later under UV transilluminator were neglected. The appearance of bands was interpreted as a possible positive result for DNA, and therefore the samples containing it were stored at -20^0C until further analysis.

2.4.2.2 DNA identification

After the samples containing DNA were confirmed using agarose electrophoresis following the WGA procedure, 16S rRNA was first attempted on all DNA-positive tubes; if this failed to work (i.e. the sample does not contain a pure isolate), then the samples were analyzed using an Illumina next generation sequencer to reveal the mixed culture within the tube.

2.4.2.2.A 1*6S rRNA PCR amplification*

The DNA extracts for each isolate were later used in a PCR thermocycler as templates to amplify the 16S rRNA gene for 35 cycles, the universal primers F27 (5′-AGAGTTTGATCMTGGCTCAG-3′) and R1492 (5′-TACGGYTACCTTGTTACGACTT-3′) were used. Both target universally conserved regions to enable the amplification of about 1500bp (Heuer *et al.*, 1997). The themocycler T3-0150 Sensoquest Thermal Labcycler (SensoQuest GmbH Company, Göttingen, Germany) was used for the PCR amplification. Each tube contained the following reaction mixture: 6 µl of D.W, 1 µl from each of F27 and R1492 primers(20 pmol/ µl), 2 µl template

DNA, and 10 µl of AmpliTaq Gold® Fast PCR Master Mix - UP (2×) (Applied Biosystems, California, USA) (total reaction mixture volume: 20µl). Initial denaturation and activation of enzyme step was performed at 95°C for three minutes, this was followed by 35 cycles of a denaturation step 94°C for one minute, annealing at 60°C for one minute, and an extension step at 72°C for 1 minute. Finally one extension step at 72°C for five minutes. After that, the PCR products (16S rRNA gene) presence and yield was determined by running the samples on 1% agarose gel at 200 V for one hour in 1× Tris-acetate-EDTA buffer, made visible by ethidium bromide staining and subsequent UV transillumination. Later, the PCR products were sent for sequencing to the Core Genomic Facility, University of Sheffield-UK, using the Applied Biosystems' 3730 DNA Analyser.

2.4.2.2.A.i Sequence analysis

After receiving the sequencing data, nucleotide sequences were analysed using the Finch TV software, Version 1.4.0 (Geospiza Inc, USA). Those sequences were then used to identify their species origin, using the Basic Local Alignment Search Tool (BLAST) by making matches with the closest reported sequence uploaded to the National Centre for Biotechnology Information (NCBI) Genbank database.

DNA sequencing in mixed species samples: Since many of the tubes that were amplified using the REPLI-g® Single Cell Kit did not contain pure genome of single species, the use of 16s rRNA PCR to identify the microbes present using 27R and 1492R primers proved not to be efficient at identifying the microbes present, also, the use of the mentioned primers only allows for the identification of specific range of bacterial species, and excludes many others, such as Cyanobacteria (Heuer *et al.*, 1997); it also cannot be used to identify eukaryotic cells which might be present on the stubs. This is why the samples which showed positive DNA presence which were not axenic were sent for the Illumini Next generation sequencing and subsequent analysis.

2.4.2.2.B Next-Generation Sequencing (NGS)

Seven DNA positive samples from the REPLI-g® Single Cell Kit amplification product were selected for sequencing. The selection process excluded the samples successfully identified using the 16S rRNA. The samples were sent to the Sheffield Institute for Translational Neuroscience (SITraN) where a Next-Generation Sequencing device (NGS) – Illumina was available to sequence the mixed population of DNA inside each of the tubes. A Nextera® XT DNA kit was used by the SITraN technical staff to prepare indexed paired-end libraries from the DNA for the following cluster generation and DNA sequencing; multiplexed sequencing libraries were generated by fragmentation and addition of adapter sequences into the template DNA in the samples in a tube containing the Nextera XT tagmentation reaction. The Nextera XT DNA Library Prep Kit – Illumina was used as described by the kit's handbook. After running the samples through the Next-Generation Sequencing device (NGS); results were obtained from SITraN in the form of large (around 2.6 gb) computer (fastq) files and subsequently sent for further analysis to a bioinformatician at the Kroto Research Institute.

2.4.2.2.B.i *De Novo* Sequencing

The seven fastq DNA library files were sent to the Computational Systems Biology unit, Department of Computer Science at the Kroto Research Institute, University of Sheffield, for the purpose of conducting *De novo* assembly, followed by a BLAST search; Metagenomic assembly against 35000+ microbial reference genomes downloaded from NCBI, followed by BLAST search were performed before the results were returned.

2.4.3 Control Flights

Separate control flights were also performed before each of the sampling flights. In this case, the balloons were sent up into the stratosphere but the sampling drawer was kept shut, so that the stubs were never exposed to the stratosphere; however, all other analysis techniques were followed in an identical manner to those conducted on the sampling launches. When SEM

analysis was conducted on the control stubs, no particulate matter was found, thereby showing the sealing of the drawer was airtight and that none of the stubs were exposed to any particles from Earth of any height during the balloons ascent or descent. The negative findings from the controls also prove that contamination did not occur during the processing and analysis of the samples, thereby countering contamination arguments, which might be directed towards to the work.

2.5 Results and Discussion

2.5.1 Findings from the first sampling flight

When the balloon, plus sampler, ascended above 22km, the sampler drawer (shown in Figure 2-10) was opened outwards, thus enabling the SEM stubs mounted on it to be exposed to the conditions of the surrounding stratosphere, allowing particles in the air to alight onto the mounted stubs. A single SEM stub was also mounted on the outside of the sampler (Figure 2-10) so that it was exposed, during both the launch and descent, to both the lower atmosphere and the stratosphere. Figure 2-13 shows that the surface of the exposed stub was contaminated with a diverse range of biological material, include grass shards, pollen and fungal spores. Such particles were never observed by SEM on any of the stubs exposed to the stratosphere within the sampling box on any launches. This finding as, will be discussed below is of crucial significance to the formulation of our conclusion regarding the stratosphere sampling studies.

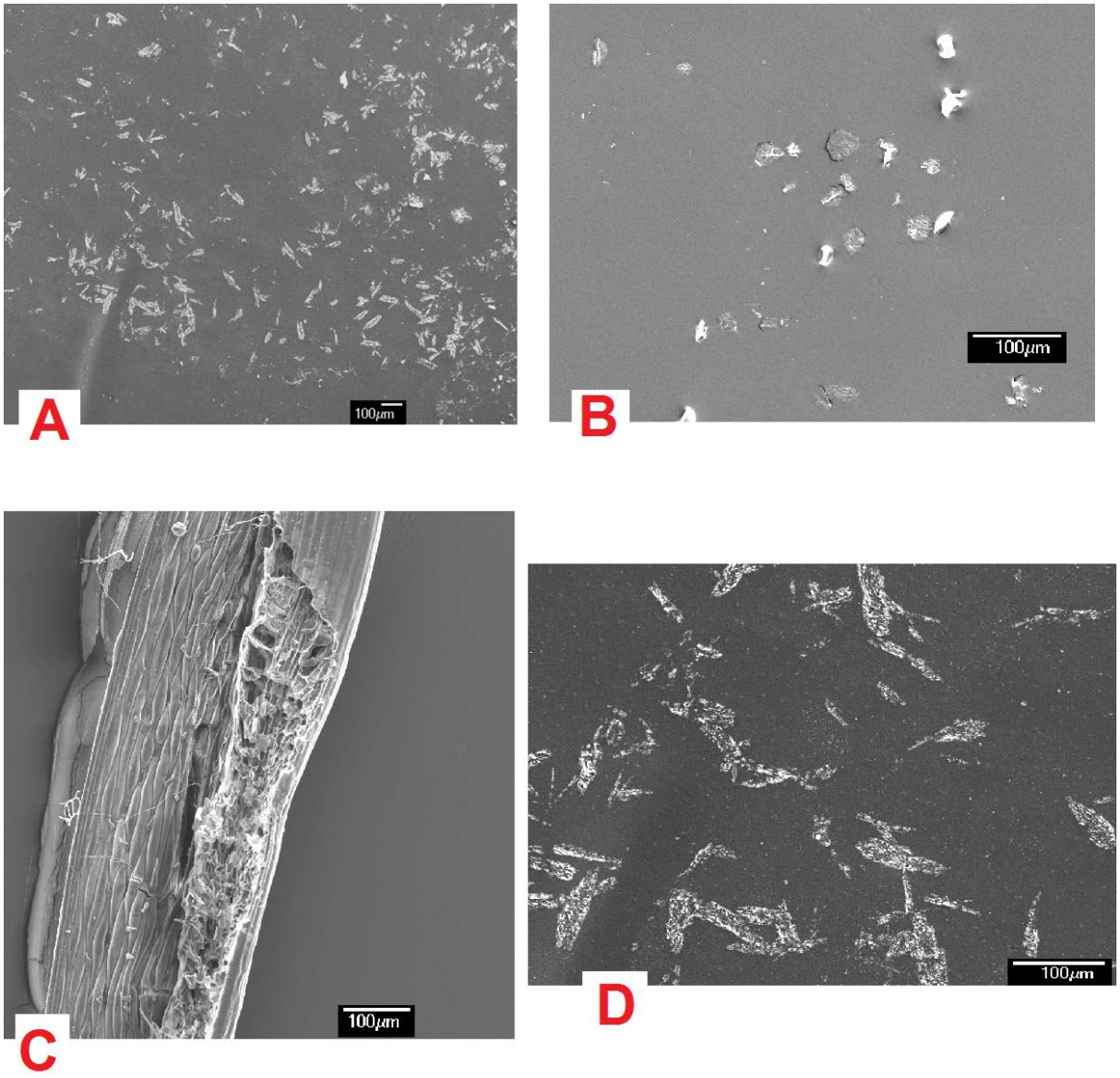

Figure 2-13: SEM images of Earth-related biological material found on outside of sampler

A. Pollen and fungal spores and B, C, and D, grass particles found only on the stubs placed on the outside of the sampler (Wainwright *et al.*, 2015a).

Figure 2-14 shows that stubs exposed on the open sampler in the stratosphere had clear impact events caused by high-speed micrometeorites, which created “bullet-hole” impacts on the surface of the

stubs. These impact events were found alongside biological entities (see below), in addition to inorganic dust particles (Figure 2-15).

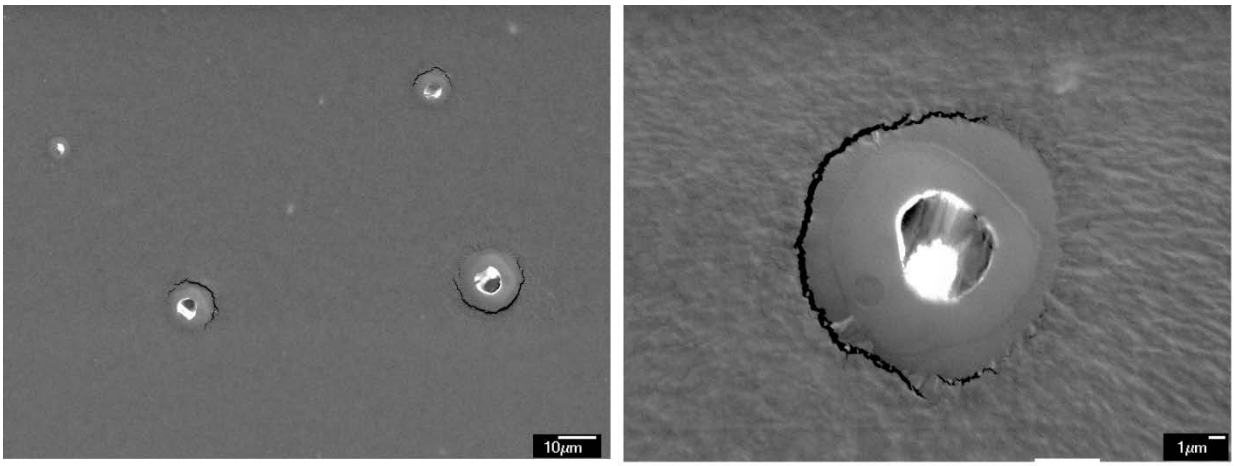

Figure 2-14: Impact craters on the sampling stubs

Impact events resulting from high-speed incoming micrometeorites are shown in A and B.

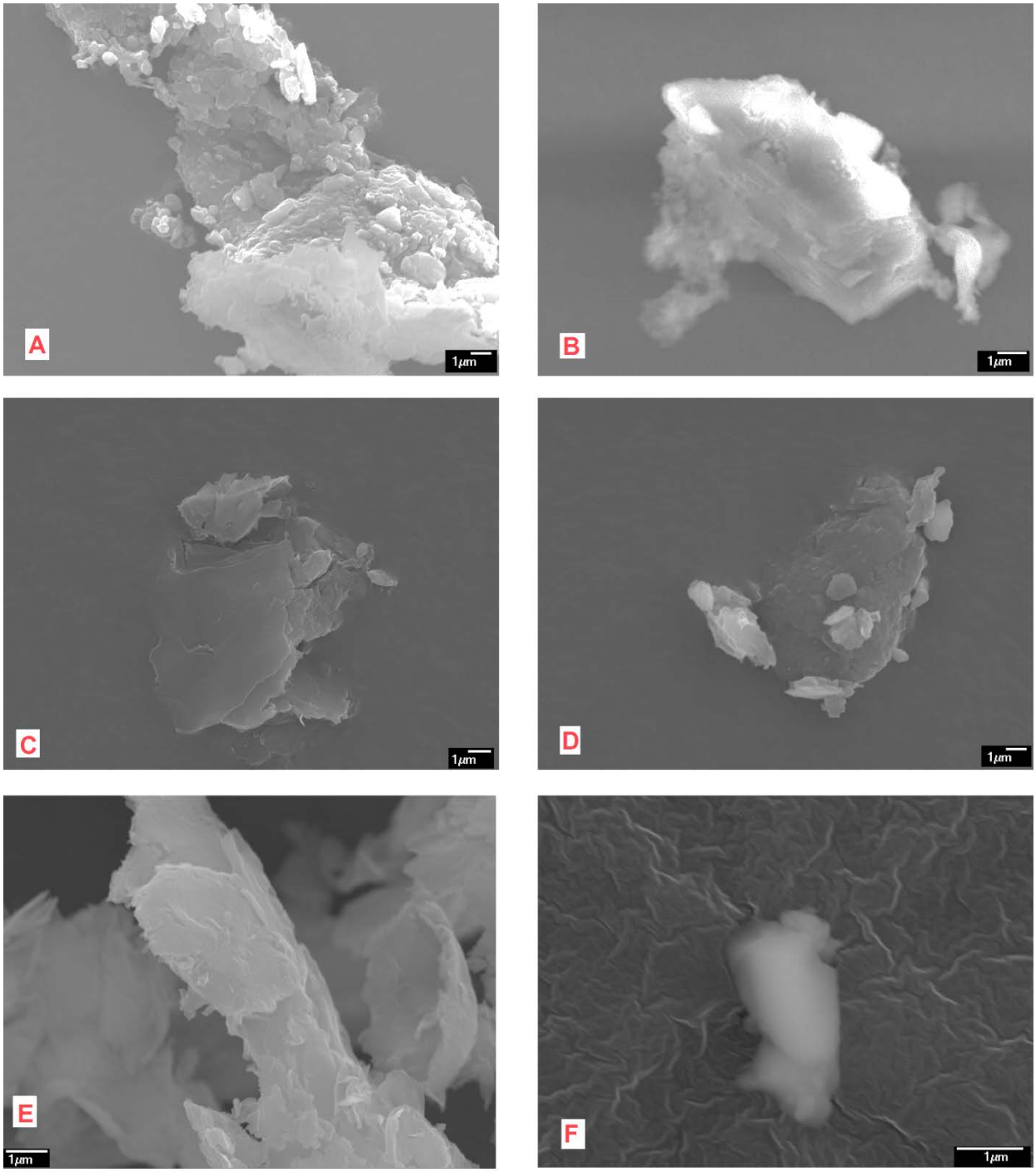

Figure 2-15: Examples of cosmic dust and other inorganic particles collected from the stratosphere

Collected during the first launch, A-F shows amorphous, irregular structures, clearly different from what are interpreted as biological entities.

Other samples from the same flight were analysed with EDAX. The complex mass shown in Figure 2-16, is clearly biological due to its filamentous-slimy appearance that resembles a mass of bacterial cells covered with a slime-based biofilm. The long threads seen in the centre of the images have been analysed using EDAX, and the results (Figure 2-17) show that the threads are composed of carbon and oxygen, and lack significant amounts of inorganic ions such as silicon iron or calcium. What is particularly noticeable in both Figure 2-16 and Figure 2-17, is that the filaments appear to be flattened, an effect typical of when observing ordinary filamentous microbes (e.g. fungal hyphae) using the scanning electron microscope.

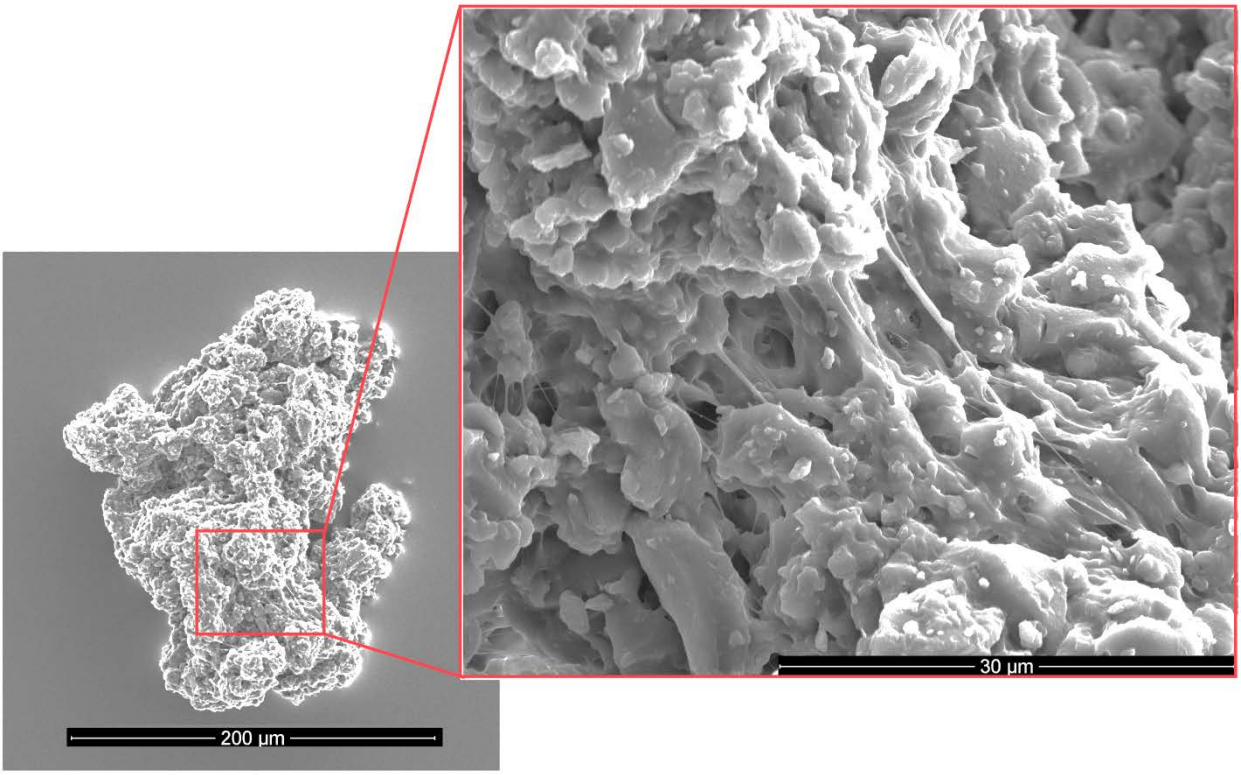

Figure 2-16: Large, mucus-based biological entity isolated between 22-27km

Showing filamentous branching structures, which appear biological.

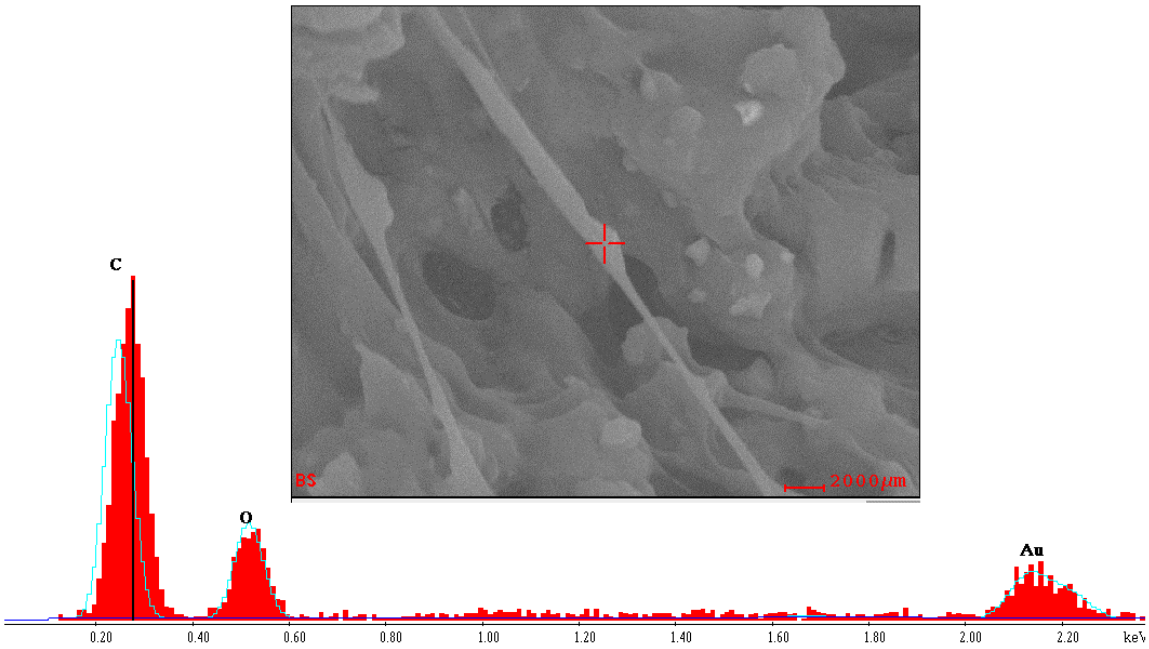

Figure 2-17: EDAX analysis for one of the filaments shown in Figure 2-16

The collapsed tube, we suggest, is due to the pressure difference in the SEM, and indicate it is not a solid rod.

Another complex entity primarily made of C and O is shown in Figure 2-18, the biofilm-complicated morphology, and the distinct "spiracle-like" pores of it is a clear indication of it not being an inorganic particle. This particle pertains a clear impact zone around it on the stub, meaning it came at speed, possibly encased in an ice particle, which later melted away.

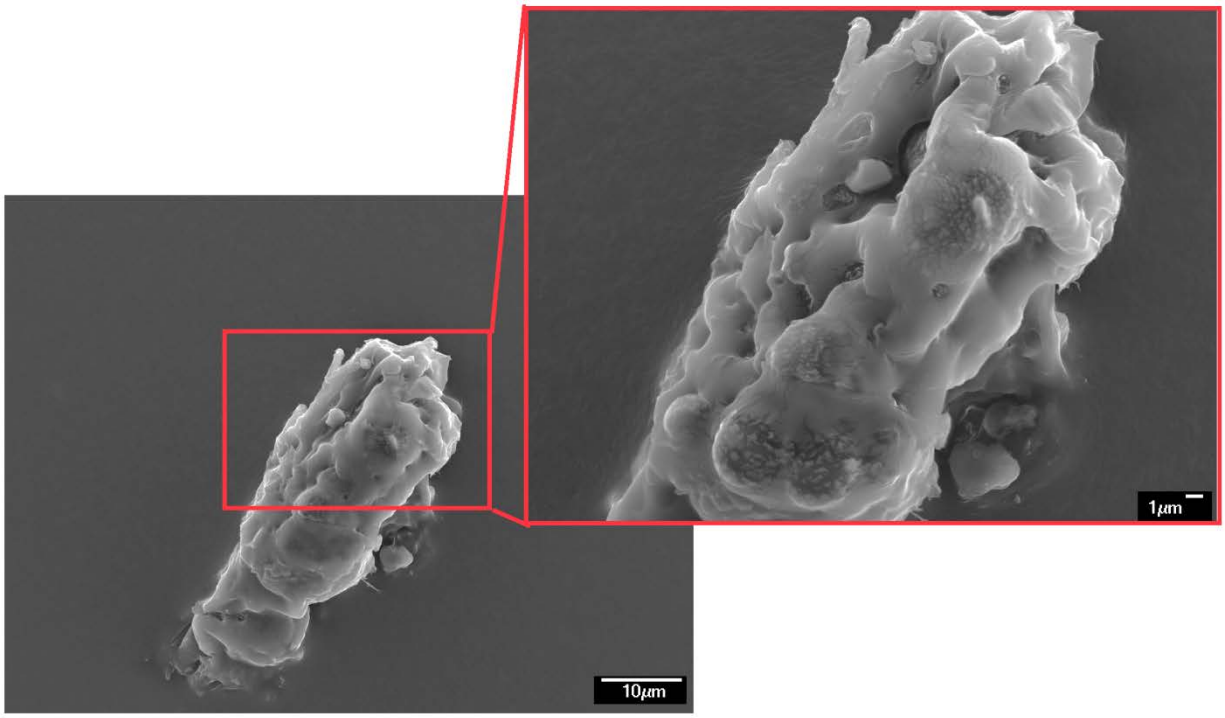

Figure 2-18: Large biofilm covered BE that impacted the SEM stub at speed

EDAX for this entity showed C and O composition, an impact crated on the stub is also visible, showing the particle to impact at speed.

The entity shown in Figure 2-19 is difficult to interpret, whether a single entity or originally belonged to a bigger one is unknown, it also might be a group of single organisms attached together to a single “back plate”. What is certain, however is that this entity is biological, for two main reasons, the abnormal morphology of it, which does not resemble any inorganic dust particles, also, EDAX has shown that the main components are C, O, and silicon (Si), which was different from other inorganic particles that were collected during the same sampling flight, for example, the one shown in Figure 2-20 is clearly inorganic since it is almost entirely made of aluminium. It is possible however; that the Si reading picked up by EDAX is due to the possibility of the “back plate” having this element within it. It should be noted too that this BE does not resemble any yet known terrestrial organisms.

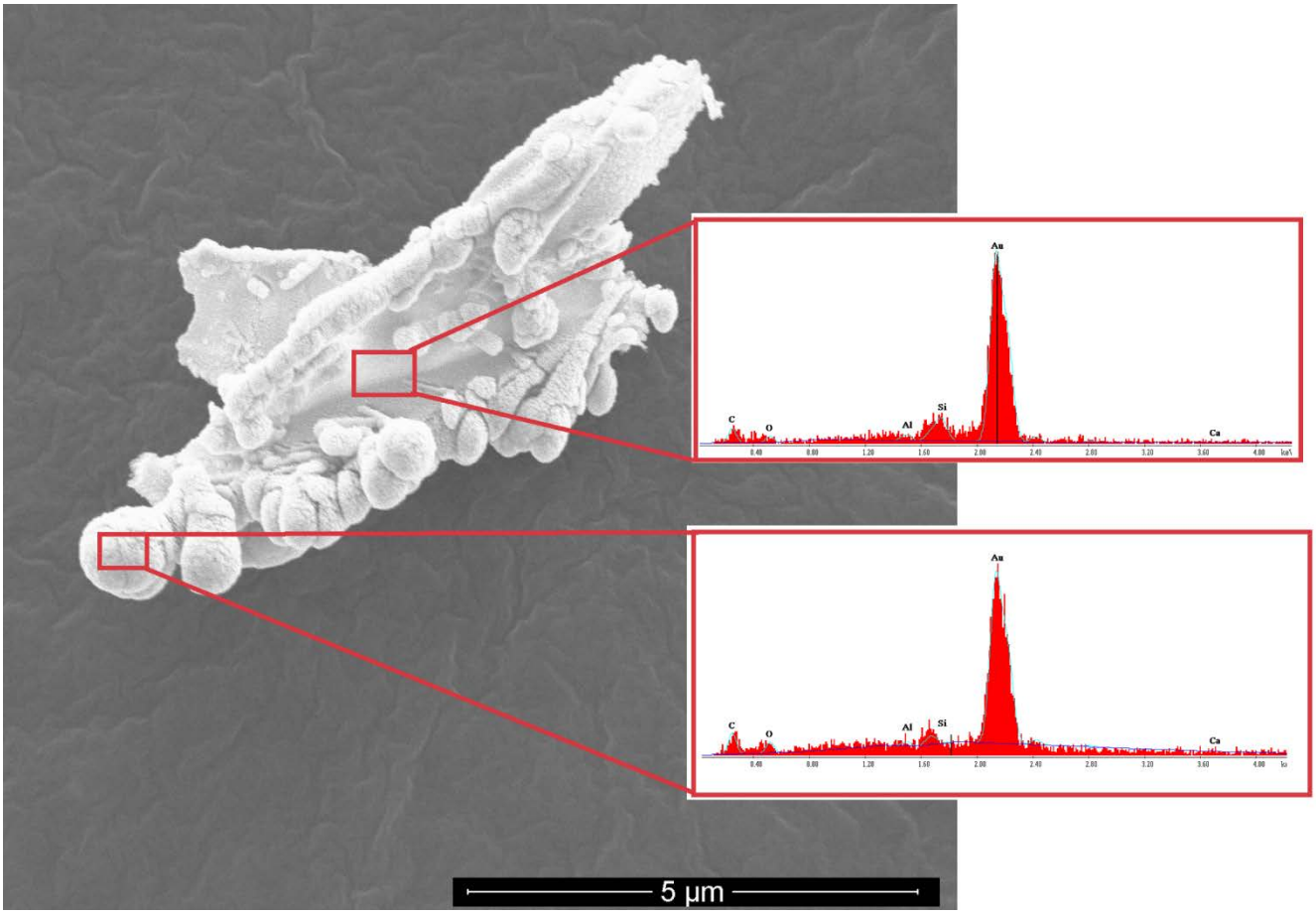

Figure 2-19: A complex biological entity that was isolated from the stratosphere

The insets on the right show EDAX readings from two locations within the BE, showing a prevalence of C and O, in addition to Si. The Au peak is due to the gold coating used when preparing the sample for SEM examination.

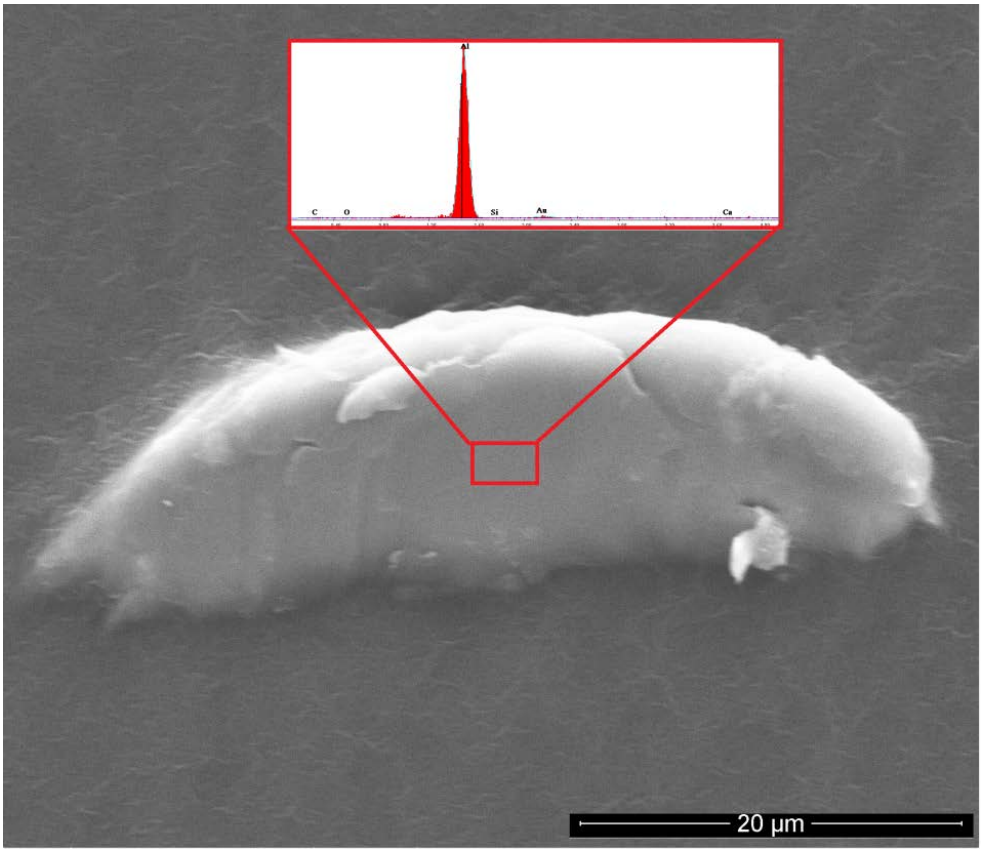

Figure 2-20: Amorphous particle recovered from the first stratosphere-sampling mission

The relatively large size and the impact crater it created on the stub indicate it to be incoming from space, EDAX results show only aluminium, thus not biological.

When analysing the remaining stubs from the first launch, SEM revealed what appears to be a Large Spherical Object (LSO), with a diameter of about 30 µm that has impacted the surface of one of the stubs. Using Nano-manipulation, this LSO was pushed away from the impact site, thus revealing a large impact crater caused by it, meaning high-speed impact. Upon impact, the LSO entity was damaged, and when dislodged from the impact site a mucus-based substance began to ooze from the LSO. Figure 2-21 (A-D) highlight images taken during the stages before, during, and after Nano-manipulation. Closer examination of the LSO revealed another smaller spherical object (SSO) attached to it (Figure 2-22), in addition to non-

biological cosmic dust particles which were attached to the LSO. There are also distinct fault lines on the LSO which might have been the result of the impact.

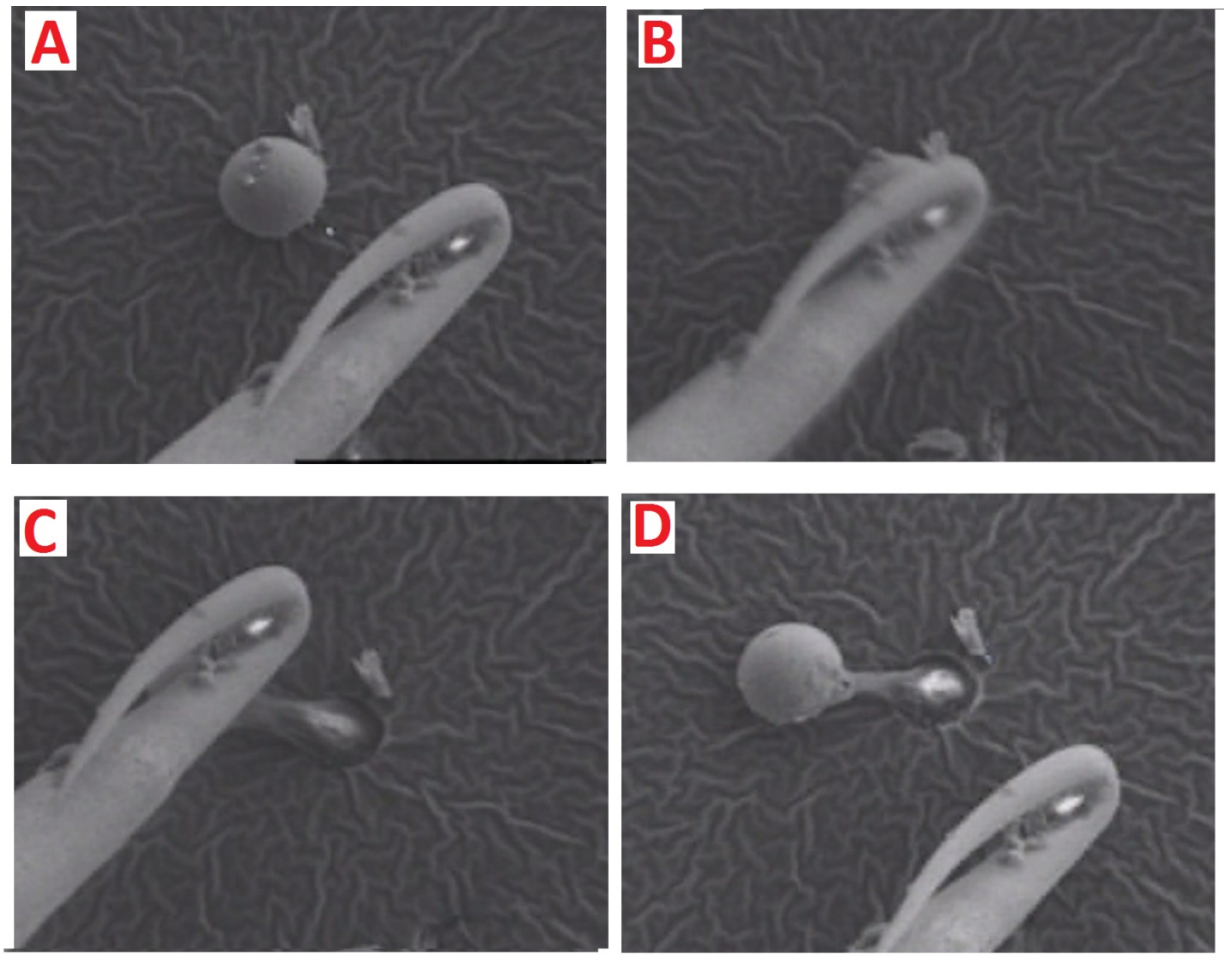

Figure 2-21: SEM images for the Large Spherical Object (LSO)

The entity was removed from its impacting site by Nano-manipulation technology using Nickel-Chromium nano-tips. A- Shows the LSO before attempting to remove it, B, and C- during the manipulation and D- after removing the needle away.

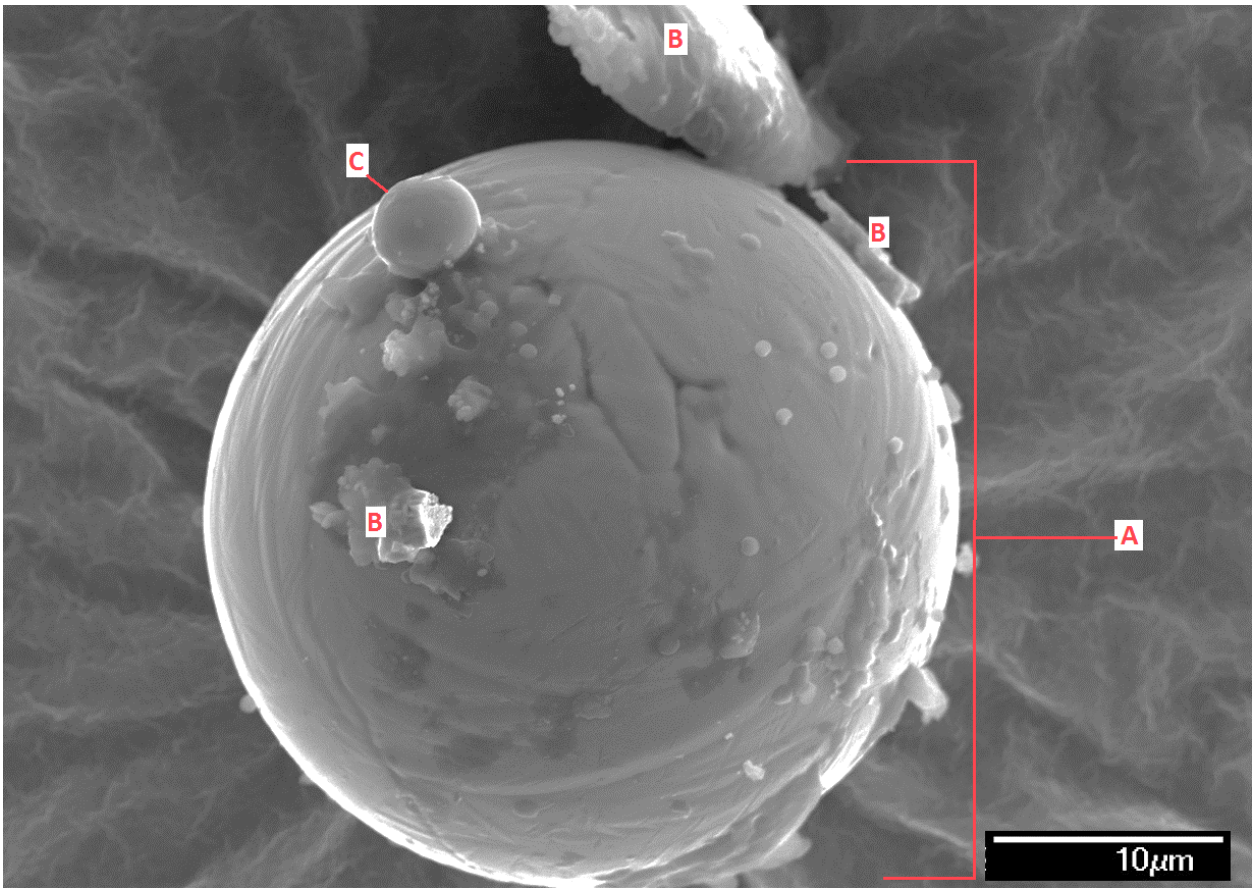

Figure 2-22: Detailed SEM image for the LSO prior to dislodging it from the impacting site

A: show the LSO, the impact on the stub around it is also visible. B: show the inorganic cosmic dust particles. C: the SSO attached to the larger sphere.

EDAX results for the outer surface of the LSO showed that it is made mostly of titanium (Ti), with a small amount of vanadium (V), and traces of carbon and nitrogen. After the ball was removed from the impact location, the issuing material coming out of it was analysed with EDAX, revealing it comprising mainly of carbon and oxygen (carbonaceous material), thus

suggesting it to be biological material encased in the titanium sphere (Figure 2-23).

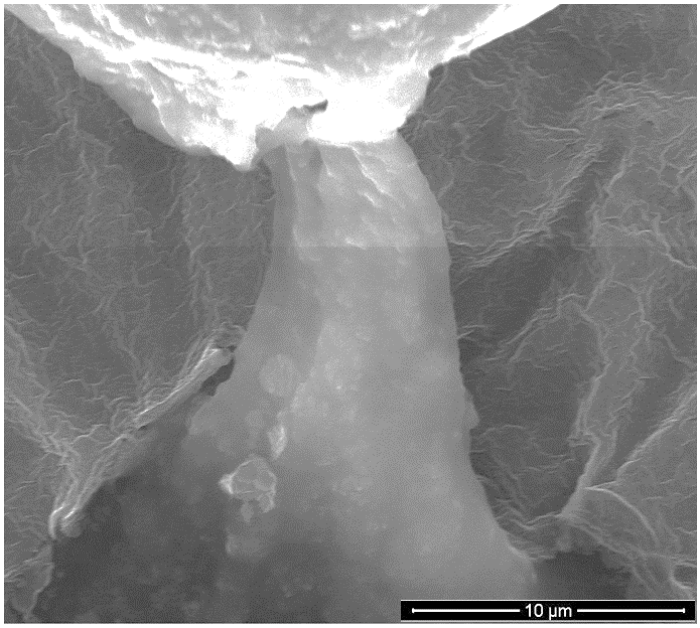

Figure 2-23: Close-up SEM image for a section of the LSO

Showing the carbonaceous material coming out of the titanium sphere.

2.5.2 Findings from the second sampling flight

Results from the second stratospheric flight, despite following the exact same procedures of the first one, did not yield in any type of biological entities. However, SEM images for the stubs did show some inorganic material that belong to the infalling cosmic dust particles, some created the same type of “bullet-holes” impact craters found in the first launch; This, in addition to the video recorded proving the opening of the sampling drawer, evidence sampling to be successful, and no malfunction happened since stratospheric material were recovered.

The absence of BEs does not affect the credibility of the first launch’s findings, for a number of reasons:

- Findings of BEs appeared again in many of the subsequent sampling missions.
- If the BEs recovered from the first launch are terrestrial on origin, why have they not been picked up in the second launch? Considering the immense terrestrial biological pool, it is logical to find BEs on every sampling trip if they were, being lifted from the troposphere.
- As the cometary panspermia theory suggests: meteorites, that might or might not be carrying biological entities, are not continually arriving to Earth, but rather intermittently, for example, the Perseid meteor shower happens between July and August every year (Mead, 2010), which might be the source of the BEs recovered from the first launch since it matches the window time of the meteorite event.

2.5.3 Findings from the third sampling flight

In the third launch, BEs appeared again, making it likely that results from the first are repeatable and not due to contamination. Several entities showed shapes and EDAX readings which highly suggest them to be biological in origin, when compared to the dust particles and micrometeorites present on the same samples.

In Figure 2-24, a BE with unusual appearance is shown along with its EDAX reading, the surface of this particle, as SEM shows, has clear wrinkle marks, thus might indicate that it was previously expanded, as evidenced by the thick ridges instead of thin edges on the BE. Meaning that the BE originally had a swollen structure that might have had contained liquid or gas inside of it, but collapsed following impact on the SEM with speed. This BE was also compared with SEM images for human skin and dandruff particles as an extra precautionary measure, since those too have been suggested by critics as contaminants and the explanation to our findings. Such human material was not comparable to the isolated BEs, showing that such contamination did not occur.

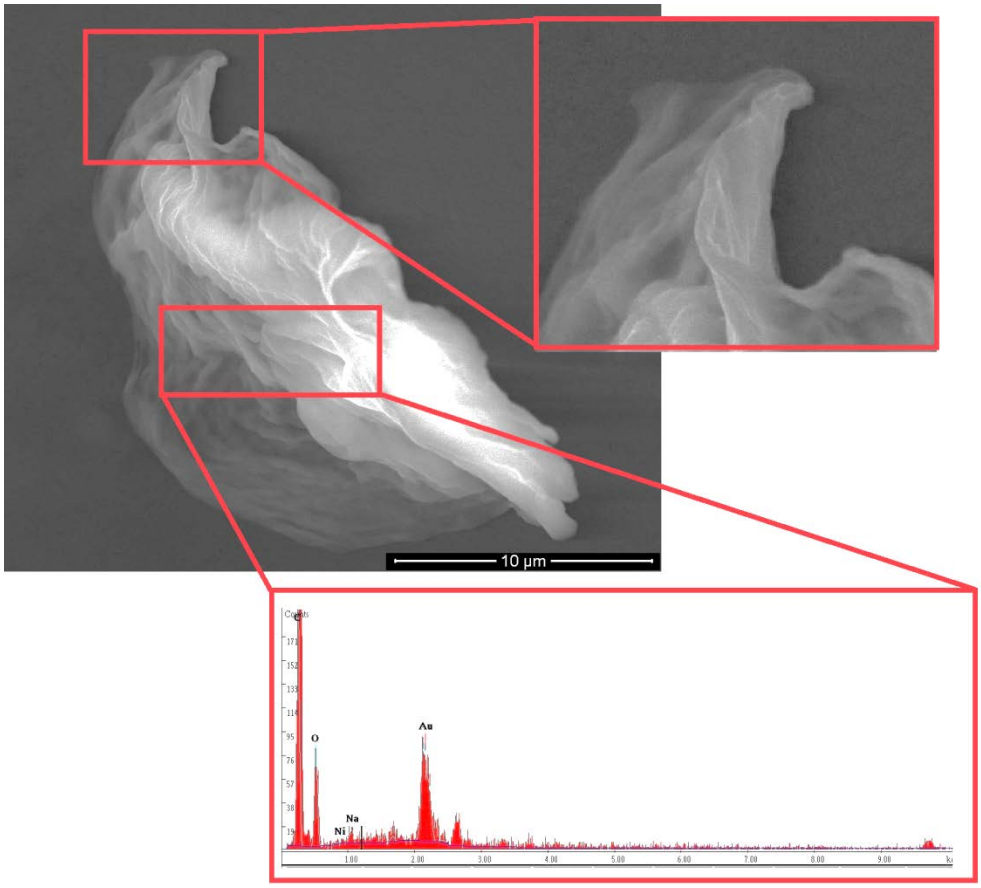

Figure 2-24: A gossamer-like particle recovered from the third stratospheric sampling trip

The thick ridge in the inset image suggests that the gossamer is not a paper-thin sheet, but a collapsed balloon-like structure. The EDAX inset at the bottom shows a prevalence of C and O.

Another entity with a collapsed appearance is shown in Figure 2-25. In our opinion, it closely resembles the BE in Figure 2-24, as it has the same collapsed appearance. The triangle shape in the foreground of the object indicate that it was also folded upon the impact on the stub. In addition, EDAX showed a prevalence of C and O, as in the previous BE.

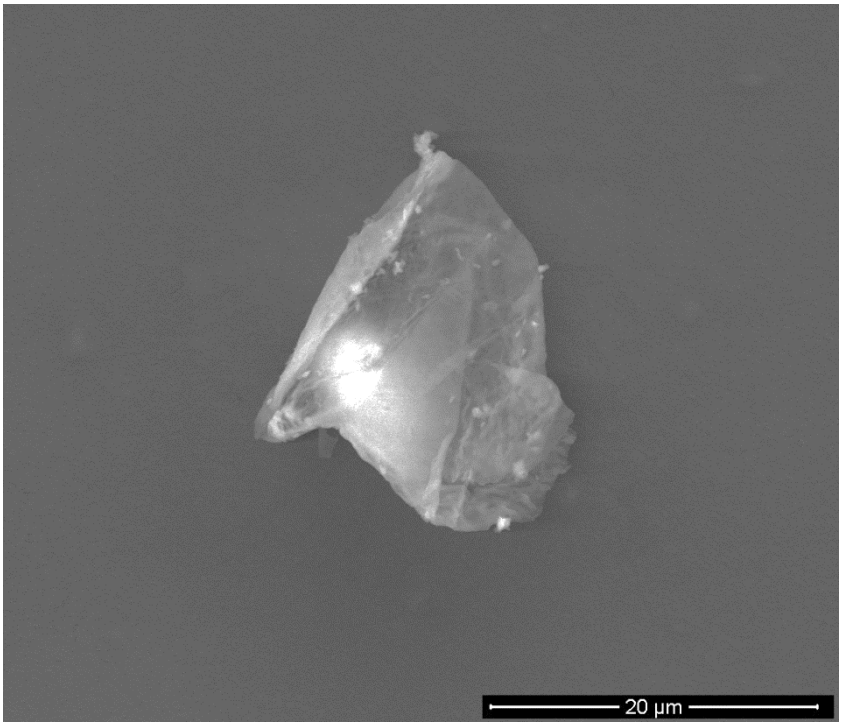

Figure 2-25: A bell-shaped BE recovered from the stratosphere

Showing on the EDAX is mainly C and O, notice the triangular corner in the foreground of the entity, which indicate a folded ridge.

The star-shaped biological entity in Figure 2-26 appears to be made of sheets of cells fused with each other, with the ones near the top smaller in diameter as it got close to the top-most edge. There also appears to be filamentous bridges connecting the cells at the top. As shown by EDAX, in addition to C and O, small amounts of sodium were present. To make sure that this entity is not a result of inorganic compounds, several concentrations of sodium bicarbonate and carbonate were prepared in the lab, and allowed to form precipitate from drying, but we were still unable to create similar morphologies when later examined under the SEM.

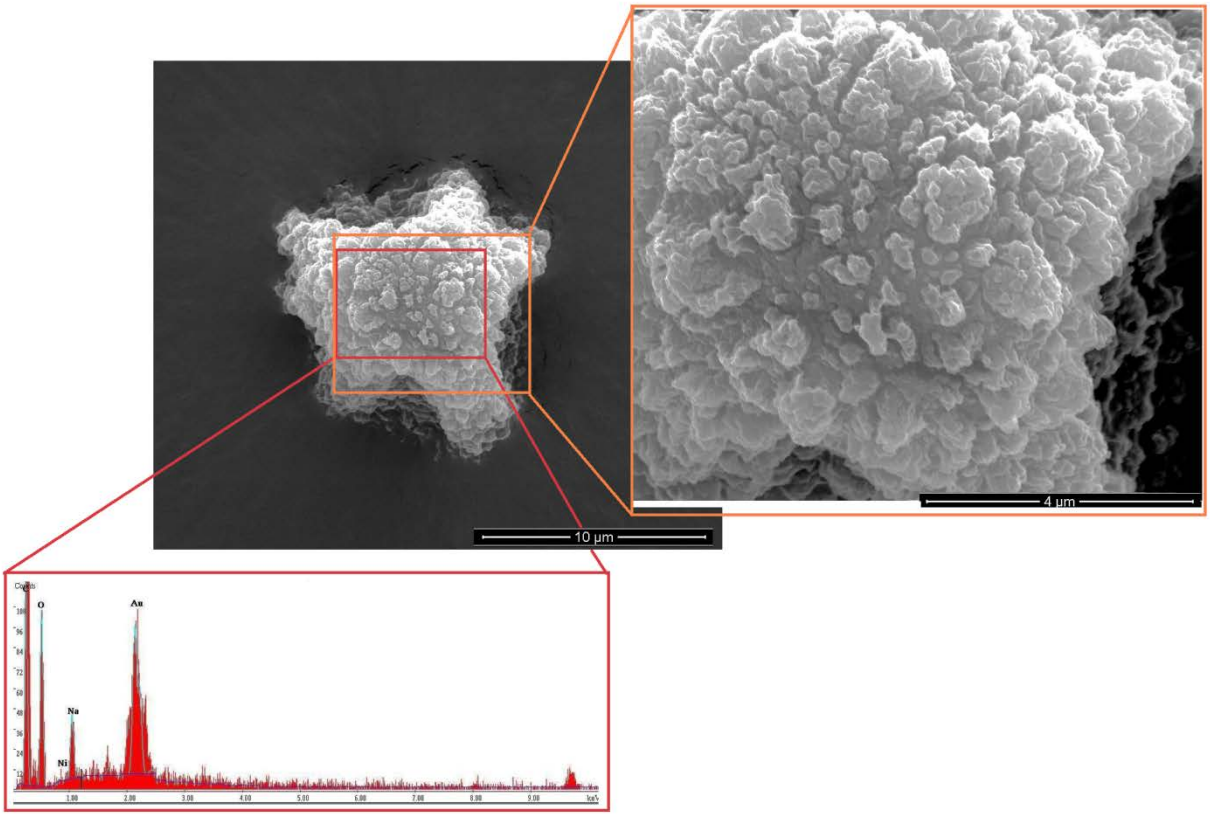

Figure 2-26: A star-shaped BE recovered from the stratosphere

The insert on the right show filament-bridges between particles on the uppermost surface, the insert at the bottom demonstrate the EDAX results, showing C and O, with a trace of Na.

The aggregation of particles shown in Figure 2-27 (A) are difficult to interpret, it could be argued to be a clump of inorganic particles; EDAX shows it contains C and O mainly, followed by other elements such as molybdenum, aluminium, magnesium, and sodium. However, when the aggregation of particles was examined in more detail (Figure 2-27 B), small entities were present which had a slimy appearance and elongated filaments, unlike the clump mentioned earlier. This one was shown by EDAX to contain C and O, with traces of Fe.

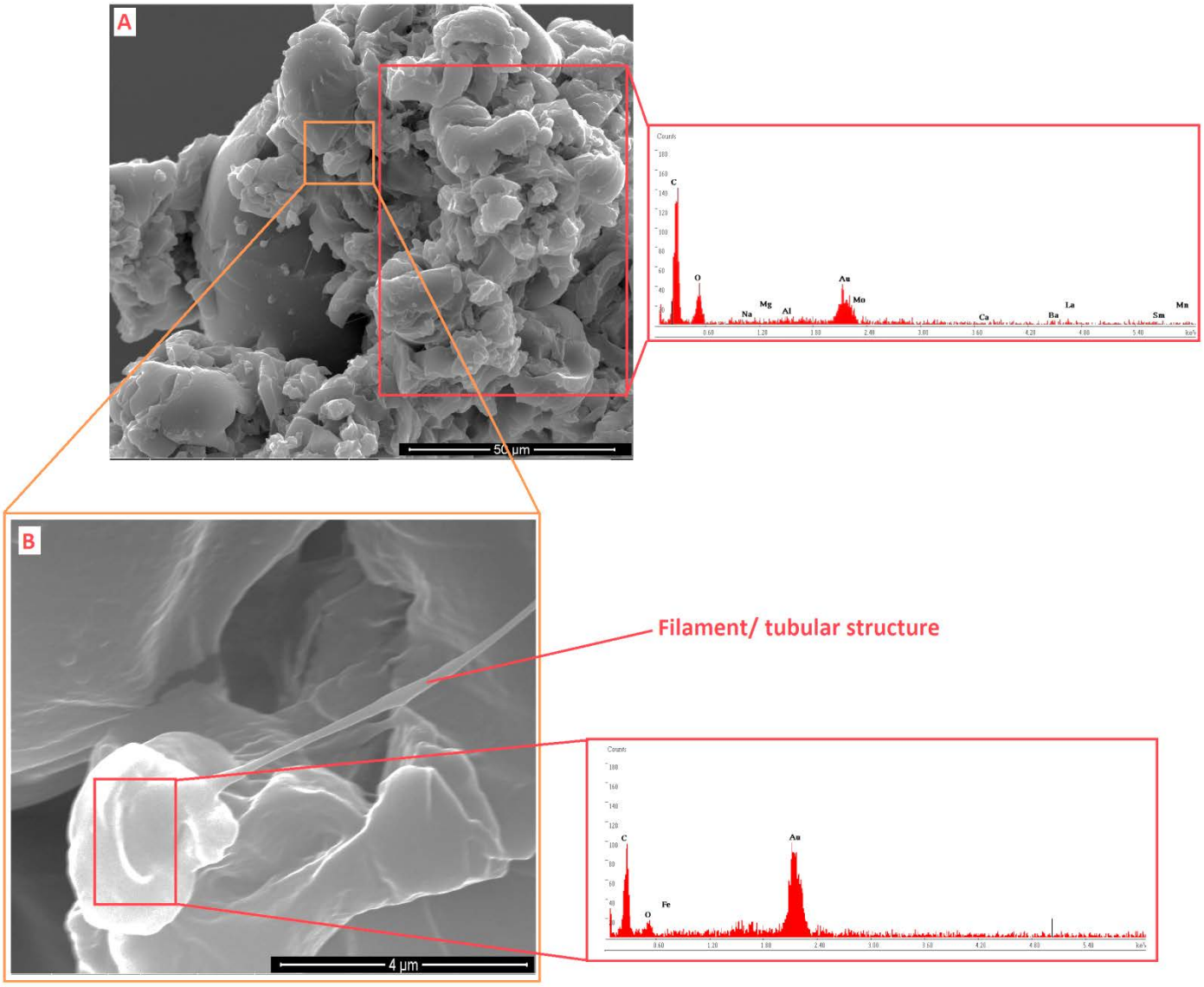

Figure 2-27: Large clump of particles captured on one of the stubs from the third mission

A- Shows the EDAX for some of the particles on the right, EDAX shows C and O, in addition to other elements. B- close-up look for a particle that has an elongated filament, EDAX shows a prevalence of C and O.

The argument that the shown above entities are biological, is further evidenced when the entities are compared to cosmic dust particles of the same size, recovered from the stratosphere; Unlike the entities shown before (Figure 2-27), the ones in Figure 2-28 are of an obvious inorganic appearance and structure, based on the EDAX for them which shows the

main element to be either silicon or aluminium, the standard ingredient in most cosmic dust particles and micrometeorites.

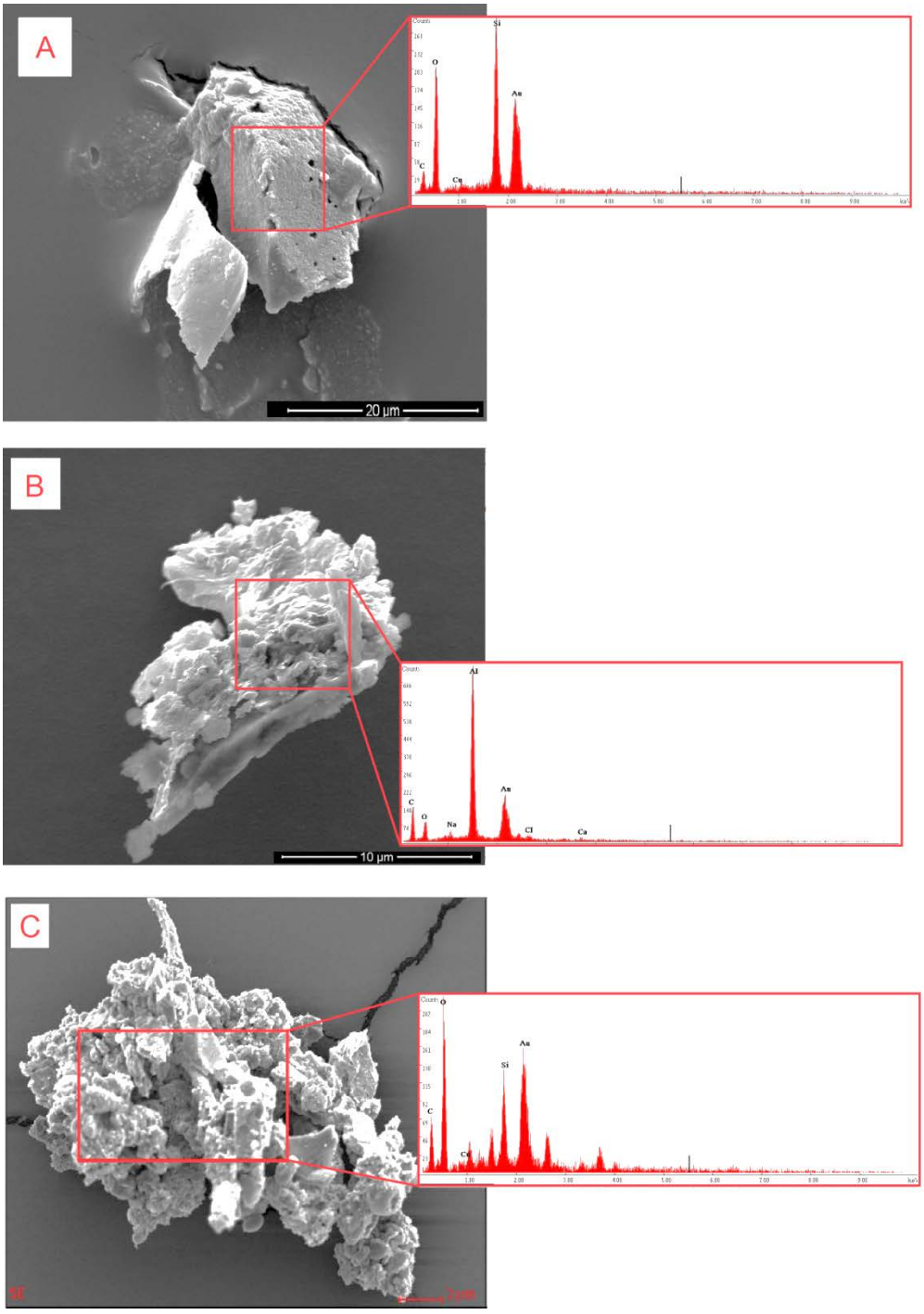

Figure 2-28: Three inorganic particles recovered from the stratosphere

Judging by their size, shape, and impact crater on the stubs, it is attributed to have been brought to earth as cosmic dust particles, considering the prevalence of silicon in A and C, and aluminium in B.

2.5.4 Findings from the Fourth Stratospheric Flight

This stratospheric launch was the first to be conducted outside of the UK. The high Altitude balloon launch was conducted in Reykjavik – Iceland. Sample acquisition was done in the same way as before by using the sampling drawer with the stubs attached inside of it facing upwards; however, polished copper stubs were used instead of carbon Lait tabs, for testing whether those stubs could provide a better clarity on the instances of particles impact on it.

There were no recovered biological entities from this launch. However, many inorganic cosmic particles were collected during the sampling flight. In Figure 2-29, three objects are shown; all appear to have impacted the copper stubs at speed, as apparent from the finely formed circular impact crater around each of the particles.

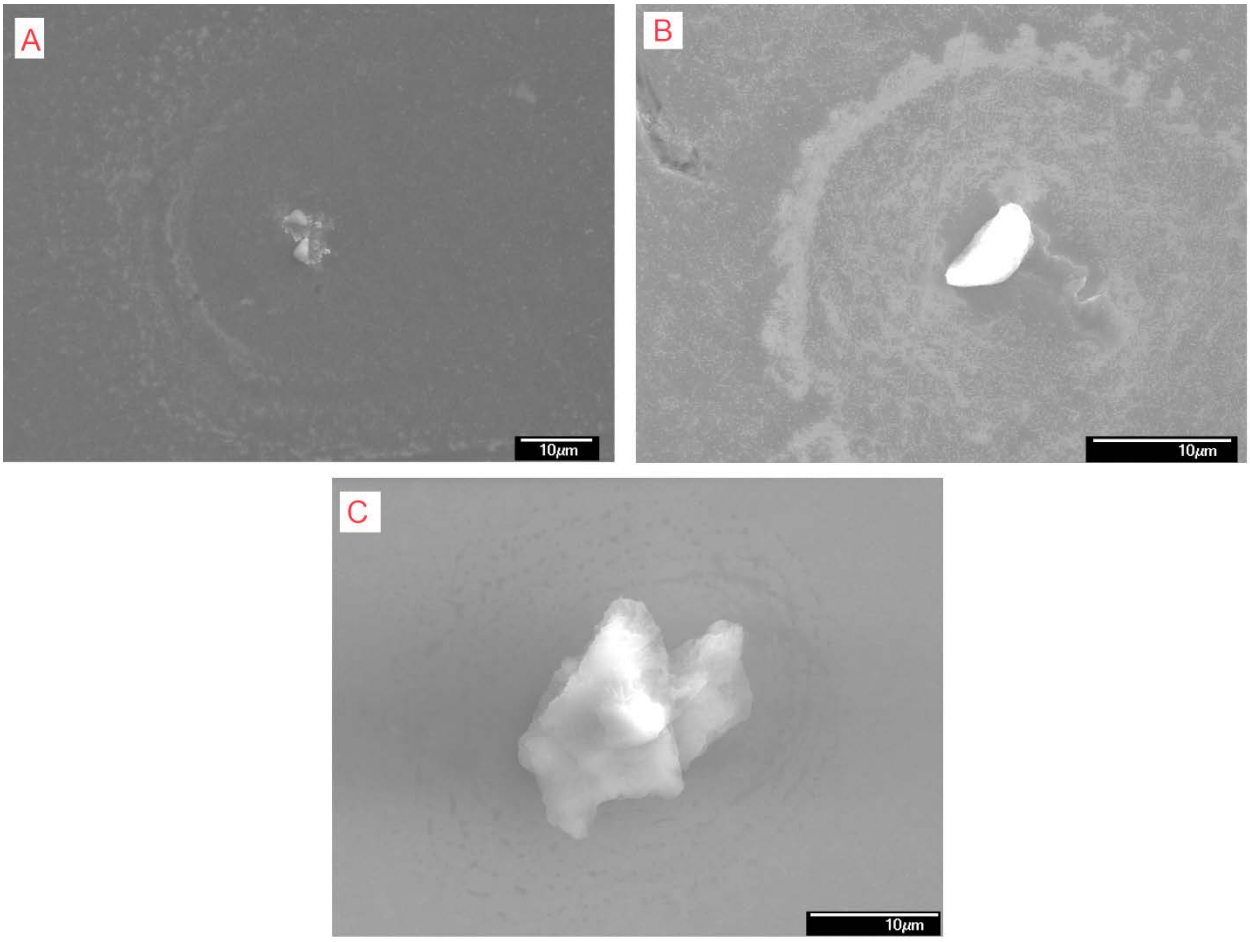

Figure 2-29: Three inorganic particles recovered from the upper stratosphere above Reykjavik – Iceland

The strong impact crated visible in all A, B and C, indicate the particles to have impacted the stubs at high speed.

As we mentioned earlier, it is believed that many of the biological entities were carried within icy comets, which breakup and burn away and melt gradually as they enter the atmosphere. Some of these comets might impact our sampling stubs, thus preserving the shape of the entities (shown in Figure 2-16 and Figure 2-18) that would have otherwise been smashed and deformed on the stubs due to the high impact speed. In the fourth launch, one of the findings on the stubs revealed a clump of around 400 small inorganic particles, arranged within a bordered somewhat oval shaped outline (Figure 2-30). The only plausible explanation for this formation

appears to be that the particles were part of an icy comet that impacted at force on the stub, hence the strong, dark border of the object; Since the particles on the outside have impacted the stub with great force, and might have also gained a fusion crust due to it being exposed, while the rest of the particles that lay within have been protected and preserved upon impact, once the ice melted, it resulted in the spread of small particles on the slide.

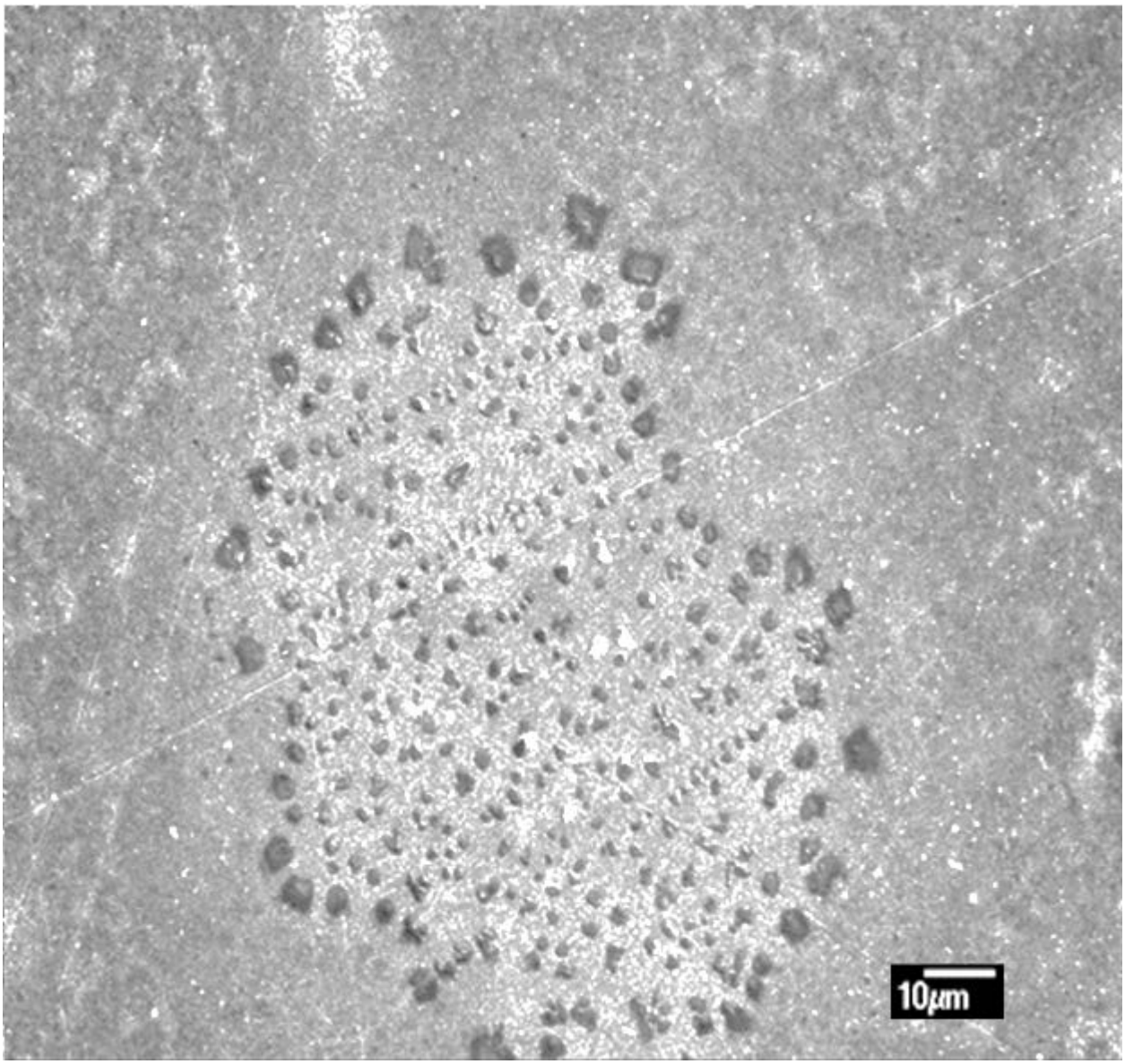

Figure 2-30: Shows scattered inorganic particles on one of the copper slides

Showing a clear, distinct border region around the clump. An indication of a comet made of ice and dirt.

The samples recovered from the fourth launch were not analysed all at once; instead, sample analysis was divided into two rounds to make it easier to handle the stubs with minimum contamination. Unfortunately, no EDAX was used for the samples analysed in the first round, including the ones shown in Figure 2-30, which requires interpreting solely on morphology and impact pattern. However, EDAX was used on the second batch of samples, and while no BEs were reported from it, the EDAX reading showed clear evidence that the particles are non-biological. Figure 2-31 shows some of the clumps and particles, along with their EDAX readings, which are notably different from the BEs that were found in the first and third launch. All four entities contain silicon as the main element, followed by oxygen, suggesting those particles to be made of SiO_2 (Silica). However, the relatively large size of the particles suggests that these are not terrestrial dust grains since these cannot be lifted above 20 km, but rather cosmic dust particles. Carbon and Manganese was present in small quantities in Figure 2-31A only. Copper, also a common component in cosmic dust particles and micrometeorites was also present in all of the particles. The elemental composition of the particles also suggests some of the particles to contain olivine, an essential component of chondrite meteorites (Peters *et al.*, 2015), thus further confirming the extra-terrestrial origin of the particles.

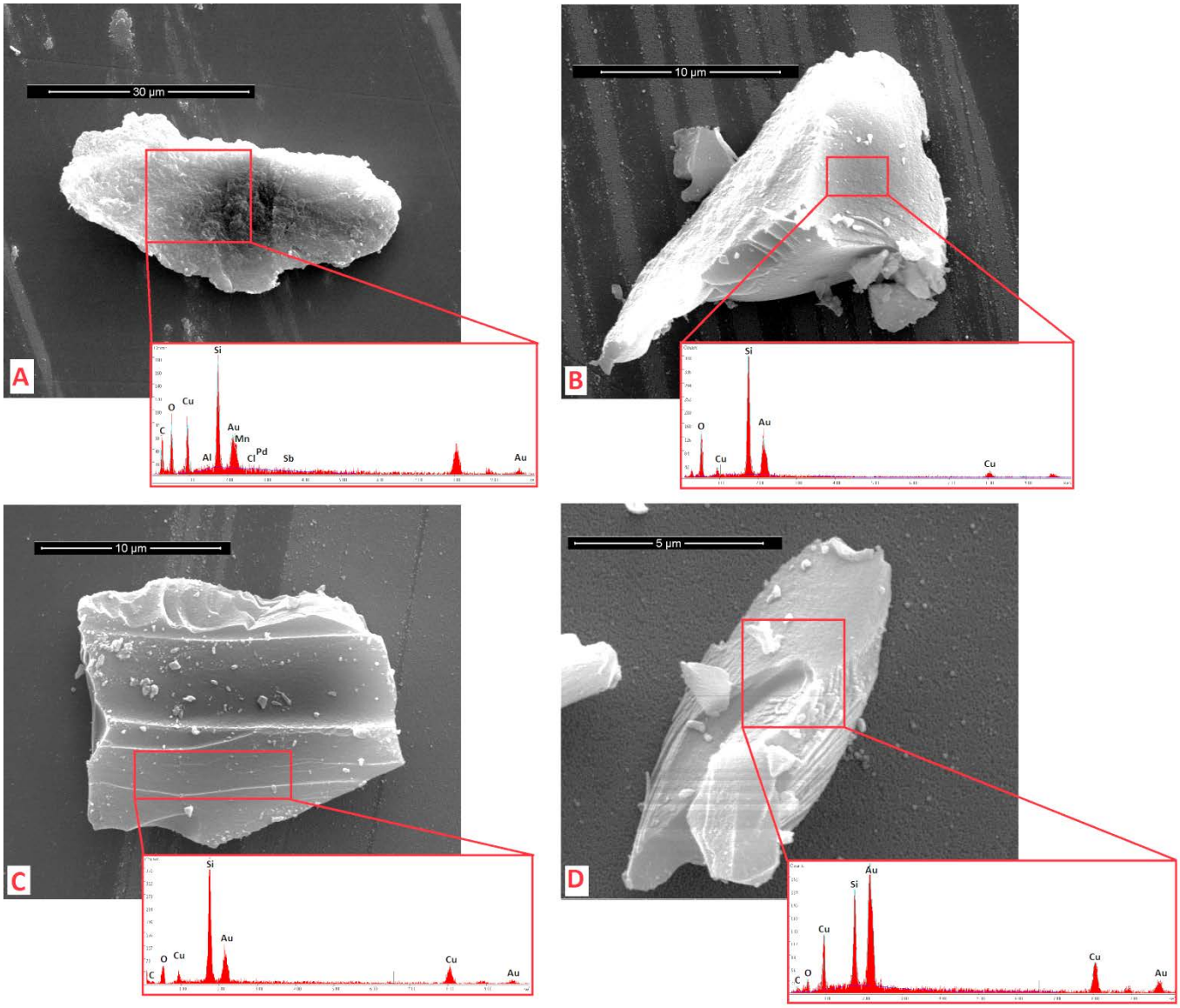

Figure 2-31: Four cosmic dust particles collected from the fourth stratospheric launch

The inset for each of A-D shows their EDAX reading, with Si being the main element present.

2.5.5 Findings from the Fifth Stratospheric Flight

In this launch, a new method for collection was introduced. Although the same carbon stubs were used as the ones from the first, second, and third missions (Carbon Leit tabs). These carbon stubs in the fifth launch were mounted on a special type of high-powered magnets, in order to collect magnetized particles which might be incoming from space, since cosmic dust particles, and micrometeorites can exhibit magnetic characteristics (Hunter and Parkin, 1960, Plane, 2012) . Neodymium magnets were used (strong, permanent magnet made from alloys of rare-earth elements). The magnets contained an alloy of neodymium, iron, and boron elements, which formed the tetragonal crystalline structure $Nd_2Fe_{14}B$; aluminium and cobalt are also part of the alloy, with smaller amounts of dysprosium and praseodymium (Table 2-2).

Table 2-2: The elemental composition of the neodymium magnets alloys

The neodymium magnets were used in the fifth stratospheric flight.

Main Elements within NdFeB	Percentage by weight
Neodymium (Nd)	29% - 32%
Iron (Fe)	64.2% – 68.5%
Boron (B)	1.0% - 1.2%
Aluminium (Al)	0.2% - 0.4%
Niobium (Nb)	0.5% -1%
Dysprosium (Dy)	0.8% -1.2%

The samples in this launch were analysed using two methods; the first was by SEM and EDAX as in all of the previous launches, the second method was using the single cell amplification technique enabled by REPLI-g Single Cell Kit – QIAGEN, as described earlier in 2.4.2.1.

2.5.5.1 SEM and EDAX results

The results show that stratosphere-derived particles were isolated on the surface of the magnets. It should be noted however, that not all of the captured particles are necessarily magnetic since non-magnetic particles may also have alighted onto the magnet surfaces.

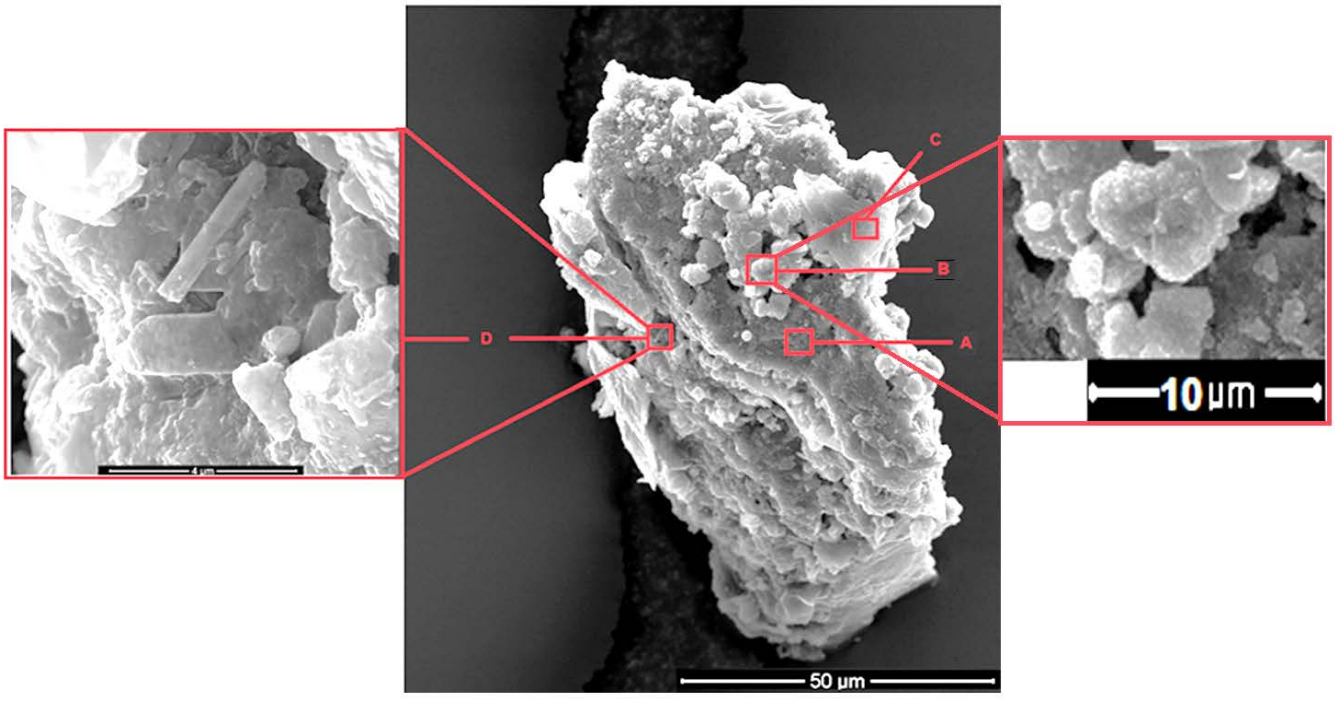

Figure 2-32: An SEM image for a large-complex entity, which was recovered from the fifth stratospheric launch

A-D are the points in which EDAX readings were taken, with two zoomed-in insets at points B and D.

A complex mass with a maximum size of approximately 100µm across is shown in Figure 2-32: An SEM image for a large-complex entity, which was recovered from the fifth stratospheric launch. The main body of the mass is made up of layers of material largely composed of iron, but it also contains C, N and O, as well as bromine, chlorine and selenium. An iron “whisker” (Figure 2-32 D) can also be observed embedded in the mass. The whisker contains calcium, chlorine and interestingly, holmium, praseodymium, and tungsten. A particle seen at Figure 2-32 C, contains tantalum and titanium. The EDX results show this to consist predominantly of iron but it also contains C,N and O (Table 2-3). Modelling studies have shown that particles bigger than 5 µm in size cannot be elevated from the Earth to the stratosphere (Kasten, 1968, Dehel *et al.*, 2008). In the following discussion, 5 µm is regarded as the theoretical elevation limit (TEL); particles substantially larger than this are therefore considered to be incoming to Earth from space and have not been elevated from Earth. Since the particle mass shown in Figure 2-32 clearly exceed the TEL it assumed to have originated from space and not Earth.

Table 2-3: Elemental results from EDAX for the A-D regions outlined in Figure 2-32.

Location	Elements	Wt%	At%
A	Carbon (C)	4.34	21.60
	Nitrogen (N)	0.90	3.85
	Oxygen (O)	1.27	4.76
	Chlorine (Cl)	3.16	5.32
	Iron (Fe)	45.36	48.54
	Gold (Au)- Used for coating	39.87	12.10
	Selenium (Se)	2.01	1.52
	Bromine (Br)	3.09	2.31
B	Carbon (C)	3.22	13.36
	Nitrogen (N)	1.55	13.36
	Oxygen (O)	9.31	29.03
	Chlorine (Cl)	4.56	6.42
	Iron (Fe)	36.15	32.28
	Gold (Au)- Used for coating	39.98	10.12
	Selenium (Se)	2.07	1.31
	Bromine (Br)	3.16	1.97
C	Carbon (C)	14.24	43.97
	Oxygen (O)	10.71	24.83
	Sodium (Na)	1.89	3.05
	Chlorine (Cl)	6.69	7.00
	Calcium (Ca)	3.51	3.25
	Titanium (Ti)	1.02	0.79
	Iron (Fe)	11.44	7.60
	Tantalum (Ta)	3.26	0.67
	Gold (Au)- Used for coating	39.44	7.43
	Thallium (Tl)	7.80	1.42
D	Chlorine (Cl)	0.30	0.76
	Calcium (Ca)	1.77	4.02
	Praseodymium (Pr)	1.36	0.88
	Iron (Fe)	35.00	56.93
	Holmium (Ho)	2.86	1.57
	Tungsten (W)	1.61	0.80
	Gold (Au)- Used for coating	42.66	19.68
	Rubidium (Rb)	14.44	15.35

Figure 2-33 shows a “scaly” mass isolated from the stratosphere, this mass is notable for containing the rare earth element, dysprosium. Like the particle shown in Figure 2-32, this particle clearly exceeds the TEL and as result, we assume it to be incoming into the stratosphere, not elevated to this region from Earth, the element composition is shown in

Table 2-4.

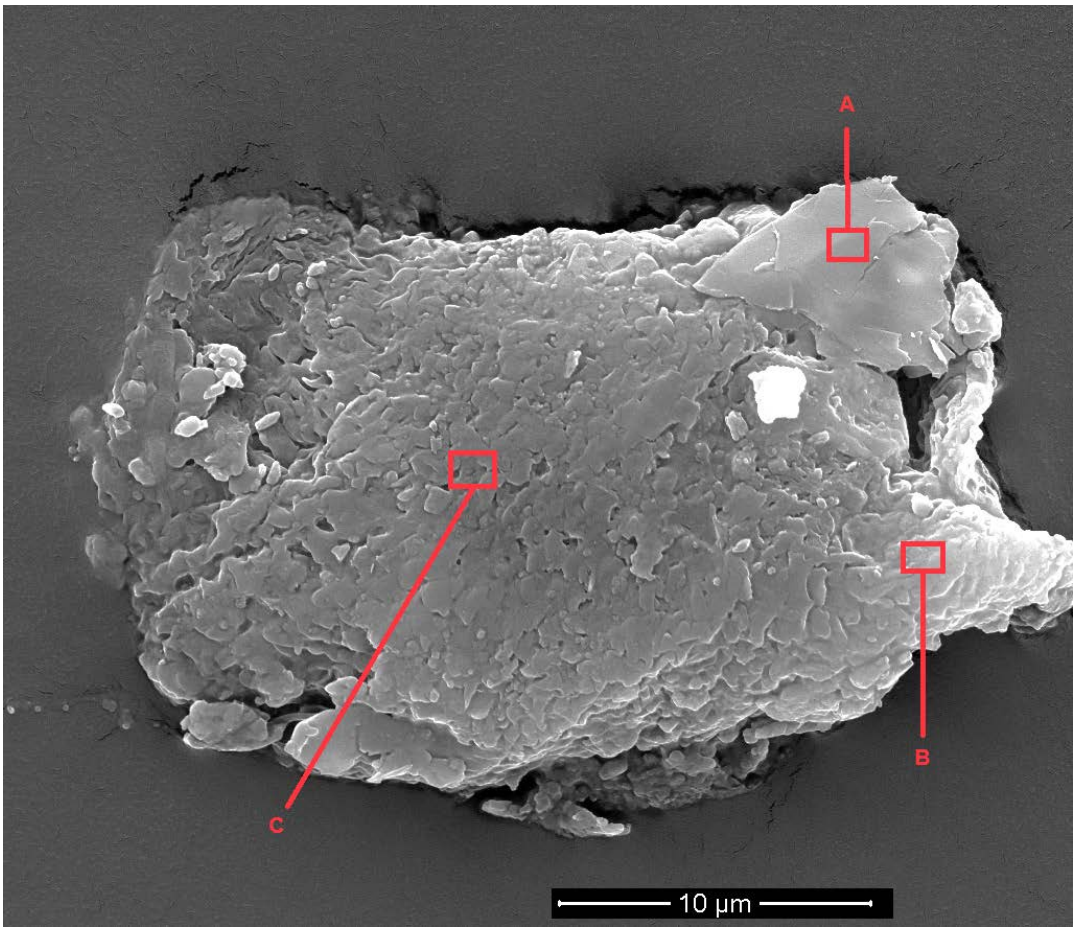

Figure 2-33: A large stratospheric masses sampled from the fifth launch

Viewed under SEM and analysed for elemental composition using EDAX.

Table 2-4: Elemental results from EDAX for the A-C regions outlined in Figure 2-33

Location	Elements	Wt%	At%
A	Carbon (C)	42.66	66.69
	Oxygen (O)	18.22	21.38
	Cobalt (Co)	1.41	0.45
	Sodium (Na)	3.32	2.71
	Magnesium (Mg)	2.73	2.11
	Silicon (Si)	3.60	2.41
	Chlorine (Cl)	3.63	1.92
	Gold (Au)- Used for coating	24.43	2.33
B	Carbon (C)	45.11	74.85
	Oxygen (O)	10.85	13.52
	Sodium (Na)	3.77	3.27
	Chlorine (Cl)	5.97	3.36
	Potassium (K)	3.21	1.64
	Barium (Ba)	1.16	017
	Manganese (Mn)	0.56	0.20
	Dysprosium (Dy)	1.08	0.13
	Gold (Au)- Used for coating	28.29	2.86
C	Carbon (C)	25.13	56.52
	Oxygen (O)	5.25	8.87
	Sodium (Na)	9.08	10.66
	Chlorine (Cl)	22.30	16.99
	Potassium (K)	2.50	1.73
	Barium (Ba)	1.06	0.21
	Manganese (Mn)	0.63	0.31
	Dysprosium (Dy)	1.59	0.26
	Gold (Au)- Used for coating	32.48	4.45

Figure 2-34 shows an unusual shaped particle composed of a non-regular amorphous broadly rectangular mass with distinctive projections emerging from the upper corners and beginning to emerge at the bottom corner. The projections are tube–like and sealed. Similar projections were seen to be forming on other adjacent, amorphous masses and in the lower centre of the image. Analysis using EDX shows that the particles contain carbon and oxygen, but are mainly composed of, or covered in, sodium and potassium chloride (Table 2-5); the projections have a similar composition. The amorphous masses were centred on distinct, square crystals which EDX analysis shows to be crystals of sodium chloride, i.e. salt crystals. We are unable to come to a conclusion about the nature of these “horned particles”; It contains C and O and possess bilateral symmetry and may be biological entities which are covered in, or containing sodium and barium chloride; alternatively, it might be inorganic structures. Similarly, the origin of the particles seen in Figure 2-34 is unclear; The overall size (4 µm) suggests it to be small enough to have been elevated to the stratosphere from Earth. However, the large mass of the associated salt crystals would make it unlikely that the “horned particles“ salt crystal combination could be lifted from Earth to a height around 25 km, as result, we suggest it is incoming to Earth from space.

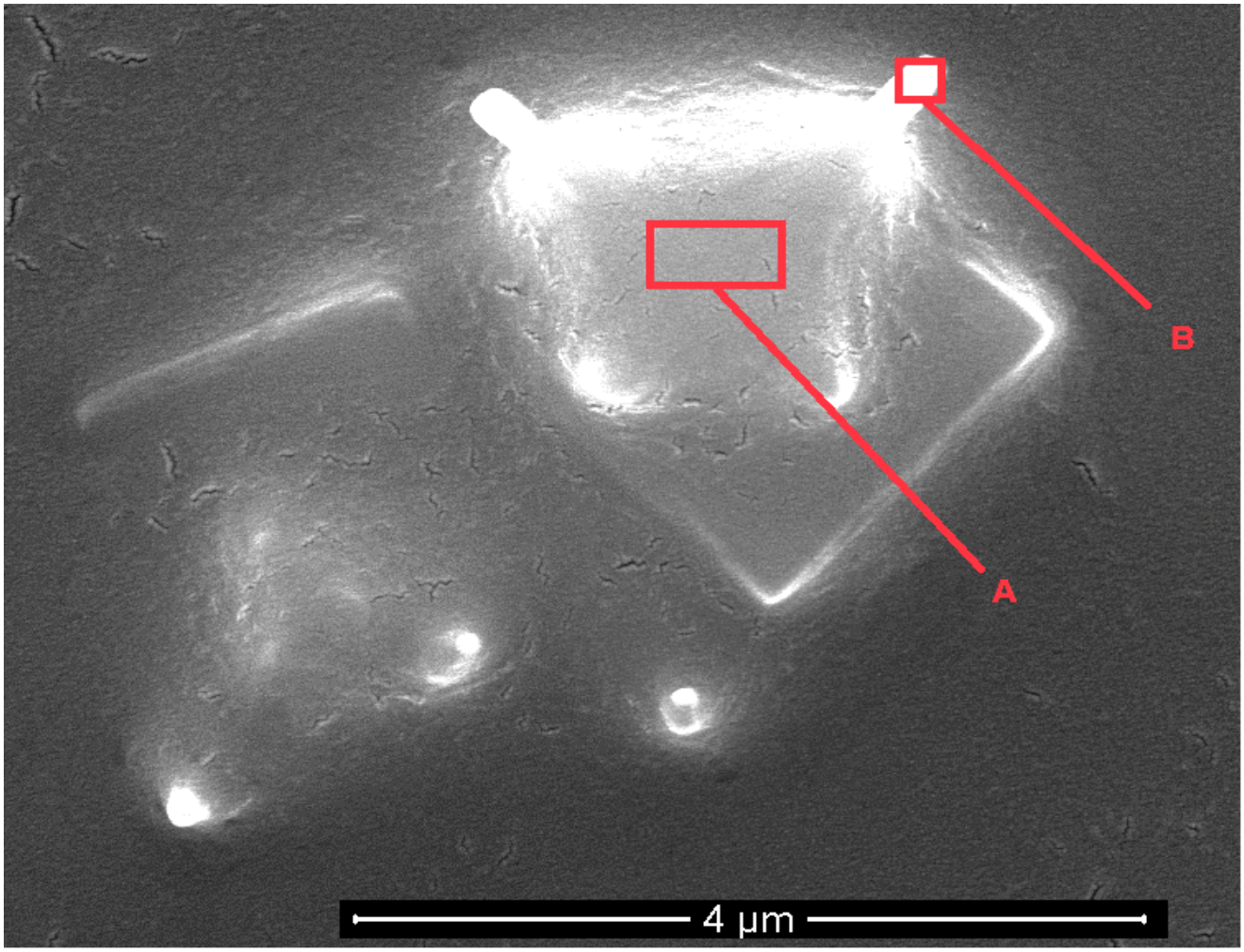

Figure 2-34: SEM image for one of the entities recovered from the fifth stratospheric flight

Showing an unregulated amorphous mass attached to cubical-shaped-inorganic crystals of sodium chloride.

Table 2-5: The elemental composition for the entity shown in Figure 2-34.

Location	Elements	Wt%	At%
A	Carbon (C)	13.37	38.65
	Oxygen (O)	1.40	3.03
	Sodium (Na)	14.14	21.35
	Chlorine (Cl)	27.41	26.84
	Potassium (K)	3.27	2.90
	Barium (Ba)	1.30	0.33
	Gold (Au)- Used for coating	39.11	6.89
B	Carbon (C)	15.25	51.53
	Oxygen (O)	2.37	6.01
	Sodium (Na)	7.57	13.36
	Chlorine (Cl)	13.54	15.50
	Potassium (K)	1.12	1.17
	Barium (Ba)	0.50	0.15
	Gold (Au)- Used for coating	59.65	12.29

Figure 2-35 shows two particles masses which exceed the TEL and which contain large percentages of C,O and N. The bottom particle is of particular interest since it appears to be a collapsed, ridged sphere. These particles may be biological, and since their size clearly exceeds the TEL we suggest it incoming to Earth from space.

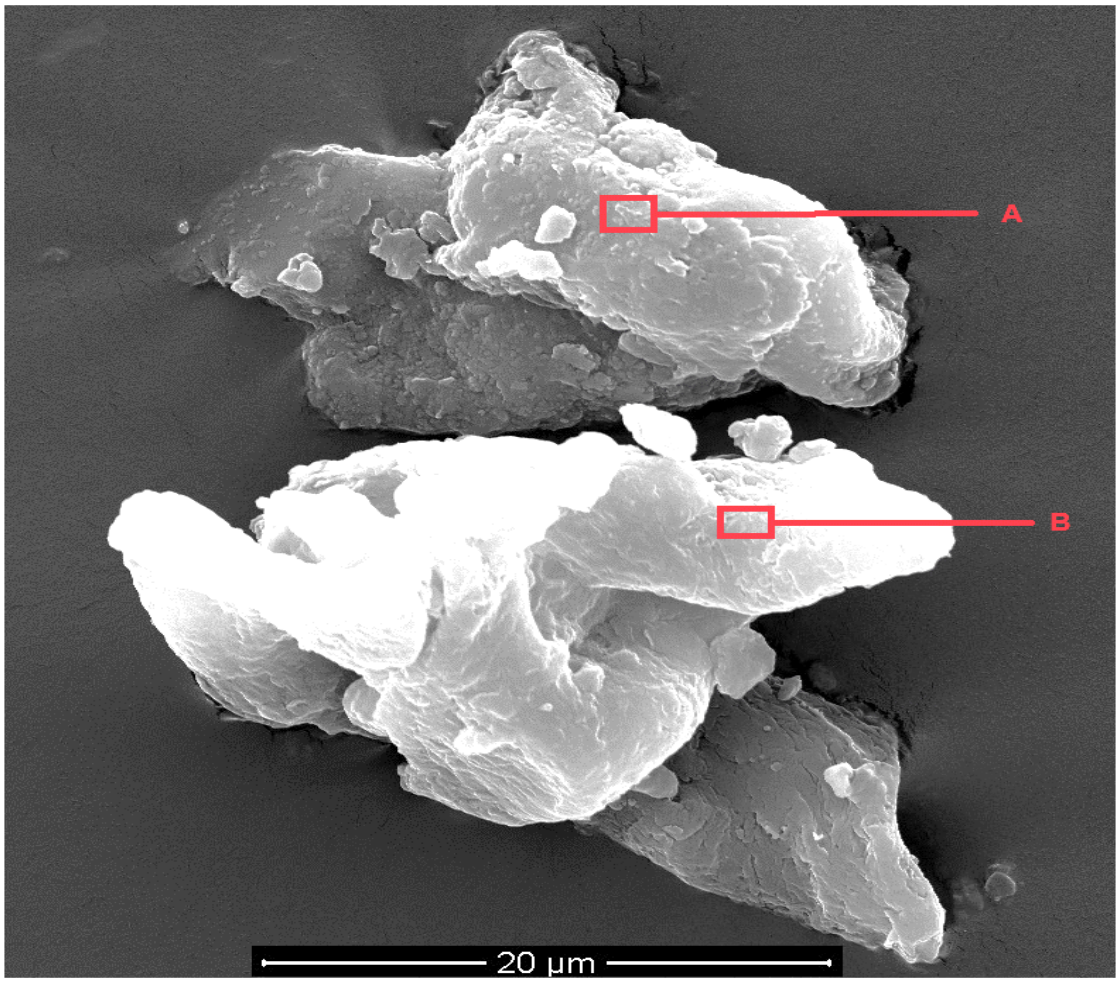

Figure 2-35: SEM of two masses recovered from the fifth stratospheric flight

With the mass at the bottom appearing to have been collapsed upon impact on the stub.

Table 2-6: The elemental composition for the entity shown in Figure 2-35.

Location	Elements	Wt%	At%
A	Carbon (C)	40.58	64.62
	Nitrogen (N)	7.97	10.88
	Oxygen (O)	13.99	16.72
	Sodium (Na)	2.48	2.06
	Chlorine (Cl)	3.75	2.03
	Potassium (K)	1.02	0.50
	Copper (Cu)	1.23	0.37
	Gold (Au)- Used for coating	28.99	2.82
B	Carbon (C)	43.28	63.71
	Nitrogen (N)	10.67	13.47
	Oxygen (O)	15.17	16.76
	Sodium (Na)	1.29	0.99
	Silicon (Si)	1.36	0.86
	Chlorine (Cl)	2.99	1.49
	Potassium (K)	1.23	0.56
	Gold (Au)- Used for coating	24.01	2.15

Figure 2-36 shows another mass, which is rich in C, O, and N (Table 2-7). It is approximately four times the TEL and we therefore assume that it is incoming to Earth. The main mass shows a region which rich in C, O, and N, made up of a mass of particles of around 1 μm and may consist of an individual bacterium. An amorphous particle in Figure 2-36-C is also rich in C N and O; We suggest therefore that this is biological material incoming to Earth from space.

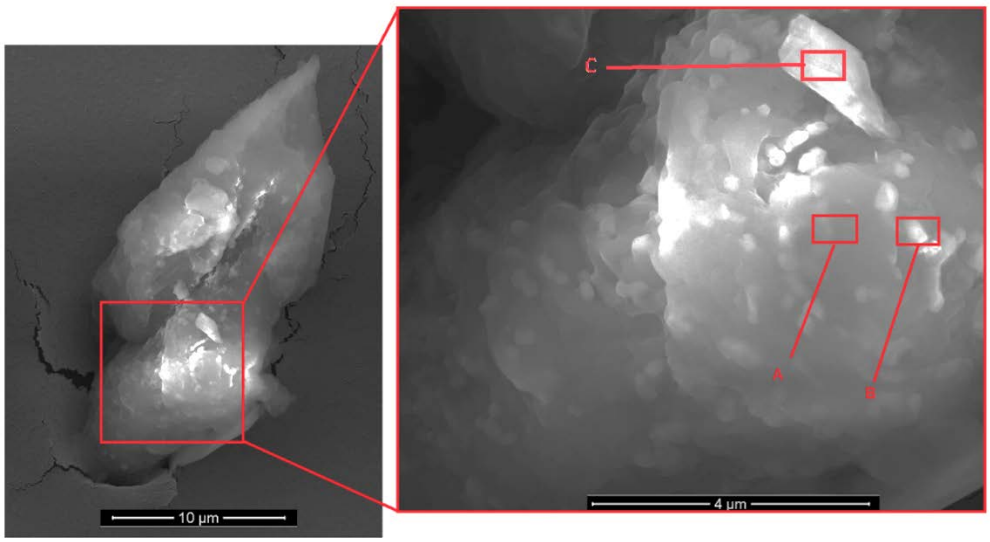

Figure 2-36: SEM image for an amorphous entity recovered from the fifth launch

The EDAX analysis revealed it rich in C, O, and N content.

Table 2-7: The elemental composition for the amorphous entity shown in Figure 2-36.

Location	Elements	Wt%	At%
A	Carbon (C)	52.15	63.60
	Nitrogen (N)	12.28	12.84
	Oxygen (O)	17.17	15.72
	Sodium (Na)	5.20	3.31
	Aluminum (Al)	0.69	0.37
	Silicon (Si)	0.46	0.24
	Niobium (Nb)	1.75	0.28
	Molybdenum (Mo)	2.07	0.32
	Chlorine (Cl)	6.34	2.62
	Potassium (K)	1.41	0.53
	Calcium (Ca)	0.48	0.18
B	Carbon (C)	50.77	64.34
	Nitrogen (N)	9.37	10.18
	Oxygen (O)	19.09	18.16
	Sodium (Na)	3.27	2.17
	Magnesium (Mg)	0.51	0.32
	Aluminum (Al)	0.73	0.41
	Silicon (Si)	1.22	0.66
	Gold (Au)- Used for coating	5.36	0.41
	Molybdenum (Mo)	2.60	0.41
	Chlorine (Cl)	4.50	1.93
	Potassium (K)	1.89	0.73
	Calcium (Ca)	0.69	0.26
C	Carbon (C)	40.51	53.22
	Nitrogen (N)	6.82	7.68
	Oxygen (O)	28.70	28.30
	Sodium (Na)	5.15	3.53
	Magnesium (Mg)	0.30	0.19
	Aluminum (Al)	2.07	1.21
	Silicon (Si)	4.19	2.35
	Gold (Au)- Used for coating	3.37	0.27
	Molybdenum (Mo)	2.29	0.38
	Chlorine (Cl)	4.91	2.19
	Potassium (K)	1.10	0.44
	Calcium (Ca)	0.58	0.23

A particle mass which only marginally exceeds 5 µm TEL is shown in Figure 2-37. The particle (EDAX at A) contains C, O, and N, with smaller amounts of aluminium, calcium and bismuth; the particle may be biological. Location B shows particles containing C and O as well as aluminium, calcium, neodymium, nickel, lutetium and gallium Table 2-8.

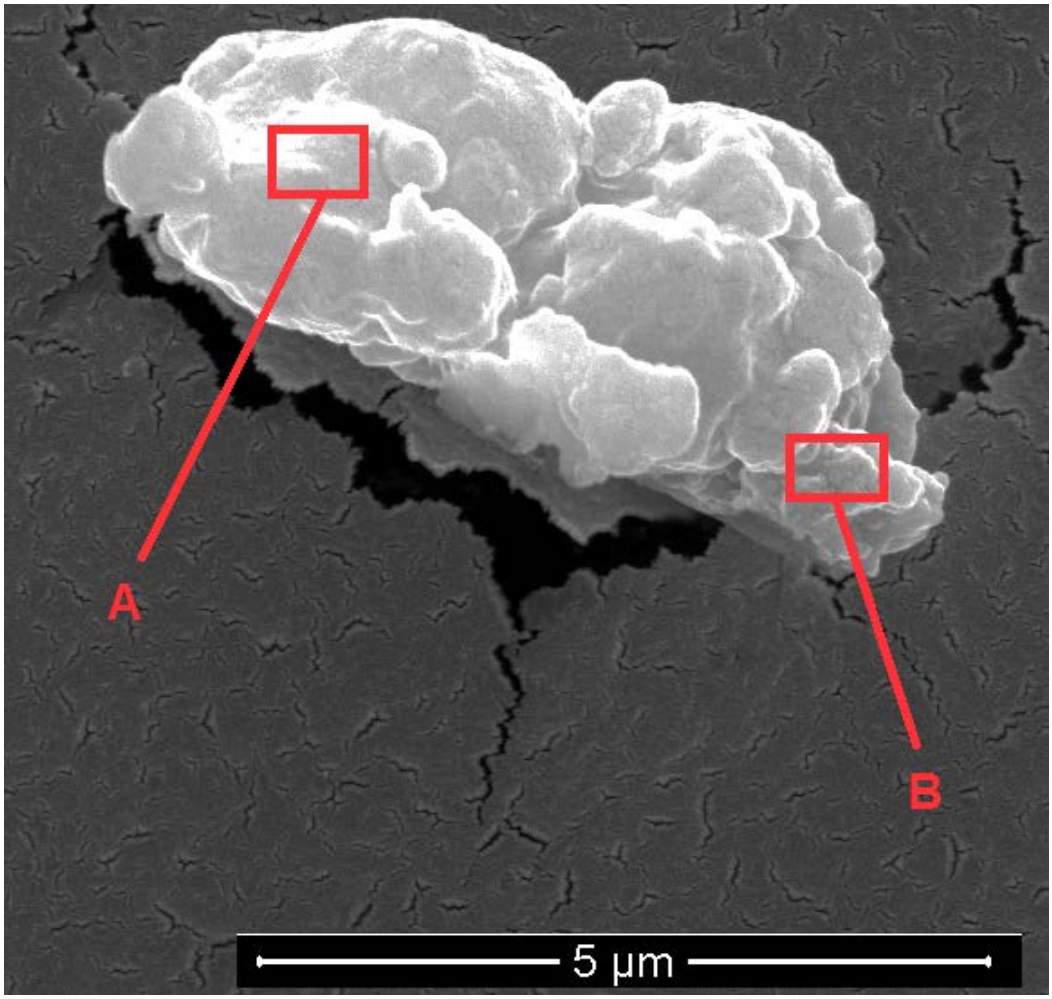

Figure 2-37: SEM image of relatively small particle close to the TEL limit in size

The noticeable impact on the slide suggest the object fell with speed on the stub.

Table 2-8: The elemental composition revealed EDAX analysis of the small particle shown in Figure 2-37.

Location	Elements	Wt%	At%
A	Carbon ©	18.06	58.51
	Nitrogen (N)	3.69	10.25
	Oxygen (O)	5.63	13.68
	Aluminum (Al)	1.69	2.43
	Bismuth (Bi)	5.27	0.98
	Calcium (Ca)	1.52	1.48
	Gold (Au)- Used for coating	64.14	12.67
B	Carbon ©	29.86	77.36
	Oxygen (O)	4.75	9.23
	Aluminum (Al)	1.38	1.59
	Calcium (Ca)	1.15	0.89
	Neodymium (Nd)	0.97	0.21
	Nickel (Ni)	1.08	0.57
	Lutetium (Lu)	2.89	0.51
	Gallium (Ga)	1.66	0.74
	Gold (Au)- Used for coating	56.27	8.89

Damage to the surface of the carbon SEM stubs can be clearly seen in Figure 2-37. In our previous studies, when such stubs were sent directly into the stratosphere, we suggested that similar (although less apparent) damage is caused by the biological entities impacting the stubs at high speed, i.e. adding further weight to a space origin. In the case of the particles shown here however, such damage is clearly apparent, and occurred when the carbon stub was adpressed onto the surface of the magnet, as a result it does therefore indicate an impact event.

2.5.5.2 Single-cell amplification and subsequent DNA sequencing analysis:

2.5.5.2.A *Confirmation of positive DNA from the MDA technique using agarose gels*

As explained earlier, twenty-four tubes were used with the REPLI-g® Single Cell Kit, the procedure was performed as explained in 2.4.2.1. As mentioned earlier, one of the samples was a control taken from a sterile stub. After completion of the MDA technique using the REPLI-g® Single Cell Kit; the products from the 24 tubes were ran on agarose gel to confirm the presence of DNA, as shown in Figure 2-38; out of the 24 samples, only two failed to show any DNA, one of which was the negative control, all the remaining 22 samples were confirmed at this stage to contain DNA. The remaining two negative tubes were disregarded.

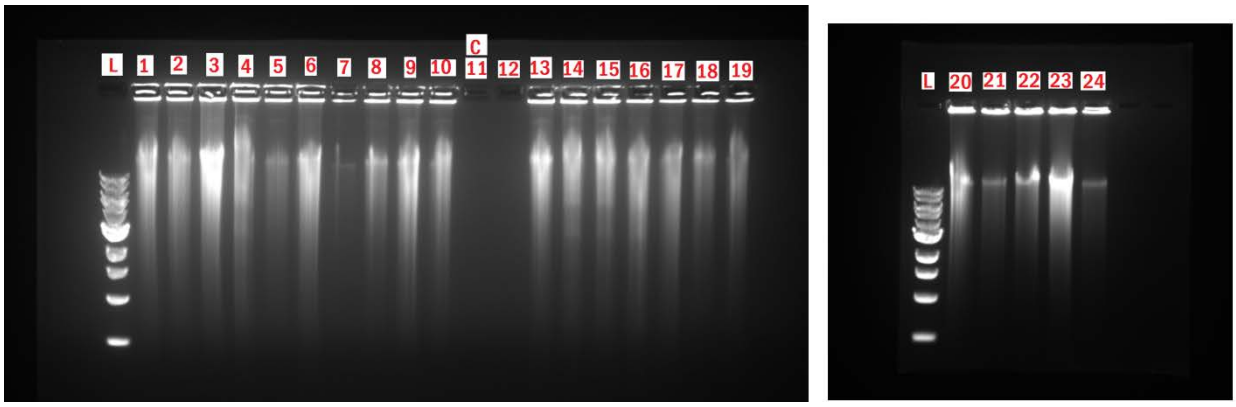

Figure 2-38: Negative image of an ethidium bromide-stained 1% agarose gel of the REPLI-g® Single Cell products

Two gels were prepared as shown to demonstrate all of the twenty-four samples, two of which failed to show DNA; 11 – Control (C), and sample 12. L: L: 1kb BIOLINE HyperLadder.

2.5.5.2.B *The use of 27F and 1492R primers for 16S rRNA PCR amplification, and identification of axenic DNA*

The 27F and 1492R primers are universal primers that can be used for a wide variety of bacterial species, with some exceptions (Heuer *et al.*, 1997). We

decided to use 16S rRNA PCR amplification at this stage because it will give faster results than when sending the samples for Illumina Next-Generation sequencing and subsequent *De Novo* assembly. However, 16S rRNA PCR amplification and subsequent sequencing give the best results when there was only axenic DNA in the tubes. All of the 22 DNA-positive samples were subjected to the 16S rRNA PCR amplification; following it, the amplification products were ran on 1% agarose gel and the results are shown in Figure 2-39. Out of the 22 samples, only seven shown a clear single band of DNA, all the bands appeared to be in the same length (with the help of the DNA 1kb ladder, the PCR DNA product is estimated to be around 1500 bp, compatible with the primers F27 and R1492). The reason why the other fifteen samples failed to show clear bands is most likely attributed to them containing nonaxenic DNA, this was confirmed later by the Illumina-Next Generation sequencing.

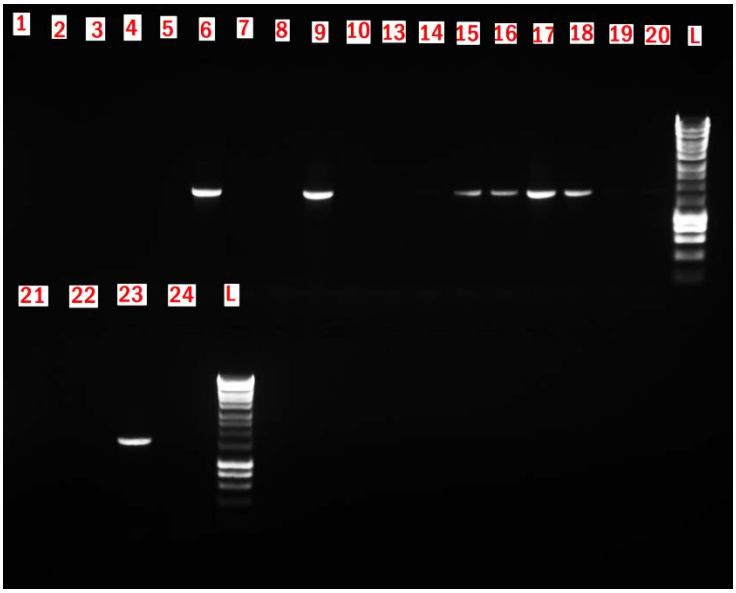

Figure 2-39: Negative image of an ethidium bromide-stained 1% agarose gel

Showing DNA bands for the PCR 16S rRNA products, a single band of DNA is apparent for some of the samples. L: 1kb BIOLINE HyperLadder.

The seven samples which showed positive DNA bands were sequenced at the Core Genomic Facility, when the sequencing data were received, it was used to identify their species origin, using BLAST search; Below is the identification results for each:

- Sample tube number 6: *Staphylococcus aureus* (99% match) (See Appendix A: A1 and A2).
- Sample tubes number 9 and 16: *Streptococcus thermophilus* (99% match) (See Appendix A: A3, A7, and A4).
- Sample tube number 15: *Staphylococcus saprophyticus* (99% match) (See Appendix A: A5 and A6).
- Sample tube number 17: *Staphylococcus sciuri* (99% match) ((See Appendix A: A8 and A9).
- Sample tube number 18: *Propionibacterium acnes* (99% match) (See Appendix A: A10 and A11).
- Sample tube number 23: *Aquicella siphonis* (98% match) (See Appendix A: A12 and A13).

The most notable finding, obtained from the seven identified samples mentioned above, is the one which contained *Aquicella siphonis* (Sequence ID: ref|NR_025764.1|), because unlike the other five species, which critics might argue results were human contamination (since it can occur as normal skin flora) (Kloos and Musselwhite, 1975, Fredricks, 2001, Findley *et al.*, 2013), *Aquicella siphonis* is extremely unlikely to be a laboratory contaminant because of the unique and geologically limited environments from which it has been isolated. *Aquicella*, belongs to the γ-proteobacteria, and was first reported and named by Santos *et al.* (2003) who isolated two species, *Aquicella lusitana* gen. nov., sp. nov., and *Aquicella siphonis* sp. nov.; the isolates originated from a borehole (i.e. a drilled well) in central Portugal. Bastain et.al., (2009) also reported isolating *Aquicella siphonis* from the Lascaux Cave, showing a 96% sequence similarity to Santos's original isolate. At the time of writing this report, no other study has reported finding this microbe elsewhere. *Aquicella siphonis* is closely related to *Legionella* which live within protozoa as part of their life cycle and it has been suggested that *Aquicella siphonis* also possesses an intracellular life

cycle involving an, as yet, unidentified eukaryotic host (Santos *et al.*, 2003, Bastian *et al.*, 2009); the organism is therefore clearly unlikely to be a laboratory air contaminant. It could be argued that the isolate originated from the balloon, during in-flight sampling. This seems unlikely since the manufacturers cover the balloon in talc which would be expected to similarly contaminate the sampler; no talc however was found on the sampling discs when these were viewed under the scanning electron microscope.

Unlike other findings, the seven microbial species isolated using 16S rRNA PCR amplification all seem to have a cellular size of around 1µm in diameter. If we accept that those microbes were isolated in the stratosphere and are not laboratory contaminants, especially in the case of *Aquicella siphonis*, then the question of whether or not they have an Earth origin remains open because they are all below the size limit of 5 µm which have been determined by previous studies to prevent the uplift of an organism from Earth to the stratosphere (Kasten, 1968, Dehel *et al.*, 2008). However, the fact that they are small does not *a priori* exclude the possibility that they came from space, although Occam's Razor would suggest that this is unlikely. The fact is that 16S rRNA PCR amplification is a rather limiting tool for this purpose; it solely identifies axenic DNA for bacteria, therefore leaving out any potentially mixed population of microbes, or eukaryotic DNA. Which was why the other samples were sent for NGS *and De Novo* assembly combined with BLAST in order to identify more diverse populations that might be present in the samples.

2.5.5.2.C *Illumina Next Generation sequencing results, and identification of non axenic DNA*

As stated earlier, the limitation with using 16S rRNA is the specificity for only a certain group of prokaryotes, and the need to have a pure isolate presents a problem when working with samples that have more than one cell type. Usually in similar cases, e.g. when working with soil samples, the standard protocol is to dilute the samples enough to get CFU on the culture-media

plates, identify the microbial species of each pure isolate, and then estimate the percentage of microbial species in the sample (Torsvik and Øvreås, 2002). This method however, has several shortcomings, such as the vast difference between the direct number of microbial count and the number of culturable bacteria (Amann *et al.*, 1995). In the work reported here on the stratospheric sampling, since only a limited number of cells were isolated on each SEM stub, and because of fears of leaving out microbes that are unculturable on routine media plates, this direct culturing and identification technique is of only limited use. Therefore, it was concluded that the most suitable means of identifying the entire DNA present in non axenic samples (which were obtained from the MDA) was to sequence it using the Illumina Next Generation sequencing technique.

As explained earlier (section 2.4.2.2.B), seven DNA positive non axenic samples (REPLI-g® Single Cell Kit product) were selected randomly for NGS. The results from NGS (fastq DNA library files) were sent to the Computational Systems Biology Unit, Department of Computer Science at the Kroto Research Institute, were the following was performed:

- Quality control for all seven samples was performed using FastQC (A simple quality control for raw sequence data produced from the sequencing pipeline, it aims to verify the quality of the data before progressing to conduct further analysis) (Andrews, 2010).
- *De novo* assembly for all samples was performed, followed by BLAST search; results were interpreted based on the techniques used when handling the samples.
- 35,000+ microbial reference genomes downloaded from the National Center for Biotechnology Information (NCBI). Metagenomic assembly against downloaded reference genomes performed for all samples, followed by BLAST search.

The results showed a surprisingly large number of microorganisms in each of the seven samples, as evidenced in (Figure Figure 2-40,Figure 2-41, Figure 2-42, Figure 2-43, Figure 2-44, Figure 2-45, and Figure 2-46).

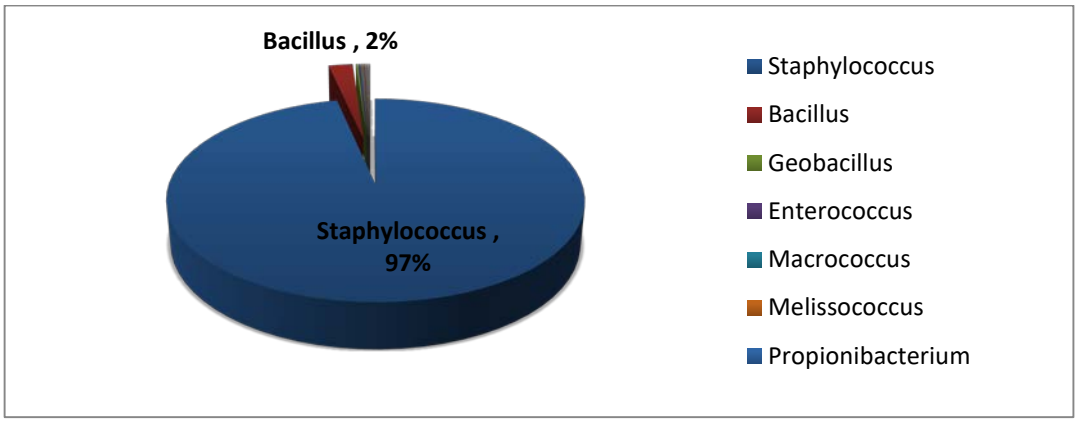

Figure 2-40: Total sequence count, grouped by species name, for sample 1 of the seven non-axenic DNA samples:

Following *De novo* assembly and BLAST, grouped by species family name, showing a prevalence of Staphylococcus (sequence count 5771940, Representative 96.590%). (See Appendix D for full results, including each species name)

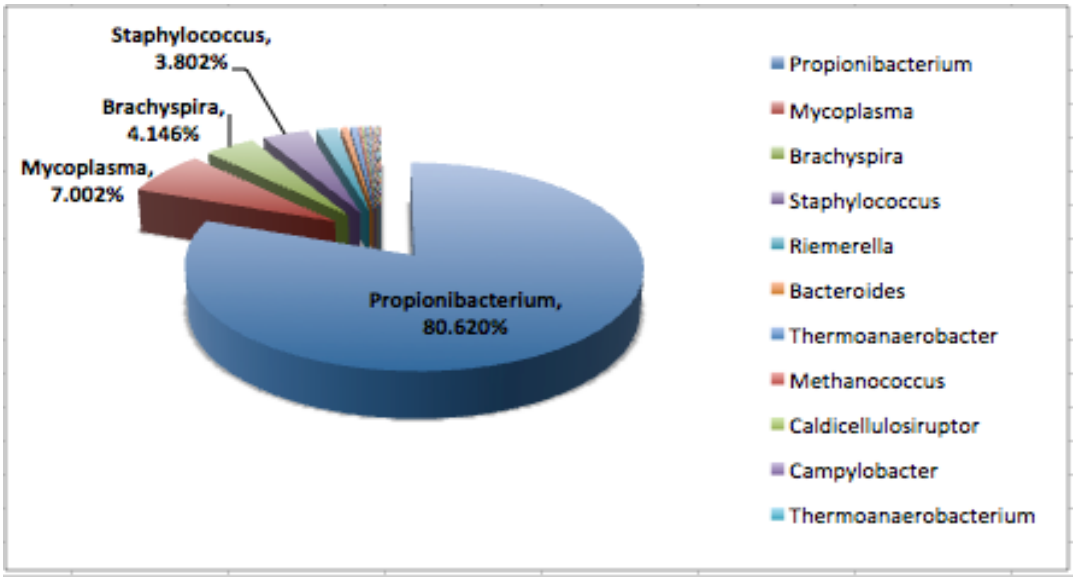

Figure 2-41: : Total sequence count, grouped by species name, for sample 2 of the seven non-axenic DNA samples:

Following *De novo* assembly and BLAST, grouped by species family name, showing a prevalence of *Propionibacterium* (sequence count 17305, Representative 80.620%).

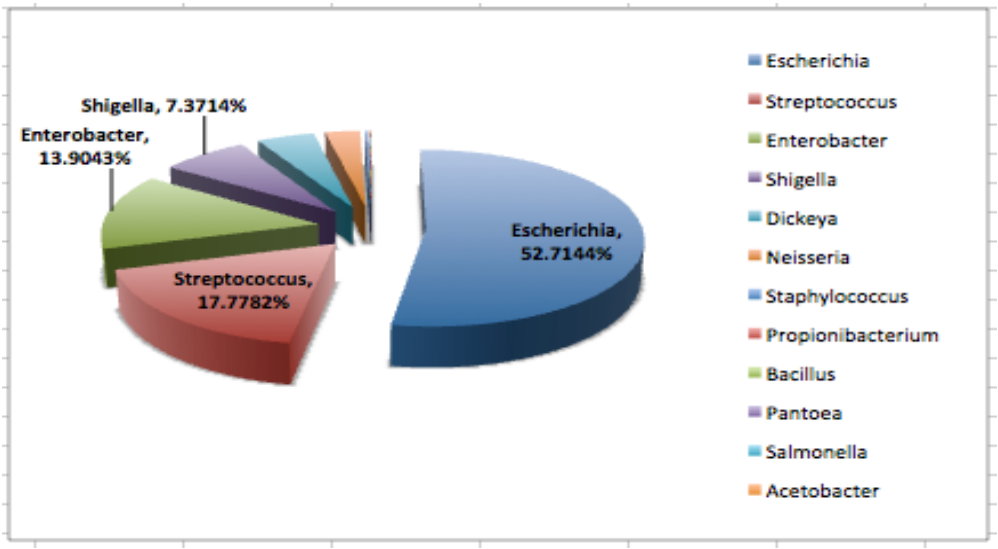

Figure 2-42 : Total sequence count, grouped by species name, for sample 3 of the seven non-axenic DNA samples:

Following *De novo* assembly and BLAST, grouped by species family name, showing a prevalence of *Escherichia* (sequence count 107948, Representative 52.7144%).

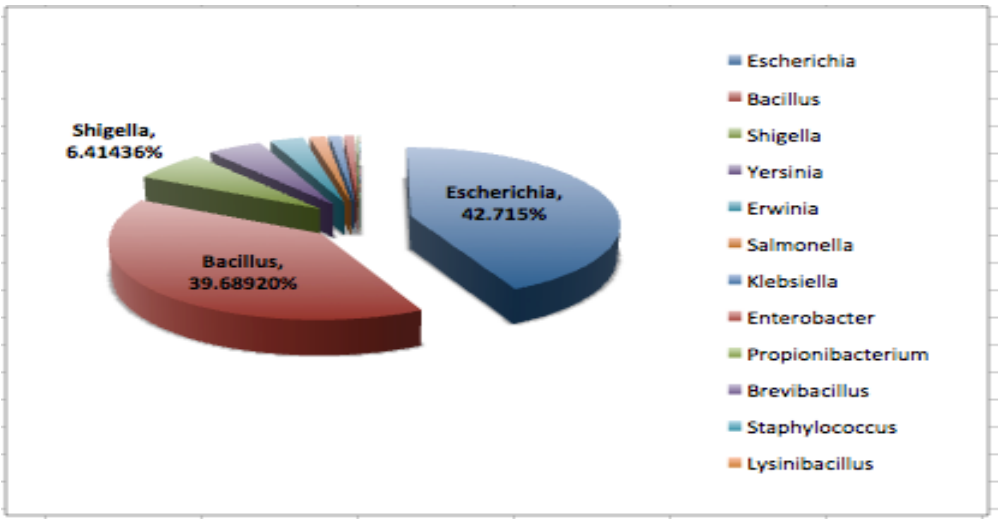

Figure 2-43: Total sequence count from sample 4 of the seven non-axenic DNA samples:

Following *De novo* assembly and BLAST, grouped by species family name, showing a prevalence of *Escherichia* (sequence count 2835826, Representative 42.715%).

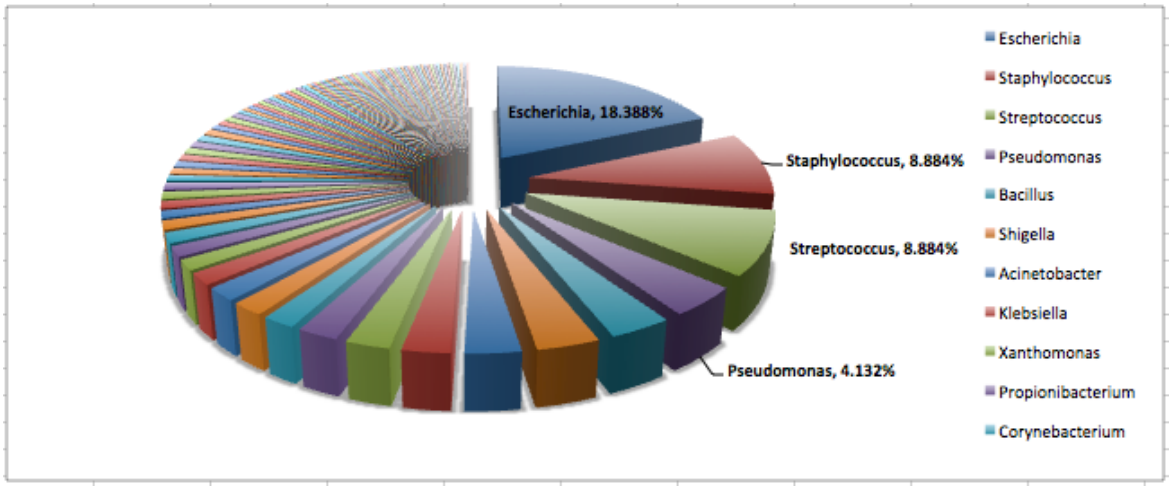

Figure 2-44: : Total sequence count, grouped by species name, for sample 5 of the seven non axenic DNA samples:

Following *De novo* assembly and BLAST, grouped by species family name, showing a prevalence of *Escherichia* (sequence count 89, Representative 18.388%).

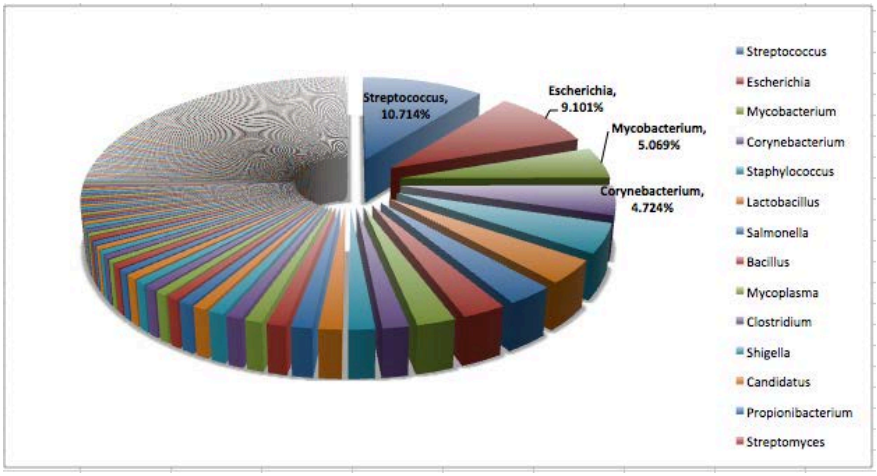

Figure 2-45: : Total sequence count, grouped by species name, for sample 6 of the seven non-axenic DNA samples:

Following *De novo* assembly and BLAST, grouped by species family name, showing a prevalence of *Streptococcus* (sequence count 93, Representative 10.714%).

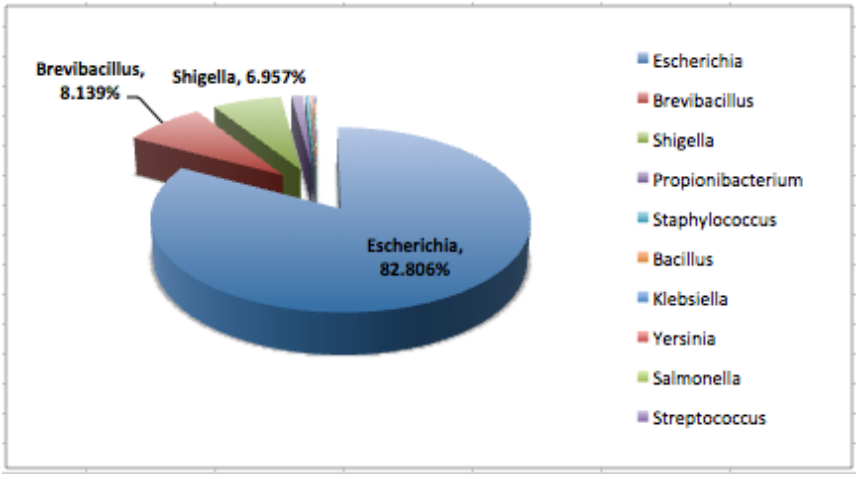

Figure 2-46: Total sequence count, grouped by species name, for sample 7 of the seven non-axenic DNA samples:

Following *De novo* assembly and BLAST, grouped by species family name, showing a prevalence of *Escherichia* (sequence count 114677, Representative 82.806%).

As seen in all of the NGS results from the seven samples, there is a strikingly large diversity of microbes in each of the tubes. If it is accepted that these results are not the result of contamination, then the stratosphere host a microbial community that is as complex and diverse as the soil and water environments. Although previous studies have already showed microbes that exist in the stratosphere (Wainwright *et al.*, 2004, Yang *et al.*, 2008a), the problem with previous methods is its reliance on culture-based analysis techniques, and 16S rRNA PCR, both exclude a significant number of microbes which might be present. The NGS results for the samples is unlikely to result from contamination for many reasons; since single-cell amplification steps were performed within a single tube, it minimised the possibility of contamination. The use of negative controls also failed to show any microbes, demonstrating the sterility of the experiments. Perhaps the strongest argument that the single-cell amplification and NGR results are not due to laboratory contamination is the presence of a number of microbes which are extremely unlikely to exist in a laboratory environment; Some of

the microbes from sample 1 (Figure 2-40) are mentioned below, (See Appendix D for details of all isolated microbes):

- *Oceanobacillus iheyensis* an extremely halotolerant and alkaliphilic microbe, isolated from deep sea sediment at depth of over a thousand meter on the Iheya Ridge (Lu *et al.*, 2001).
- *Prochlorococcus marinus*, a dominant photosynthetic microbe in the ocean (Chisholm *et al.*, 1988).
- *Flexistipes sinusarabici*, a type of Eubacteria isolated from Atlantis II Deep brines in the Red Sea (Fiala *et al.*, 1990).
- *Persephonella marina*, a thermophilic microbe, previously isolated from deep hydrothermal vents (Götz *et al.*, 2002).
- *Salinispora tropica*, an obligate marine actinomycetes microbe (Maldonado *et al.*, 2005).
- *Kineococcus radiotolerans*, a radiation resistant microbe, previously isolated from a heavily irradiated area of the Savannah River, a nuclear reservation in South Carolina, USA (Phillips *et al.*, 2002).
- *Marinithermus hydrothermalis*, a thermophilic marine bacterium isolated from over a 1,300 m deep-sea hydrothermal vent chimney - Suiyo Seamount in the Izu-Bonin Arc, Japan (Sako *et al.*, 2003).

Due to their unique properties and environments from which they have been isolated, the microbes, mentioned above are highly unlikely to be laboratory contaminants. The question of how they became resident in the stratosphere can be easily explained using the model studies by (Kasten, 1968, Dehel *et al.*, 2008) which suggests that microbes with a size below 5 µm in diameter can be lifted from the troposphere below; Judging by the large diversity of the microbes recovered and analysed here using NGS technique, this the most likely source, although a space origin cannot be *a priori* excluded. It is concluded, however, that these organisms likely have an Earth origin.

A notable conclusion which emerged from the NGS analysis results is that none of the sequenced DNA belonged to cells which exceed the size limitation proposed by (Kasten, 1968, Dehel *et al.*, 2008), proving that

large cells cannot be lifted from the troposphere. As evidenced by the lack of DNA from those sources, this strongly evidence that the large biological entities (exceeding 30 µm in many cases) have an extra-terrestrial origin, and are not from the troposphere.

2.5.6 Findings from the Sixth sampling flight

The same launch and analysis protocols were followed in this sampling mission as the ones from the first, second, and third missions; SEM stubs were used to collect stratospheric samples, which upon retrieval, were analysed using SEM and EDAX. The reason why no DNA sequencing techniques were performed during this launch is that at the time, the analysis was still undergoing on the cells recovered from the fifth launch, therefore there was no way at that point of confirming the effectiveness of using the Single-cell amplification using WGA technique.

Various entities have been found from this sampling mission, many of which left a visible impact crater as a sign of the object coming at speed into the stubs; The entity shown in Figure 2-47 appear to have collapsed upon impact on the stub at high speed as shown by the circular damaged area of the SEM stub as a result of the impact. The BE itself has also deformed after impact thus making it very difficult to determine its original morphology, however, what is noticeable from the EDAX readings (Figure 2-48) is the persistence of the same chemical elements, and their percentages compared to each other, which a high prevalence of C, O, Mg, Si, and Al. Whether this entity is biological is not easy to determine though, since its morphology was altered greatly after impact.

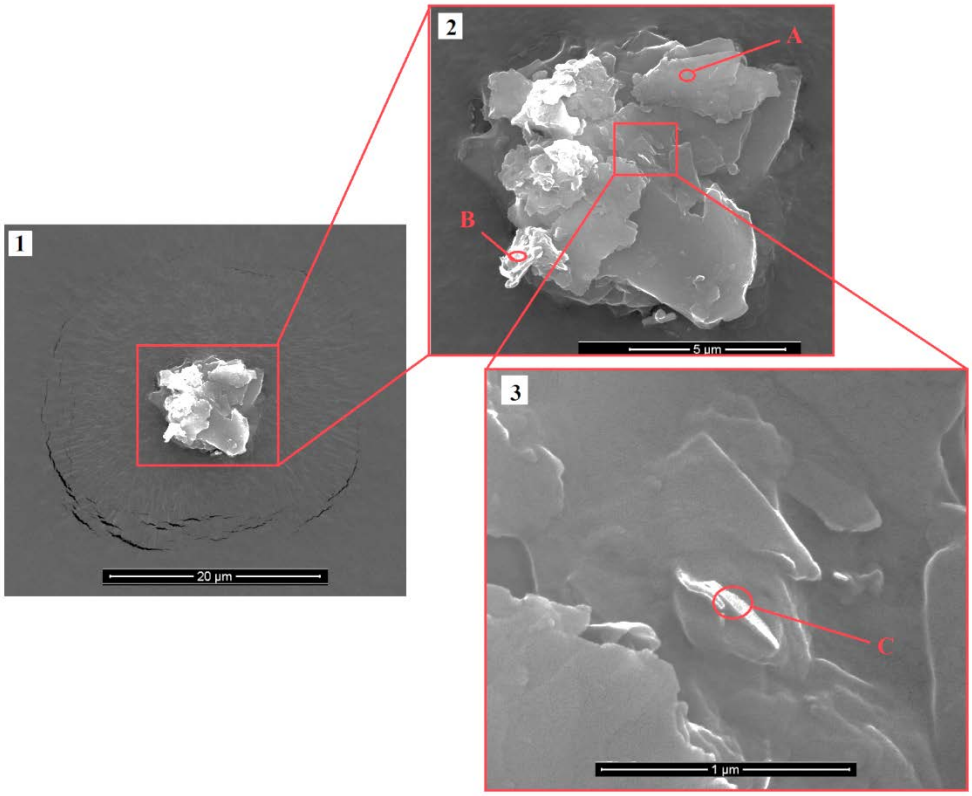

Figure 2-47: A collapsed particle that impacted the SEM at speed

Inset 1 shows the circular rim of the crater, inset 2 and 3 show a zoomed-in view of the particle with A, B, and C representing the different spots of which EDAX measurements shown in Figure 2-48 were taken.

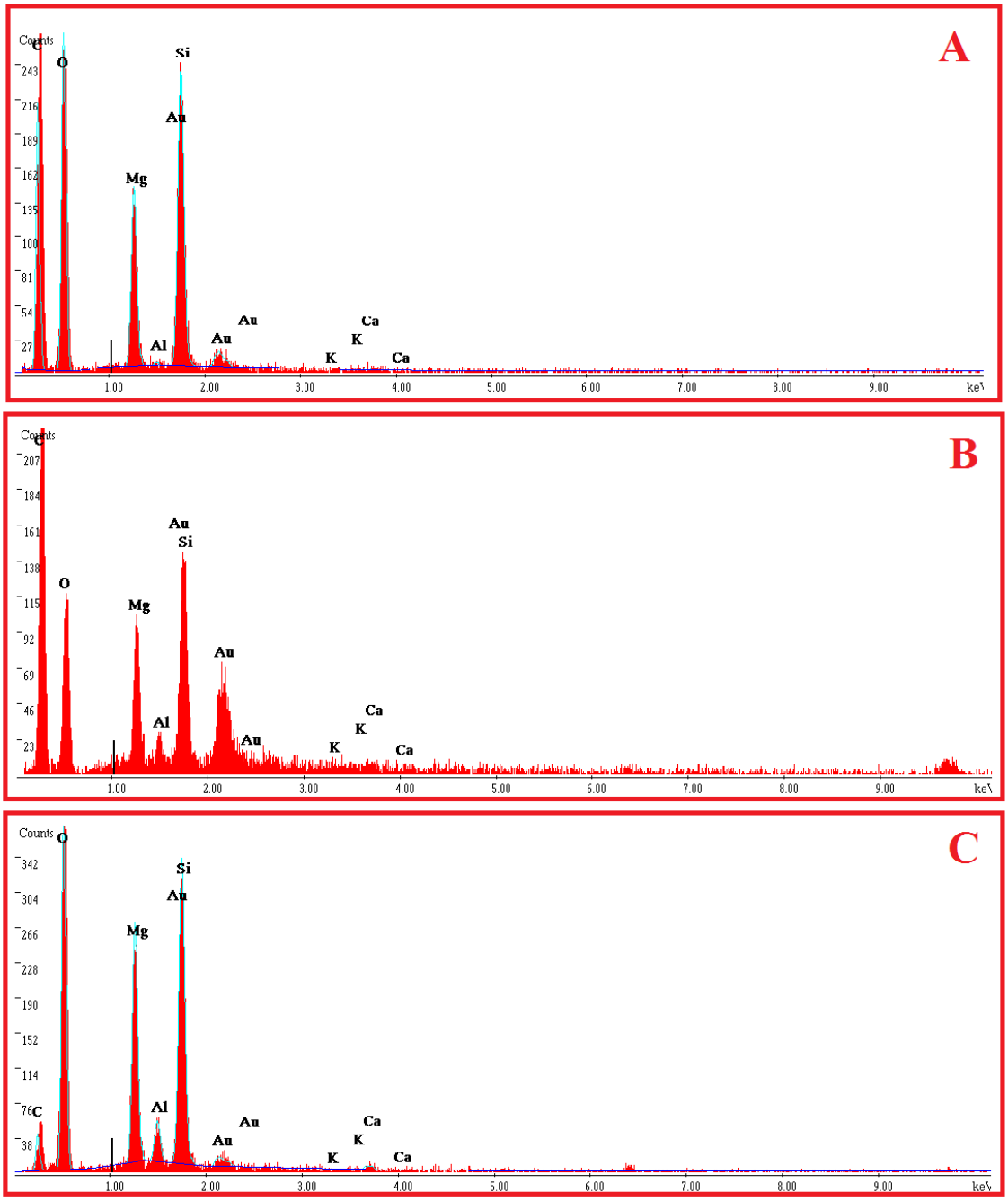

Figure 2-48: Extremely close similarity in EDAX reading between three different regions

Taken for A, B, and C areas which are shown on Figure 2-47 , this indicate a consistent uniform chemical composition for the BE.

The “mucus-based” appearance of the BE shown in Figure 2-49 and the presence of small spherical structures and filaments in many regions of the entity strongly suggest a biological origin for it. As evidenced by the percentage of elemental composition of C and O, in addition to other elements as outlined in the EDAX results. We believe that this particular entity represents a group of microbes which were all surrounded with a biofilm formation; because biofilms are usually formed by microbes when adsorbed to a surface while in an aquatic environment, which is compatible with the theory of microbes surviving inside the comet’s molten core (Wickramasinghe *et al.*, 2007). In addition, Ca is an essential component for the biofilms for structural integrity (Turakhia, 1986), which was also present in the EDAX results.

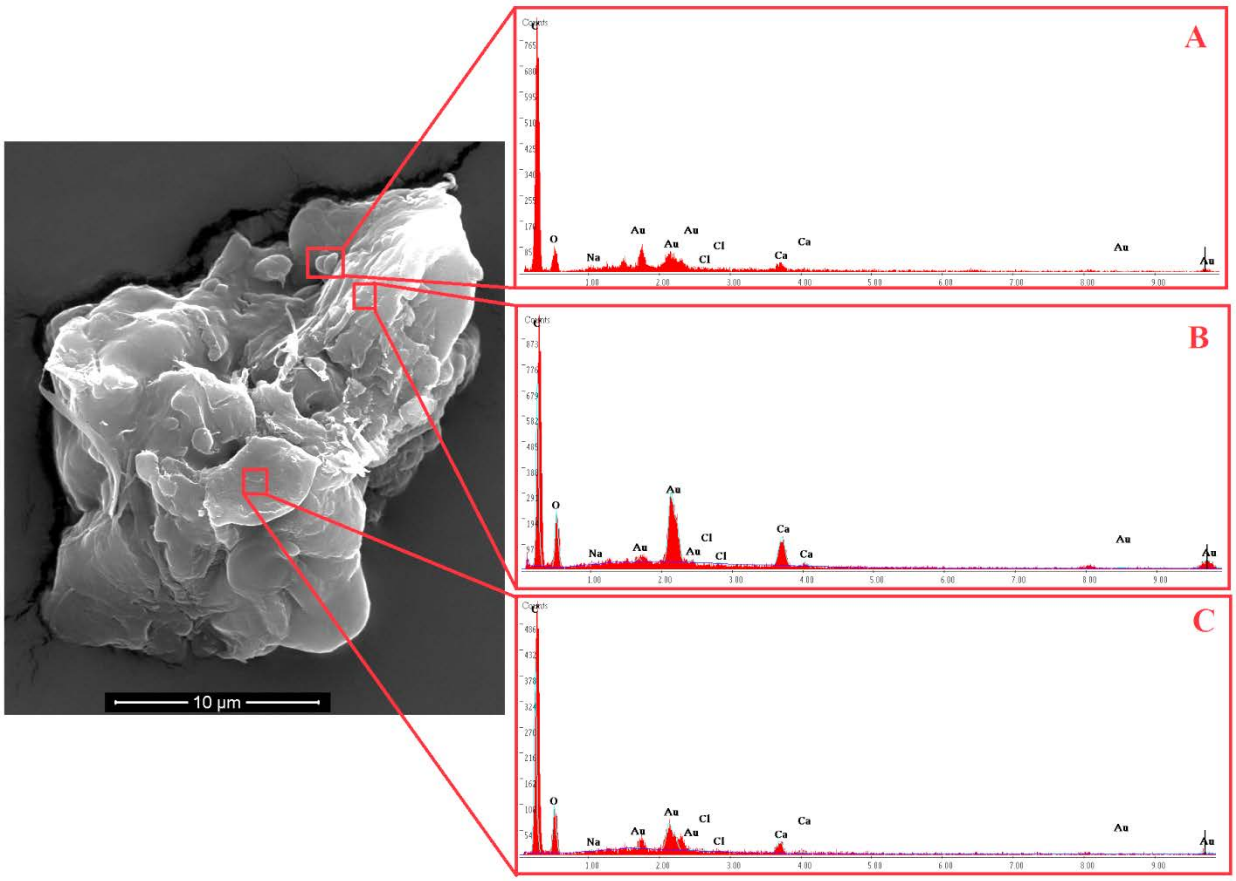

Figure 2-49: A complex entity which appears to be surrounded by a biofilm formation

Showing a prevalence in C and O, as indicated by EDAX readings on the outlined areas in A, B, and C.

The complex formation in Figure 2-50 is a good example of the difference between non-biological particles and the ones we believe to be belonging to living cells; It appears to be comprised of two types of formations: One is closely similar to the membranous-deflated entities shown previously in Figure 2-8 and Figure 2-24 both in morphology and chemical structure (Figure 2-50 C), while the other has the appearance and chemical elements of abiotic dust particles (Figure 2-50 A and B).

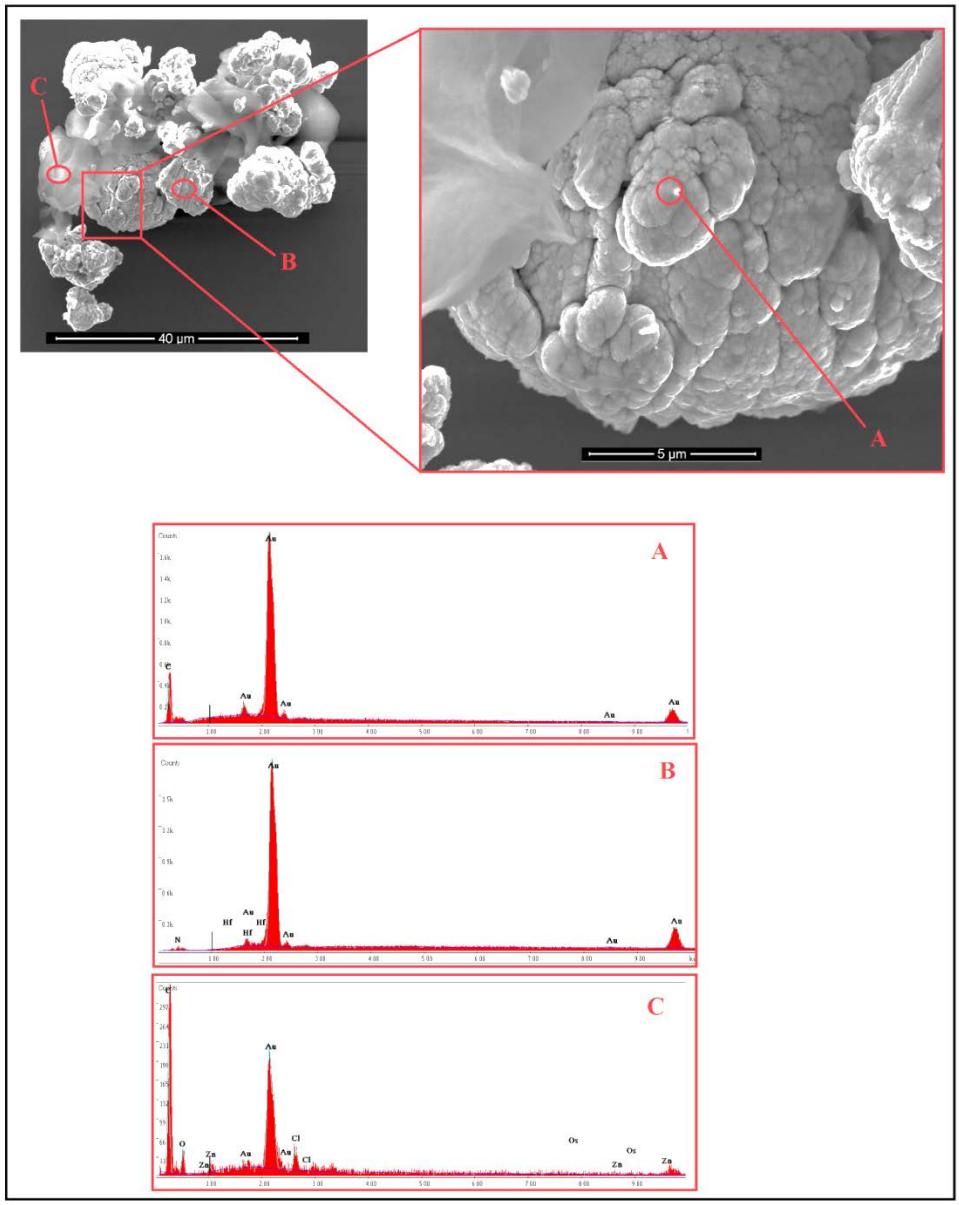

Figure 2-50: An SEM for an entity recovered from the sixth stratospheric flight

In C: a membranous deflated structure, possibly biological with a chemical composition of carbon and oxygen mainly. While A and B appears to belong to an aggregate of non-biological cosmic dust particles; C is almost entirely composed of carbon, and B does not appear to have carbon nor oxygen.

The difference between entities, which we believe to be biological versus none biological, can be seen more clearly by looking at the large entity shown in Figure 2-51, due to its “fragmented” morphology and chemical structure made mostly of Si, followed by elements such as Al, K, and Na, there is little doubt of it being a non-biological cosmic dust particle, the large size of it also eliminates the possibility to have been elevated from the troposphere. The extra-terrestrial origin for the particle is even more evident when considering the clear impact and cracking marks on the SEM stub due to the high-speed impact.

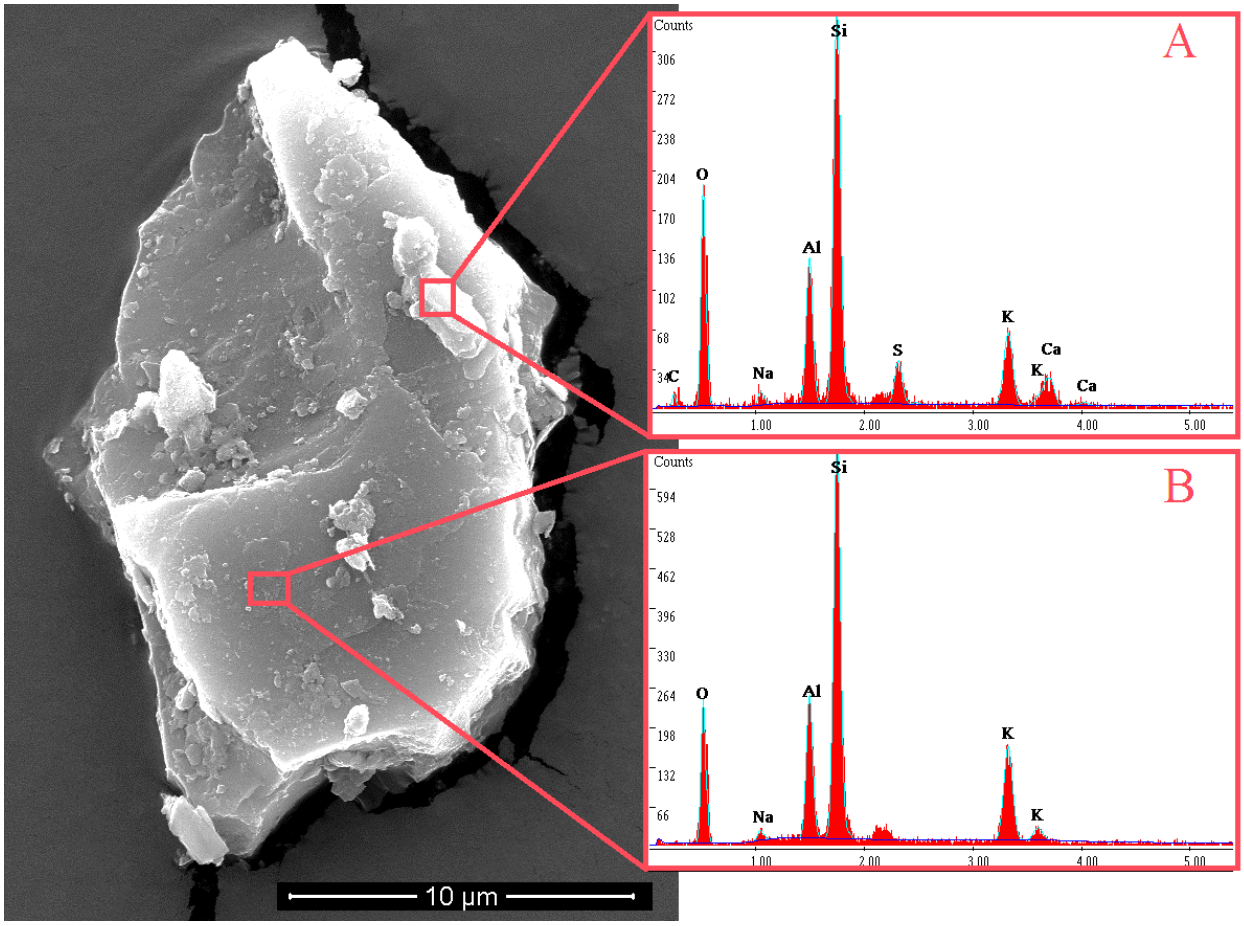

Figure 2-51: An SEM for a large particle, comprising mainly of silicon

The EDAX readings are shown in the two insets to the right, the breakage points in the background behind the particle can also be seen.

It must also be mentioned that all of the launches were made there was no volcanic launches in the short periods prior to it. Although volcanic launches could lift terrestrial microbes above the tropopause, anything lifted will still be brought down due to gravity within a few days (Kasten, 1968). In addition, we analysed (using SEM) particles of the Eyjafjallajökull 2010 volcanic eruption in Iceland (samples were collected by an external partner), and compared them to our recovered BEs; as shown in Figure 2-52, the volcanic ash particles show a clear morphology of being non-biological, unlike the BEs which possess evidently obvious different morphologies.

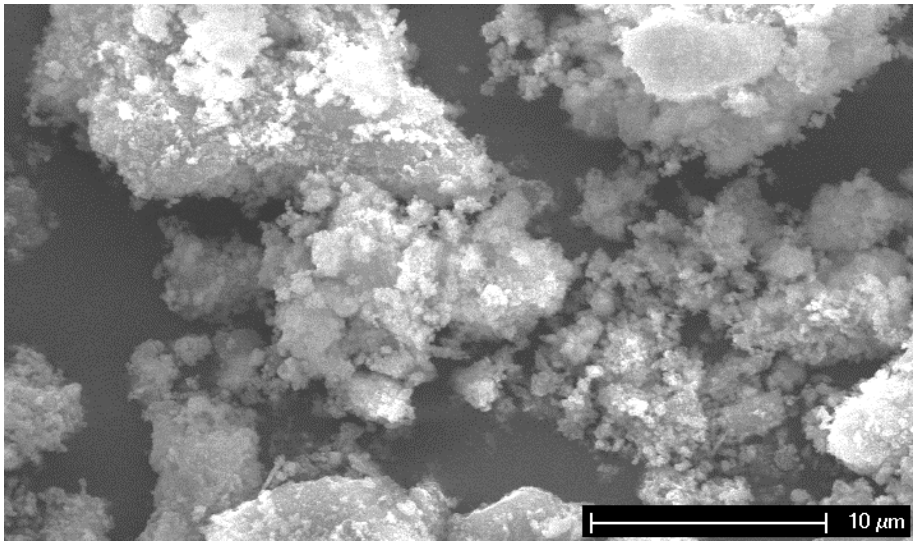

Figure 2-52: Image of the SEM analysis for volcanic dust

Collected from the Eyjafjallajökull 2010 volcanic eruption – Iceland, showing large non-biological particles of the volcanic ash.

2.6 The argument for a space origin for the stratospheric findings

Considering the conditions and facts about space travel, meteorites, and microbial survivability, which were discussed in the introduction, and when reviewing the results obtained over the course of the six balloon launches, we conclude that the biological entities found in the stratosphere have not

been there due to elevation from the troposphere. Instead, we believe that those entities have been entering our atmosphere from space, and are being brought to us through meteorites and comets as their means of delivery. No pollen seeds or grass debris has been ever recovered from any of the SEM stubs which were sent and exposed to the stratosphere, despite that such particles can be of the same size to the ones we reported in this work. The recovered BEs were always found at extremely low frequencies, and occur as isolated pristine entities, and have not been found associated with common-terrestrial organisms. As shown previously in Figure 2-13, the entirety of the sampling box was covered with grass particles and pollen on its outer surface, but never on the inside. The explanation of a terrestrial origin for the stratospheric-isolated particles might be proposed by critics arguing via the application of Occam's razor. However, we view this explanation as a flawed one, since there is no known mechanism that can selectively lift one type of particle (e.g. BEs) into the stratosphere while leaving out others of the same size (known terrestrial microbes and entities). Because such a "sieve" mechanism of lifting our discovered particles is not currently described, we believe that the BEs have been incoming from space; This argument was presented at early stages of the work (Wainwright *et al.*, 2015a) although it did expose us to being "hostages to fortune", because if any of the subsequent missions collect stratospheric pollen grains, then our argument of a space-origin would be weakened. Now, after the completion of six launches, no such terrestrial particles have ever been recovered, a finding compatible with the conclusion reached by other researchers (Kasten, 1968, Dehel *et al.*, 2008) who have calculated the extreme improbability of particles above 5 μm in diameter being elevated to heights above 20 km.

Another reason to conclude the BEs are from space relates to them being associated with impact events on the SEM stubs, manifested by either a crater, such as the one associated with the titanium ball (Figure 2-21), or as a crack or damage on the stub's surface (e.g. Figure 2-19 and Figure 2-49). If those BEs were from the troposphere, they should have impacted with low force on the stubs, and have not made such a visible impact event. Even

when we replaced the SEM stubs in the fourth launch with copper slides instead, we still saw impact events which failed to show on the controls. However, there exists the possibility of those BEs being lifted from the troposphere by an unknown mechanism to extreme heights, then impacting the stubs on their return at speed. That, however, would seem unlikely. The presence of micrometeorite impact on the SEM stubs also helps to address another argument presented by critics; which concerns the presumably low chances of us picking up life-forms on the stubs, because even if life was distributed in the universe, the chances of capturing it on small SEM stubs would be extremely low. Our counter argument is that considering that the amount of cosmic dust entering our atmosphere can reach up to 100,000 metric tons annually (Peucker-Ehrenbrink and Ravizza, 2000), the chances of capturing such particles on the SEM stubs does not appear improbable, and when other factors are put into consideration, like the presence of over 10^9 bacteria per a gram of soil (Whitman *et al.*, 1998), and the timing of many of our launches with or slightly after the Perseid meteor shower event, then the likelihood of capturing extra-terrestrial microbes on the stubs does not appear unlikely. While many of the recovered BEs do appear to have been collapsed upon impact (Figure 2-7 and Figure 2-9), we believe most of those which reaches the surface of sampling stubs while encased in minute ice grains, later to melt leaving the BEs on stubs relatively intact.

Our only case of a BE that is similar to terrestrial organism is the diatom fragment (Figure 2-5), which was evidently broken and damaged. Since diatoms occur in vast numbers in Earth's fresh water and seas, one might use Occam's razor to suggest a terrestrial origin for it, but given the large size of the particle, the improbability of it being lifted up according to the calculations of Dehel *et al.* (2008) remains however, a strong argument. Therefore, we conclude it must have arrived to Earth from space.

The unquestionable detection of DNA from the fifth launch, identification of the microbes from it, and the complete lack of any large eukaryotic cells, illustrate two important points; First: The stratosphere is full of countless types of microbes, as was shown by the sequencing results, some of which have so far only been isolated from extreme and very specific locations (e.g.

Oceanobacillus iheyensis, *Flexistipes sinusarabici*, *Kineococcus radiotolerans*, and *Marinithermus hydrothermalis* - Section 2.5.5.2.C) and are therefore, not laboratory contaminants. Secondly: large cells cannot be lifted from the Earth, despite the strikingly large number of microbial species discovered in the stratospheric samples, none belong to recognizable large-celled organisms, such as fungal of algal cells which are larger than 5µm in diameter. Our results are therefore in agreement with the virtual simulations made by other researchers (Kasten, 1968, Dehel *et al.*, 2008) which state that cells smaller than 5 µm in diameter (e.g. bacterial cells) can be elevated above 20 km, but anything larger cannot (e.g. fungal spores, tardigrades). Therefore, we conclude that the large BE we recovered on the SEM stubs were not terrestrial, but instead were brought in by meteorites and comets. Our findings and argument of the improbability of anything larger than 5 µm in diameter to have been lifted to the stratosphere is supported by the sampling attempt made by Yang *et al.* (2008a) using an aircraft to collect samples; only bacterial strains were found which tended to form small aggregates which were highly tolerant to UV (Figure 2-53).

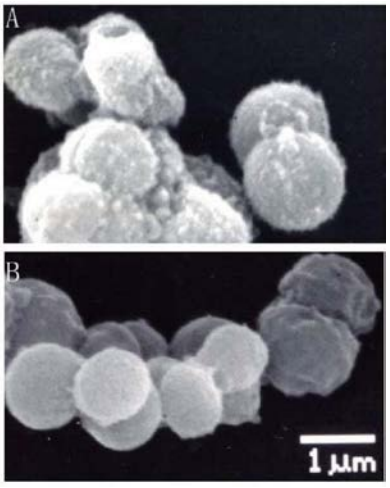

Figure 2-53: Small bacterial cells isolated from the stratosphere by Yang *et al.* (2008a)

The size of the cells means that such cells can be lifted from the troposphere into higher altitudes.

CHAPTER 3

3 Chapter 3: Lithopanspermia - Microbial survival in terrestrial samples, terrestrial rocks, amber and halite.

3.1 Introduction

One of the principal assumptions in the cometary panspermia theory is that microbes can survive long transit times, up to millions of years, when inside meteorites and comets (Horneck *et al.*, 2002b), a possibility which is discussed in this Chapter. UV- radiation survival is then discussed in Chapter 5. The present Chapter also deals with the theory of Archipanspermia, i.e. the possibility of the transfer of microbes from Earth in manufactured building materials. The question of how long microbes can remain dormant will also be considered here.

Aims- The following questions will be considered:

- Can bacteria regain viability after remaining dormant for more than 1 million years?
- How often microbes are found in terrestrial samples? Including rocks, pellets, and manufactured (formed) materials, relating to the reverse-lithopanspermia and the archipanspermia theories.

3.2 Microbial transfer through space within rocks

The effect of meteorites and comets impacting planets like Earth obviously depends on the bolide size, leading to possibly altering the distribution of life-forms on the planet (Gladman *et al.*, 1996, Cockell *et al.*, 2006). Despite the life-threatening impacts of meteorites, they also provide the necessary ejecting force to lift and throw some of the planet's terrestrial rocks away to escape the planet's gravity, some of the rocks may contain embedded microbes, which might survive the associated shock and heat conditions. Such impact ejecta can leave the planet and carry life through the cosmos, or subsequently return to Earth and possibly re-populate it with life should

the conditions again become suitable. Such possibilities are referred to as lithopanspermia; the theory that microbes can be transported throughout space inside rocks, and seed other planets with life (Horneck *et al.*, 2002a, Valtonen *et al.*, 2009). The theory of lithopanspermia assumes that microbes do not grow in the ejecta, but survive for the necessary long transit periods, by being protected from adverse conditions. It is becoming increasingly fashionable to suggest that life may have been transported to and from Mars during the heavy bombardment period (Mileikowsky *et al.*, 2000). Although there is, as yet, no direct evidence for this, the discovery of water on the ancient and contemporary surface of the red planet (Ojha *et al.*, 2015), suggests that Mars may have been previously habitable (Knoll and Grotzinger, 2006, Tosca *et al.*, 2008), which together with the fact that some 40 Martian meteorites have been found on Earth (Weiss *et al.*, 2000), backs up this possibility should signatures of past or present life be ever discovered on Mars.

A study by Worth *et al.* (2013) has attempted n-body simulations, to predict the final end-destination within the solar system for ejected Martian and Earth rocks; they conclude that it is highly probable that material can be transferred between planets (e.g. from Mars and Earth to the moons of Jupiter and Saturn), with most of the transfers happening during the last stages of the heavy bombardment period and beyond (i.e. up to two billion years ago), thus showing relevance to the new investigation of the possibility of life on the moons of Saturn and Jupiter (Parkinson *et al.*, 2014, Mayson and Morris, 2015).

The main question considered in this Chapter is not however, whether microbes can survive the ejection and the re-entry stages of panspermia, but to investigate if microbes could survive the long transit time through space and retain the ability to seed new habitable planets. The transfer of rocks throughout space, even within relatively short distances such as between Earth and Mars would take about one to twenty million years (Nyquist *et al.*, 2001), although shorter timescales for meteorite transfer have been proposed by Gladman and Burns (1996).

3.3 Long-term preservation of bacteria in various samples

As stated earlier, an essential aspect of lithopanspermia-related long transit time is for microbes to be able to survive long “hibernation” periods, assuming that lethal factors are to be avoided. For obvious reasons, it is not possible to study the survivability of bacteria over long geological time periods. However, the potential long-term preservation of microbes can be still evaluated from the many types of ancient samples existing on Earth, including salt crystals, drilled ice and deep earth cores, fossilized remains of plants and animals, and amber (Hoyle and Wickramasinghe, 1981a, Cano and Borucki, 1995, Wainwright *et al.*, 2009).

Lipman (1931) reported finding living bacteria in anthracite coal from Pennsylvania, and subsequent studies also identified viable bacteria in ancient samples; however, critics have always invoked contamination to explain such results. Estimates based on survival curves for extant bacteria also suggest and that accumulating damage over long time-scales, and macromolecular decay would limit the long-term viability of bacterial cells (Hebsgaard *et al.*, 2005, Sankaranarayanan *et al.*, 2011, Paéibo, 2012).

The long term survival of bacteria in ancient samples is generally attributed to the formation of endospores, especially in relation to members of the genus *Bacillus*, the contents of which are dehydrated and encased in a protective, thick protein coating which allows the endospore to endure extreme condition such as heat, radiation, shock and pressure, in addition to a range of chemical factors. The resistance of the spore to such factors is due to its reduced metabolic activity, the slowing or halting of enzymatic activity, loss of fluids, and conformational changes of the DNA, possibly allowing for a “hibernating” state lasting millions of years (Nicholson *et al.*, 2000, Atrih and Foster, 2002). A unique quality in endospores is that, despite their apparent inactivity and persistence against outside harmful factors, they can maintain a special sensory alert mechanism, which allows them to respond to the availability of certain nutrients; thus leading to germination and the subsequent outgrowth of a new vegetative cell.

Cano and Borucki (1995) attempted to isolate bacteria from Dominican amber samples in order to determine if microbes can survive for extremely long periods. They used amber samples containing an embedded species of an extinct bee. This research was based on the fact that modern bacteria often exhibit a symbiotic relationship with modern bees, in which they occupy the abdominal area of the insect, e.g. *Proplebeia dominicana*. Those extinct bees have been preserved in amber for a period of 25-40 million years. Extensive sterilization techniques to clean the amber from the outside were employed by the above mentioned authors, before breaking and attempts at culturing any bacteria present. By using 16S rRNA, an amber isolate was found to be closely related to *Bacillus sphaericus*. The implication of this study, regardless of the type of the isolated microbe, is that an organism, which has been "dormant" for close to about 20- 40 million years, was apparently revived, and regained the ability to multiply and be fully metabolically active, thereby providing evidence to argue that microbes can survive during the long-times required for panspermia.

The fact that amber-bacterium isolated by Cano and Borucki (1995) belongs to the spore forming and ubiquitous genus *Bacillus*, is obviously important in relation to its claimed long term survival. However, despite the claimed care that was taken to avoid contamination, the obvious criticism to such studies is that the apparent amber-related bacterium is a modern bacterium (Willerslev *et al.*, 2004). One of the few studies dedicated to isolating microbes from amber in relation to lithopanspermia was undertaken by Wainwright *et al.* (2009), two microorganisms were isolated from the amber samples, which were then identified using 16s rRNA as *Bacillus amyoliquifaciens*, and *B. cereus*, the study concluded that microbes can survive being dormant for long geological periods which could be transferred throughout the cosmos within meteorites and comets.

In the last two decades, many researchers have concentrated their attempts to isolate microbes embedded in glacial ice and permafrost (i.e. soils that are permanently frozen); the reason for this is because of the assumption that owing to the permanent-stable low temperatures of such environments, they represent an ideal environment for microbial preservation over extremely

long periods. Viable microbes and nucleic acids have been isolated from both ice-cores of glacial ice (dating up to 100k years), and permafrost soils (2-3 Million years) (Catranis and Starmer, 1991, Castello *et al.*, 1999, Christner *et al.*, 2000, Ma *et al.*, 2000, Willerslev *et al.*, 2004), results which have obvious implications for panspermia. However, contamination issues were again brought up to discredit such findings; Willerslev *et al.* (2004) argue for example, that DNA and RNA would degrade overtime, with a maximum “shelf-life” of one million year.

Fluid inclusions in evaporate minerals (halite, gypsum, etc.) have also been studied in relation to panspermia because salt deposits, which forms by the evaporative concentration of brines on the surface of the Earth, can then be buried in the sub-surface and remain unaltered and locked away from external conditions for periods reaching up to millions of years (Benison and Goldstein, 1999, Satterfield *et al.*, 2005). Such environments are considered good repositories for the survival of microorganisms and the preservation of DNA based on their dark, hypersaline, and low O_2 environment, which makes them resistant against oxidative damage, radiation, and hydrolysis (Schubert *et al.*, 2010). Subsequent studies have attempted to use PCR and nucleic acid sequencing to examine the bacterial diversity within the fluid inclusions on the genetic level (Park *et al.*, 2009). In a recent study Sankaranarayanan *et al.* (2011), reported that although the surface sterilization protocols for the halite samples within the previously mentioned studies can be efficient in rendering any contaminants non-viable and thus enable the extraction of viable ancient ones from the samples; however, their effectiveness against contaminating DNA, which might interfere with the PCR investigation, is still unclear.

3.4 Predicting the long-term survival for nucleic acids

A number of studies have attempted to put a “shelf-life” for the survivability of DNA, including the racemization of nucleic acid, extrapolations of DNA in solution, and the thermal age (Hebsgaard *et al.*, 2005). Most of the earlier studies have relied on the simplistic approach based on hydrolytic

depurination as the only source of significant destabilization for DNA, although cross-linking may be more significant to the retrieval of the nucleic acid sequences (Willerslev *et al.*, 2004). However, although more is now understood about DNA degradation rates during different geological conditions, accurate theoretical calculations for the long-term survival of DNA are still not available (Hebsgaard *et al.*, 2005, Paéibo, 2012). Some bacterial cells might be able to maintain a continuous, yet slow metabolic activity, which might allow for genomic DNA repair to proceed overtime (Rivkina *et al.*, 2000); alternatively, long-term survival can be attributed to a yet non-measurable alternative pathway, which might employ the H_2 content of spores (Morita, 1999).

In summary, although most of the previous models have predicted a survival time of around 100K years maximum for short pieces of amplifiable DNA (Hebsgaard *et al.*, 2005), more recent studies have shown that in many cases, DNA can be recovered from samples dating to 300–400 K years. Those findings are now widely accepted by the scientific community, and a maximum age for DNA survival of 1 million year is now considered feasible (Paéibo, 2012). However, as Hebsgaard *et al.* (2005) comment that “Despite the problems of modelling the long-term survival of DNA in the geosphere, empirical claims of geologically ancient DNA (gaDNA) in the order of 1000-fold older than theoretical predictions for maximal DNA survival are cause for considerable concern”. If any of the numerous results reported for the isolation of microbes over a 1 million years old is to be accepted (Cano and Borucki, 1995, Greenblatt *et al.*, 1999, Wainwright *et al.*, 2009, Sankaranarayanan *et al.*, 2011), then the theoretical maximum life limit of DNA (which is currently 1 million years) clearly needs some re-evaluation.

The work described in the Chapter was aimed at isolating and then identifying microbes from a variety of potential panspermia “vehicles” using what we suggest is a contamination-proof approach.

3.5 Materials and Methods

3.5.1 Isolation of Microbes from Baltic Amber samples

3.5.1.1 The amber pieces used for the study

Authentic Baltic amber samples were obtained from various suppliers, who estimated them to date between between 35- 44 million years ago; all contained fossilized insect remains of Long-Legged Flies (Diptera: Dolichopodidae). The authenticity of each piece was verified by submerging it in salt water (when the sample floats), and by the emission of a pine resin odour when exposed to a red hot needle (Poinar, 1992). Before starting with any work on the amber samples, they were checked thoroughly with a low resolution microscope to check for the absence of deep cracks which might contain contaminants; only perfect samples were then used. Six amber samples were finally selected; all were confirmed as genuine samples and crack-free, as shown in Figure 3-1.

Figure 3-1: The amber samples selected for the attempted microbial isolation

The scale shown in the lower left is for all of the samples.

3.5.1.2 The sterile-breaking apparatus

In order to guarantee a contamination-free environment, a modified 50ml Duran bottle was used in which a steel plunger passed through a hole in the plastic cap reaching the bottom of the bottle. The top of the cap and the plunger were completely sealed with an autoclavable bag using autoclave tape as shown in Figure 3-2. A thick rubber plate was placed on the inside base of the vessel to strengthen it and prevent the accidental breakage of the glass by the steel plunger. The bottles were then filled up with Nutrient Broth (20 ml), re-sealed, and autoclaved for 15 min at 15 psi pressure–121°C.

Figure 3-2: The sterile samples breakage apparatus

Modified Duran bottles were used with a steel plunger; an autocleavable bag was used as a seal.

Each amber sample was then submerged in commercial bleach (10% v/v) for 30 minutes, transferred to 70% (v/v) alcohol for 5 minutes, then into sterile water for washing, and finally transferred into the modified Duran bottle using an alcohol-flamed forceps; the bottles were then sealed immediately. The whole process described above was performed in a Class II laminar flow hood, the sterility of which was checked periodically. Control samples were also used to test the sterility of the process by performing the same steps but without adding any samples into the bottles.

After the addition of the amber, the vessel was incubated for 72 hours at 25°C and then another extra 72 hours at 37°C, while being examined by eye daily for signs of growth; if any of the bottles showed an indication of microbial growth they were immediately disregarded and the experiment was repeated from the start until a contamination-free medium, with no growth obtained.

When no growth was observed after the incubation period, the samples in the growth-free bottles were cracked *in situ* and the bottles were again incubated at 25°C and 37°C respectively for 3 days. If the bottles showed positive growth for bacteria, the growth was streaked onto Nutrient agar, and incubated at 37°C for 24 hours to obtain single colonies of pure isolates. Single colony forming units (CFU) were then selected and transferred into Nutrient Broth (5ml) and incubated for 18 hours at 37°C; extraction of bacterial nucleic acids and PCR 16S rRNA was performed.

3.5.1.3 DNA Extraction

A PowerSoil®DNA Isolation Kit (Cat: 12888 - MO BIO laboratories Inc.) was used to isolate the DNA from the amber samples for the purpose of 16s rRNA PCR. Lysozyme and various buffers (supplied by the manufacturer) were used to lyse the cells, the resulting soluble fraction was then treated with protein precipitation reagent, and filtered through a spin column containing a silica membrane to catch and hold the DNA, purification was done for the DNA using ethanol and buffer washing solutions; 100µ of elution buffer was then added, the diluted DNA was stored to be confirmed later by gel electrophoresis. The procedure is described in detail in the handbook for the kit; here, the basic steps undertaken and modifications made on the original protocol are mentioned:

From the microbial growth in the Nutrient Broth, 100 µl of was added to the PowerBead tubes (in the original protocol, 0.25 gm of soil is added), and vortexed briefly, then, about 60µl of solution, C1 was added, and the mixture is inverted several times. The tubes were then all secured horizontally on a flat-bed vortex pad, and were fixed firmly using tape, and vortexed at the maximum setting for 10 minutes. After vortexing was finished, the tubes were centrifuged for half a minute at 10,000 x g, and the supernatant was transferred to 2ml collection tubes, where 250µl of solution C2 was added and then the tubes were vortexed for five seconds, followed by a five-minute incubation at 40C. Later, the tubes were centrifuged at room temperature for 60 seconds at 10,000 x g, 500µl of the supernatant was then transferred to a new 2ml collection tube, where 200µl of solution C3 was added, and the mixture was then vortexed for a few seconds before being incubated for five

minute at 40C. Later, the tubes were centrifuged for one minute at room temperature at 10,00 x g, and then 600µl of the supernatant was transported into another sterile 2ml collection tube, 1200µl of C4 solution was then added and the mixture was vortexed for five seconds. Then, about 675µl of the mixture was loaded onto a spin filter, and centrifuged at 10,000 x g for one minute at room temperature, the flow through was disregarded and additional 675 µl of the supernatant was added again to the spin filter, and centrifuged again at 10,000 x g for one minute, finally, the remaining supernatant was loaded on to the spin filter and centrifuged as before for one minute. solution C5 was then added 500µl and centrifuged for 30 seconds at 10,000 x g, the flow through was discarded and the filters were centrifuged again at room temperature for an additional minute at 10,000 x g, then the spin filter was placed in a clean 2 ml collection tube, and 100µl of solution C6 was added to the centre of the white filter membrane, before centrifuging at room temperature for 30 seconds at 10,000 x g. As a final step, the spin filter was disregarded, with the DNA remaining ready in the tube for other downstream applications. The DNA extracts were kept at -20°C when not in use. The diluted DNA was stored to be confirmed later by gel electrophoresis.

3.5.1.4 Agarose gel electrophoresis

Extracted genomic DNA and PCR products were examined using gel electrophoresis, in all cases, 10 µl of the samples were mixed with 2 µl of 6X loading dye and were set to run on a 1% Agarose gel (w/v), the gels were submerged in 1X TAE buffer supplied by (Fisher Scientific, cat.BP1332), Hyper Ladder 6 µl was used to help confirm the existence of DNA in the samples.

The gel was prepared by adding 1gm of agarose into 100ml of 1X TAE in a 250 ml flask, complete dissolving of the agarose was achieved by placing the flask in the microwave for complete homogenization, then the mixture was allowed to cool down to 55°C before the addition of 4µl Ethidium bromide stain (Fisher Scientific, cat.E/P800/03), in order to demonstrate the DNA under the UV light later. Then, the mixture was poured in the BioRad Subcell GT electrophoretic tank and allowed to harden. Subsequently, an

electric current of 80 volts was ran through the gel for 40 minutes, viewing and photographing of the DNA's bands was performed using a Uvitec "Uvidoc" mounted camera system.

3.5.1.5 Amplification, extraction and purification of 16S rRNA

After successful extraction of the bacterial genome, the amplification of 16S rRNA gene from the rest of the DNA extract was achieved by the Polymerase Chain Reaction (PCR) technique, Table 3-1 shows the various components and quantities used for the 16S rRNA bacterial gene amplification.

Table 3-1: PCR reaction mixture (Weisburg *et al.*, 1991)

Component	Bacterial 16S rRNA
Sterile Milli-Q water	27.0 – 31.0 µl
dNTP mix (2.5 mM each)	5.0 µl
MgCl2 solution (50 mM)	6.0 µl
AmpliTaq polymerase (5 U/µl)	0.5 µl
10x Taq buffer	5.0 µl
Forward primer (10 ppmole.l^{-1})	0.5 µl
Reverse primer (10 ppmole.l^{-1})	0.5 µl
DNA template (10 – 100 ng)	1.0 – 5.0 µl

For the amplification of 16S rRNA gene; bacterial universal primers detailed in Table 3-2, were used, supplied by Eurofins (mwg/operon), Germany (Heuer *et al.*, 1997).

Table 3-2: The nucleotide sequences of the two primers used for 16S rRNA PCR

Primer name	Sequence (5'-3')	Target Gene
F27	5′-AGAGTTTGATCMTGGCTCAG-3′	Bacterial 16S rRNA
R1492	5′-TACGGYTACCTTGTTACGACTT-3′	Bacterial 16S rRNA

The settings for the thermal cycler were the following: denaturation step at 94°C for three minutes, followed by 30 cycles of DNA denaturation at 94°C for one minute, annealing 45°C, and strand extension at 72°C for 2 minutes. This thermal profile was set onto 30 repeated cycles for denaturation, annealing and extension.

Confirmation of positive PCR products was by agarose gel electrophoresis with 10 µl from each amplification mixture, purification of the products was achieved with QIA quick® PCR Purification kit by following manufacturer's instruction (Qiagen, UK). After that, the PCR products (16S rRNA gene) presence and yield was determined by running the samples on 1% (w/v) agarose gel at 200 V for one hour in 1X Tris-acetate-EDTA buffer, made visible by ethidium bromide staining and subsequent UV transillumination. Later, the PCR products were sent for sequencing to the Core Genomic Facility, University of Sheffield-UK, using the Applied Biosystems' 3730 DNA Analyser.

3.5.1.6 Sequence analysis

After the sequencing data were received back, nucleotide sequences were analyzed using the Finch TV software, Version 1.4.0 (Geospiza Inc, USA). Those sequences were then used to identify their species origin, using the Basic Local Alignment Search Tool (BLAST) by matching it with the closest reported sequence uploaded to the National Centre for Biotechnology Information (NCBI) Genbank database.

3.5.2 Isolation of microbes from terrestrial rock samples

Seventeen rock samples were collected from various urban areas around the University's campus (Figure 3-3); samples were placed in sterile petri dishes until used.

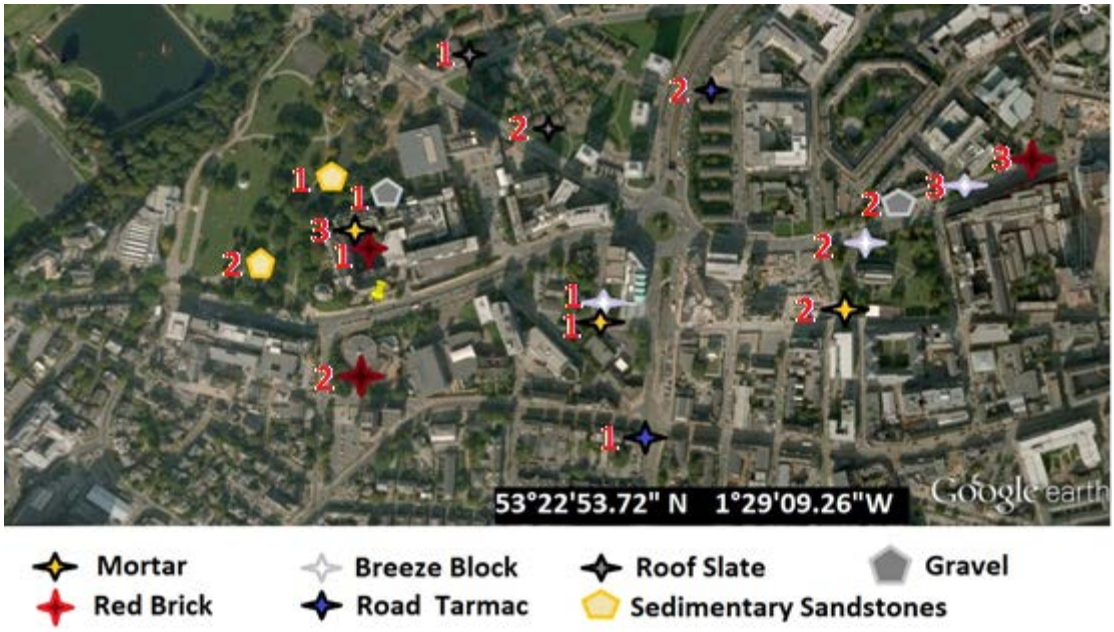

Figure 3-3: A Google aerial image showing the collection sites of the rock samples

The samples were collected from the areas surrounding the main University campus.

The selected samples included: Manufactured or modified building material and rocks that occur in nature, which were: roof slate (2), road tarmac (bitumen)(2), red brick (3), mortar (the material between bricks)(3), breeze block (3) , natural geosamples included, sedimentary sandstone (2) and gravel (2).

All the subsequent handling of the samples, including breaking the rocks, growth of the microbes, DNA extraction, gel-electrophoresis, 16S rRNA PCR amplification, and DNA sequencing were performed using the same materials and techniques as used previously with the amber samples.

3.5.3 Isolation of microbes from halite crystals

Salt deposits, formed by evaporative concentration of brines at the Earth's surface, can be buried in the subsurface in relatively unaltered condition for hundreds of millions of years (Hardie *et al.*, 1985). Salt is an abundant and valuable natural resource in Kansas, USA, from where the halite samples

used here were obtained. Halite is the mineral name for salt (i.e. NaCl, sodium chloride), and is typically white in colour; however, it can appear in a spectrum of other colours depending on the impurities present (Carter and Heard, 1970). In Kansas, salt is usually extracted from the Hutchinson Salt Member of the Wellington Formation (Figure 3-4). It was deposited during the Permian Period, about 275 million years ago, and covers about 37 thousand square miles of the subsurface of central and south central of Kansas. The majority of the rocks in the Hutchinson Salt Member are salt, with only less than 20 percent being shale, with the result that this region contains more salt, with less impurities, than most other salt beds (Dellwig, 1968).

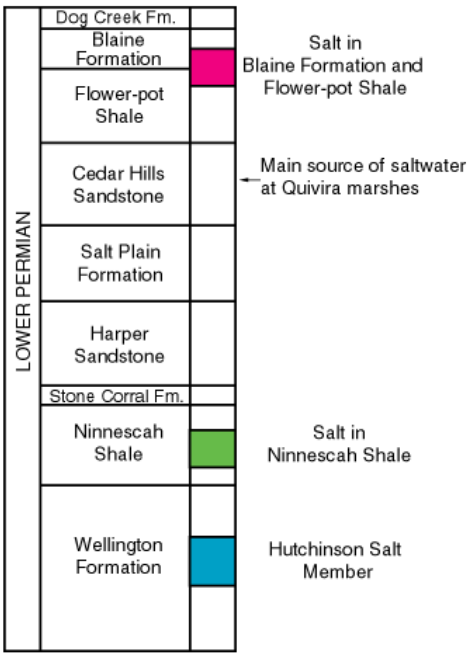

Figure 3-4: Sequence of rocks associated with salt deposits in Kansas

Data taken from Kansas Geological Survey, Public Information Circular 2002.

Five salt crystals were selected for this study, all taken from the Hutchinson, Kansas salt mine (Strata) in the USA. The presence of delicate crystal structures and sedimentary features are signs that these salt minerals have

not recrystallized since the time they were formed. The following methods to study the crystal were modified after the techniques described by Vreeland *et al.* (2000):

The selected five crystals, between 5-10 mm in diameter, all contained brine inclusions (Figure 3-5). They were cleaned and polished using distilled water in order to remove any soil contaminants and dissolve and minimize any small fissures that might block the sterilizing liquid from reaching into the complete outer surfaces of the crystal. Another benefit of the water washing is it increases transparency and makes it easier to see brine inclusions and monitor the subsequent drilling process.

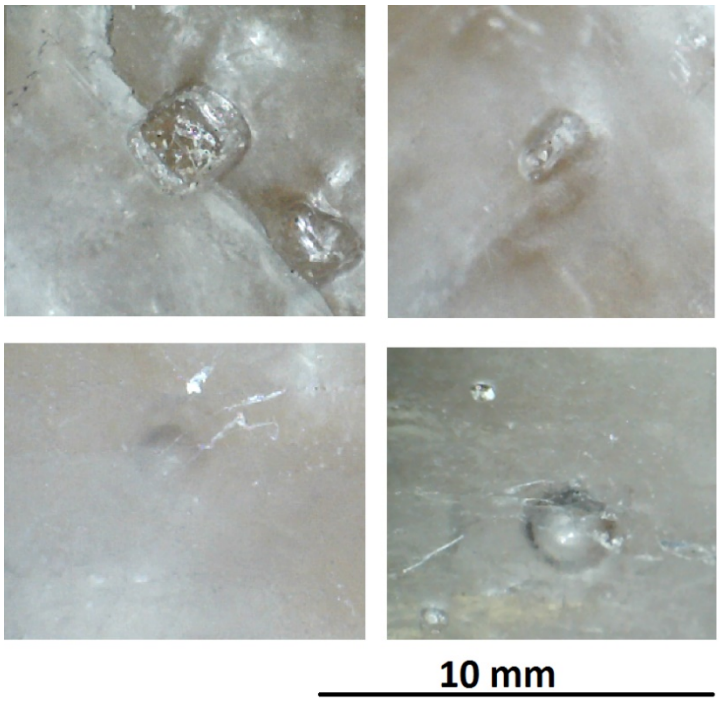

Figure 3-5: Some fluid inclusions in the halite salt crystals

The scale bar shown at the bottom is the same for all images.

The cleaned samples were then transferred into a class II laminar flow hood, the sterility of which was checked periodically. Sterile gloves were used all the time when handling the samples and every precaution was undertaken to avoid contamination from the lab, a UV-C sterilizing lamp was used to decontaminate the hood for a period of two hours before use; all equipment,

including the glassware, culture media, forceps and tweezers were sterilized by autoclaving at 121^0 C for 15 minutes. The media culturing any potential recovered microbes from the halite crystals were prepared into 250 ml flasks (50 ml of casein-derived amino acids liquid medium (CAS) in each flask). In order to make sure that the media were completely sterile, after sterilization of the flasks, all were incubated at 37ºC for 72 hours before use. Only when no signs of microbial growth is observed, the medium was used further.

After the initial sterilization of the crystals by washing, the samples were placed in previously sterilized beakers and covered when not in use. Later, each of the crystals was immersed in 10 M of NaOH for five minutes, then washed briefly in a saturated brine solution for a couple of minutes, before immersing in 10M HCl for five minutes, finally the crystals were washed again in the saturated brine solution for another two minutes. The solutions used during the sterilization and washing processes were replaced after use for each crystal, in order to avoid cross contamination. While the crystals were inside the sterile, decontaminated laminar hood, they were held carefully by hand, using sterile gloves, and a sterile needle and syringe were used to slowly drill a narrow shaft into the inside of the crystal, this was done by repeatedly rotating the syringe in order to drill the sample. When the brine inclusion was finally reached, the needle and the syringe were disregarded, and a new one was used to aspire the liquid from the inclusion, and carefully place it in the CAS flasks. The flasks were then placed in the incubator for 72 hours at 25ºC, and then for another 72 hours at 37ºC.

As a precautionary step to ensure sterility of the work, some crystals were drilled in locations other than the inclusions, and then a needle was use to simulate the aspiration action as before, this acted as the negative control for the experiment, if the work is sterile, no growth should be observed in the flasks that were inoculated with these randomly selected drilling locations on the crystals.

When the flasks of the brine inclusions samples showed positive signs of growth, the DNA extraction protocol, gel electrophoresis, 16S rRNA PCR

amplification, DNA sequencing, and sequence analysis were all done with the same material and steps as was previously used in the amber and terrestrial rock samples.

3.6 Results

3.6.1 Growth from the Amber and the terrestrial rock samples

None of the six amber samples showed any sign of microbial growth in the medium prior to cracking, demonstrating the efficiency of the surface sterilization procedure before the breaking of the amber in the sealed vessels. However, all of the amber samples showed no growth signs after smashing them inside the media within the sterile breakage containers. It is worth mentioning, that the containers giving negative results for growth were kept in room temperature after the experiment for a period of three months, and still did not show any growth. This provides good evidence for the contamination-proof guarantee of the technique.

AsTable 3-3 shows, most rock samples showed initial growth after sterilizing and placing them in the container without breaking, despite several repeats the result were the same. We excluded contamination and instead explain this by the fact that the rocks were porous by nature, and since they can never be truly sealed, this suggests that microbes can enter the rock samples and be lifted form Earth into space, while being shielded from radiations, heat and shock stresses. To confirm this, we isolated bacteria from the rock, and compared the sequence with that of bacteria isolated from the same rocks after sealing the pores with melted paraffin wax (this time there was no growth prior to the cracking), breaking the wax-coated rocks *in situ* and then isolating any microbes which grew. Both isolated bacteria turned out to be identical which further confirms the above-mentioned conclusion. The suitability of such porous rocks for providing protection against intense solar UV radiation during panspermia is further confirmed by a study from Bryce *et al.* (2014) which shows that certain

microbes can grow within rock-cracks and pores and thus be protected from any harmful radiation.

The igneous pebble samples did not show any sign of microbial growth prior and after the breaking, presumably because these rocks have a smooth non-porous surface which creates a physical barrier against the entrance of microbes.

Table 3-3: Growth results of the rock samples after and before breaking, and the DNA sequencing results.

Rock Samples	Growth prior to cracking	Growth after cracking	DNA sequencing results
Roof slate 1	Positive	Positive	*Bacillus subtilis*
Roof slate 2	Negative	Positive	*Bacillus cereus*
Road tarmac 1	Negative	Negative	-
Road tarmac 2	Negative	Negative	-
Red brick 1	Positive	Positive	Rhizobium sp. IRBG74
Red brick 2	Negative	Negative	-
Red brick 3	Positive	Positive	*Bacillus licheniformis*
Mortar 1	Positive	Positive	*Bacillus subtilis*
Mortar 2	Positive	Positive	*Bacillus subtilis* & *Bacillus cereus*
Mortar 3	Negative	Positive	*Bacillus subtilis*
`Breeze block 1	Positive	Positive	Bacillus sp. FJAT-17862
Breeze block 2	Positive	Positive	*Bacillus subtilis*
Breeze block 3	Positive	Positive	*Bacillus subtilis*
Sedimentary sandstone 1	Positive	Positive	*Rhizobium sp.* IRBG74 & *Bacillus subtilis*
Sedimentary sandstone 2	Positive	Positive	*Bacillus subtilis* & *Bacillus licheniformis*
Gravel 1 (Pebble)	Negative	Negative	-
Gravel 2 (Pebble)	Negative	Negative	-

3.6.2 Growth from the halite mineral samples

As explained earlier in section (3.5.3), the brine within the inclusions from the five mineral samples that were selected and used in this study was aspirated and transferred into flasks containing sterile CAS media; of the five flasks, only one showed a positive sign of growth after the incubation period. About 100µl was taken from the flask showing growth, and streaked on a Nutrient Agar plate and incubated for 48 hours at 37^{o}C to obtain single colonies. All of the colonies showed the same characteristics, and were shown under the light microscope to belong to the same species. One CFU was then selected for subsequent DNA extraction and identification protocols.

3.6.2.1 DNA Extraction results

The extraction protocol was applied on all the pure isolates from the nutrient broth tubes, and the presence of genomic DNA was confirmed by gel-electrophoresis procedure before proceeding to the next step, Figure 3-6A shows the HyperLadder 1 used to determine the size of DNA molecules to help in recognising successful genomic DNA extractions, while Figure 3-6B shows the Hyperladder 1 in action along with the successfully extracted DNA which was unidentified at the time prior to sequencing.

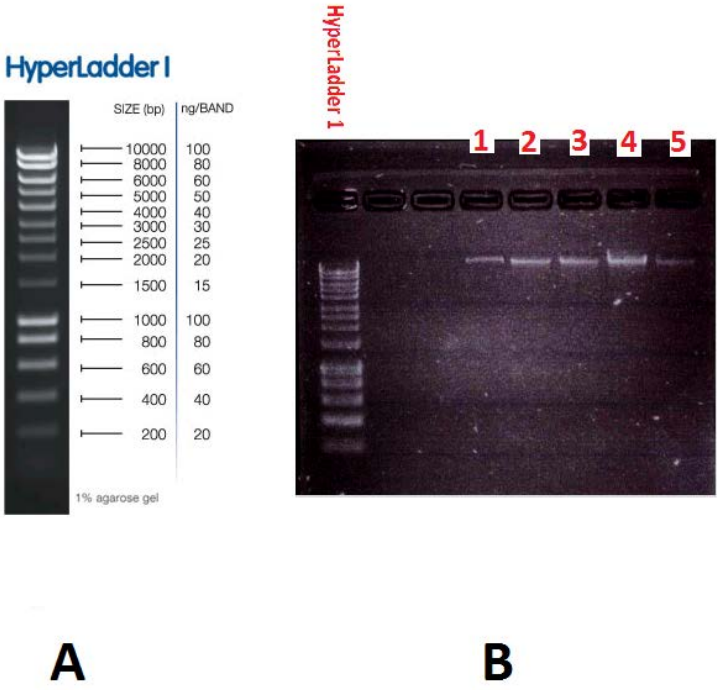

Figure 3-6: DNA bands visualized on Agarose gel for microbes within terrestrial rocks

A: Standard hyperladder I with 14 lanes indicating higher intensity bands, 1000 and 10,000 and each lane (5µl) provides 720ng of DNA (BIOLINE supplier), B: Successful nucleic acid extraction from five microorganisms which were unknown prior to DNA sequencing: (1- *Bacillus licheniformis* 2- *Bacillus subtilis* 3- *Rhizobium sp*. *IRBG74* 4- *Bacillus cereus* 5- *Bacillus sp. FJAT-17862*).

3.6.2.2 PCR amplification of extracted DNA

After the successful extraction, the PCR amplified 16S rRNA gene for all samples was visualised by gel electrophoresis, the amplified 16S rRNA are shown in Figure 3-7.

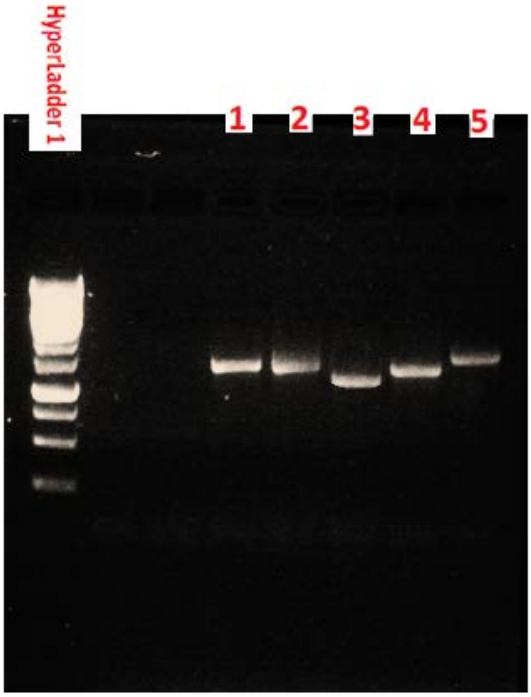

Figure 3-7: Successful DNA amplification by PCR in which the products are demonstrated on a 1% (w/v) agarose gel

The same standard Hyperladder 1 was used here. DNA in the five lanes were identified later as (1- *Bacillus licheniformis* 2- *Bacillus subtilis* 3- *Rhizobium sp. IRBG74* 4- *Bacillus cereus* 5- *Bacillus sp. FJAT-17862*).

3.6.2.3 Identification of the unknown bacteria

The PCR 16S rRNA products were sent to the University of Sheffield Medical School, Core Genetics Unit to sequence their DNA, the returned sequencing results were submitted to BLAST search to compare it with other sequences from the database of the National Centre for Biotechnology Information (NCBI) (http://www.ncbi.nlm.nih.gov) (Altschul *et al.*, 1997), Finch TV software (Version 1.4.0/Geospiza Inc.) was used to manually fill in the unidentified nucleotides (N) according to their colour coding (Mishra *et al.*, 2010), using these data; a phylogenic tree was made to facilitate effective phylogenic investigation of each genus.

As mentioned previously, no positive growth was observed from the Amber samples, however, five bacterial species were recovered from the terrestrial rocks samples (Table 3-3), and only one halite sample showed a positive growth of a single microbial species, which was revealed by sequencing analysis and BLAST search to be *Bacillus amyloliquefaciens* (See Appendix B: B1 and B2).

3.7 Discussion

The fact that no growth resulted from the sterile breakage of the amber samples might mean the spores have not survived the long hibernation period, alternatively, there were no spores present. There is also the possibility that the set of environmental conditions we selected to grow the microbes (incubation temperatures, oxygen availability, nutrients present within the media, etc.) were not suitable in this instance. However, it is worth mentioning that most previous similar studies confirmed finding living spores inside amber samples, which later regained the ability to grow (Cano and Borucki, 1995, Wainwright *et al.*, 2009); both of those studies clearly indicated the microbial recovery ratio from amber samples is relatively low; Out of the twenty amber samples that were used by Wainwright *et al.* (2009), only one sample showed a positive presence of microbial spores, the same low recovery ratio of viable bacteria was also reported in the work of Cano and Borucki (1995), out of the twelve used amber samples, only one yielded a positive recovery of a single microbial species. Since in the work reported here only six amber samples were used, the result may simply due to probability. The percentage of successful recovery of microbial isolates from the amber samples might also depend on other factors, such as the type of the amber used, and its age; out of the four amber pieces which were used by Greenblatt *et al.* (1999), three yielded positive recovery of bacterial spores. The amber used, in this case, was an Israeli amber from Earth-corings removed from the slopes of Mt. Hermon, dating back to 120 million years.

Although we failed to recover any microbes from the amber pieces, one important observation must be noted here; the sterile breakage apparatus which we used (modified Duran bottles with the plunger and the overlaying autoclavable cover) was successful in preventing outside contamination; once the bottles were sealed and lacked any growth after incubation, they then remained sterile even when unopened for more than three months.

The sampling of the terrestrial rocks for microbes also presented a few issues. Despite the laborious sterilization efforts performed on the outer surface of the rocks, some of the samples deposited in the sterile breakage vessels showed positive microbial growth prior to breaking. Initially, this was put down to contamination resulting from handling, but despite several repeats and additional sterilization procedures growth kept appearing in the vessels containing the unbroken rock. It was eventually concluded that this was due to the porous nature of these rocks allowing the entry of bacteria into their interior and that they can never be truly “sealed” from the outside. To confirm this, we left some of the rocks from which microbes were readily isolated in a 70% alcohol solution for one week, when we later placed those rocks in the breakage vessels, no growth was ever observed, even when they were broken open. Presumably, because the rock was left for a long period in alcohol, the sterilizing solution managed to reach the core and the entirety of the rock, thereby effectively killing all microbes inside. We conclude that porous terrestrial rocks can successfully harbour microbes in their interior and thereby protect them from the extreme conditions following ejection and inter-cosmic travel, as was indicated by the study of Bryce *et al.* (2014) which showed that porous meteorites can provide sufficient protection to allow for the survival of microbes in space.

As shown in (Table 3-3), five samples of bacteria were recovered from terrestrial rock samples and some rocks were shown to contain more than one microbial species within the same sample. The recovered bacteria are all ubiquitous in nature, and common soil microbes (Van Der Heijden *et al.*, 2008). Some of the microbes recovered from the rocks have already had

their survivability tested in real space exposure conditions (Horneck, 1993), where the spores of *B. subtilis* were exposed to the vacuum of space and the solar UV and cosmic rays. It was found that if the spores were protected against those radiations (e.g. inside a terrestrial porous rock), then they can survive up to several years. However, the same study shows that spores left unprotected in the vacuum of space are exposed to an increased mutation frequency, the UV negative effect on the spores will also be augmented, leading to an increased rate of mutagenesis. In a recent study by Wassmann *et al.* (2012), spores of *B. subtilis* were exposed to the harsh conditions of the low-earth orbit for a period of 559 days, this study was carried on board the ESA's agency EXPOSE-E facility, the results demonstrated the importance of an effective shielding (such as in a porous meteorite) against the high inactivation potential by solar radiation.

The isolation of microbes from terrestrial rock samples strongly suggests that rocks can be used as a transporting vehicle for lithopanspermia, the presence of microbes in surface rocks has been investigated previously by (Myers and McCready, 1966), however, it could be argued that since those earlier studies did not use the cracking vessels used in our work, which act as a contamination-proof vessel, such findings were invalidated by contamination.

In our studies of halite crystals, the sterility of our work was confirmed by the use of negative controls; The crystals were drilled in randomly selected locations that did not contain a brine inclusion, and then underwent the same treatment of the other samples, including inoculation in the culture media and checks for growth. None of the controls ever showed positive growth for bacteria in the media, thus providing proof of the effectiveness of the sterilization procedures followed. In addition, the techniques which we adapted and modified, were evaluated extensively by Sankaranarayanan *et al.* (2011), who checked the effectiveness of the sterilization protocols by testing for residual spiked *Homo sapiens* DNA (following surface sterilization of the crystals) using PCR primers targeting specific regions for human mitochondrion; Table 3-4 outline their findings regarding the

effectiveness of each of the sterilization techniques undertaken by them as well as other studies.

Table 3-4: List of some of the surface sterilization protocols evaluated, with the washing steps employed for each

Data from (Sankaranarayanan *et al.*, 2011).

Protocol Name	NaOH 10N Halite Saturated	HCl 10N	Halite Saturated Na_2CO_3	Halite Saturated 6% Sodium hypochlorite (Bleach)	Halite Saturated Brine	Ethanol
Al	+	–	–	–	+	–
AlB	+	–	–	+	+	–
AlAc	+	+	+	–	+	–
AlAcBl	+	+	+	+	+	–
Ac	–	+	+	–	+	–
AcBl	–	+	+	+	+	–
Bl	–	–	–	+	+	–
Et	–	–	–	–	–	+
BlEt	–	–	–	+	+	+
AcBlEt	–	+	+	+	+	+
AcEt	–	+	+	–	–	+

The only microbe that was isolated from any halite crystals was the common soil bacterium *Bacillus amyloliquefaciens*, a gram positive bacterium very similar to *Bacillus subtilis*. These two species share many homologous genes as well as many phenotypic characteristics, which makes them difficult to differentiate using routine microbiological techniques (Welker and Campbell, 1967, Palva, 1982, Nicholson *et al.*, 2000). As with *B. subtilis*, the endospores of *B. amyloliquefaciens* enable the bacterium to survive for long periods (Nicholson *et al.*, 2000). However, two important characteristics distinguishes *B. amyloliquefaciens* from *B. subtilis*. The former produces α-Amylase in 50-150 folds more than the latter, and more importantly, in relation to it being isolated from halite, is the ability of *B. amyloliquefaciens*

to grow well in 10% NaCl, an ability not possessed by *B. subtilis* (Welker and Campbell, 1967). This last fact is significant in relation to the aim of recovering bacteria, which may have survived for geologically long periods in the brine inclusions of the halite crystals. A number of studies reported finding bacteria such as *Halococcus salifodinae*, from salt crystals (Vreeland and Huval, 1991, Norton *et al.*, 1993, Denner *et al.*, 1994). Another feature of the spores of *B. amyloliquefaciens* is their ability to maintain viability following high-pressure (Ahn and Balasubramaniam, 2007), which is relevant considering that halite crystals buried in the sub-surface layer of the Earth's crust will be exposed to a range of high temperature and pressure conditions (Carter and Heard, 1970).

Microbial survivability in the liquid inclusions inside halite and amber has been previously investigated and most of the studies which have reported positive findings usually involve isolates of *Bacillus*, as was the case here with halite. Cano and Borucki (1995) isolated a strain of *Bacillus sphaericus* from an amber sample, Vreeland *et al.* (2000) isolated a previously undiscovered *Bacillus* species, which they suggested might be an ancestor to the currently existent microbes.

Most of the previous reports mentioned above which concern the isolation of bacteria from ancient salt crystals and amber were met with scepticism, mainly due to concerns over contamination. Also, many of the previous studies have used salt samples that had been isolated from contaminated sources; having been young in age and resulted from flowing brines or salt efflorescence, in addition, some salts might have been recrystallized, which might make them on an undetermined age (Vreeland *et al.*, 2000). In our halite isolation, however, our findings are substantiated with the use of the contamination-proof breakage vessel, the use of controls, and an overall strict-sterility maintained protocols during laboratory handling. Our results agree with Vreeland *et al.* (2000), and if both are taken to be correct, it will double the length of time microbes are known to survive inside ancient geological samples.

CHAPTER 4

4 Chapter 4: Indications of the presence of microbial fossils in recovered meteorite samples.

4.1 Introduction

Meteorites which survive entry to Earth present us with “free” samples that provide clues to the different environmental conditions present on other cosmic worlds. For example, the geological rock composition, volatile content, and even atmospheric conditions of the planet from which meteorites originate can be determined by studying such samples (Herd *et al.*, 2002). The detection of extraterrestrial amino acids in numerous meteorites, identical to those found on Earth, have led to the suggestion that the building blocks of life may have a space origin (Engel and Macko, 1997, Burton *et al.*, 2012). More relevant to the present study, meteorites might: a) contain bio-signatures (McKay *et al.*, 1996), or microfossils , which could hint at past extra-terrestrial microbial activity (Staplin, 1962, Hoover, 1997, Hoover *et al.*, 2003), or b) live microbial cells or spores relevant to the theory of cometary panspermia (Hoyle and Wickramasinghe, 1981a, Hoyle and Wickramasinghe, 1981b, Wickramasinghe *et al.*, 2013b).

This Chapter will review some of the controversial studies relating to claims concerning detecting signs and remains of past-life in meteorite samples. Studies on the analysis of some of the meteorite samples will also be discussed in relation to the above mentioned possibilities.

4.2 Meteorites, transporters of the building blocks of life

The Murchison meteorite, a type II carbonaceous meteorite, is one of the most studied of all meteorites and has contributed more than any other extraterrestrial sample to the field of astrobiology It has a relatively large mass, and its provenance is secure since it was observed when it fell to Earth in 1969 (Kvenvolden *et al.*, 1970, Engel and Macko, 1997, Hoover *et al.*, 2003, Wickramasinghe *et al.*, 2013b).

The detection of extra-terrestrial amino acids and hydrocarbons within the Murchison meteorite (Kvenvolden *et al.*, 1970), caused a radical shift in the field of astrobiology, and encouraged scientists to further analyse recovered meteorites in the aim of obtaining information on how life may have started on the early Earth. A racemic mixture of an equal amounts of both L- and D-enantiomers is expected if abiotic amino acids were synthesized on the early Earth (Cohen, 1995). and the possibility is now seriously entertained that a significant fraction of amino acids and other organic compounds present on the early Earth may have been brought originally by comets and meteorites impacting the planet (Chyba and Sagan, 1992). Since the Murchison meteorite contained an excess of L-enantiomers, it can be argued that a similar excess might have been present on the early Earth, suggesting that the excess of L-enantiomers found in the solar system can be attributed to an extra-terrestrial origin (Engel and Macko, 1997). Martins *et al.* (2008), suggest that organic compounds, the indispensable component of any genetic code, predate the existence of the solar system, and possibly have played an essential role in life's origin, a view enhanced by the discovery of purine and pyrimidine compounds in the Murchison meteorite, their non-terrestrial origin being confirmed by determination of carbon isotope ratios for uracil and xanthine.

4.2.1 Biosignatures in the ALH84001 meteorite

Of particular interest in relation to investigating life on Mars are the Shergotty-Nakhla-Chassigny (SNC) meteorites class, which were delivered to Earth following impact events on Mars (Ott, 1988). McKay *et al.* (1996) provided the most cited of such studies when they reported claimed bio-signatures in the ALH84001 Martian meteorite, retrieved from Antarctica. ALH84001 is an igneous orthopyroxenite meteorite consisting of coarse-grained orthopyroxene [(Mg,Fe)SiO3] and minor maskelynite (NaAISi3O8), olivine [(Mg,Fe)Si04], chromite (FeCr204), pyrite (FeS2), and apatite [Ca3(PO4)2]. It is also reported to have been crystalized 4.5 billion years ago, close to the time of formation of Earth (Chapman and Morrison, 1994). The focus of the study by McKay *et al.* (1996) was on the secondary

carbonate minerals present in the ALH84001 meteorites, which formed globules ranging in diameter between 1-250 µm, this feature having not previously been reported in any other SNC meteorite, which ordinarily contain only trace carbonate phases. It was suggested that these unique globules were formed about 3.6 billion years ago, in other words, almost at the same time as life is estimated to have appeared on Earth, i.e. when the conditions became relatively stable (Ohtomo *et al.*, 2014). Oxygen isotopic data suggest the globules were formed at temperatures ranging between 0-800C, which falls within the optimum temperature for most terrestrial microbes. The globules were reported to be located in the spaces between fractures (Figure 4-1), and pore cavities, which is as expected if they represents remnants of microbial growth (Bryce *et al.*, 2014). The globules, it was claimed, are unlikely to be of terrestrial origin because many of them had signs of being shock-damaged, which might had happened either on Mars or in Space, but following the meteorite's residence on Earth (Wentworth and Gooding, 1995). The association with the meteorite oxygen and carbon isotopic composition (McKay *et al.*, 1996) apparently presents further proof for the globule being indigenous to the ALH84001 meteorite, rather than forming during the 13,000 years of being preserved in Antarctica.

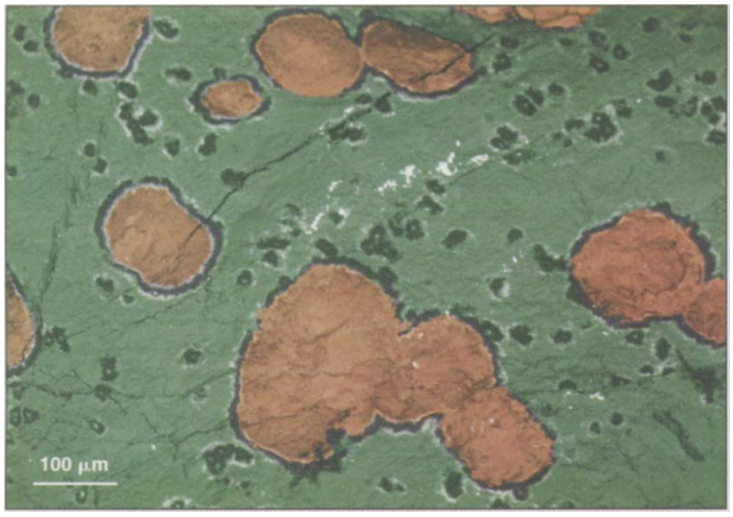

Figure 4-1: False-colour backscatter electron microscopy image for the surface of one of the chips of the ALH84001 meteorite

Showing the carbon globules (orange coloured), also visible is the fracture lines, the black rim around the globules is for magnesite (McKay *et al.*, 1996).

Researchers also note that since those globules were located within the fractures of the meteorites, it makes it “somewhat friable and breaks relatively easily along pre-existing fractures.”. It is these, fractured surfaces that were examined by McKay *et al.* (1996) when looking for the presence of polycyclic aromatic hydrocarbons (PAHs), which might have acted as a biomarker. High resolution SEM and TEM of the surface textures and some of the selected internal structures of these globules indicated that they possess fine grained, secondary phases of single domain magnetite and Fe-sulfides. The study also noted the similarity of those carbonate globules in size and textures to some recognized terrestrial carbonate precipitates, which are formed by terrestrial microbes (Figure 4-2).

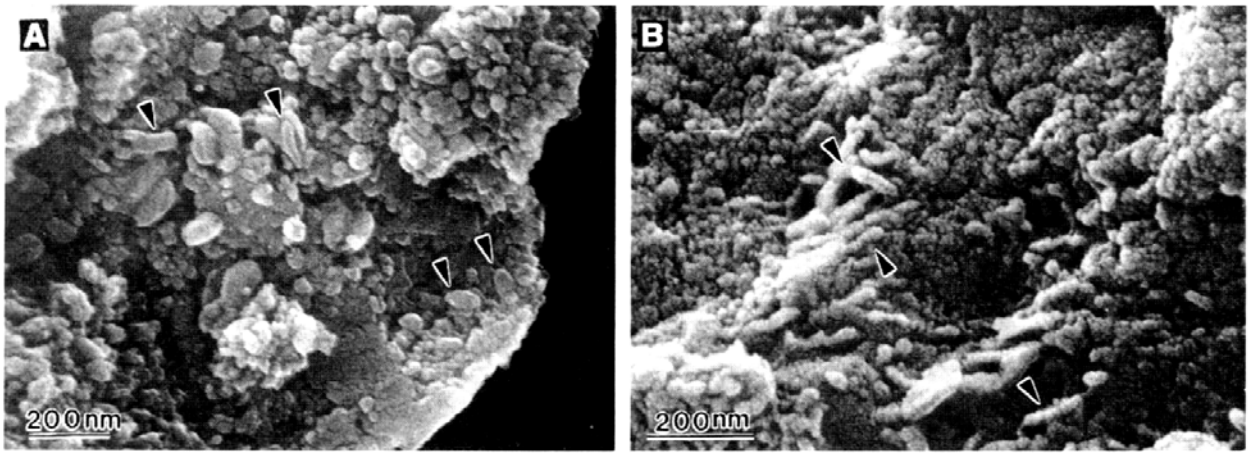

Figure 4-2: Two SEM images for sections of the ALH84001 meteorite

Showing an elongated and ovoid structures that are associated with the carbonate globules, the arrows in both A and B outline the nanometer elongated forms and ovoid structures that might be attributed to biogenic activity (McKay *et al.*, 1996).

It is important here to note that McKay *et al.* (1996) was careful in not stating conclusively these globules formed as the result of biogenic activity. The paper explained that although a biogenic process can explain the various features within the sample, mainly the PAHs (which might then make them a remnants of fossils belonging to past Martian microbes) an inorganic formation, is also possible.

MacKay's findings were soon investigated further by many other scientists who examined the ALH84001 meteorite for potential bio signatures. One of the strongest evidence for past biogenic activity within the rock comes from (Thomas-Keprta *et al.*, 2001) who reported discovering many nano-sized magnetite crystals (Fe_3O_4) located within the globules and their rims, those crystals show strong chemical and physical similarity to magnetite particles produced by terrestrial magnetotactic microbes. Such magnetite particles have not been found to be produced by abiotic processes, either in the lab or in natural geological processes and it was suggested that they may be Martian "magnetofossils".

Many scientists doubted that these findings can be explained by biogenic activity although, as Thomas-Keprta *et al.* (2002) concluded only a biogenic interpretation is consistent with the bigger picture with how these carbonates were formed.

Sears and Kral (1998) analysed a lunar meteorite using similar techniques and methods of those described by McKay *et al.* (1996), and the findings of the two studies were similar (Figure 4-3). However, those authors suggested that the structures they contain might have a terrestrial and not a Martian origin.

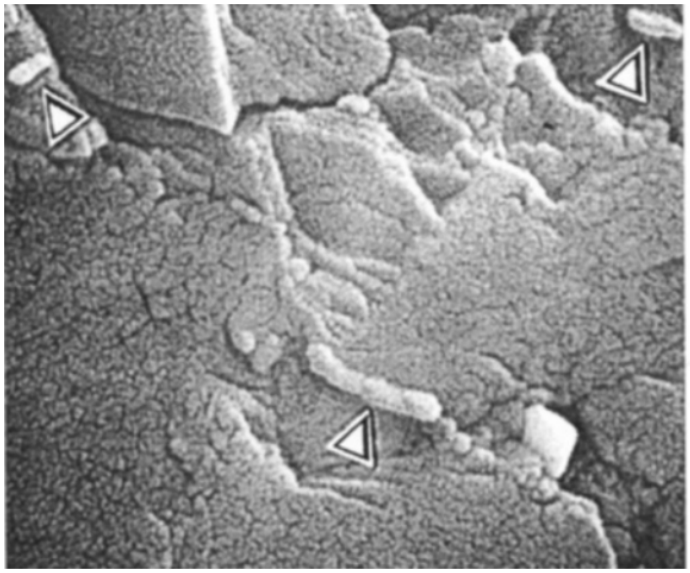

Figure 4-3: An SEM image for a section of the lunar meteorite QUE 94281

Showing three elongated objects demonstrated by the arrows. The horizontal field of view are 1 μm (Sears and Kral, 1998).

4.2.2 Microfossils in meteorites

Many of the structures within the ALH84001 meteorite which resembled microfossils were on the nano-scale, i.e. around 100-400 nm in length (McKay *et al.*, 1996), and many scientists argued that these dimensions were below the minimum size for an organism (Bradley *et al.*, 1997, Koziol and Brearley, 2002). Many reports have however, shown that so-called nano-microbes exist; Huber *et al.* (2002) for example, reported finding a nanoarcheon symbiont having a size of less than 400 nm which are smaller than the nano-forms found in ALH84001. Another study reported the isolation of anaerobic hyper-thermophilic nanobes from which were reported to be autonomous hyperthermophiles and obligate sulfurophiles, with a size range between 100nm - 1μm; phase-contrast microscopy showed that the organisms are flagellated and actively motile (Figure 4-4) (Hoover and Rozanov, 2003).

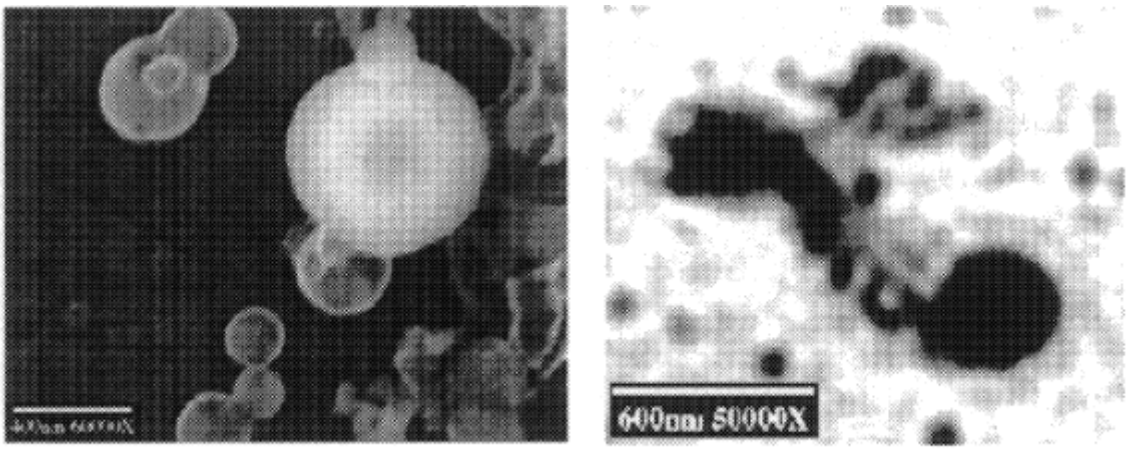

Figure 4-4: Nanobes isolated from Rainbow hydrothermal vents

a. under the SEM, b. a stained nanobe in order to show the flagella (Hoover and Rozanov, 2003).

The Orgueil meteorite, which fell in France in 1864, has been extensively studied for the presence of microfossils. Tan and VanLandingham (1967) for example, reported finding numerous biological cylindrical structures, which bears close similarity to the bacterium *Rhodopseudomonas rutilis*, mainly in relation to the presence of similar arrangements of magnetosomes. The Murchison meteorite has been similarly examined and a claimed Acritarch was found; these are extinct microbes with uncertain affinity but possibly a phytoplankton (Hoover and Rozanov, 2003) (Figure 4-5).

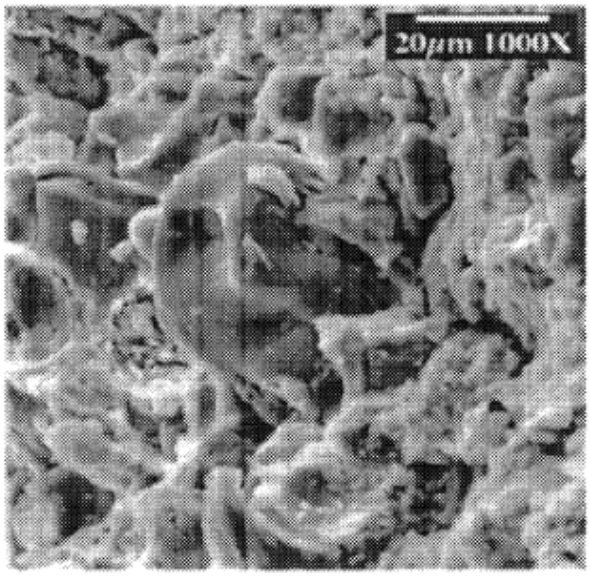

Figure 4-5: SEM image of an Acritarch

Recovered from a pristine meteorite sample (Hoover and Rozanov, 2003).

Hoover (2011), also examined various CI1 carbonaceous meteorite samples for potential microfossils; many claimed micro-structures were found having a complex-filament morphology indigenous to the meteorite samples. Many of these showed unique shapes, such as tubular bodies with tapered ends, and were always found from within freshly fractured pieces of the meteorite; contamination was thereby excluded (Figure 4-6). The size and the many visible features of those microfossils suggest affinity with the modern Cyanobacteriaceae usually found in microbial mats in aquatic environments. Analysis using EDAX reported the sheathes of those microfossils to be enriched in carbon while the internal body is filled with minerals containing magnesium and sulphur, the study also failed to detect nitrogen which was said to confirm that the observed formations are ancient microfossils.

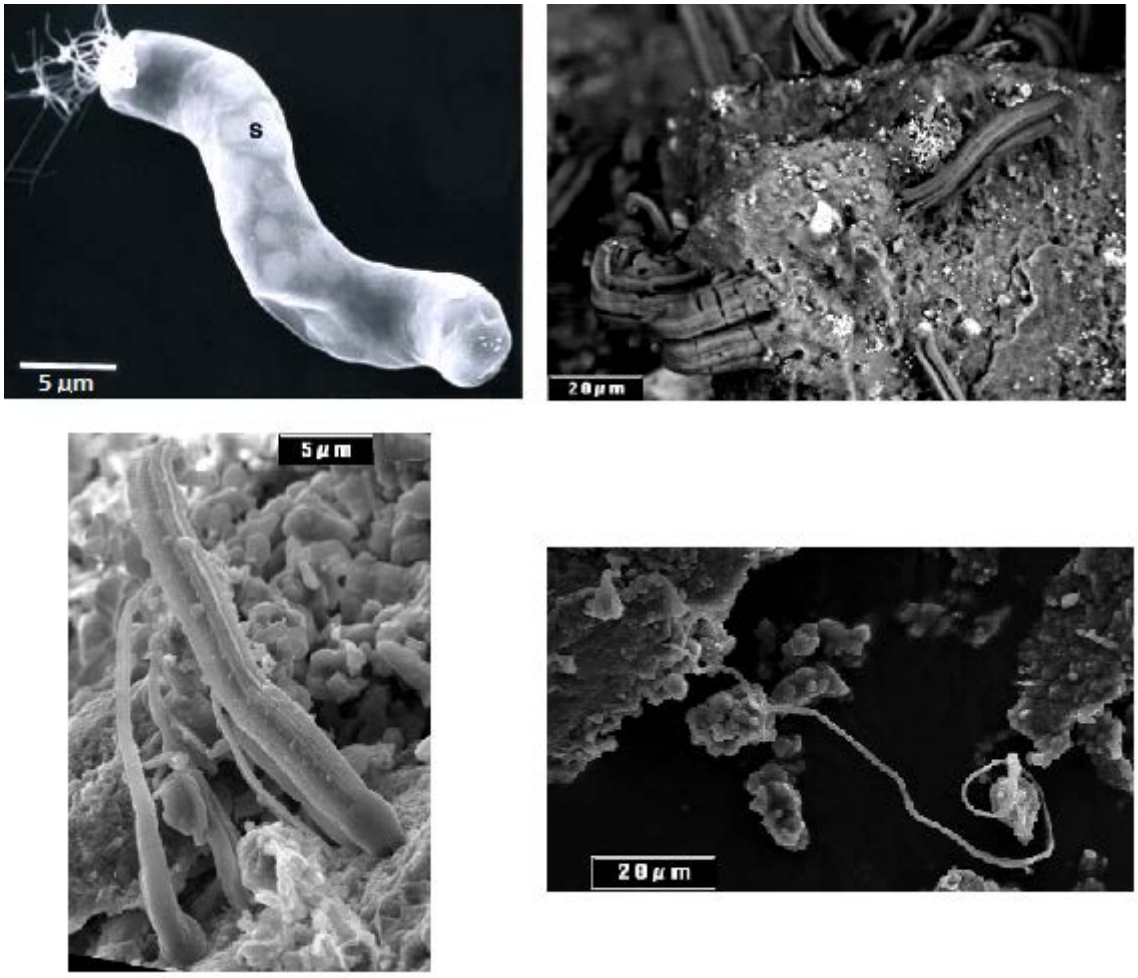

Figure 4-6: Some of the microfossils recovered from the CI1 meteorites

Showing filamentous formations, Hoover (2011).

In 2013, a meteorite was observed as it fell in the city of Polonnaruwa, Sri Lanka, the authenticity of it was confirmed by SEM, triple oxygen isotope analysis, and X-Ray Diffraction analysis (XRD), all of which confirmed it to be a carbonaceous chondrite (Wallis *et al.*, 2013). Many microfossils were reported within the meteorite, however, what is particularly notable was the discovery of fossils of diatoms which it was claimed to provide evidence for extra-terrestrial life (Wainwright *et al.*, 2013a, Wickramasinghe *et al.*, 2013c, Wickramasinghe *et al.*, 2013d) (Figure 4-7).

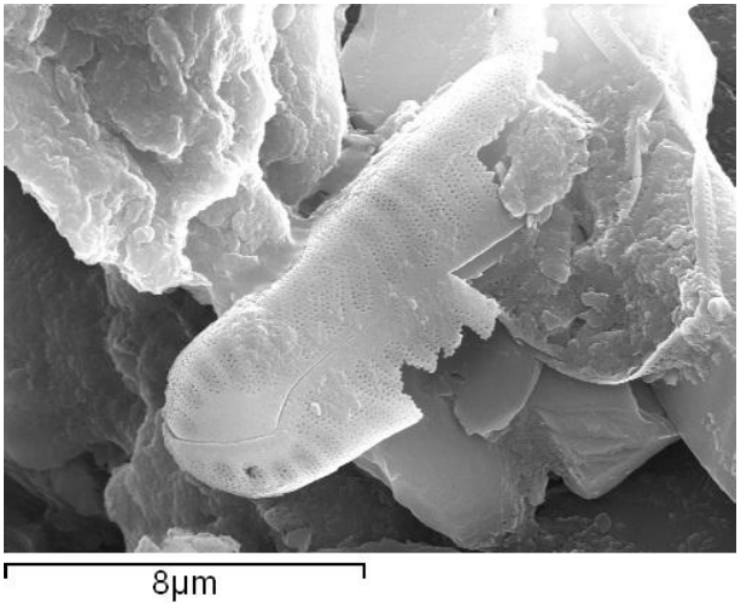

Figure 4-7: An SEM for a diatom fragment

Fused into the rock structure of the Polonnaruwa meteorite (Wainwright *et al.*, 2013a).

In a subsequent study, further analysis into the Polonnaruwa meteorite revealed microfossils having worm-like forms. Which, it was claimed, are indigenous to the meteorite (Figure 4-8) (Wainwright *et al.*, 2013b).

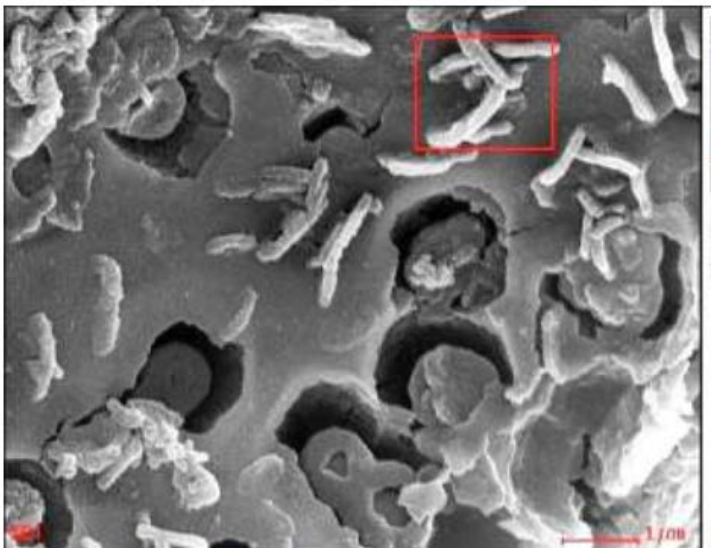

Figure 4-8: A section of the inner surface of the Polonnaruwa meteorite

Examined by SEM showing the worm-life structures (Wainwright *et al.*, 2013b).

As Wainwright *et al.* (2013b) noted, reproducibility of the results, and reporting microfossils in new meteorite samples is the best way to ensure findings from previous studies are not due to contamination. Work described in this Chapter aimed at identifying microfossils from meteorite samples by repeating the methods used in the previously mentioned studies; EDAX analysis was also conducted wherever possible.

4.3 Materials and methods

4.3.1 Northwest Africa 4925 meteorite sample:

The single sample supplied from a dealer was cut from an originally larger meteorite sample, which was catalogued as Northwest Africa 4925 NWA 4925; the authenticity of the sample was confirmed by the fellow members of the International Meteorite Collectors Association. The meteorite was recovered in 2007 from Erfoud, a town in the Sahara Desert, in the Meknès-Tafilalet of the Maghreb region in eastern Morocco. This meteorite is classified as an anachondrite, (i.e. a Martian, olivine-phyric shergottite). The fragment which was used was covered partially with a fusion crust, and showed a porphyritic texture with large chemically zoned olivine megacrysts set into a fine-grained groundmass composed of pyroxene and maskelynite; minor phases include chromite, sulphides, phosphates, and small Fe-rich olivines. Olivine megacrysts often contain melt inclusions and small chromites. Its mineral composition (EMPA): Olivine, $Fa_{27.6–46.8}$; pyroxene, $Fs_{20.0–37.7}Wo_{3–14.8}$; maskelynite, $An_{67–69}$. It is classified as an achondrite (Martian, olivine-phyric shergottite); severely shocked with some melt pockets; moderately weathered.

4.3.1.1 Sterilization of the meteorite sample, and lysis of potential contaminants modern biofilms

The sample was immersed in 70 percent ethanol for an hour, then washed twice with sterile, deionized water, before being transferred to a sterile petri dish prior to being examined under the SEM. The water used in the sterilization process was sterilized in the autoclave at 120^0C for twenty minutes, and then filtered through 0.1 µm micropore filter (Nalgene).

4.3.1.2 Scanning electron microscopy Examination

After sterilization, the meteorite sample was positioned inside a staging chamber, with the side to be analysed flush to the base. Konductomet phenolic mounting compound (20-3375-016) was used to stage the sample. Similar procedures usually involve grinding then polishing of the surface of the sample during this stage, however, during the work described here, only an instantaneous process of grinding was performed, in the aim of removing any build-up that might be present on the upper surface to be examined, so that only freshly exposed material would be viewed. The coarseness of pile used was 120 microns using a Bueler Automet 250 for 5 seconds with a touch force of 20N, a head speed of 50 RPM and a Platen speed of 140 RPM. A second sample was prepared presenting the outside surface of the meteorite. This was staged on top of a conductive carbon tab. Due to its relatively low conductive nature the sample was coated using an Emscope gold sputter coater, so as to minimize charging effects and optimise image acquisition. The sample was coated for a deposition-duration of 1 minute at 15 milliamps. Before being introduced into the SEM the sample was placed in a vacuum chamber overnight to remove any remaining moisture from the porous sample. No chemicals or concentrated alcohols were introduced at any stage as a cleaning step. The sample was finally delicately irrigated using de-ionised water.

4.3.2 The Polonnaruwa meteorite sample

A meteorite fall event occurred on 29 December 2012, in the Araganwila village, near the city of Polonnaruwa - Sri Lanka, the event was witnessed by many of the locals, where the large meteoritic bolide exploded and disintegrated, with countless pieces falling. Some were collected by researchers collaborating with our team, and identified as a carbonaceous chondrite containing an aggregate of fine minerals (Wainwright *et al.*, 2013a, Wallis *et al.*, 2013, Wickramasinghe *et al.*, 2013d). This was further confirmed by the distribution of the stable isotopes of oxygen (Wallis *et al.*, 2013). Many studies reported finding various fossilized diatoms and other microfossils within the meteorite samples (Wainwright *et al.*, 2013a, Wainwright *et al.*, 2013b, Wainwright *et al.*, 2013e). Here results are presented of further analysis for a recovered meteorite fragment obtained from the region of the meteorite fall.

4.3.2.1 Sterilization of the meteorite sample

A piece of the meteorite was sterilized in the same way as used for the Northwest Africa 4925 meteorite, after washing, the meteorite was then sectioned prior to being examined under the electron microscope. The protocol described here is the same used by Wainwright *et al.* (2013e). A hot plate was used to fix the sample using wax into a polymer stub, for the purpose of staging the sample into a wire saw (Well 3241 Wire Saw) setup; a subtle slope is used by the setup to enable the wire to gradually press up to the opposing face of the staged meteorite sample. In order to increase or decrease the amount of force in which the wire puts on the sample, the slope's gradient is altered for this purpose. The thickness of the wire was about 0.17mm; fine diamonds coat the wire, mode size, circa 30 microns. The activation of the device causes the wire to cut slowly and accurately through the rock substance, once the sample is split in half; one of the pieces was fixed inside a staging chamber, while the freshly cut face, which was to be analysed was fused to the base. Konductomet Phenolic mounting compound (20-3375-016) was used to stage the sample. As with the Northwest Africa 4925 meteorite, instantaneous grinding was performed to

remove any build-up on the freshly broken surface. The coarseness of the used pile was 120 microns; a Bueler Automet 250 was used for five seconds with a 20N touch force, a head speed of 50 RPM and a Platen speed of 140 RPM. Because of the low conductivity of the sample, and to minimize the charging effect and for better image acquisition optimization, an Emscope gold sputter coater was used to coat the sample with gold at a deposition duration of one minute at 15 milliamps. To remove the remaining moisture from the sample, it was left in a vacuum chamber overnight before finally being examined by the SEM (JEOL 6500F).

4.3.3 The Carancas meteorite samples

On the 15th of September 2007, an impact event by a meteoroid created a 13 meters wide crater in the area near the Carancas community, Desaguadero town, near Chucuito in the Puno region of Peru, not far from the Bolivian border (Rosales *et al.*, 2008, Kenkmann *et al.*, 2009). It was identified as an ordinary chondrite and its fall was unique because stony meteorites usually disintegrate when entering the Earth's atmosphere. According to Borovička and Spurný (2008), the Carancas meteoroid is "monolithic" in nature and lacks internal cracks.

Nine Carancas meteorite pieces were used for this study, all obtained from a commercial supplier, and the authenticity of the samples was confirmed by fellow members of the International Meteorite Collectors Association. The meteorite samples were collected within one week following the impact event. The sizes of the obtained pieces ranged between 0.4- 4.5 cm in diameter, Figure 4-9 show one of the largest pieces used here.

Figure 4-9: One of the recovered Carancas meteorite samples

The monolithic inner surface can be seen on the right side in this image, green olivine crystals that are embedded in the meteorite matrix.

4.3.3.1 Sterilization of the meteorite sample, and lysis of potential contaminants

The same treatment used for the sterilization of the Northwest Africa 4925 meteorite was performed here; eight samples were immersed in 70 percent C_2H_5OH, followed by washing in sterilized, deionized water; they were then kept in sterile petri plates for subsequent analysis. The remaining sample was not washed or sterilized, but instead used as a control to evaluate meteorite surface contamination from the environment.

Two of the sterilized larger samples were selected for SEM examination, while the other seven samples were to be placed in the sterile-breakage bottle in an attempt to isolate any viable microbial spores or cells present inside the samples.

4.3.3.2 Scanning electron microscopy Examination

The same protocol used for the Northwest Africa 4925 meteorite sample preparation for SEM analysis was used for the two selected Carancas meteorite samples.

4.3.3.3 Isolation of Microbes from the Carancas meteorite samples

As mentioned earlier, seven Carancas meteorite samples were selected for the attempt to isolate microbial spores or cells (one sample was not subjected to the surface decontamination process). The same isolation technique used for amber samples was used to isolate microbes (3.5.1.2), using the sterile breakage containers, shown in Figure 3-2. As mentioned previously, the sterile –breakage bottles are modified 50ml Duran bottles, with a steel plunger going through the cap into the bottom of the bottle, the base of the bottle contained a rubber plate to prevent the breakage of the glass, and an autoclavable bag covered the plunger and the cap. The bottle contained 20 ml of Nutrient Broth. Prior to use, the bottles were autoclaved for 15 min at 15 psi pressure-121°C.

The Carancas samples, were then inserted into individual modified Duran bottles using an alcohol-flamed forceps, and the bottles were sealed immediately. The whole process was performed in a Class II laminar flow hood, sterility of which was checked periodically. Control samples were also used to test the sterility of the process by performing the same steps but without adding any samples into the bottles.

After the addition of the meteorite pieces, the vessel was incubated for 72 hours at 25°C, followed by a period of 72 hours at 37°C, while being examined by eye daily for signs of growth; if any of the bottles showed an indication of microbial growth they were immediately disregarded and the experiment would be repeated until a contamination-free medium was obtained.

When no growth was observed after the incubation period, the samples in the growth-free bottles were cracked *in situ* and the bottles were again incubated at 25°C and 37°C respectively 3 days for each. Where the bottles showed positive growth for bacteria an aliquot was streaked onto Nutrient agar, and incubated at 37^{o}C for 24 hours to obtain single colonies of pure isolates. Single colony forming units (CFU) would then be selected and transferred into Nutrient broth 5ml tubes and incubated for 18 hours at 37°C, extraction of bacterial nucleic acids and PCR for 16S rRNA would follow for the identification of bacteria.

4.3.3.4 DNA extraction

The kit used to extract DNA from the bacteria growth was “QuickExtract™ Bacterial DNA Extraction Kit” (Epicentre – Nos. QEB09050). This kit was selected because the whole process for DNA extraction would be performed in a single tube, thus minimizing contamination. It is used to extract the DNA for most of the bacterial types, and it contain the Ready-Lyse lysozyme solution, which possess 200 more the specific activity of hen egg lysozyme, and the QuickExtract solution formulated for microbial DNA extractions. In short: to extract the DNA, the QuickExtract solution and Ready-Lyse Lysozyme solution were added to the pelleted microbial growth, and then incubated at room temperature for the cells to be lysed. This was done by firstly centrifuging 1.5 ml of microbial growth at 1,700 x g (5,000 rpm) in a microcentrifuge for three minutes in order to pellet the bacterial cells. Then the bacterial pellet was suspended with 0.5 ml of sterile water, and recentrifuged at 1,700 x g (5,000 rpm) in a microcentrifuge for three minutes. The supernatant was then disregarded carefully by pipetting, and 100µl of QuickExtract Bacterial DNA Extraction solution was added to the cell pellet. This was followed by the addition of 1µl of Ready-Lyse Lysozyme solution to each tube; then, it was mixed briefly by inverting the tube several times for complete dispersion of bacteria and the Ready-Lyse Lysozyme within the solution. The suspension was then left at room temperature for 15 minutes; if the solution was still not clear, the tube was left for an additional hour on the

bench. After this step is completed, the DNA in the solution is ready for downstream applications, including PCR.

In order to confirm the presence of DNA within the samples, gel electrophoresis was used, in which 10µl of the samples was mixed with 2µl of 6X Loading dye and set to run on a 1% agarose gel (w/v), the gels were submerged in 1X TAE buffer supplied by (Fisher Scientific, cat.BP1332). Hyper Ladder (6 µl) was used to help to confirm the existence of DNA in the samples.

The gel was prepared by adding 1gm of agarose into 100ml of 1X TAE in a 250 ml flask. Complete dissolving of the agarose was achieved by placing the flask in the microwave for complete homogenization, then the mixture was allowed to cool down to 55°C before the addition of 4µl Ethidium bromide stain (Fisher Scientific, cat.E/P800/03), in order to demonstrate the DNA under the UV light later, then the mixture was poured in the BioRad Subcell GT electrophoretic tank and allowed to harden. Later, an Electric current of 80 volts was ran through the gel for 40 minutes, viewing and photographing of the DNA's bands was performed by the Uvitec "Uvidoc" mounted camera system. Samples which failed to show positive DNA bands when viewed later under UV transilluminator were neglected. The appearance of bands was interpreted as a possible positive result for DNA, and therefore the samples containing it were stored at -20^{o}C until further analysis.

4.3.3.5 PCR Amplification and sequence analysis

DNA extracts for each isolate were later used in a PCR thermocycler as templates to amplify the 16S rRNA gene for 35 cycles, the universal primers F27 (5′-AGAGTTTGATCMTGGCTCAG-3′) and R1492 (5′-TACGGYTACCTTGTTACGACTT-3′) were used. Both target universally conserved regions to enable the amplification of about 1500bp (Heuer *et al.*, 1997). The themocycler T3-0150 Sensoquest Thermal Labcycler

(SensoQuest GmbH Company, Göttingen, Germany) was used for the PCR amplification. Each tube contained the following reaction mixture: 6 µl of D.W, 1 µl from each of F27 and R1492 primers (20 pmol/ µl), 2 µl template DNA, and 10 µl of AmpliTaq Gold® Fast PCR Master Mix - UP (2✕) (Applied Biosystems, California, USA) (total reaction mixture volume: 20µl). Initial denaturation and activation of enzyme step was performed at 95°C for three minutes, followed by 35 cycles of a denaturation step 94°C for one minute, annealing at 60°C for one minute, and an extension step at 72°C for 1 minute. Finally, one extension step at 72°C for five minutes. After this, the PCR products (16S rRNA gene) presence and yield was determined by running the samples on 1% agarose gel at 200 V for one hour in 1× Tris-acetate-EDTA buffer, made visible by ethidium bromide staining and subsequent UV transillumination. Later, the PCR products were sent for sequencing to the Core Genomic Facility, University of Sheffield-UK, using the Applied Biosystems' 3730 DNA Analyser. After the sequencing data were received, nucleotide sequences were analysed using the Finch TV software, Version 1.4.0 (Geospiza Inc, USA). Those sequences were then used to identify their species origin, using the Basic Local Alignment Search Tool (BLAST) by matching it with the closest reported sequence uploaded to the National Centre for Biotechnology Information (NCBI) Genbank database.

4.4 Results and Discussion

4.4.1 Analysis of the Northwest Africa 4925 meteorite

The sample we used for this analysis were cut from a larger piece, as evidenced in Figure 4-10 which shows the meteorite sample under the SEM, as the exterior surfaces appearing in the image would have originally been within the inner matrix of the meteorite. The surface of the cut sample was scanned and imaged.

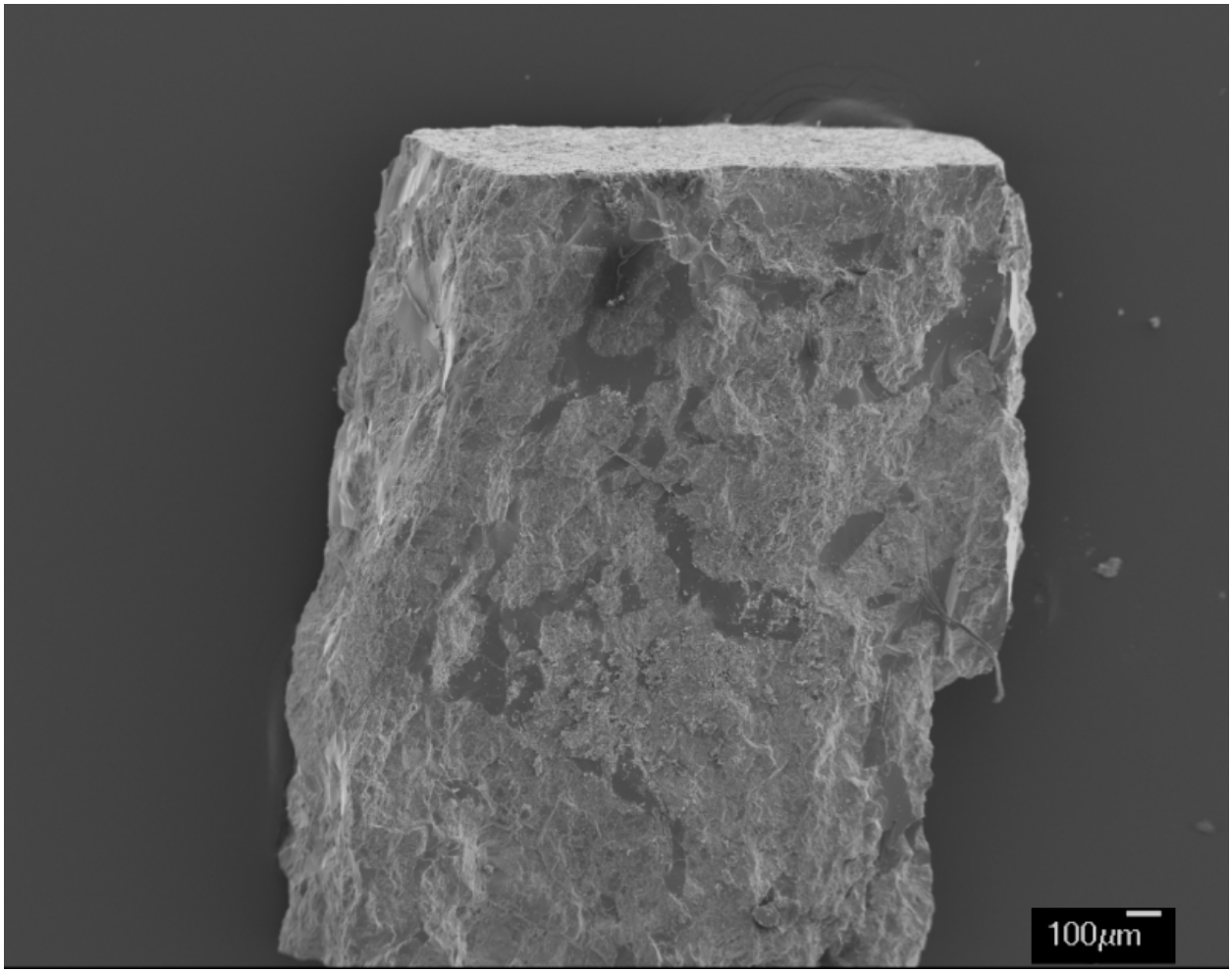

Figure 4-10: An SEM image for the analysed meteorite sample

The images shown below were taken from this side of the meteorite, which was originally located in the inside of the large meteorite.

The images from SEM analysis revealed areas that contain presumptive microbial biofilms consisting of smaller forms, which resembles a biofilm of modern bacteria found on the surface of terrestrial soils of rock samples (Figure 4-11).

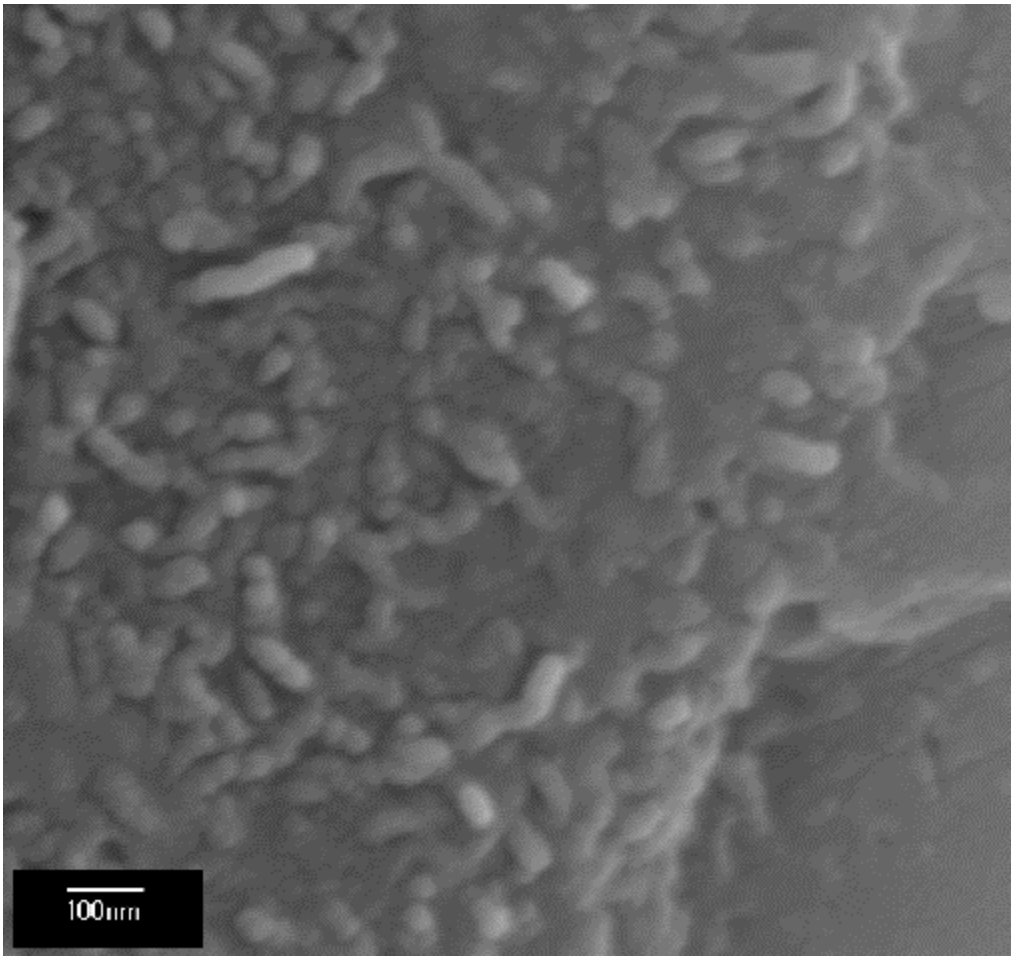

Figure 4-11: Presumptive bacterial biofilm within the freshly cut Northwest Africa 4925 meteorite

Showing a number of bacteria-like morphologies such as cocci, rods, and other forms.

In Figure 4-12, details for each of the individual microbial types are shown, such as rods, cocci, and spiral shaped bacteria-like chains, with also individual rods occurring in complex grouping such as star-shaped formations. Both the presumptive biofilm area and the adjacent non-biofilm region are shown to be identical by EDAX analysis in regards to their chemical composition; Mainly silicon, iron, magnesium, calcium, and oxygen, i.e. a composition expected of an anachondrite and not modern, contaminating bacteria (Wainwright *et al.*, 2014).

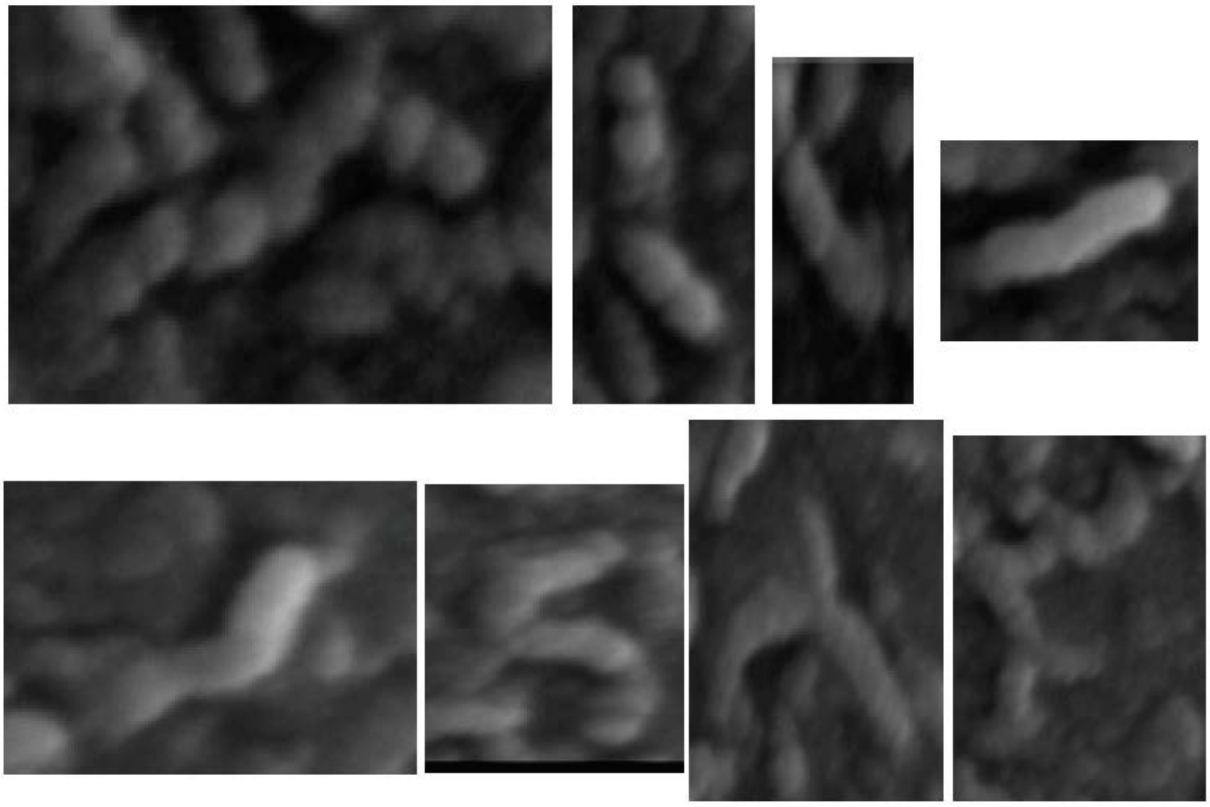

Figure 4-12: SEM images showing details of the many presumptive bacteria-like forms

Recovered from the Northwest Africa 4925 Martian meteorite (Figure 4-11 for scale reference).

The entities shown in Figure 4-11 appear to be fossilized bacterial biofilms composed of recognizable bacterial forms which would originally have been within the inner matrix of the meteorite prior to the sample being cut. Two arguments can be made against this suggestion a) the image shows terrestrial-derived biofilms, which fossilized on the meteorite following its fall, or b) the image shows a modern biofilm composed of living bacteria, these possibilities appear unlikely however, since the imaged entities show no signs of lysis following the 70 percent ethanol treatment. The possibility that terrestrial biofilms underwent mineralization during the period the meteorite have resided on Earth also seem to be highly unlikely, nor is the possibility

that modern terrestrial biofilms formed from an air-derived bacterial inoculum while the sample was in storage.

When the presumptive biofilm region was analysed with EDAX (shown in Figure 4-13), the region appeared to be mineralized and was essentially of the same chemical composition as the adjacent regions of the Martian meteorite in which presumptive biofilm formations were absent. These findings appear to confirm the conclusion that the presumptive biofilm belongs to the Martian meteorite, and not attributed to a modern contamination biofilm due to modern terrestrial bacteria.

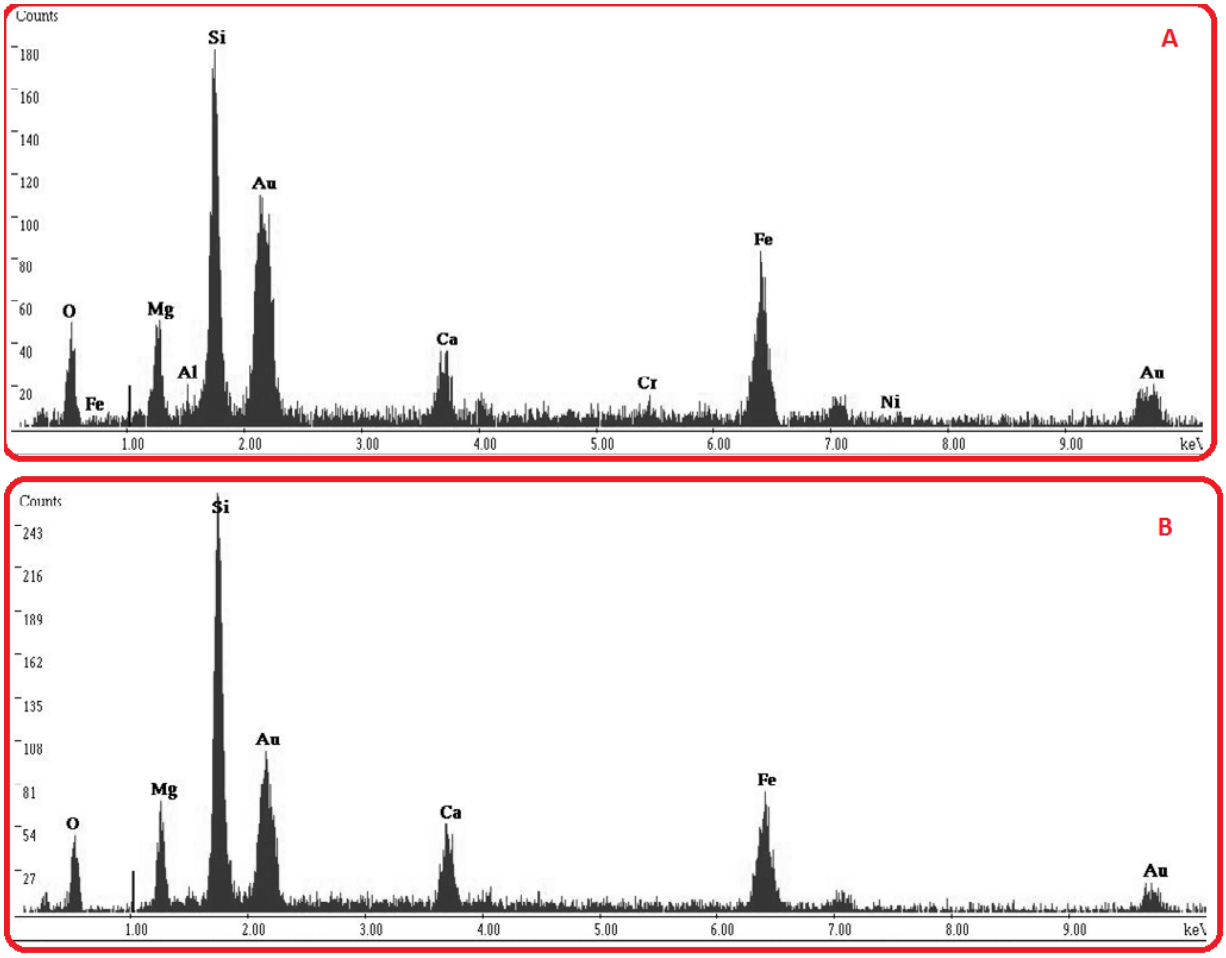

Figure 4-13: Two almost identical EDAX readings for different regions within the same sample

Northwest Africa 4925 Martian meteorite, A) is for the “biofilm” region, and B) is for another area within the broken sample distant from the “biofilm” region.

It is possible that the formations seen inside the Northwest Africa 4925 meteorite are mineral artifacts which mimic bacteria, a possibility used by critics to attribute similar, previously observed meteorite found structures to non-biological causes, e.g. the nano-bacteria like formations within the ALH84001 meteorite (Sears and Kral, 1998). It would seem to be remarkable coincidence however, that such a broad variety of microbial forms be so closely packed into an apparent biofilm. Unlike the forms observed within the Allen Hill meteorite (McKay *et al.*, 1996), the presumptive bacterial fossils seen here are not nano-sized, but instead, circa 0.2 µm, in other words, similar in size to many types of terrestrial bacteria that can be found in naturally occurring in nutrient-limited environments on Earth. The relatively large size of our reported putative bacteria is also sufficient to avoid arguments over whether those cells can contain a complete bacterial genome, as commented upon by Mushegian (1999) who estimated the approximate size for a small cell cannot be less than 0.14µm, a diameter well below the size of the structures found here.

A final criticism is that the claimed bacterial fossils (i.e. Martian-derived forms) appear to be too much like terrestrial bacteria, an argument which would be logical only if it is assumed that extra-terrestrial bacterial are fundamentally different from terrestrial forms. However, according to the panspermia theory, both Earth and Martian environments are likely to have obtained their bacteria from a common source, if this is the case then microbes present on both planets would be expected to have closely similar morphologies (Hoyle and Wickramasinghe, 1981a, Wickramasinghe and Wainwright, 2015).

Figure 4-14 another biomorph, which was reported from the same meteorite. This filamentous structure appears to be attached to the body of the meteorite from one end, and resembles a bundle of long fibres folded back on itself. Data from EDAX analysis shows it to be primarily composed of carbon, oxygen, silicon and magnesium in smaller amounts, i.e. a

composition is suggestive of a mineralized biological entity (or possibly a carbon-rich magnesium silicate) (Figure 4-15). The fact that it is attached to the meteorite excludes the possibility that it is a stray terrestrial fibre or hair; in fact, its morphology is reminiscent of a filamentous microbe, possibly a Cyanobacteria. Those filaments also appear analogous to the structures found inside the Orgueil carbonaceous meteorite reported by Hoover (Tipler, 2011), in which the author claim it represent fossilized Cyanobacterial filaments originating from Mars.

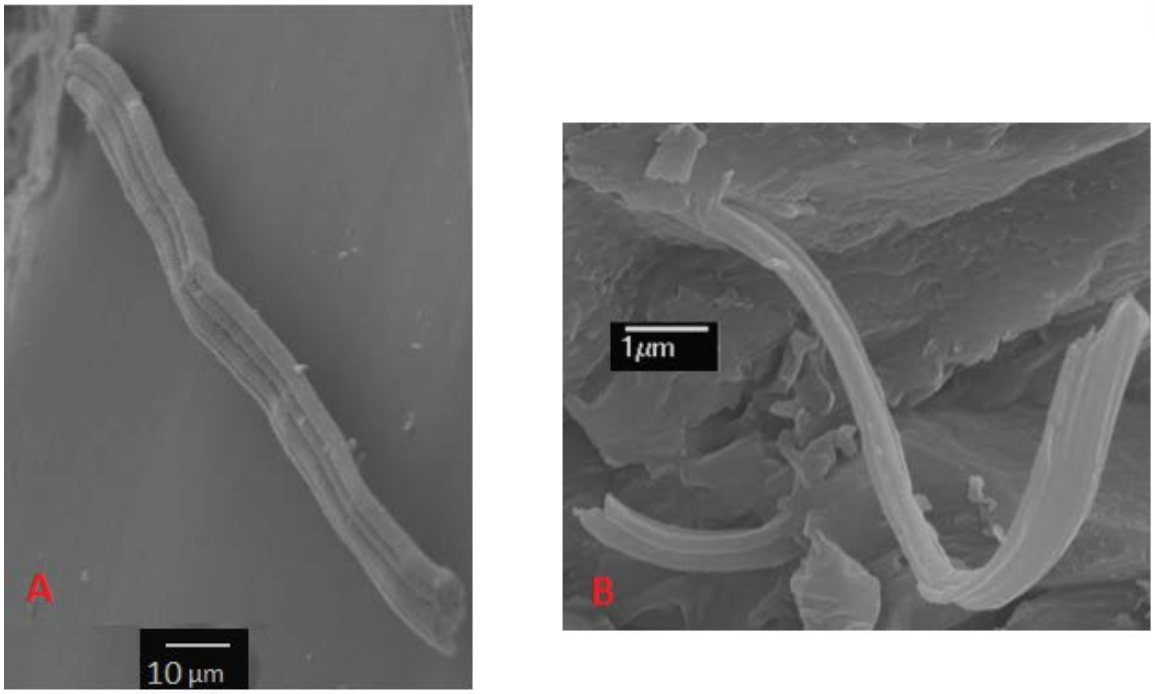

Figure 4-14: An SEM of filaments observed on the surface of a fragment of the Mars meteorite

A) Filament bundle folded up at the top. B) The attachment of the filament body to the meteorite.

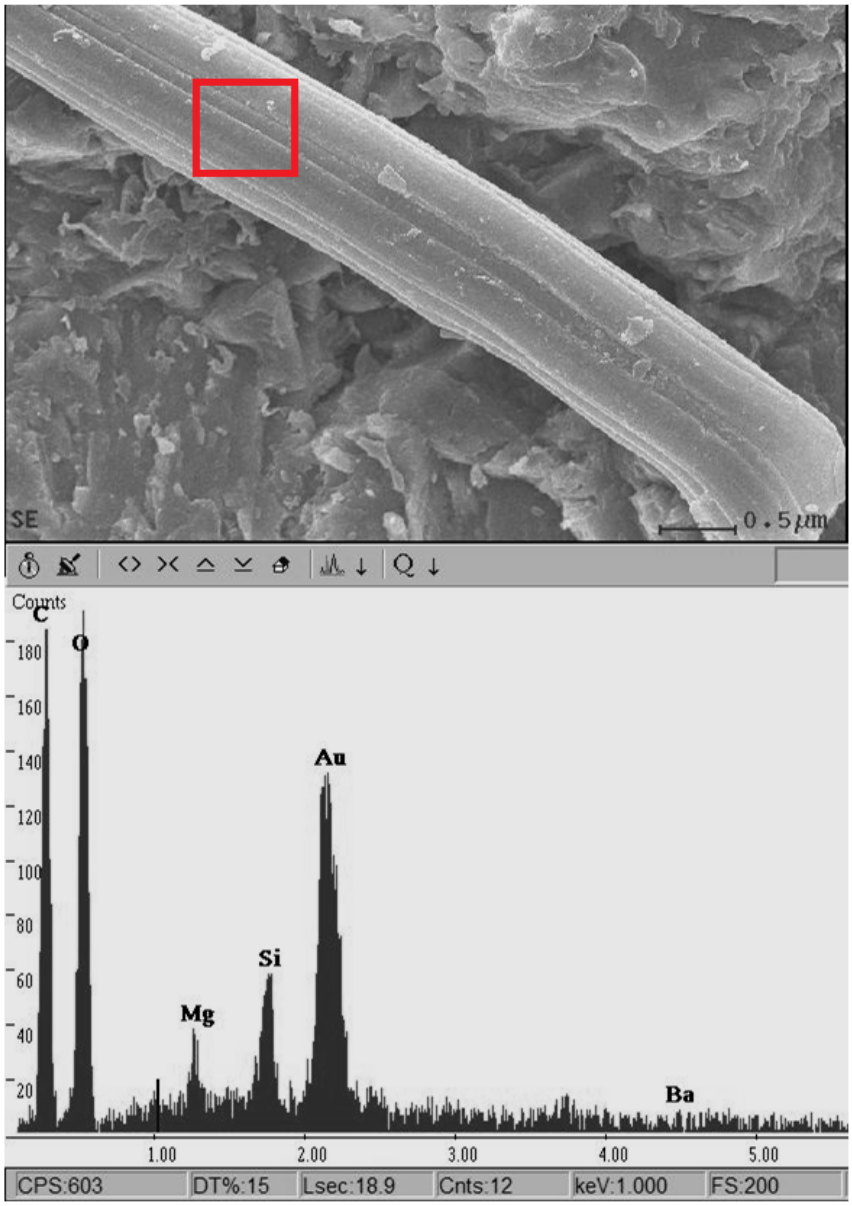

Figure 4-15: Results for the EDAX analysis for the fiber bundle

Upper image indicates the area for the EDAX, the data in the image below show the preponderance of carbon and oxygen.

Since biofilms appear mostly in water-rich environments, we suggest the presumptive bacterial biofilm reported by us to have been formed in a watery Martian environment, such a conclusion appear to be consistent with the reports recently originating from the NASA Mars Curiosity Rover of fine-grained sedimentary rocks, which are interpreted to represent an ancient

lake preserving evidence of an environment that could have supported life (Grotzinger *et al.*, 2014). Recent evaluation of the Labelled Release Experiment results from the Mars-Viking probe of 1976 have also shown that current Martian surface microbiology are likely to exist (Bianciardi *et al.*, 2012).

4.4.2 Analysis of the Polonnaruwa meteorite

Many small pieces of this meteorite were retrieved from the fall-site shortly after the impact event. Tests were then conducted on the samples in an attempt to validate their authenticity, origin, and to search for the presence of potential fossil microbes. Reports appeared to suggest the presence within the meteorites of indigenous diatom fossils (Wainwright *et al.*, 2013a, Wainwright *et al.*, 2013b, Wainwright *et al.*, 2013e, Wallis *et al.*, 2013, Wickramasinghe *et al.*, 2013a, Wickramasinghe *et al.*, 2013d). Wickramasinghe *et al.* (2013d) suggest that microbes can survive entry to our terrestrial biosphere by being in a freeze-dried state inside the pores and cavities. The same study also declared finding living microbes, besides fossils within the meteorite piece which was studied within the Medical Research Institute in Colombo. Figure 4-8 show some of the recovered microbes (Wickramasinghe *et al.*, 2013a). However, since we tested the sample only by using SEM and EDAX, we cannot validate such claims nor refute them. Further studies showed that this meteorite is distinct from fulgurite (material formed on Earth when lightning strikes sand) (Wainwright *et al.*, 2013a). Wallis *et al.* (2013) have shown the oxygen isotope data from the recovered meteorite fragments prove the fragments originated from the witnessed bolide event over Polonnaruwa city. The samples which we analysed for the Polonnaruwa meteorite was the same as that was investigated earlier by (Wainwright *et al.*, 2013b, Wainwright *et al.*, 2013e). Those studies reported the presence of microspherules which were revealed by EDAX to be carbonaceous, biomorphs, such as fossilized diatoms were also found.

Further analysis by us of data acquired from SEM and EDAX revealed many types of presumed fossilized entities occurring within the meteorite, some having relatively small sizes, with an average diameter of 0.5 µm, as shown

in Figure 4-16 which shows an aggregate of small structures similar to terrestrial bacilli. Their size is well above the nano-size of the ALH84001 fossils, and fairly similar in morphology to many well-known terrestrial bacteria. EDAX showed that chemical composition of the formation and the surrounding region, lacking microfossils, was identical, showing that the *Bacillus*-like structures are not modern bacterial contaminants. The biomorph-aggregate is also seen to be located within a depressed region of the meteorite, and appear to be interlocked with the topographically complex body of the rock, showing that they are highly unlikely to result from recent contamination.

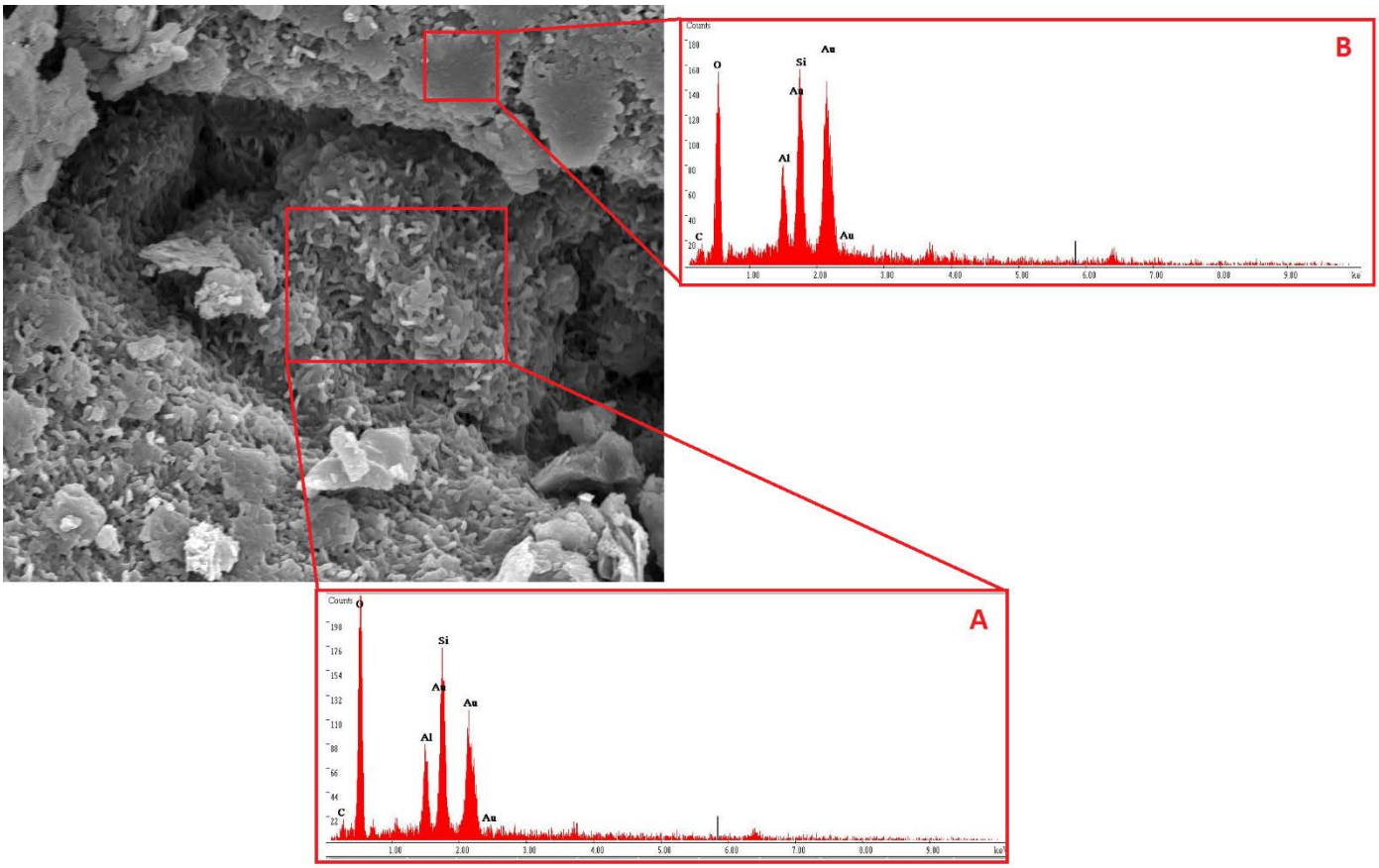

Figure 4-16: SEM image for a section of the Polonnaruwa meteorite, EDAX signatures for two locations is shown

A) an aggregate of biomorphs which are similar to rod shaped bacteria. B) EDAX for a featureless region within the meteorite section. Both A and B carry almost the same EDAX signatures.

Using the techniques available to us we cannot confirm that the biomorphs shown in Figure 4-16 are microfossils, since they may be mineral artefacts simulating biological structures (Koziol and Brearley, 2002). On the other hand, the relatively large microfossil shown in Figure 4-17 definitely appears to be biological in nature. The most striking feature (in addition to its size, around 600 µm in diameter) is its complexity, the upper half of the structure is missing, lost as the meteorite was cut. It possesses what appears to be a multilayered cell wall, suggestive of a single cellular eukaryote organism. EDAX analysis for areas within this entity revealed a consistency in the elemental composition, similar to the surrounding regions, meaning it is indigenous to the meteorite and not a modern contaminant, as evidenced by the presence of Si and Al which presumably replaced the original structures through the process of permineralization (Oehler and Schopf, 1971). The layered outer “cell wall” shown in Figure 4-17A is similar in some aspects of appearance to the cellulose in plant cell walls. However, we were not able to find an exact match for this microfossil from any previous studies.

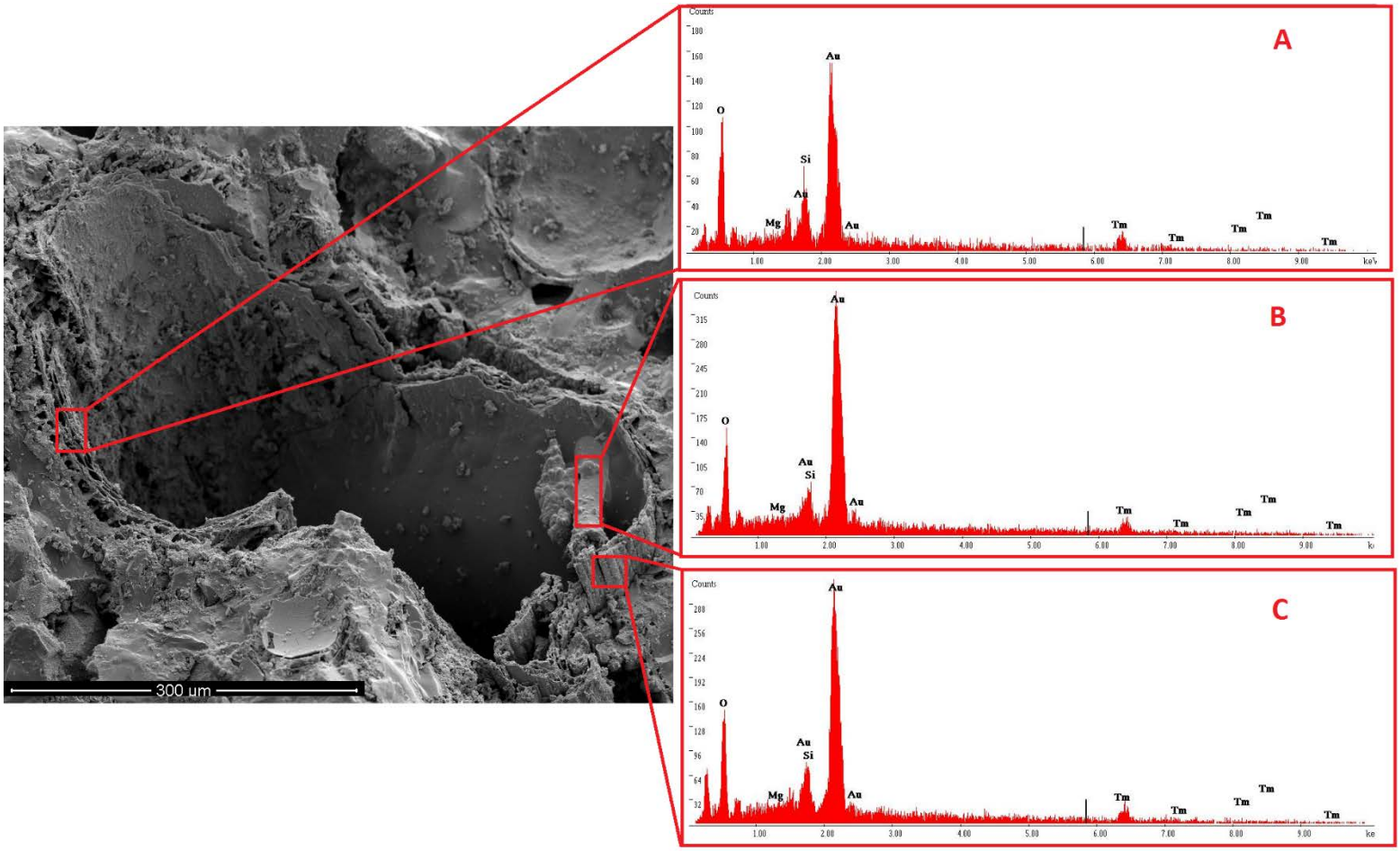

Figure 4-17: SEM and EDAX data for a large microfossil, identified within the Polonnaruwa meteorite

The EDAX measurements for three locations is shown. All of A, B, and C showed a similar chemical composition, suggesting a common origin.

Another large fossil shown in Figure 4-18 is also difficult to interpret, it appears to be a spherical object with a diameter of around 250µm, as before, EDAX analysis revealed an elemental composition of mainly Si and Al, with no nitrogen or carbon, thus excluding modern contaminants, what is noticeable here is the high O content.

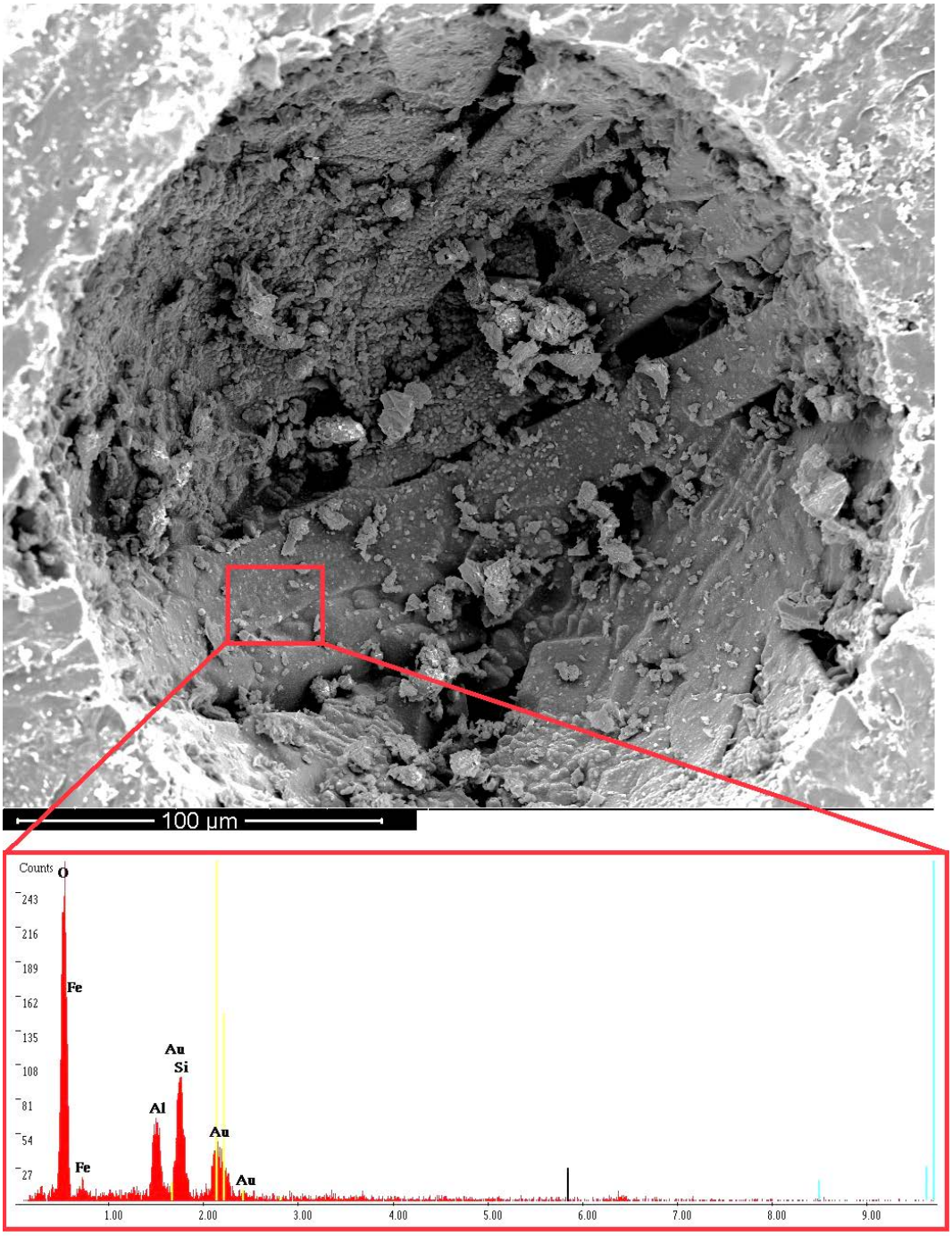

Figure 4-18: A view of a section of the Polonnaruwa meteorite showing a large spherical hollow structure

Possibly a micro-fossil, EDAX data showed a relatively similar chemical composition of this structure with the surrounding regions in the meteorite.

The structures shown in Figure 4-17, Figure 4-18 (Wainwright *et al.*, 2013a, Wallis *et al.*, 2013, Wickramasinghe *et al.*, 2013a, Wickramasinghe *et al.*, 2013d) are indicative of microfossils and not non-biological geological activity, or recent microbial contamination. Wallis *et al.* (2013) have shown that oxygen isotope results from the examined samples are in line with CI chondrites (Figure 4-19), and inconsistent with other samples from a terrestrial origin.

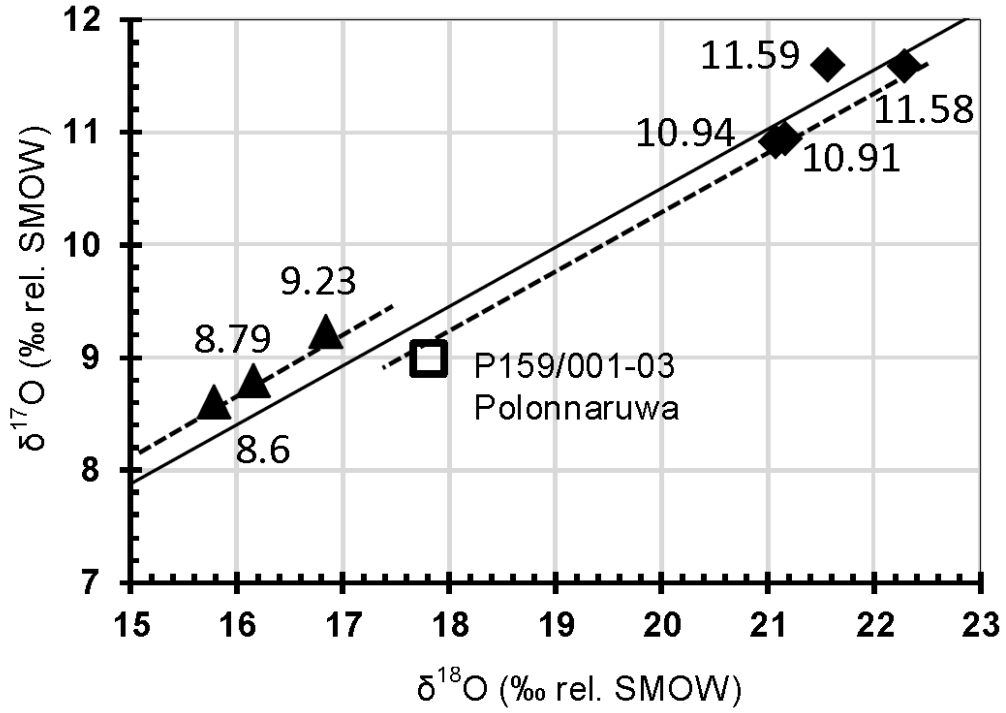

Figure 4-19: Oxygen isotopic composition data

Taken from Wallis *et al.* (2013) for a sample of the Polonnaruwa meteorite (sample P159/001-04), compared with data from other CI chondrite and CI-like chondrite meteorite samples (Alais (8.6), Ivuna (9.23) and Orgueil (8.79), (Meta-C) B-7904 (10.91), Y-82162 (11.59), Y-86720 (11.58) and Y-86789 (10.94)).

4.4.3 Analysis of the Carancas meteorite

The Carancas meteorite was observed by locals when it fell. The people near the area of the fall reported experiencing nausea, vomiting, and other medical symptoms. Mineralogical analysis of the Carancas meteorite fragments revealed it to be a chondrite with a fine-grained, grey light-

coloured texture, embedded with a rich composition olivine (Macedo and Macharé, 2009), the distinct coloration of olivine was easily recognized using light microscopy (Figure 4-9).

4.4.3.1 Scanning electron microscopy Examination

Images obtained using SEM for the fractured Carancas samples revealed a prevalence of minerals with varying morphology and sizes, showing mostly a conchoidal fractured appearance, with other irregularly shaped bodies (Figure 4-20 A and B).

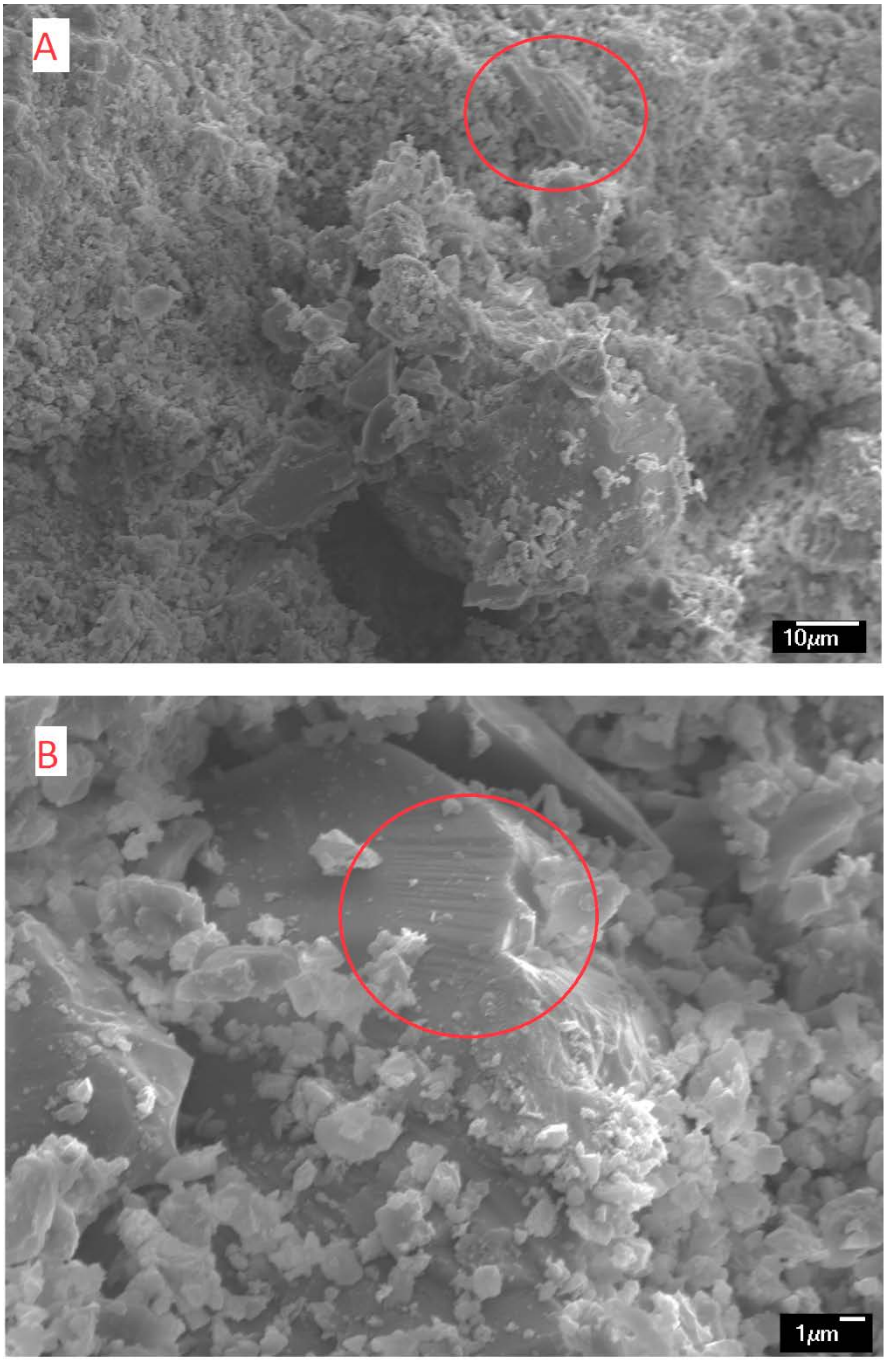

Figure 4-20: SEM section from the Carancas meteorite particles

Various irregular structures are apparent in both A and B, a couple of the locations which show conchoidal fractured appearance are encircled with red.

Rauf *et al.* (2011) presented SEM images of this meteorite which showed the presence of regions containing individual particles with small elongated features. When it was viewed using higher magnification, was shown to contain ovoid and rod-shaped formations. A similar looking structures have been found within the sample used here, Figure 4-21 comparing images from this work and Rauf *et al.* (2011).

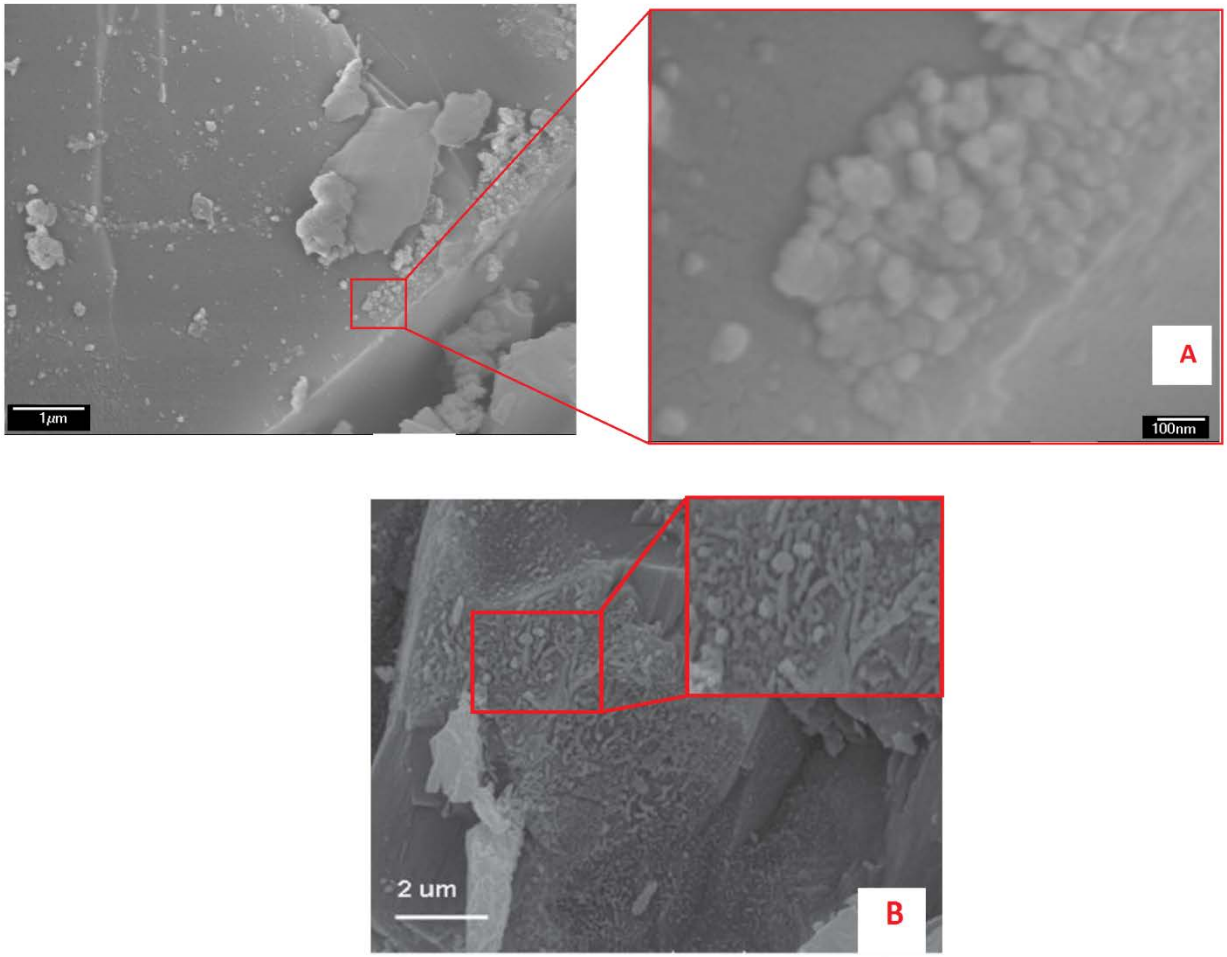

Figure 4-21: SEM images for sections of the Carancas samples showing ovoid and rod-shaped formations

A: shows one of the images from the work presented here; the nano-formations can be observed in the magnified image on the upper right inset. B: a SEM image from Rauf *et al.* (2011) showing formations that are closely similar to the findings presented here.

Another feature found by us, which was also reported by Rauf *et al.* (2011) is the mud-crack like formations, shown in (Figure 4-21). Those formations are seen to be intermixed with nano-ovoid, and rod-shaped structures, however, despite their similarity to known terrestrial microfossils in appearance, and with many of the microfossils reported within the ALH84001 Martian meteorite (McKay *et al.*, 1996), as well as the carbonaceous chondrites examined by Hoover *et al.* (2003), it is suggested that these structures are abiological, as are the forms shown in Figure 4-22, which are probably crystal-bundle precipitates.

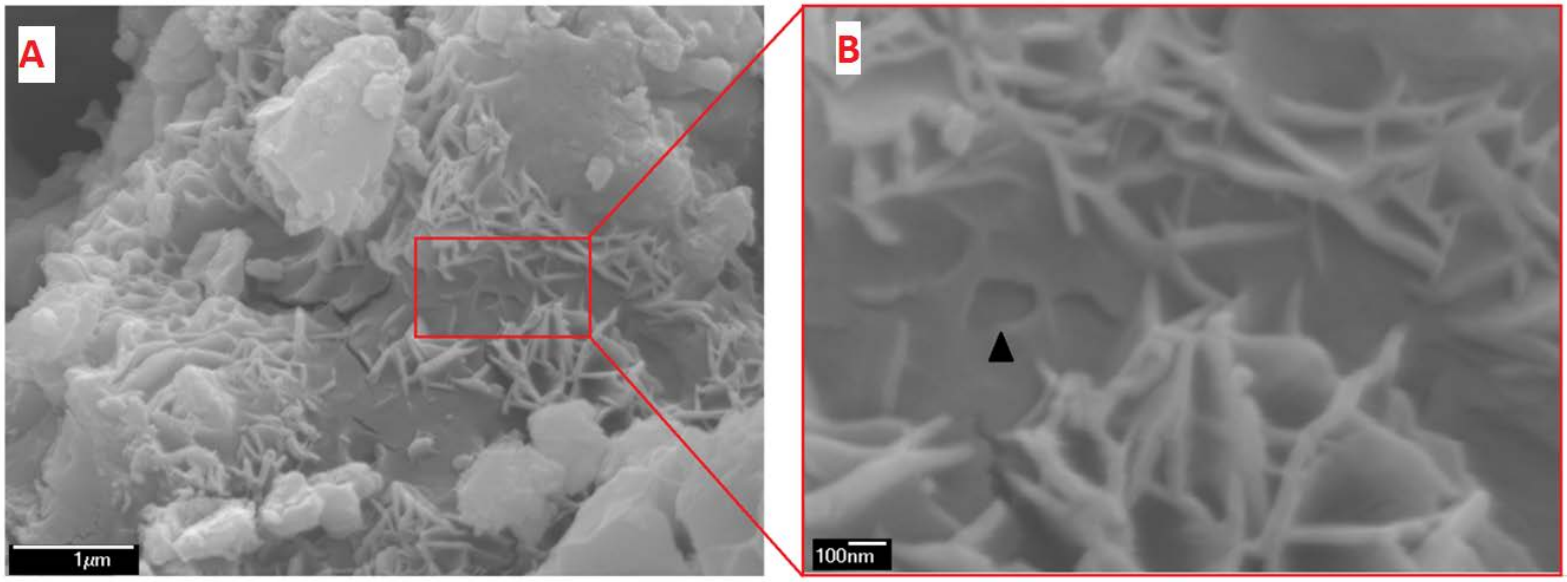

Figure 4-22: An SEM image for a section of the Carancas meteorite

A: the mud-cracked formation can be seen clearly in the centre of the image. B: an enlarged inset showing the intercomplex elongated structures, which we suggest to be carbonate crystal bundle precipitates, although we cannot entirely exclude a biological origin for it. A set of uniquely-shaped cavities can be also seen (black triangle in B).

Another interesting feature is also shown in Figure 4-22B, comprising unusual cavities, resembling those reported by Rauf *et al.* (2011) using

similar SEM analysis techniques, and might be attributed to a steam-phase formation as suggested by Miura (2008). In which the Carancas meteorite has undergone two significant processes; a high temperature following entry in the stratosphere (melting phase), and the subsequent event when the hot meteorite reacted with the cold-ground water at the impact site (steaming phase). The fact that this meteorite was fragmented relatively easy as it approached the impact site (Borovička and Spurný, 2008), also adds to this scenario.

The Carancas meteorite also contains various types of minerals that are expected to be present in space-derived samples. Optical microscopy, and EDAX results from previous studies showed a rich content of olivine, pyroxene supporting the suggestion of this meteorite as an ordinary H4/5 chondrite (Macedo and Macharé, 2009, Rauf *et al.*, 2011). The clear presences of a fusion crust on the outer-rim of the broken samples (Figure 4-9), and the presence of magnetism, further confirm the authenticity of the samples.

4.4.3.2 Microbes isolated from the Carancas samples

The second part of the Carancas meteorite analysis was devoted to an attempt to isolate viable microbes from its centre using the sterile-breakage vessel described in 3.5.1.2. Seven samples were used for this purpose, six of which were surface-sterilized thoroughly, while the seventh sample was used without sterilization as one positive control and a sterile-breakage vessel lacking a sample (with only the growth media inside) were also used as negative controls.

None of the six decontaminated samples showed any initial signs of microbial growth (no turbidity in the clear-liquid of the nutrient broth), showing that the external surface of these samples were sterile. The next step involved breaking the six meteorite pieces while still sealed within the vessels, and then incubating to see if there was any growth; the nutrient broth, remained clear in all of the six vessels, showing that the Carancas samples did not contain any viable microbes. This was further confirmed later by taking some of the nutrient broth from the vessels and examining it

under the light microscope when no signs of microbial cells was observed. However, the single meteorite sample which left unsterilized, did show signs of growth in the liquid culture within the vessel, which was expected since it was likely to possess surface contamination. DNA extraction and 16S rRNA PCR protocol as described in 4.3.3.5, was used on a single colony isolate. The BLAST search for the DNA sequences which were later obtained following 16S rRNA PCR revealed the presence of three bacteria, namely: *Bacillus megaterium*, *Bacillus gelatini*, and *Bacillus aryabhattai* (See Appendix C: C1, C2, and C3). These bacteria are normal inhabitants of soil and ground-water (McCune *et al.*, 2002, Liu *et al.*, 2009), *Bacillus aryabhattai* has been isolated from the stratosphere between 24-41 km (Shivaji *et al.*, 2009), and may have been picked up by the meteorite as it crossed this region.

To recap on the findings from the Carancas meteorite, neither the SEM analysis, nor the sterile isolation techniques showed strong evidence for the presence of past or present life within the samples. This does not weaken the panspermia theory, since it is unlikely that every meteorite and comet contains biological relics or entities within it.

CHAPTER 5

5 Chapter 5: Microbial Survivability Under Exposure to UV in Extreme Cosmic Conditions

5.1 Introduction

The theory of Panspermia has impact on many areas of Astrobiology. For example, information on microbial survivability is important in order to limit potential interplanetary contamination by spacecraft and the refinement of planetary protection protocols (Crawford, 2005), for maintaining life support systems (Hendrickx and Mergeay, 2007), and finally in relation to the searching for life elsewhere in the cosmos (Abrevaya *et al.*, 2011).

According to the modern panspermia theory, in order for microbes to survive interplanetary transport, they must survive all the three stages of the transfer process; (i) The ejection (escape) stage, which involves the ejection of planetary material, with microbes in it into outer space, possibly due to a strong impact such as a meteorite or a cometary impact, (ii) The extended journey of the ejected matter through space between planets (1-15 million years), (iii) The entry stage, in which the microbes are safely deposited on a recipient planet (Homeck *et al.*, 2002b).

Numerous studies have been conducted to investigate each of the above three stages of panspermia. In this work, an attempt is made to a) simulate the conditions facing microbes in icy comets, b) test if microbes can be shielded against lethal UV radiation by the shading effect of nano-particles. In addition, investigatethe novel concept that visible light generated indirectly from UV radiation supports photosynthesis, which might protect microbes in an atmosphere-stripped planet.

5.2 Microbial survival during the stages of panspermia interplanetary travel

Microbes face critical survival conditions during the ejection and the landing stages suggested by the Panspermia theory (Burchell *et al.*, 2004, Cockell *et al.*, 2007, Moeller *et al.*, 2008, de La Torre *et al.*, 2010a). A range of microbes (bacteria, fungi, and viruses) have been tested for their survival abilities, as have biomolecules, such as nucleic acids, amino acids, and liposomes. All have been exposed to space conditions outside of the protective magnetic field of the Earth (Apollo 16), or on board the Earth-orbiting missions, including the Spacelab1, Spacelab D2, BIOPAN mission, and EXPOSE on the ISS (Olsson-Francis and Cockell, 2010). In such experiments, microbes have been exposed to high vacuum, intense UV, temperature extremes, and cosmic radiation, all of which may affect the stability of genetic material leading to high mutation rates and inactivation and damage to the nucleic acids. A factor which was found to have the most lethal effect on unprotected (i.e. naked) microbes, is extraterrestrial solar UV radiation, although when sufficiently shielded, spores of *Bacillus subtilis* were able to survive in space for over 5 years (Horneck *et al.*, 2008).

Horneck *et al*,. (2008) investigated the ejection stage of panspermia by subjecting bacterial spores, and certain lichen species to shock pressures ranging between 5-40 GPa. The results indicated that microbes are able to survive planetary ejection, in a scenario that might have occurred during Earth's early history when life may have been “inoculated” to the planet. Another study by Burchell *et al.* (2017) also showed that fossil fragments can survive 20 GPa shock pressures. The effect of extreme UV radiation (30.4 nm) on *Bacillus* sp. and *Deinococcus radiodurans* was tested during a rocket flight by Saffary et al., (2002). The survival rate decreased by an extra order of magnitude under desiccation for both organisms, presumably due to cellular damage on the outer membranes and proteins, rather than DNA denaturation. Lichen can also colonize and photosynthesize following sixteen days of full exposure to the space conditions on board of the Biopan-5 research facility (de La Torre *et al.*, 2010a). The STONE experiment, by the European Space Agency (ESA), was also used to test the re-entry step

of the panspermia theory. Cockell et al., (2007) reported on the gneissic rock samples that contained within it *Chroococcidiopsis sp*, an endolithic photosynthetic microorganism, was unable to survive re-entrance to the atmosphere due to extreme temperatures penetrating down to more than 5mm deep into the rock.

A significant recent investigation of the feasibility of microbes surviving entrance to Earth-like atmospheres was conducted in relation to microbes contained in meteorites was carried out by Slobodkin *et al.* (2015) as part of the METEORITE experiment on the FOTON-M4 satellite. These experiments involved using *Thermoanaerobacter siderophilus*, a spore-forming, anaerobic, and thermophilic bacterium, which was placed inside small basalt discs (1.4 cm in thickness) and fixated on the exterior hull of the space capsule. After being exposed to space conditions for 45 days in orbit, the landing module re-entered the Earth, during which, the outer surface of the basalt discs melted due to the extreme heating of the atmospheric transit. However, out of the 24 wells of the discs, viable microbes were recovered from 4 and confirmed by PCR 16S rRNA identification. This experiment is significant because it provides good evidence of the ability of a microbe to survive inside an “artificial” meteorite during the re-entry process.

The possibility of Mars to Earth exchange of microbes within meteorites is of particular interest because of the relatively short distances involved. Mileikowsky *et al.,* (2000) calculated that in order for microbes to be protected from harmful extraterrestrial UV radiation, shielding by rock material around microbial cells and spores is necessary. He also predicted that in order for microbes to survive a one million-year interplanetary trip between Mars and Earth with a viable minimal population, microbes must be shielded deep (0.33m) in rock. The same study also estimated that during the last four billion years on Earth, more than 100 billion meteorites, each with a temperature under 100^{o}C, have landed on the surface of Earth. Numerous recovered meteorites have been confirmed to have a Martian origin (Fritz *et al.*, 2005), therefore suggesting the possibility of interplanetary transfer of matter within the solar system.

5.3 Composition of Asteroids, Comets and Meteoroids

Asteroids are relatively small bodies made of rocky materials including carbon. Comets, in contrast, are made of ice, organics, and dust particles (carbon, silicon, minerals etc.), and when close to the sun; a visible tail of dust and gas can be observed. Meteoroids can belong to either asteroids or comets and when they burn up in mid-air they become meteors; if the meteoroid then succeeds in reaching the Earth's surface the surviving piece is referred to as a meteorite (Campins and Swindle, 1998). As mentioned earlier; microbes need to be protected from harmful radiation when in deep space; opaque materials in asteroids provide an obvious means for this purpose (Rettberg *et al.*, 2002a). Unlike asteroids, comets are mainly icy volatiles of frozen gases mixed with cosmic dust (Bockelée-Morvan, 2011). Pristine, thin ice is unlikely to protect microbes against harmful radiations, although the presence of dust particles within an ice comet will tend to shield microbes from harmful UV radiation.

5.4 Cosmic radiation in the universe

Three bands of solar radiation intensity are present (from the least to most biologically harmful, respectively), namely UVA from 320 to 400nm has the longest wavelengths, UVB from 290 to 320nm, and UVC, a shortwave ionizing radiation, which is the most lethal of the three, and ranges between 200 to 290nm; following sufficient dosage exposure it can kill or, at least damage, most microorganisms including viruses (Chang *et al.*, 1985, Gascón *et al.*, 1995, Paul and Gwynn-Jones, 2003).

UVA is prevalent on the surface of the Earth, while only small amounts of type UVB reaches us since the ozone layer absorbs most of it (about 90%) as well as all of the UVC. So life forms on the Earth's surface are virtually safe from radiation's harm (Organization, 2002), but as we go higher into the atmosphere the ultraviolet levels increase at around 10-20% with each kilometre (Blumthaler *et al.*, 1997), The exposure dosage for other cosmic

radiations also increases exponentially with altitude, although these are not as significant as UVC when it comes to causing damage to living organisms (Galante and Ernesto Horvath, 2007). It's worth noting that the harsh conditions of the upper atmosphere induce survivability traits in microbes residing here; Studies have shown for example, that dried microbes in cold and extremely low pressure environments exhibit higher survivability rates than microbes normally found at room temperature and pressure (Miyamoto-Shinohara *et al.*, 2006). This means it is logical to assume that "Ultraviolet-sensitive bacteria could also have been isolated from our upper atmospheric samples, if they were not exposed to ultraviolet radiation." (Yang *et al.*, 2008a).

Four types of cosmic radiation can potentially harm microorganisms where they are not adequately shielded (Mileikowsky *et al.*, 2000):

- Solar Ultraviolet radiation.
- Solar energetic particles in interplanetary space.
- Diffuse X-rays.
- Galactic cosmic rays; (γ) rays and charged particles.

The lethal effects of UV and to a lesser extent, X-rays and solar particles, can be mitigated by even the thinnest layer of rock or other materials (Nicholson *et al.*, 2005). Protection against galactic cosmic rays differs a little; the thicker the initial coating, greater ultraviolet exposure will induce cell- damage until it reaches a threshold, then the more coating is increased in thickness the more protective the shielding against ultraviolet will be, providing the microbes with the required protection (Mileikowsky *et al.*, 2000).

5.5 Relevance of microbial resistance against cosmic UV to the panspermia theory

A major reason why the lithopanspermia theory has started to gain popularity in recent years is based on the discovery on Earth of lightly-shocked Lunar and Martian meteorites, suggested the possibility of

interplanetary exchange of meteorites (Mileikowsky *et al.*, 2000, Nicholson *et al.*, 2005). The transit time for Mars to Earth meteorite-transfer it is estimated at between 10^5-10^7 years (Gladman *et al.*, 1996), although shorter transit times are possible with more direct trajectories (Gladman and Burns, 1996). In stark contrast, the transit times for spaceships and probes is significantly shorter, although such transfer is only relevant to directed panspermia (Crick and Orgel, 1973). The transfer of microbial spores is particularly relevant to panspermia because of their resistance to most extreme environments including extended transit time and UVC (Joseph and Schild, 2010). Most studies for microbial survivability in space experiments involve microbial spores (Horneck *et al.*, 2008, de la Torre *et al.*, 2010b, Olsson-Francis and Cockell, 2010, Wassmann *et al.*, 2012), such as *Bacillus* species, which can be 10-100 times more resistant than vegetative cells to UV radiation (Nicholson *et al.*, 2002).

In spores, the component which presents the target for inactivation by UV is mainly DNA, and this appears to be applicable for the whole spectrum of UV. The UV radiation can generate lesions directly on the DNA, in addition to the producing of reactive oxygen species (ROS) which can kill spores by the generation of single and double strand breaks in the genome of the microbial spore (Nicholson *et al.*, 2005). One mechanism which bacterial spores might use to shield itself from UV is by concentrating absorbing pigments within its spore-coats and outer layers (Hullo *et al.*, 2001). However, as mentioned earlier, the UV wavelength which is most efficient in killing both vegetative and spores of bacteria is UVC, estimated to be ≥300-fold more efficient than UVB and UVA. When actively growing microbes, such as *B. subtilis* are exposed to UVC directly, cyclobutane-type dimers are primarily generated between adjacent pyrimidines on the same strand of DNA. Those cyclobutane pyrimidine dimers (CPDs), can be generated by adjacent cytosines (CC), thymine and cytosine (TC, or CT), and thymines (TT). Potentially lethal lesions can then result from the various photoproducts generated between adjacent pyrimidines (Nicholson *et al.*, 2005).

The loss of bacterial diversity and biomass for life travelling in space can be attributed to any of these inhibitory factors: high vacuum, solar UV radiation, desiccation, temperature fluctuations, Earth's Van Allen Belt's charged particles, solar particle events, and galactic cosmic rays (GCR). Most recent studies have indicated that a spore-forming microbes are better protected from these factors than are non-sporing species (Wassmann *et al.*, 2012, Kawaguchi *et al.*, 2013b, Bryce *et al.*, 2014). Also, many studies have shown consistently that despite the strong lethal effect of space UV radiation against microorganisms, the effect of UV can be easily avoided by thin layers of UV absorbent pigments in the spores, dust, metal oxides, or any kind of opaque materials (Cockell, 1998, Horneck, 1998, Horneck *et al.*, 2001). It is unlikely however, that any naked microbe, even a spore former, could travel through space and retain its viability instead organisms need to be protected by being present within meteorites or covered with cosmic dust. Although the Earth's Van Allen radiation belts, SPE, and GCR can affect deeper layers inside meteorites, they require long exposure times to be considered significant in reducing microbial numbers and activity (Nicholson *et al.*, 2005).

5.5.1 Microbial embedment and UV penetration of ice

As mentioned earlier, icy volatiles are an important component of comets. However, most proposed scenarios for the interplanetary transfer of biological material have concentrated on attempting to explain microbial shielding against UV in meteorites and rocky substances, without focusing on the ice component of comets. In fact, almost all survivability experiments have used only dried microbial cells and spores (i.e. samples not suspended in liquid) (Horneck *et al.*, 2001, Rettberg *et al.*, 2002b, Slobodkin *et al.*, 2015). According to Wickramasinghe's version of Cometary Panspermia, microbes are able to survive within the comet's core, surrounded by outer layers of ice as well as in transient cometary "lakes" and "ponds", the outer layers being stripped through the action of sublimation as the comet voyages through space (Wickramasinghe *et al.*, 2009).

Although freezing can be lethal to some microbes, many bacteria can survive and metabolize in ice, a medium in which it is suggested life may have originated (Price, 2007). Many physical and chemical factors that kill microbes become ineffective when bacteria are embedded in ice. UV radiation is an exception in that it can penetrate ice sheets and blocks and kill microbes embedded within the ice (Ladanyi and Morrison, 1968). When the ice is free of solid particles and pure its transparency is similar to that of distilled water and in normal lake waters UV can penetrate to depths of 5-10 meters (Berkner and Marshall, 1965).

5.5.1.1 Bacterial resistance to ultraviolet radiation in water and ice, with and without suspended particles

It is imperative when investigating panspermia to assess the lethal effect of different types of UV on a selected microbial samples which are embedded in ice, and compare them to ones that are in water (Ladanyi and Morrison, 1968), and also determine whether the size of inorganic particles embedded in ice play a role in providing shielding for microbes from UV.

The theoretical predictions of a study by Trodahl and Buckley (1990) have showed that for ice, UV absorption coefficients are similar to the water values. This was confirmed further by the practical work they reported within the same study, showing that UV transmittance in seawater with an over-layer of ice above it decreased through different periods of the year due to an increased turbulence of the ice, therefore limiting the amount of UV reaching the layers below.

5.6 Exploiting UV as an in indirect energy source for microbes

A few microorganisms, such as *Deinococcus radiodurans*, can live in heavily irradiated environments such as nuclear reactors (Cox and Battista, 2005). However, gaining such an exceptional ability to withstand radiation may have taken millions of years of evolution, while the first time such conditions existed on Earth is during the 1940's when the first nuclear reactors were made (Narumi, 2003). This leads to the conclusion that, these microbes, millions of years ago, lived in an environment with strong ionizing radiation. Later, when *Deinococcus radiodurans* was brought to earth and lived in relatively stable conditions, the need for irradiation-response genes subsided, therefore they were locked away until the needed, when manmade nuclear reactors were developed (Pavlov *et al.*, 2002, Wainwright, 2003, Pavlov *et al.*, 2006). Even bacteria, such as *E. coli*, have been found by Pavlov *et al.* (2006) to develop high radiation-resistance when exposed to cycles of high radiations doses.

When investigating survivability in outer space and on other planets, the search is mostly for either microbes in a dormant state i.e. bacterial spores, or viable microbes which could survive cosmic radiations and nutrient deprivation; such microbes are suggested by many studies to be endolithic (Horneck *et al.*, 2008, Bryce *et al.*, 2014). Endoliths are considered prime candidates when searching for extra-terrestrial life because of their ability to be embedded in deep rock layers (Onstott *et al.*, 1997, Rettberg *et al.*, 2002a, Rastogi *et al.*, 2010), they are also protected against desiccation and rapid temperature fluctuations (Friedmann, 1982, Yoon *et al.*, 2006).

Less attention is usually given to photolithoautotrophs and photoorganoheterotroph when searching for extra-terrestrial life; since photosynthesis is not an option for endolithic microbes due to no light

reaching them. If such microbes are directly exposed to lethal conditions, either on the surface of a comet, or a planet with no atmosphere they will be eventually inactivated (Wayne, 1991). Alternative sources of light other than stars have been suggested, based on reports regarding photosynthetic deep-sea microbes on Earth which uses light from the molten volcanic rocks near it (Beatty *et al.*, 2005). Although the work proves photosynthetic organisms can survive in geothermally illuminated environments, the problem is that the released energy is relatively small, extremely localized, and it requires a geologically active planet.

A scenario which might allow microbes to survive the long duration of space travel is proposed in this Chapter, namely, microbes might be able to use energy converted from UV indirectly into visible light. Such light might then be used by photosynthetic microbes, while the system provides the additional benefit of providing protection from the lethal effect of UV radiation

5.6.1 Light conversion within fluorescent minerals

While all minerals reflect light, certain ones can absorb UV light and convert it into longer wavelengths before emitting it back; a process termed as fluorescence, in which the short wavelength of invisible light (200-400nm) is converted to any of the colours contained within the visible light spectrum (400-700nm). This phenomenon makes rocks that contain these minerals glow in the dark when exposed to UV light, the colour of the visible light produced depends on many factors, such as the UV wavelength and the type of impurities present in the rock. Out of 4,200 identified mineral species, about 566 have been identified as fluorescent (Robbins, 1983, Henkel, 1989, Robbins, 1994). Fluorescent minerals are abundant on earth and in the universe, the fluorescence property in most of those rocks is due to impurities in certain quantities within them that work as activators. However, there exist minerals that fluorescence when pure, e.g. scheelite, powellite, and many minerals of uranium (Robbins, 1994).

This section of the Thesis is devoted to the proposition that life might exist and survive in space by employing this property of fluorescent minerals,

which can be applied on comets and meteorites (panspermia), or on planets which have the surface (or part of it) covered with some of the semi-transparent rocks (Figure 5-1) containing fluorescent minerals. Such as quartz (SiO_2), which is expected to be found on countless planets and in cosmic dust (Henning, 2010) with silicon being the 8^{th} most abundant element in the universe (Mason and Mason, 1991). Those rocks can cover both watery and rocky planetary surfaces, and while no life can be present on the upper surface of such rocks because of exposure to high intensity UV atmosphere, the area beneath provides a safe environment from such damaging irradiation (Tuchinda *et al.*, 2006).

When UV from a near-star falls on fluorescent rocks, it will be absorbed and emit visible light which can be used in photosynthesis. As a result, these minerals potentially protect the photosynthetic endoliths from damaging UV and also provide sources of energy in the form of visible light and heat. A food chain could then possibly be established where carbon from photosynthetic endolithic organisms feeds nearby heterotrophs, similar to the ones found in Earth's aquatic environments.

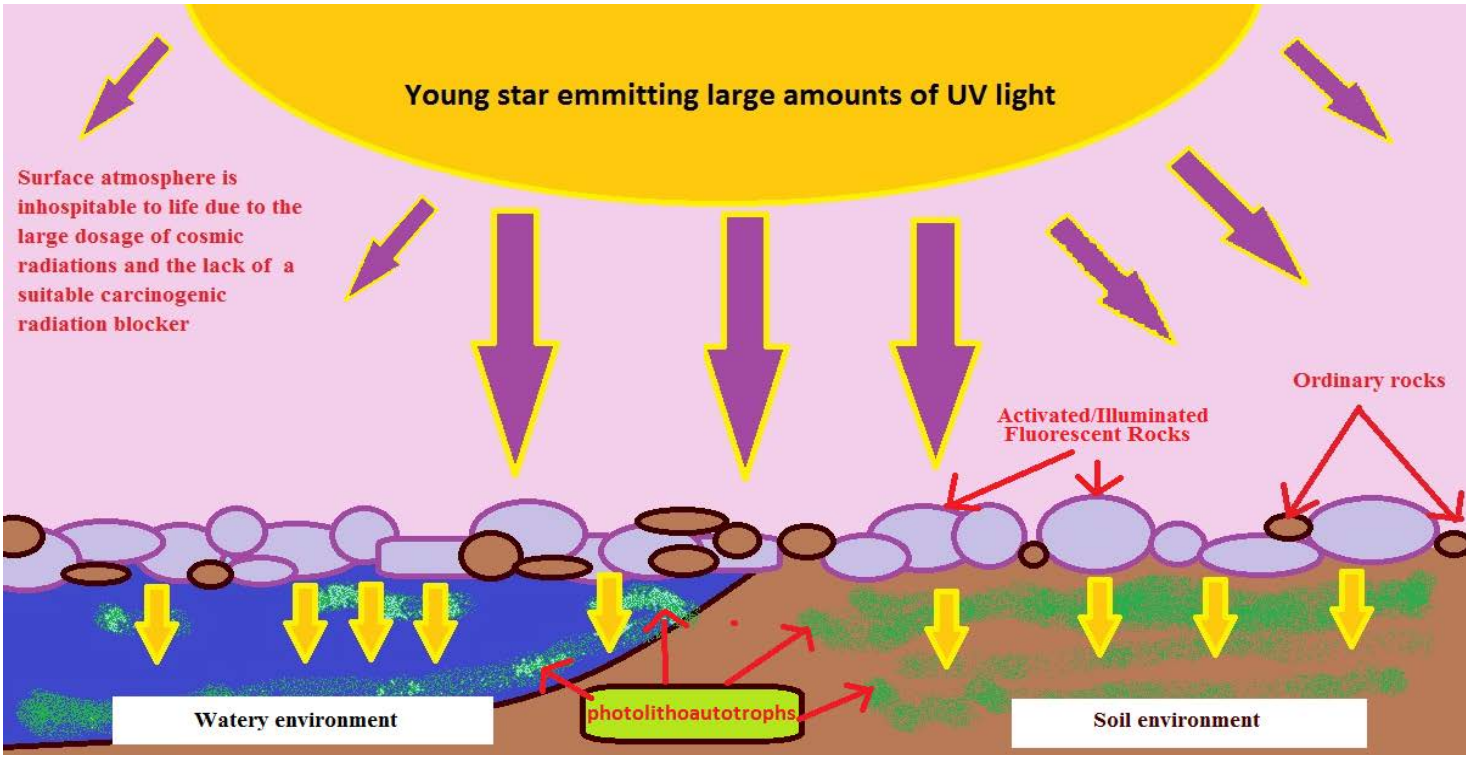

Figure 5-1: Hypothetical scenarios were the UV from a young star is absorbed by fluorescent rocks present on a planet's surface

The absorbed energy is then emitted to the underlying microbes as both light and heat, thus providing them with a constant energy supply enhancing their growth, the benefit of such system is that although the surface of the planet could be exposed to harmful radiation, it will not kill underlying microbes.

The proposed system could be particularly useful where cosmic environments are exposed to UV, but not visible light; the young Sun emitted up to 10000 more UV than it does now (Canuto *et al.*, 1982, Cockell and Horneck, 2001). The implications of this new hypothesis (suggested by us) could change our perception of the required conditions for extra-terrestrial photosynthetic microbes since it allows life to get a head start inside the subsurface of planets like early Earth, essentially because a hospitable surface environment is not needed. Such a scenario allows for an earlier starting point than what is suggested currently (Ohtomo *et al.*, 2014), this possibility is particularly relevant since the oldest known microbial fossils

belongs to the Cyanobacteria (Schopf, 1993, Simeonov and Michaelian, 2017).

In cometary panspermia, such a system, which enables microbes to gain energy indirectly holds notable advantages; It allows the microbes to metabolize and remain active instead of being dormant throughout the journey in space, meaning DNA repair mechanisms can still operate while being protected from UV and using visible light for energy. Finally, a small amount of heat also results by conversion of the excess vibrational energy, this can provide the explanation for how a micro-watery environment might be present within the comet for the microbes to metabolize (Chen *et al.*, 2003).

The aim of the work described below was to determine

1. If ice protects microbes from UV either in its pristine state or when contained within particles.
2. To provide experimental evidence in support of the above mentioned theory based on the conversion of UV to useable visible light by fluorescent minerals to support photosynthetic endoliths.

5.7 Materials and Methods

Resistance of selected microbes to UV radiation in pristine ice, and ice mixed with nanoparticles

5.7.1 Resistance of bacteria to UV radiation in pristine ice

Ten bacterial species obtained from a variety of sources, and identified using PCR 16S rRNA identification, were used:

- *Bacillus subtilis*
- *Bacillus sphaericus*
- *Bacillus thuringiensis*
- *Bacillus licheniformis*

- *Escherichia coli O157*
- *Eschericia coli DH5α*
- *Pseudomonas aeroginosa*
- *Rhizobium radiobacter*
- *Staphylococcus aureus*
- *Salmonella typhi*

Each bacterium was inoculated into (5ml) of Nutrient broth, incubated with shaking at 250 rpm in 37°C for 18 hours. The culture was then diluted to equalise 0.5 McFarland turbidity standard, later, serial dilutions of $1/10^4$ were performed for each sample by taking 1 ml and into 9ml of distilled water, then, 1ml was taken from the 4^{th} final dilution and into 10 different petri plates, labelled as shown in Table 5-1.

Table 5-1: Plates distribution used for each bacterial species for the UV C resistance in pristine ice and water.

Control: W0	**Control: I0**	**W1**	**W2**	**W3**	**W4**	**I1**	**I2**	**I3**	**I4**
Water: No ultraviolet exposure	Ice: No ultraviolet exposure	Water: UV exposure for 5 minutes	Water: UV exposure for 10 minutes	Water: UV exposure for 15 minutes	Water: UV exposure for 30 minutes	Ice: UV exposure for 5 minutes	Ice: UV exposure for 10 minutes	Ice: UV exposure for 15 minutes	Ice: UV exposure for 30 minutes

Distilled water (29 ml) was the added into each of the plates and stirred gently to mix the contents. Plates (I0, I1,I2,I3,I4) were allowed to freeze by placing them for four hours at -20° C, while the plates (W0, W1,W2,W3,W4) were stored at 4°C for the same period.

Later, control plates (W0, I0) were placed on the bench at room temperature, and all remaining plates were placed in a sterile laminar flow hood containment level 2. under an UV light type C (254nm, 8 W– UVP LLC, model number: 95-0200-02), with their plates lid removed during the exposure time, plates (W1,I1) were exposed for 5 minutes, (W2,I2) for (10) minutes, (W3,I3) for 15 minutes, and plates (W4, I4) for 30 minutes. The UV lamp was fixed to the ceiling of the laminar hood, facing down towards the plates, with the distance of 30cm from the surface of the bench.

After exposure, the lids were repositioned on the plates, and the ice plates were allowed to melt at room temperature, an amount of 1 ml was taken from every plate, including the controls, and spread onto Nutrient agar plates with a sterile glass spreader, the Nutrient plates were then incubated at 37°C for 48 hours, subsequently, observation of growth and colony count was performed for each.

5.7.2 Resistance to Ultraviolet Radiation in Ice and Charcoal Mixture

Carbon, which is the fourth most abundant element in the universe after hydrogen, helium, and oxygen, (Schramm and Wagoner, 1977) is generally abundant in comets (Hoyle and Wickramasinghe, 1985, Wickramasinghe *et al.*, 2009, Bockelée-Morvan, 2011, Goesmann *et al.*, 2015). Carbon's UV shading effect was tested in this study on six bacteria species:

- *Bacillus subtilis*
- *Bacillus sphaericus*
- *Bacillus thuringiensis*
- *Bacillus licheniformis*
- *Rhizobium radiobacter*
- *Salmonella typhi*

Growth in liquid media and serial dilutions up to $1/10^4$ was achieved as described in 5.7.1, 1ml was taken from the final dilution; (1ml) and transferred to plates (Table 5-2):

Table 5-2: Plates used for each bacterium species in the charcoal experiment.

Ultraviolet Exposure				Control: No Ultraviolet	
Ice and Charcoal 5%	Water and Charcoal 5%	Ice without Charcoal	Water without Charcoal	Ice and Charcoal 5%	Water and Charcoal 5%
5 minutes	5 minutes	5 minutes	5 minutes	30 minutes	30 minutes
10 minutes	10 minutes	10 minutes	10 minutes		
15 minutes	15 minutes	15 minutes	15 minutes		
30 minutes	30 minutes	30 minutes	30 minutes		

Plain ice and water plates were prepared in the same way as in section 5.7.1, the plates containing charcoal powder were prepared by adding 1.5 gm of carbon into the final volume of 30ml. Ice plates were prepared by placing them in the freezer at -20°C for 4 hours, all the plates except the controls will be placed under UVC in the laminar hood as before, each according to its designated exposure time and in the same way as in section 5.7.1.

After exposure, the ice plates were given time to melt at room temperature, and 1ml from every plate was taken and spread onto nutrient agar plates, and incubated at 37°C for 48 hours. Later the colonies on the plates would by observed and counted.

5.7.3 Resistance to Ultraviolet Radiation in Ice and Fumed Silica Mixture

In addition to using carbon (charcoal), the effect of inorganic nano-particles on UV shielding was tested; fumed silica (SIGMA, Product Number S 5130) was selected since it has a particle size of (0.007 µm). The steps described in section 5.7.2 were replicated, using the same bacteria and material concentrations, with the exception of using fumed silica instead of charcoal

(Table 5-3), subsequent incubation and observation of growth were conducted in the same way.

Table 5-3: Plates used for each bacterium species in the fumed silica experiment.

Ultraviolet Exposure				**Control: No Ultraviolet**	
Ice and Fumed silica 5%	Water Fumed silica 5%	Ice without Fumed silica	Water without Fumed silica	Ice and Fumed silica 5%	Water and Fumed silica 5%
5 minutes	5 minutes	5 minutes	5 minutes	30 minutes	30 minutes
10 minutes	10 minutes	10 minutes	10 minutes		
15 minutes	15 minutes	15 minutes	15 minutes		
30 minutes	30 minutes	30 minutes	30 minutes		

5.7.4 Methods for investigating the use of UV light as an indirect microbial energy source

5.7.4.1 Microbial species used in the experiment

The following photosynthetic organisms were used for this experiment; all were purchased from www.ccap.ac.uk ; two cyanobacteria: *Synechococcus elongatus* (CCAP NO. 1479/1A) and *Nostoc commune var. flagelliforme* (CCAP NO. 1453/33), and two algal species: *Chlorella variabilis* (CCAP NO. 211/84), and *Dunaliella tertiolecta* (CCAP NO. 19/6B). In the algal

experiment, a mixed culture containing *Chlorella* and *Dunaliella* were added together in the same tube, while the bacteria were used separately.

5.7.4.2 Type and preparation of the fluorescent rocks

Two pieces of rock were obtained from www.Causewayminerals.co.uk, original location of collection : El-Hammam mine -Morocco, both comprise large partial fluorite crystals in association with calcite and pyrite crystals, with approximate size of 100mm x 70mm x 50mm/ Weight – 430g for the first, and a size of 90mm x 60mm x 45mm/ Weight – 230g for the second rock (Figure 5-2). When exposed to UV A, fluorite produces a lilac blue colour, while the calcite produces a wine red coloration. Two shafts of 5mm diameter were drilled into the rocks, with a shaft length between 3.5-4 cm. The bottom hole of the shafts was sealed with paraffin-wax and then filled with distilled water and left for 15 minutes, in order to check for leakage. When no leakage was observed, the rocks were autoclaved at 120°C / 15 minutes / 15 psi, and hot-sterile wax was used to seal the bottom of the holes again in order to form wells.

Figure 5-2: Two rocks composed of fluorite, calcite and pyrite

Two shafts made in each one (circled in red) in order to inoculate with cyanobacteria later.

5.7.4.3 Inoculation of microbes into the fluorescent rocks and measuring growth

A mixed algal culture (1ml) was taken from a seven days incubated culture 25°C, and added to a Falcon tube (15ml). After that, 9 ml of growth medium Gibco, BG-11 was added and mixed thoroughly. An aliquot 400µl was then transferred into the 2 wells of a rock samples; the top of the well was then sealed with hot, sterile paraffin wax. The rock sample was then exposed to UV with incubation. A separate control sample 400µl was then transferred into a 1.5 ml Eppendorf tube and left at room temperature at a North facing window. A dark control was also set up by transferring another aliquot 400 µl to a second Eppendorf tube which was wrapped in aluminium foil to avoid any light. The rock containing the inoculum was then transferred to an incubator held at 25°C which had a UVA light source (365nm, 8 watts – UVP LLC, model number: 95-0198-02) (Figure 5-3), the UV lamp was placed horizontally on the right side on the incubator tray with the bulb facing the rocks which were placed 5cm from the UV source and the shafts were in a vertical position when facing the lamp. The dark control was also placed in the incubator (the light control was left outside at room temperature).

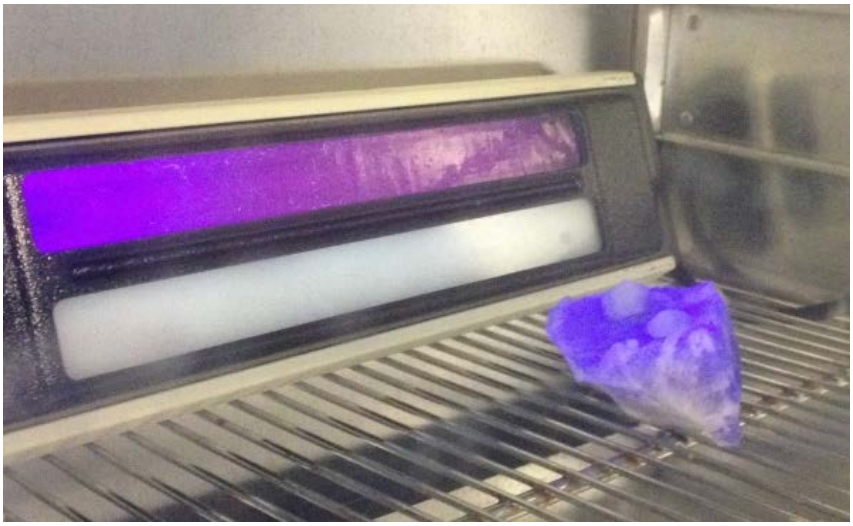

Figure 5-3: One of the rocks placed inside the incubator in front of a UV type-A lamp

After 7 days, the spectrophotometer readings for each of the samples were taken by removing 300µl, thoroughly mixed using a pipette of the culture, from inside the shafts, after the upper waxing coat was carefully removed. Sterile water 700µl was added and the mixture was transferred to a spectrophotometer cuvette. The same procedure was used for the Cyanobacteria culture, except that the 3 samples (UV exposed, light and dark samples) were incubated for 48 hours. Optical density OD for all samples was measured at 600nm using a Unicam Helisα spectrophotometer using 1ml cuvettes. Readings for the samples before incubation were made by mixing 300µl from the 15ml Falcon tube with 700µl of distilled water. The blanks used to zero the spectrophotometer employed cuvettes containing 300µl of BG-11 media with 700µl of D.W. Samples taken after incubation from within the rocks were extracted from the wells after mixing using a pipette. The OD readings for all the samples after incubation including the dark and light samples were obtained in the same manner as the one used prior to incubation, i.e. 300 µl each sample mixed with 700µl of D.W. An aliquot 25µl from all samples was taken from the Falcon tube before incubation, and then again after incubation from each well and tube, and examined under a light microscope (16X and 40X) in order to observe the respective microbial morphologies and to check for contamination. As well as UVA, the procedures were repeated using a source of UV B (302nm, 8 watts– UVP LLC, model number: 95-0199-02), and C (254nm, 8 watts- UVP LLC, model number: 95-0200-02), but only for the two cyanobacteria (*Nostoc, Synechococcus*) and not the mixed culture of algae. This was because the long incubation time for the former organism when UV B and C lamps were used lead to the generation of excessive heat.

5.7.4.4 Determination of chlorophyll content of cyanobacteria

The chlorophyll content for the cultures of all samples was also determined as follows: for Cyanobacteria, chlorophyll a (Chl a) analysis was performed as described by Meeks and Castenholz (1971). Approximately 400µl of culture was removed from each sample (i.e. before incubation and following exposure to, the dark, light and to the UV samples) and mixed with 600µl D.W in an Eppendorf tube. The samples were centrifuged at 13,000 rpm for 1 minute at room temperature (the original protocol used 1 ml of the sample, but because

in this case only a small sample was available; 400 µl of sample in 1ml of D.W. was used). Approximately 90% of the liquid from the samples was removed using a pippette, and an equal volume of 100% methanol 900µl was added to the tube; which produced a final methanol concentration of 90%. The remaining pellet was then suspended by vortexing, and the subsequent mixture was left for at least 5 minutes in the dark, to allow chlorophyll extraction; the mixture was vortexed again. The methanolic extract was centrifuged in the same manner when the cells were first harvested. Whereas the pellet remained green instead of purplish-blue, the mixture was re-vortexed and left to further extract. The OD of the methanolic-extract supernatant was then measured as described below. The extract was added to a microcuvette, and the absorbance was read at 665nm, using a 90%v/v methanol blank. Based on an extinction coefficient of 78.74 litre/gram/cm for Chl a in 90% methanol, the A665 was multiplied by 12.7 (the value 12.7 is derived from multiplying 1/78.74 by 103). This value was then multiplied by 0.4 to obtain to obtain the final concentration of Chlorophyll a in 0.4ml of culture.

5.7.4.5 Determination of chlorophyll content of green algae

Since *Chlorella* and *Dunaliella* are more easily lysed, acetone was used to determine their chlorophyll content (Zimmerman *et al.*, 2011). Aliquots 400µl were taken from each sample type (i.e. before incubation, dark, light and UVA incubation) and transferred to Falcon tubes (15ml), BG-11 growth media 4.6 ml was then added to each tube. The tubes were centrifuged at 3,500 rpm for 10 min and the supernatants were immediately discarded. Distilled water 1ml was then added to each tube in order to suspend the pellets and burst the cells. Acetone 4ml, 100% v/v was added to each tube, vortexed and left in the dark for 5 min and then centrifuged at 3,500 rpm for 5 min. If the pellet contained traces of green, it was re-suspended until a white pellet resulted. The OD value of the chlorophyll extract was then read

using an acetone 80% v/v blank at both 645 nm and 663 nm, using a 1ml glass cuvette. The chlorophyll was determined as follows:

OD_{645} X 202 = y

OD_{663} X 80.2 = z

((y+z) ÷2) = µg chl $0.4ml^{-1}$.

5.8 Results

5.8.1 CFU count of microbes exposed to Ultraviolet radiation in pristine ice, and ice mixed with nanoparticles

5.8.1.1 Bacterial CFU when exposed to Ultraviolet radiation in pristine Ice

After spreading 1 ml that was taken from each water and ice plates onto Nutrient agar plates and incubating, all of the controls showed positive growth (Figure 5-4). Although the colony forming units (CFU) count is slightly higher in the liquid water controls than in the ice controls in most plates. Not surprisingly; all the bacterial samples exposed to UV radiation under (5, 10, 15 and 30) minutes showed no growth when spread onto Nutrient agar plates, one or two CFU appeared on some plates, but they were disregarded as contaminants.

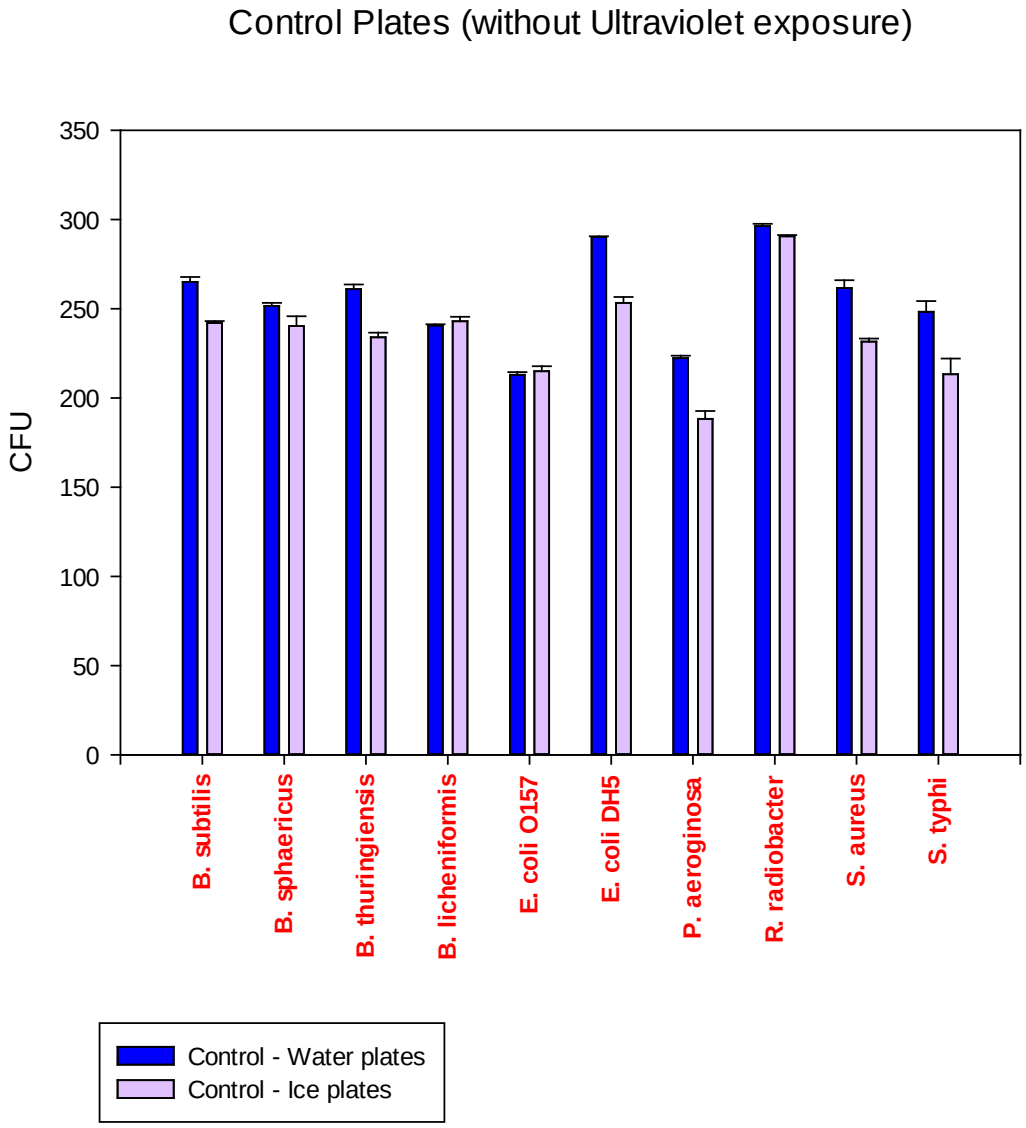

Figure 5-4: Controls for Water and Ice (CFU) count after spreading on Nutrient agar for the ten bacterial samples.

5.8.1.2 CFU when exposed to ultraviolet radiation in a charcoal mixture

After performing all the steps mentioned in (5.7.2), the colonies were counted for each plate following incubation. As can be seen in (Figure 5-5, Figure 5-6, Figure 5-7, Figure 5-8, Figure 5-9, and Figure 5-10). All the plates that contained charcoal showed an abundance of growth even after UV exposure. In the Ice plates with charcoal; The number of colony forming units (CFU) were relatively the same and have not changed significantly between the (5, 10, 15 and 30) minutes exposure times. In addition, the UV exposed ice plates lacking charcoal failed to show any significant colony count on the Nutrient plates, the charcoal-ice controls that were not exposed to ultraviolet radiation showed plenty of growth as indicated the high number of CFU.

As for the water plates, the samples with charcoal that were irradiated also did show growth in relatively large numbers compared to the extremely scarce growth on the ultraviolet exposed water-only samples, all control water samples showed higher (CFU) than the rest of the water samples, same as with the ice, since ultraviolet radiation can diffuse in some parts of the plate and effect some of the microbes.

The results also show that the colony count of the control ice was slightly higher than the irradiated charcoal-ice samples in most of the species, and that the water controls (CFU) was in turn higher than the irradiated charcoal water samples. Furthermore, only the charcoal-exposed water samples showed a consistent small decline in (CFU) count as the exposure times increased, unlike ice with charcoal particles in which the CFU remained relatively stable and did not decline with extended exposure times to UV.

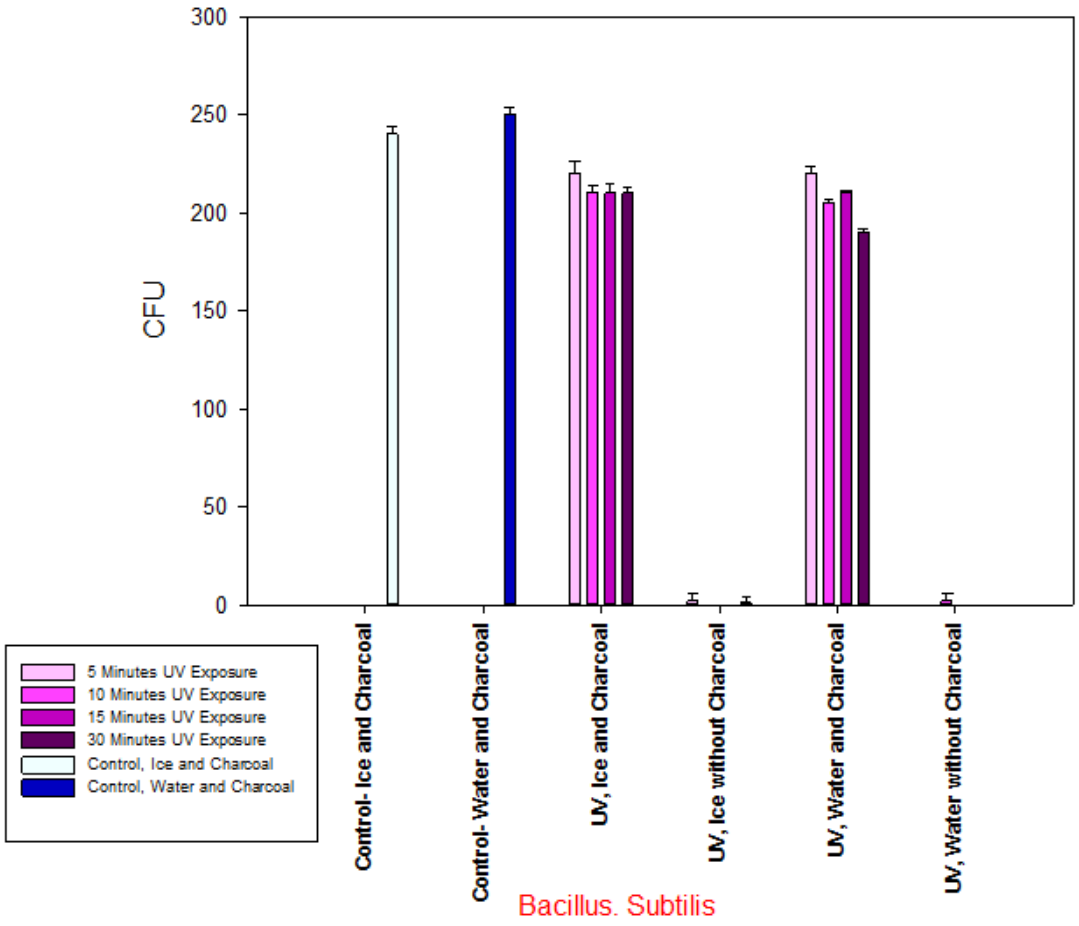

Figure 5-5: Plate (CFU) count for *Bacillus subtilis*, in the charcoal experiment.

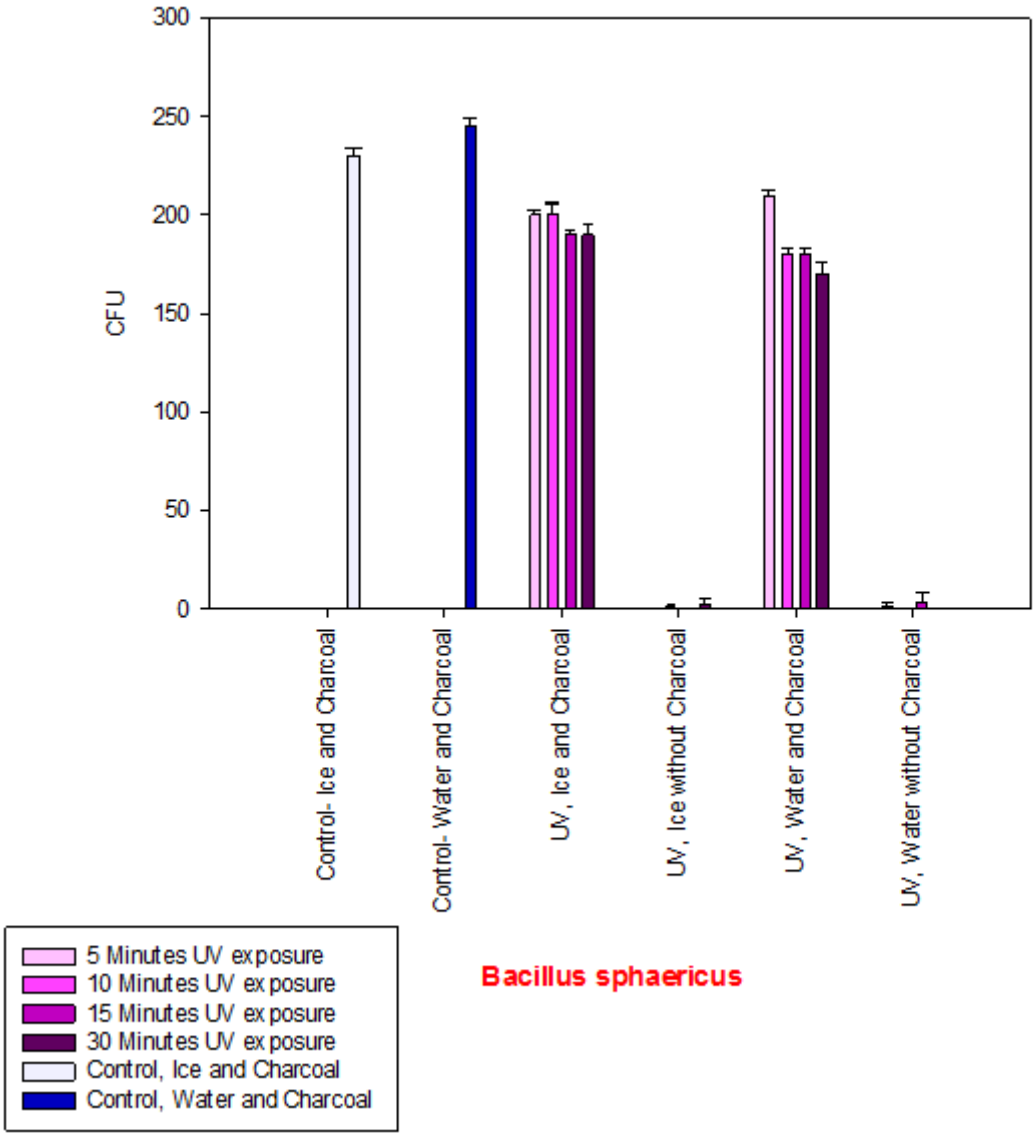

Figure 5-6: Plate (CFU) count for *Bacillus sphaericus*, in the charcoal experiment.

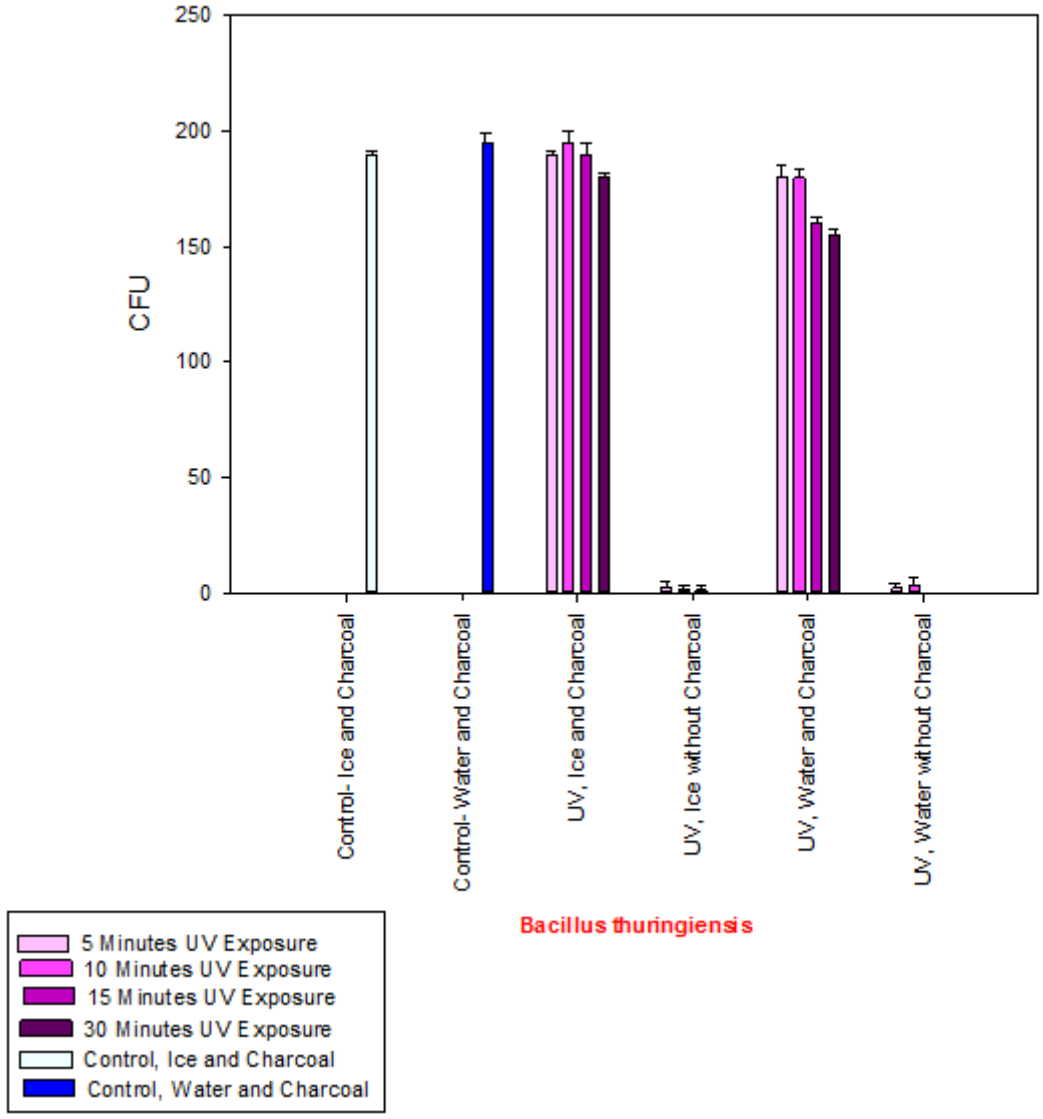

Figure 5-7: Plate (CFU) count for *Bacillus thuringiensis*, in the charcoal experiment.

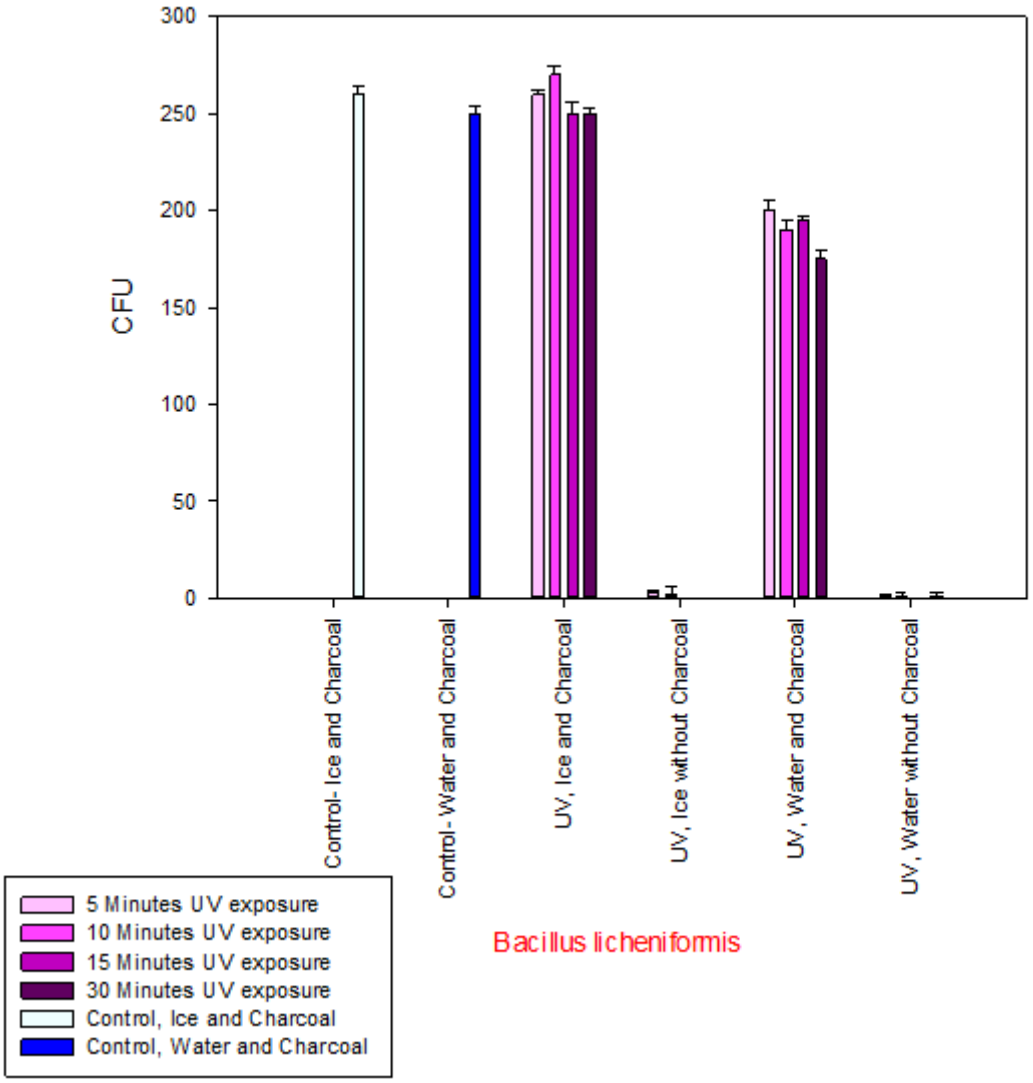

Figure 5-8: Plate (CFU) count for *Bacillus licheniformis*, in the charcoal experiment.

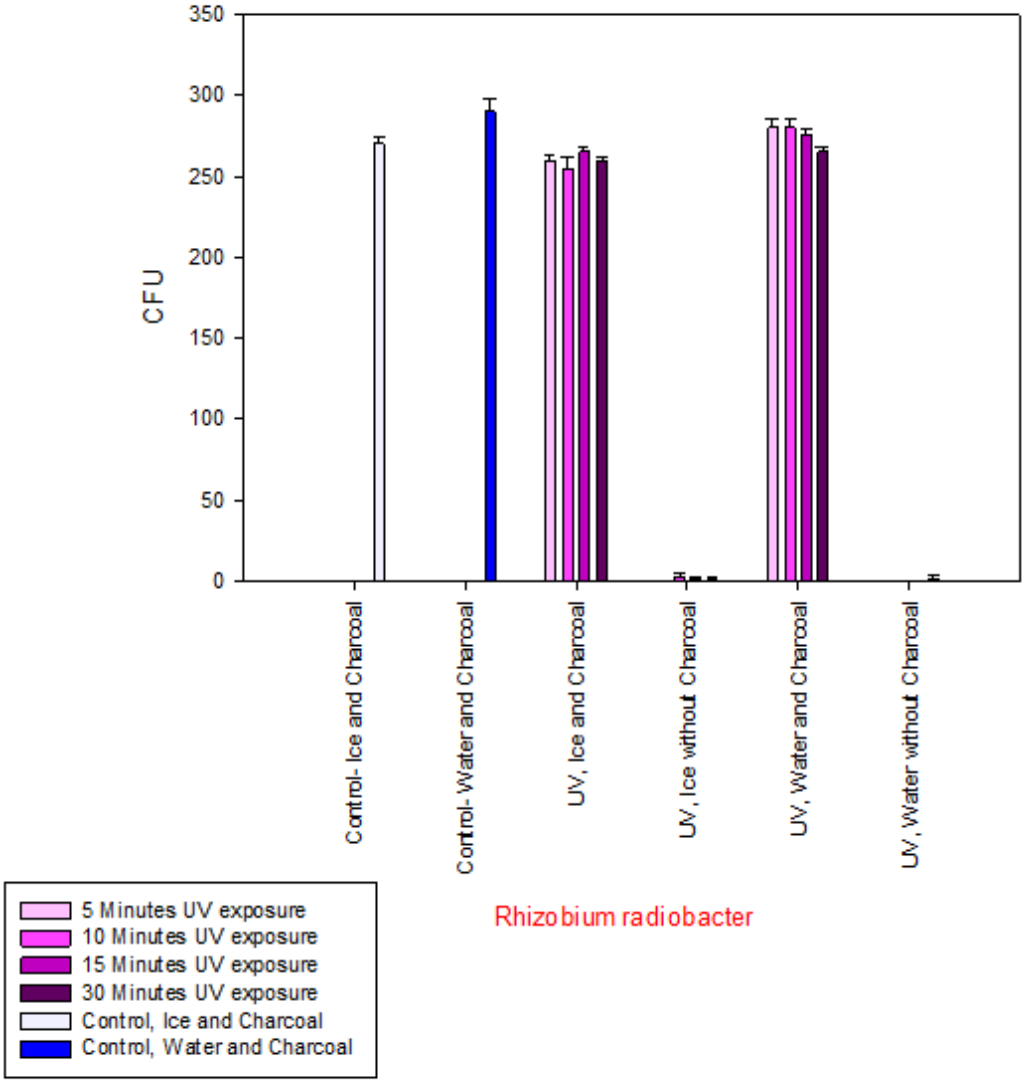

Figure 5-9: Plate (CFU) count for *Rhizobium radiobacter*, in the charcoal experiment.

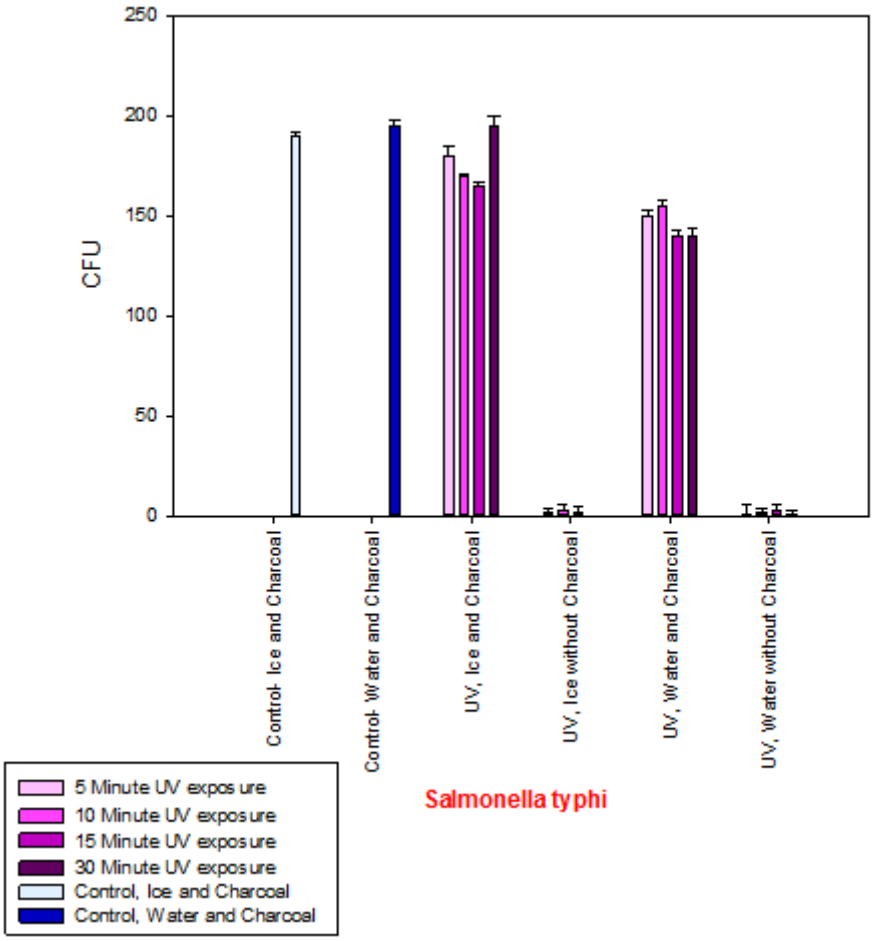

Figure 5-10: Plate (CFU) count for *Salmonella typhi*, in the charcoal experiment.

5.8.1.3 CFU when exposed to ultraviolet radiation in a fumed Silica mixture

For this experiment, fumed silica (silicon dioxide), which is produced commercially by burning silicon tetrachloride in a flame of hydrogen and oxygen at high temperature was used, the particles of the fumed silica had a diameter size of 0.007 µm. The results are shown in Figure 5-11, Figure 5-12, Figure 5-13, Figure 5-14, Figure 5-15, and Figure 5-16.

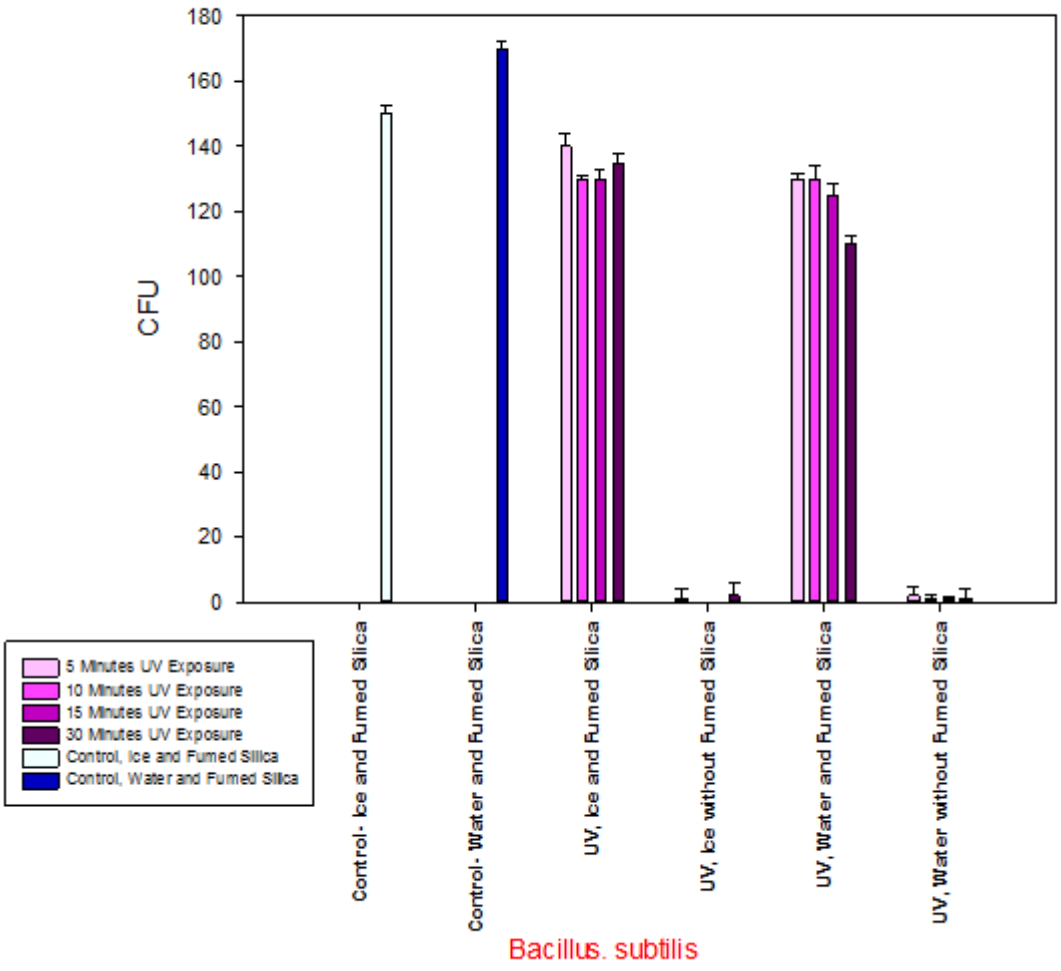

Figure 5-11: Plate (CFU) count for *Bacillus subtilis*, in the fumed Silica experiment.

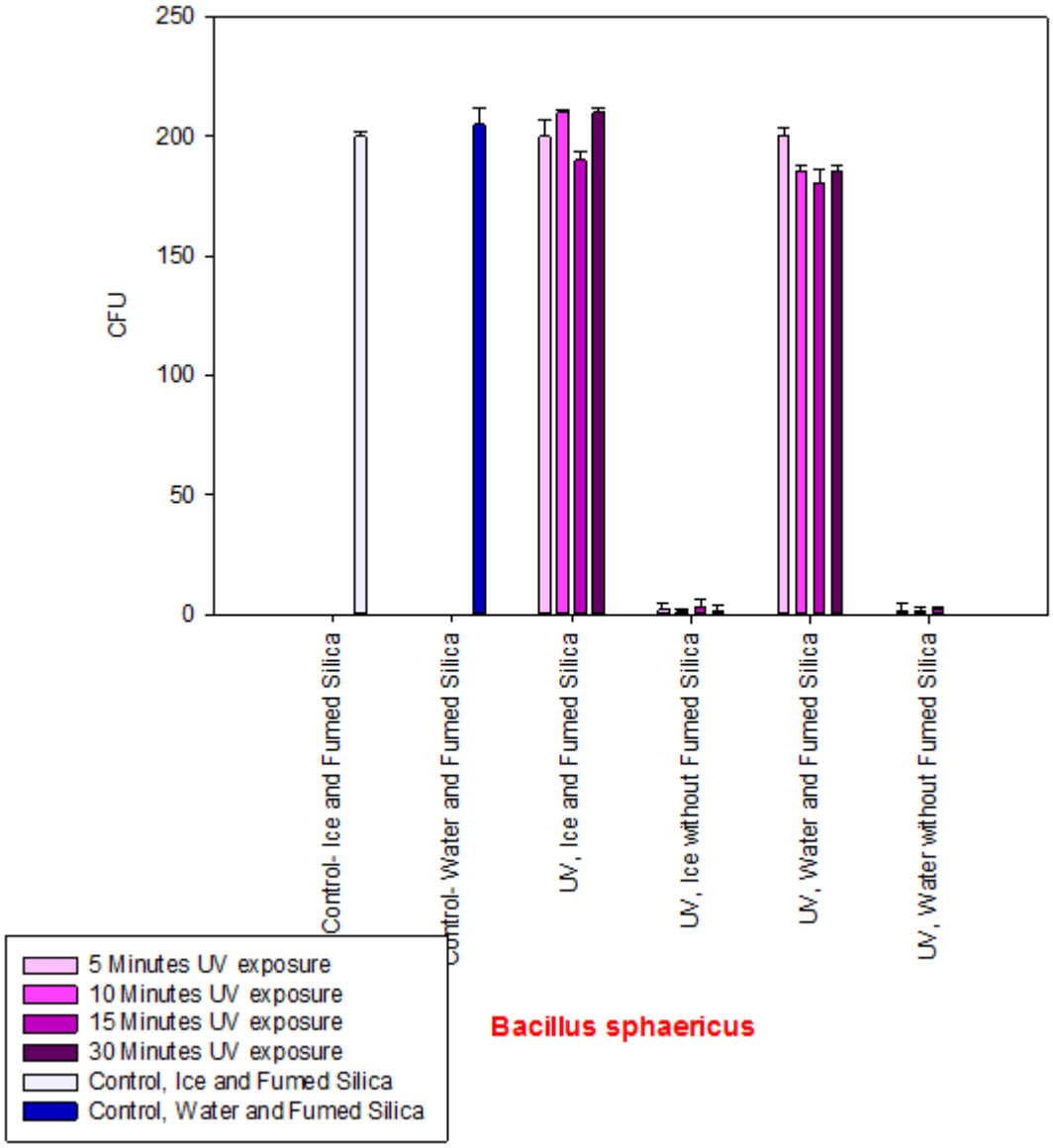

Figure 5-12: Plate (CFU) count for *Bacillus sphaericus*, in the fumed Silica experiment

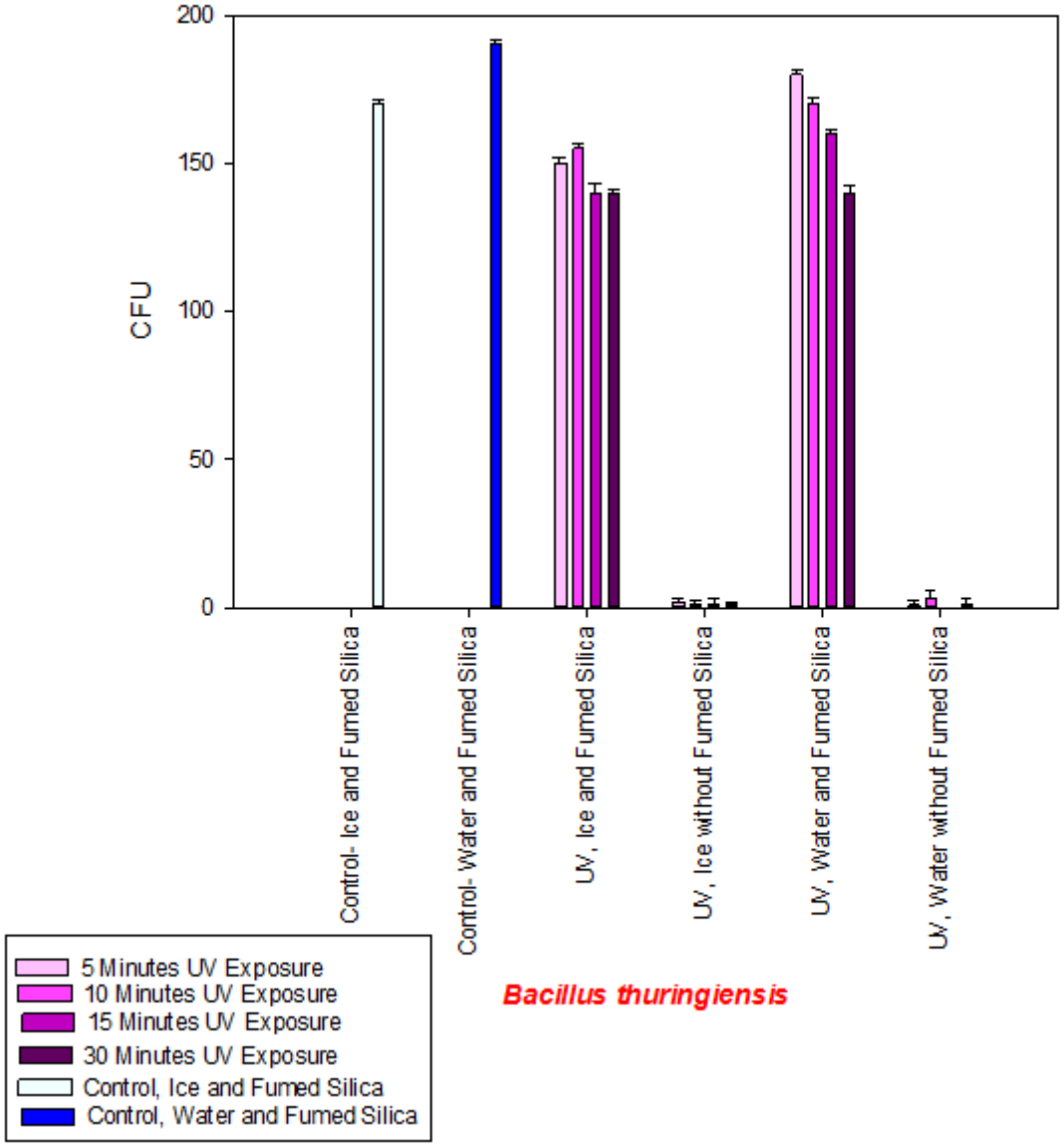

Figure 5-13: Plate (CFU) count for *Bacillus thuringiensis*, in the fumed Silica experiment.

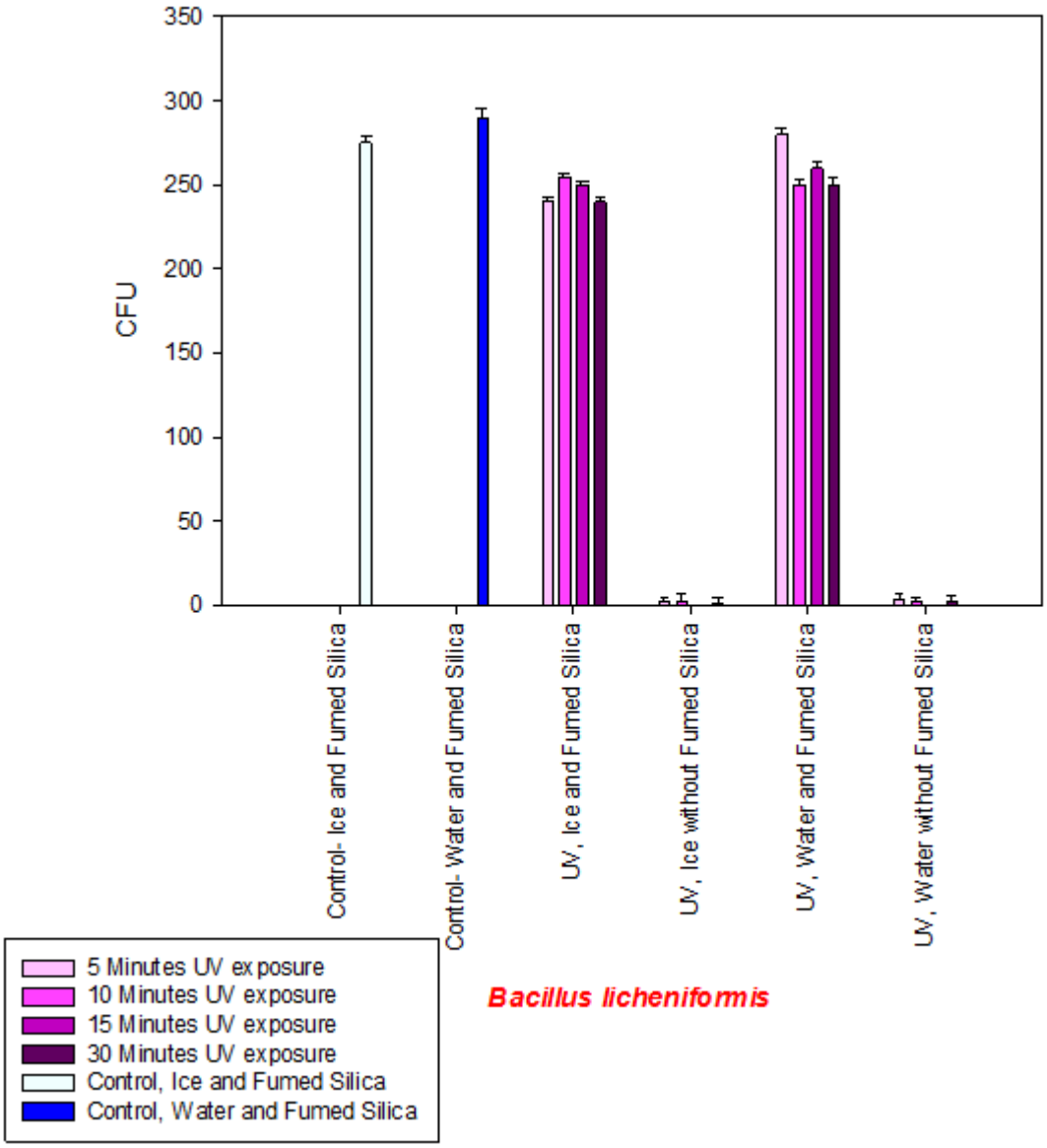

Figure 5-14: Plate (CFU) count for *Bacillus licheniformis*, in the fumed silica experiment.

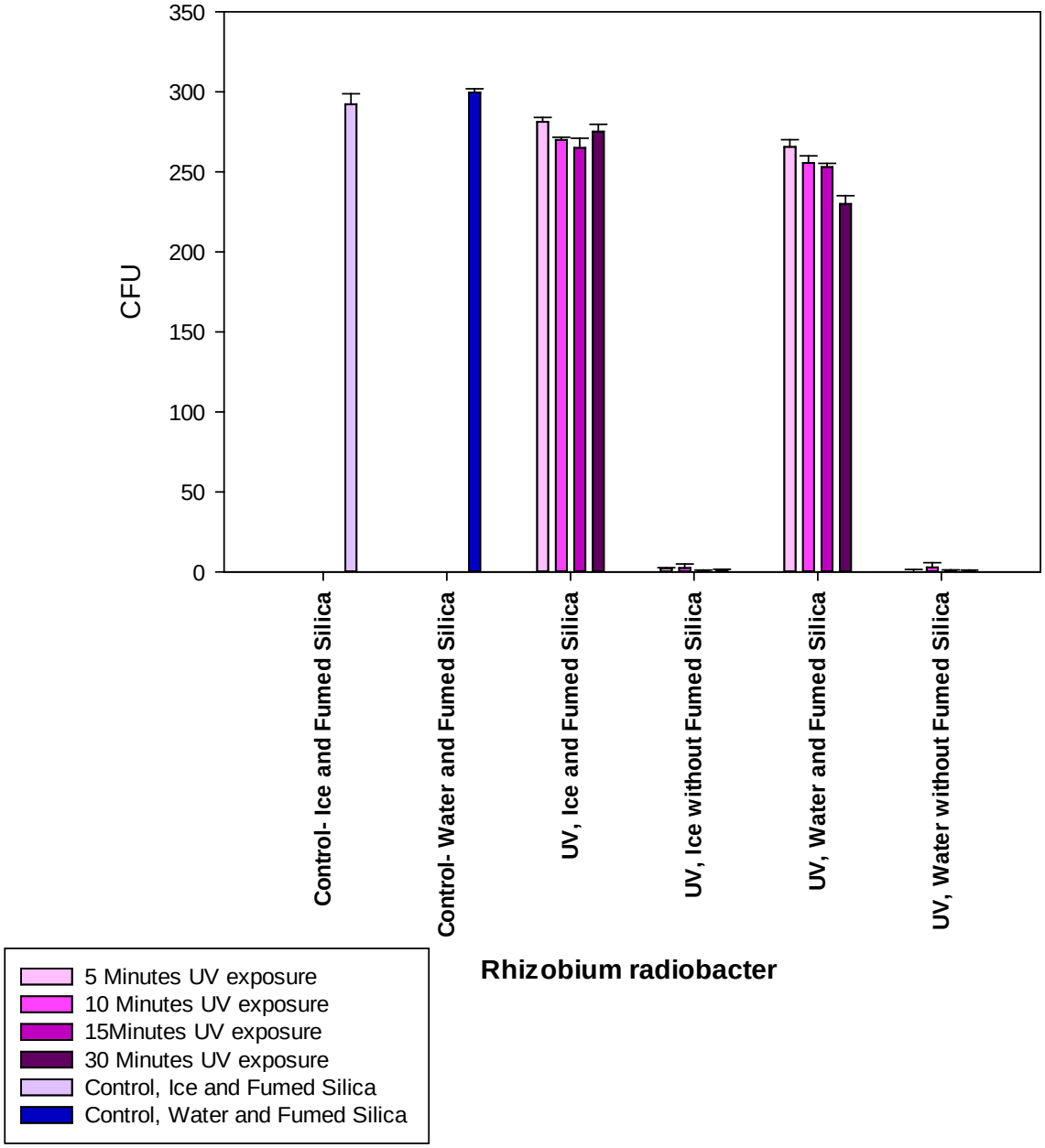

Figure 5-15: Plate (CFU) count for *Rhizobium radiobacter*, in the fumed silica experiment.

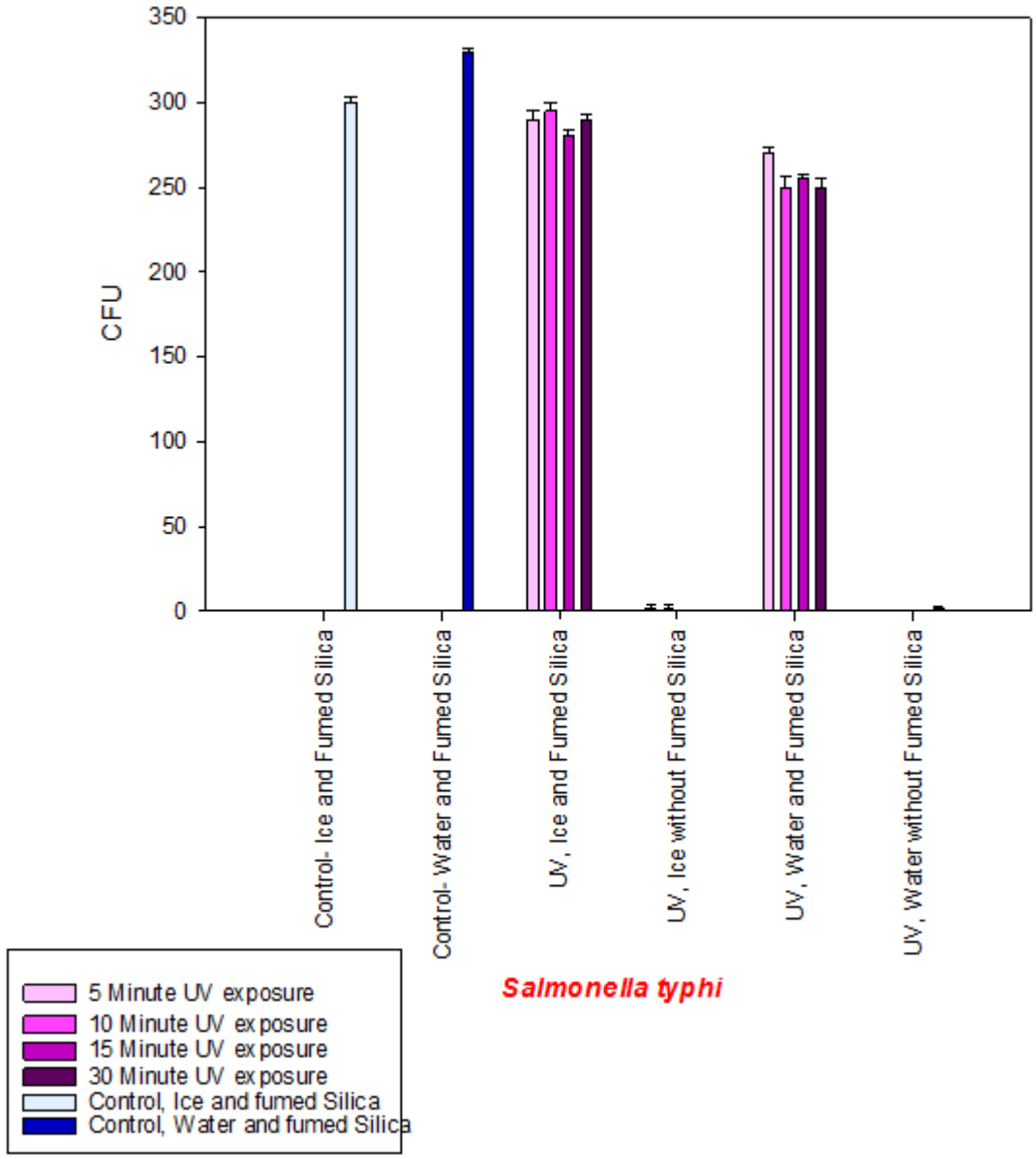

Figure 5-16: Plate (CFU) count for *Salmonella typhi*, in the fumed silica experiment.

In ice samples, same with the previous experiment (charcoal), all six species CFU numbers were consistent between the four exposure times to radiation in regards to the ice-fumed Silica plates (Figure 5-17). While the irradiated plain ice plates failed to show a significant count, compared to the controls and the silica-containing plates.

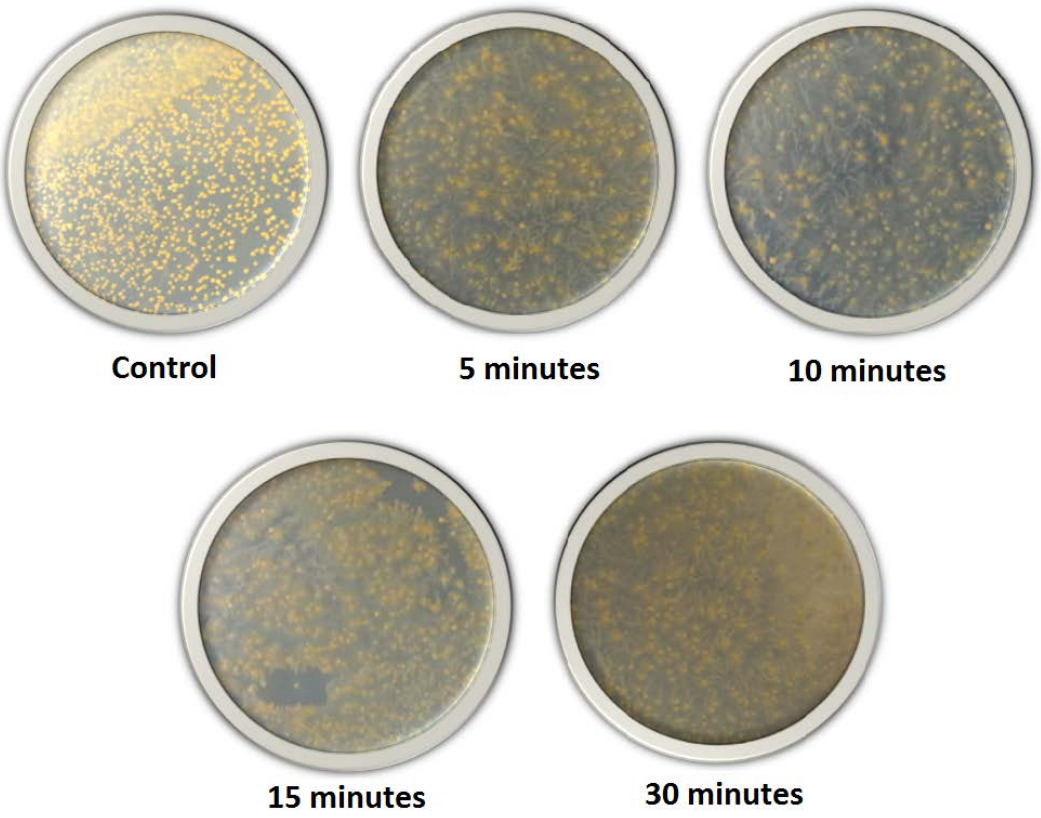

Figure 5-17: Five *Rhizobium radiobacter* plates containing fumed Silica

Four were exposed to increasing doses of UV but showed growth, morphology of growth on the plates also changed from regular round colonies to a star-shaped pattern.

ultraviolet irradiated samples showed a considerable (CFU), control water plates also showed growth, unlike the plates lacking fumed Silica in which all failed to show a significant (CFU) count.

5.8.2 The use of visible light generated from fluorescence by UV for photosynthesis

5.8.2.1 Light Microscopy

Observation of the mixed culture of *Dunaliella* and *Chlorella* was done under the light microscope before the culture from the 15ml falcon tube was incubated; typical vegetative stage for *Dunalliela* appeared as pear-shaped motile cells with two flagella from the narrow end, zygospores appeared rounded without flagella. *Chlorella* appeared as spherical single cells; both species appeared in green colour because of the presence of chlorophyll (Figure 5-18).

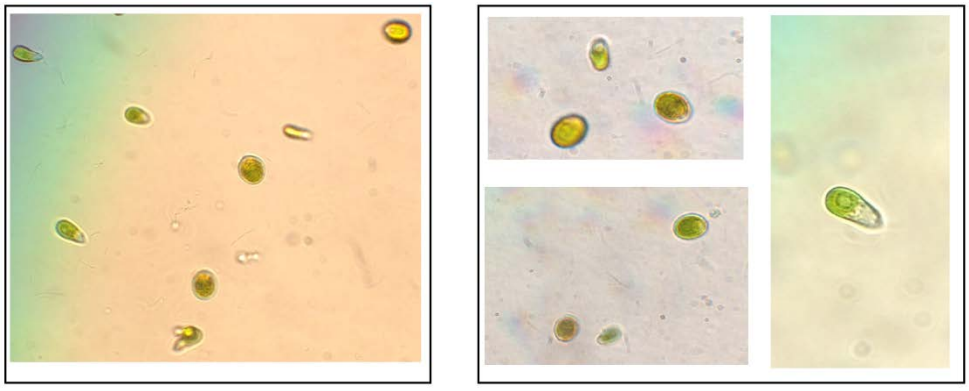

Figure 5-18: Mixed culture of *Dunaliella* and *Chlorella* under the light microscope

A: after 7 days incubation exposed to daylight, B: Cells of the same organisms taken from 7 days media exposed only to UV type A.

After incubation, the samples of algae (UV A exposed, Dark and Light tubes) were examined under the microscope, and they all showed the same cell shapes for *Chlorella* and *Dunaliella*, with the difference between them mainly in the number of cells within the field of view. Light samples showed the closest density to the original culture, and the dark sample demonstrated the lowest density, with scattered sporadic presence of cells. The dark samples also showed an extremely small number of zygospores, which can be attributed to slow growth. UV type A exposed samples cell although is smaller in numbers when compared to the light samples, it still hints for microbial growth when compared to the dark samples, especially when we consider that both vegetative and sporozygotes were observed in the UV samples, which might indicate that growth is ongoing in them.

As for the Cyanobacteria: the 25µl taken from the fresh culture before incubation showed short cells in green colour under the light microscope, which remained attached after binary fission forming long chains. After incubation, all the examined samples of *Nostoc* that were exposed to the three types of UV. Each of their light and dark samples showed the same green short cells attached to each other in one plane, and forming chains, although the dark samples showed somewhat lower density than the other samples. It is worth mentioning that short chains (4-5 cells) were also present in the UV-exposed samples, which might be an indication that growth is taking place in them (Figure 5-19).

Figure 5-19: culture of *N. commune* under the light microscope

A: some of the *N. commune* microbes taken from a culture grown in daylight, B: microbes grown in the presence of UV only, without any other source of light other than the fluorescent rocks.

Samples of *Synechococcus elongates* were also observed, but because of their extremely small size many of their features were hard to distinguish and we were only able to observe their presence which was confirmed in all the samples.

Microscopic examination was done primarily to confirm the presence of the microbes and to make sure samples were not contaminated, but the definitive comparison between the growth of samples in the different conditions was achieved through measuring the optical density (OD) for the microbial cell growth and chlorophyll measurement.

5.8.2.2 OD for Cell growth and Chlorophyll quantification

In both the cellular growth and the chlorophyll determination measurment, every experiment was repeated to obtain three measurements for each sample type; all data analysis was performed using SigmaPlot, version 12.5. Differences were considered significant for p-values less than 0.05. For

cellular growth, the OD readings were found to be higher in samples exposed to all types of UV within the rocks after incubation, compared to the dark samples. All samples left in the dark showed minimal growth, compared to when exposed to sunlight and UV. There was a slight increase in growth for the dark samples when compared to the initial seeding concentration. The percentage of growth from the samples exposed to UV was very similar to the growth seen in cultures not incubated in the minerals and exposed to ambient sunlight, although all UV exposed samples were slightly lower in growth density when compared to sunlight exposed ones (Figure 5-20, Figure 5-21, and Figure 5-22).

Results for (Chlorophyll a) content for both Cyanobacteria and algae when exposed to (UV- A) (Figure 5-23, Figure 5-24, Figure 5-25) also correlate with the OD readings for cellular growth measurements (Figure 5-20, Figure 5-21, and Figure 5-22).

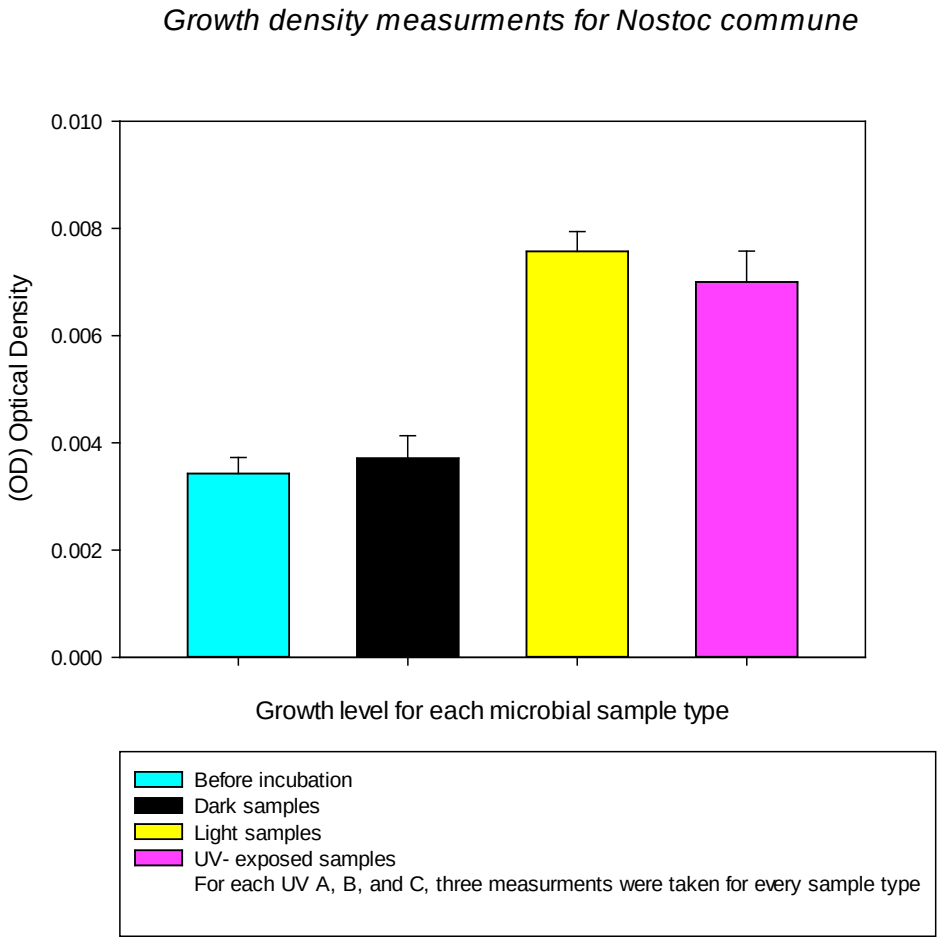

Figure 5-20: Growth measured by OD to estimate cellular density for the four sample types of *N. commune*

Bars indicate standard error, UV-samples growth rate is significantly greater compared to the dark control samples (p=0.00006).

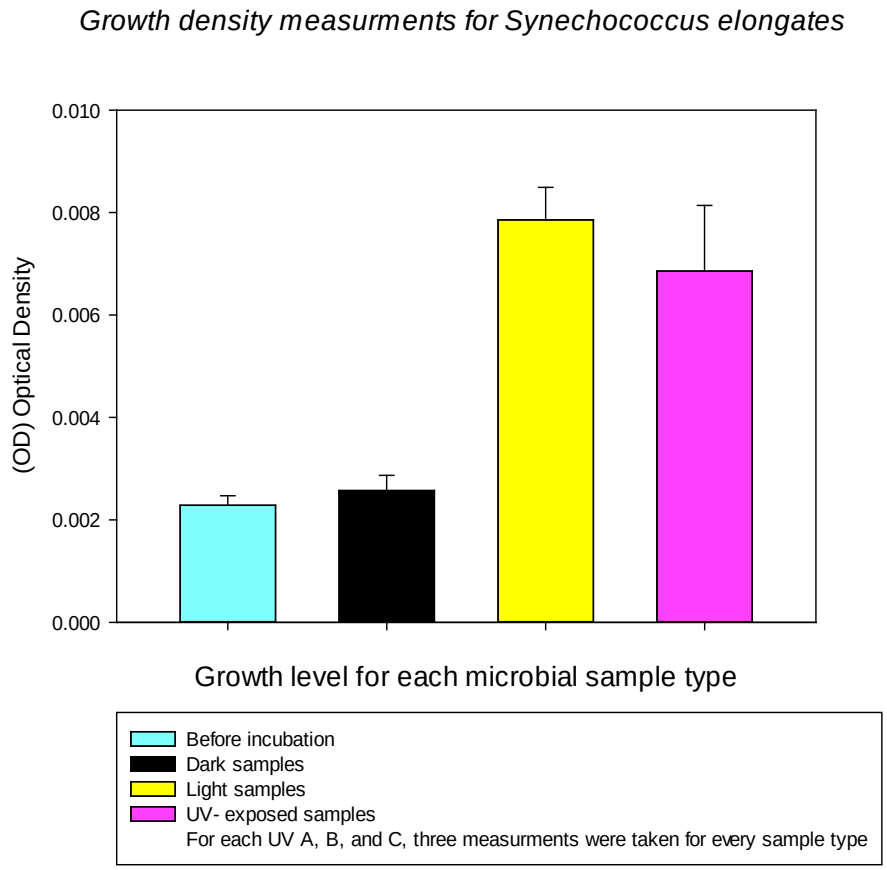

Figure 5-21: Growth measured by OD to estimate cellular density for the four sample types of *S. elongate*

Bars indicate standard error, UV-samples growth rate is significantly greater compared to the dark control samples (p=0.00007).

.

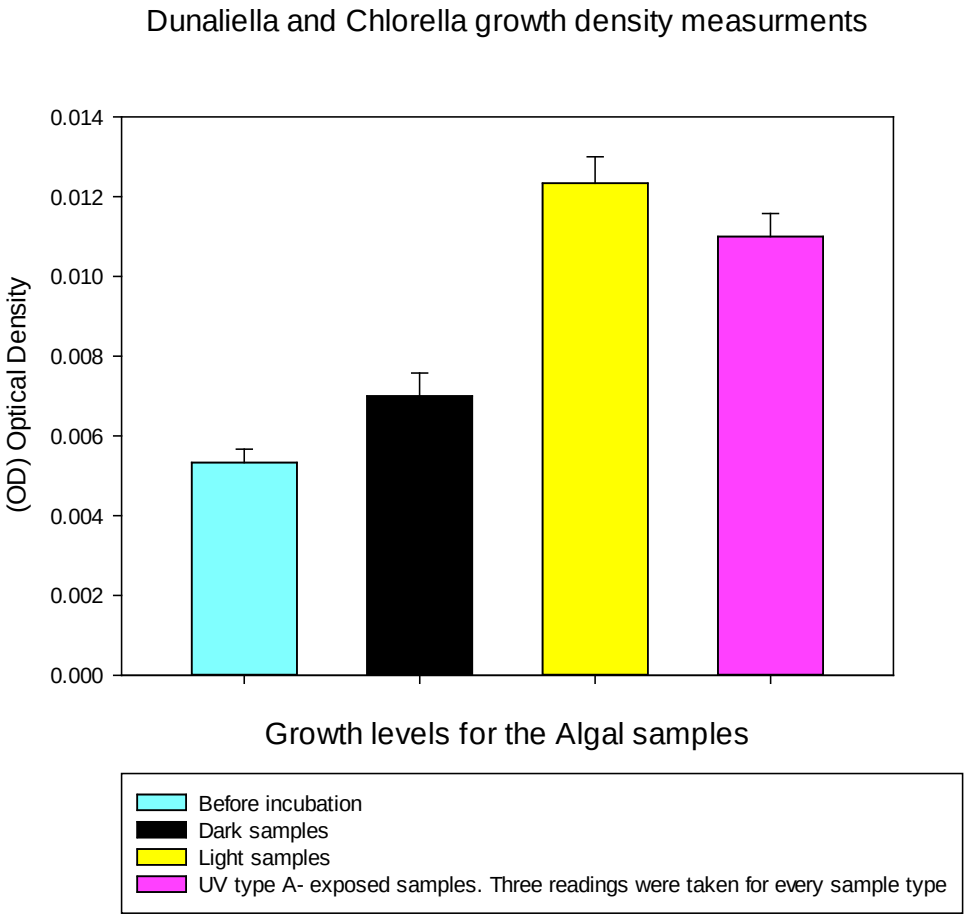

Figure 5-22: Growth measured by OD to estimate cellular density for the four sample types of the algal mixed culture (*Chlorella* and *Dunaliella*)

Bars indicate standard error, UV A-samples growth rate is significantly greater compared to the dark control samples (p=0.00008).

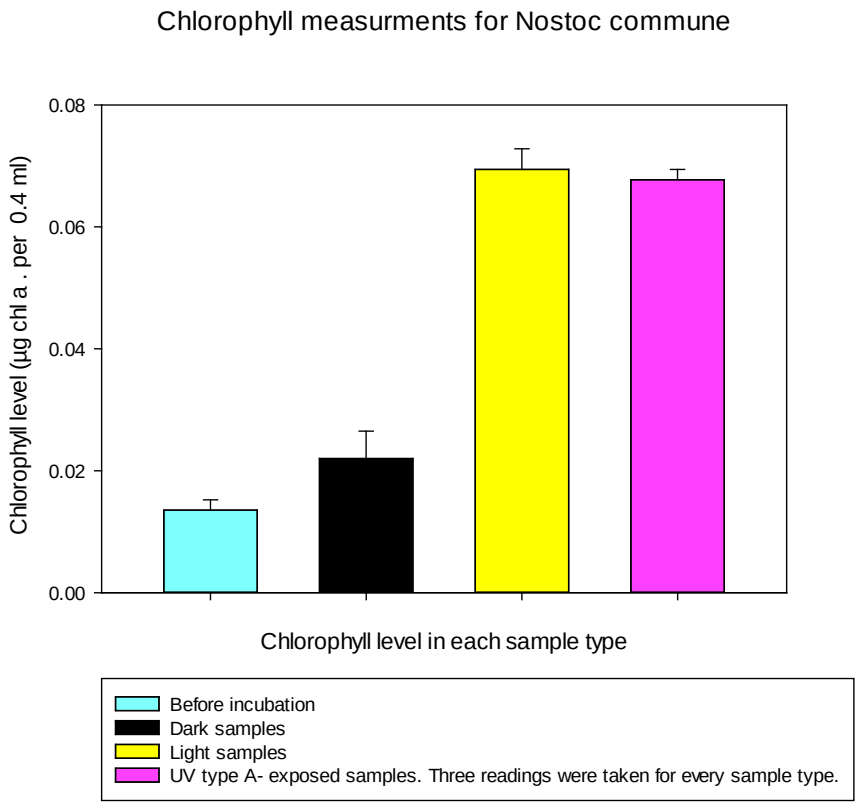

Figure 5-23: Chlorophyll measurement of the four sample types for *N. commune*

Bars indicate standard error, UV A-samples growth rate are significantly greater compared to the dark control samples (p=0.00091).

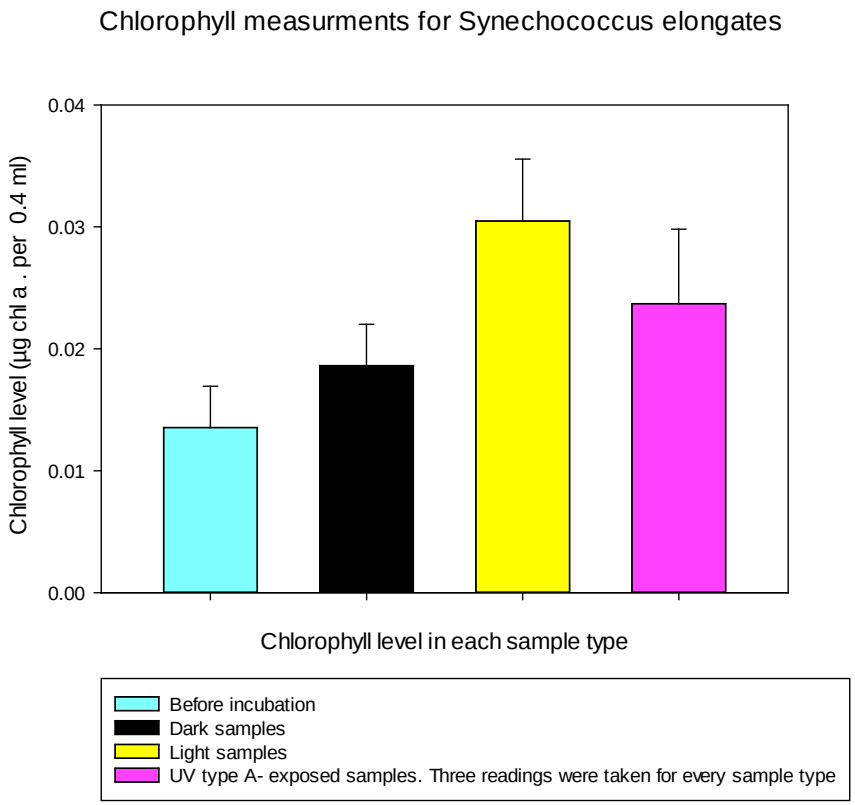

Figure 5-24: Chlorophyll measurement of the four sample types for *S. elongates*

Bars indicate standard error, UV A-samples growth rate are significantly greater compared to the dark control samples (p=0.00010).

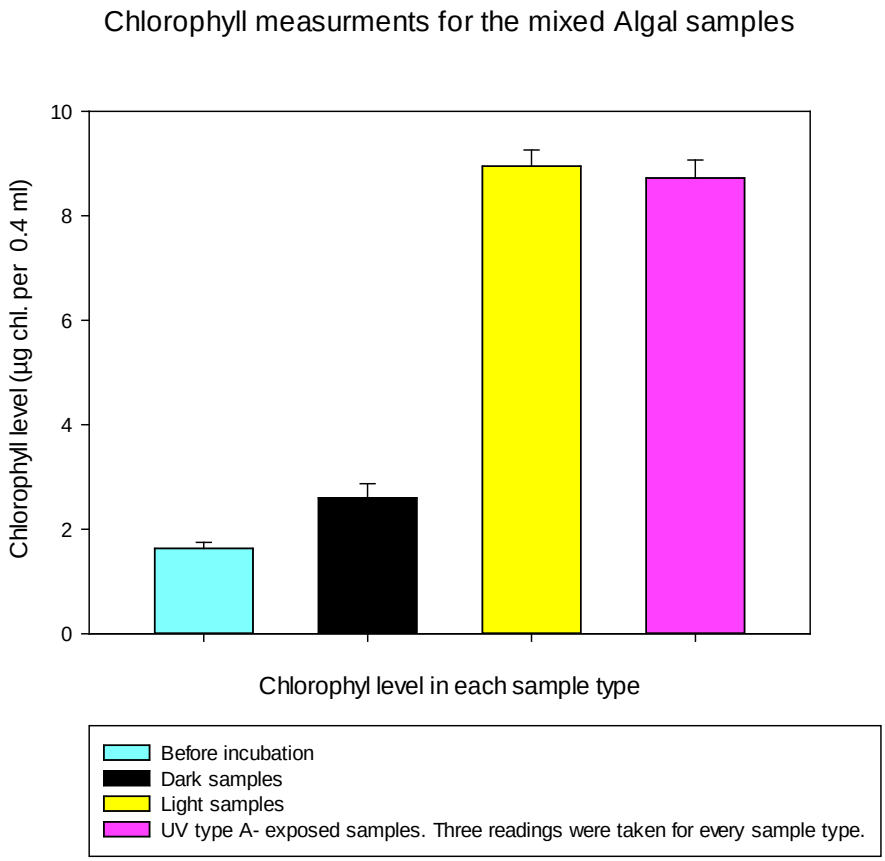

Figure 5-25: Chlorophyll measurement of the four sample types for the algal species (*Chlorella* and *Dunaliella*)

Bars indicate standard error UV A-samples growth rate are significantly greater compared to the dark control samples (p=0.00010).

5.9 Discussion

5.9.1 Microbial resistance to UV in ice or water

5.9.1.1 Bacterial resistance to Ultraviolet radiation in pristine ice

In the control plates, positive growth was observed as expected (Figure 5-4), the reason for the slightly higher CFU count in the water controls compared to the ice controls might be attributed to the microbes in water controls being able to grow and replicate more efficiently since the conditions are closer to their optimum growth conditions, also, microbes preserved in ice will be slower to regain their ability to metabolise and replicate, leading to the slight difference in the CFU count between the two.

The complete bactericidal activity of all the UV exposed samples agrees with the results from Ladanyi and Morrison (1968) who reported that most bacteria are killed within thirty seconds in 30mm ice blocks (although the paper mentions that the optical quality of the ice plays a role in the process). To our knowledge, no direct study has been done before to test whether inorganic solid particles such as dirt in ice can provide protection for microbes. Our study did not test exposure times to UV radiation below five minutes, since the aim of the study is not to determine the lethal dose of direct UV radiation against microbes, since many studies have already been published on the subject (Chang *et al.*, 1985, Harris *et al.*, 1987, Sommer *et al.*, 1998). Even *Deinococcus radiodurans*, which is one of the most resistant microbes to extreme conditions, cannot survive extended times of UV exposure (Pogoda de la Vega *et al.*, 2005). This is the reason for incorporating charcoal and fumed silica particles with the ice and water in the subsequent step of the experiment.

5.9.1.2 Bacterial Resistance to ultraviolet radiation in a Charcoal mixture

Charcoal is a black residue made mainly from carbon after the removal of volatiles, including water from animal and plants remains (Antal and Grønli, 2003). By mass; Carbon is the 4th most abundant element in the universe (Suess and Urey, 1956), and it is difficult to imagine any form of life which is not based on carbon (Pace, 2001, Cochran *et al.*, 2015, Wickramasinghe and Wainwright, 2015, Wickramasinghe *et al.*, 2015).

As was shown in Figure 5-5, Figure 5-6, Figure 5-7, Figure 5-8, Figure 5-9, and Figure 5-10, growth was reported in UV exposed plates, and in the ice samples. The lengths of time that the plates were exposed to UV did not seem to make a difference for the CFU between the 5, 10, 15 and 30 minutes exposed plates; meaning that ice and charcoal mixture did provide protection and shielding required against the radiations. This is also further confirmed when compared to the CFU count from the UV exposed plates, which did not contain charcoal, and failed to show a significant CFU count when later grown on nutrient agar plates. In the water plates samples,

results were similar to the ice samples; the water plates with charcoal showed a high CFU count, when compared to the plates that contained water with no charcoal. However, in both the water and ice controls, CFU was still higher than in the samples which contained charcoal. We believe this is because UV radiation still managed to get through to a percentage of the microbes in the plates, while the surviving microbes were successfully shielded behind charcoal particles either in water or ice.

Another difference observed from the results of CFU count between the ice and water UV exposed plates is that in water, the CFU underwent a steady decline with longer UV exposures, this is because water, unlike ice shows Brownian motion, a random movement of particles in all direction in a liquid or gaseous medium (Hida, 1980), which naturally will allow more bacteria to be exposed to radiation as time increases, unlike ice in which charcoal particles remain fixed in place providing stable shielding.

5.9.1.3 Bacterial Resistance to Ultraviolet Radiation in Ice and fumed Silica Mixture

Fumed silica was selected for this study because it comprised of Nano-particles (0.007 µm in diameter), smaller than the average size of most bacteria (0.2 µm in diameter and 2-8 µm in length) (Florke *et al.*, 2008), another reason is because Silicon dioxide is commonly used in cementitious mixtures and other building materials (Detwiler and Mehta, 1989), hence its relevance to the theory of archipanspermia (Alharbi *et al.*, 2011). Besides; Silicon, by mass, is the eighth most common element in the universe (Suess and Urey, 1956), therefore possible to be present as suspended particles within icy comets.

As can be seen from Figure 5-5, Figure 5-6, Figure 5-7, Figure 5-8, Figure 5-9, and Figure 5-10, results from this experiment agree with the charcoal experiment findings, where both water and ice mixed with fumed silica provided an adequate shielding against ultraviolet radiation. As before; water and ice controls in the fumed silica experiments both showed higher (CFU) than their irradiated samples because some microbes in the latter are

exposed to a percentage of the diffusing radiation. Also as in charcoal; the irradiated water samples showed a consistent decline in (CFU) as the exposure time increases, attributed to the Brownian motion which keeps exposing microbes to radiation unlike the situation in ice where molecules are fixed in relation to each other.

As a side observation; while most species formed separate colonies on the nutrient agar, only *R. radiobacter* and *S. typhi* demonstrated a unique branching/star-shaped growth pattern (Figure 5-26), which appeared only in the plates containing silica. Although this pattern differs slightly between the two bacteria, we believe it resulted from the presence of Nano-particles of fumed Silica, and bacterial growth behaviours. This finding does not have a direct connection to our research, it does raise the question about the role of biofilm formation and the possibility of using these by microbes to form aggregates to protect themselves from radiation. The extent of interaction between microbes and the inorganic particles when forming colonies, and whether microbes are able to assemble and employ this as a physical protective barrier could be investigated in the future.

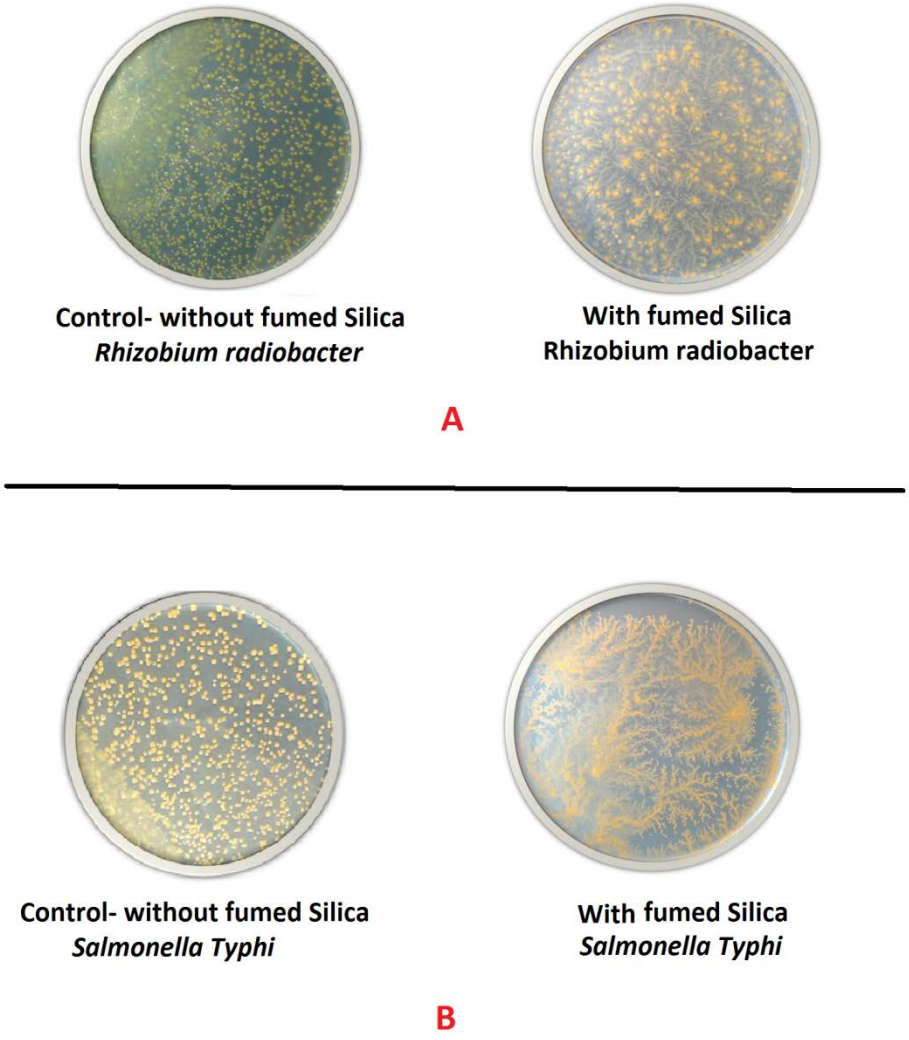

Figure 5-26: Morphological changes in growth of bacteria on the plates

Both *R. radiobacter* (A), and *S. typhi* (B) showed unique branching/star-shaped growth in plates containing small amounts of Fumed Silica, compared to the controls lacking Silica which showed regular round colonies.

5.9.2 UV as an indirect energy source for Cyanobacteria

As can be seen from the results in Figure 5-20, Figure 5-21, Figure 5-22, when cellular growth was measured using OD_{600nm}, all the samples that were exposed to the three types of UV (A, B, and C) inside the fluorescent rocks showed higher OD readings at the end of the incubation period when compared to the dark samples (samples grown in the same temperature but with no light) This provides clear evidence that microbial growth was not inhibited by any of the three UV sources. As expected, the dark samples of the photosynthetic microbes showed the lowest growth, compared to the sunlight and UV exposed samples. The slight increase of the growth of the dark samples from the initial seeding concentration is attributed by us to the presence of a few microbes that were already undergoing replication. The close similarity of the percentage of growth between the UV, and sunlight exposed samples suggests that, in fluorescent rocks, damaging UV light was converted to visible light by the fluorescent minerals and that this acted as a light source enabling both types of algae and Cyanobacteria to grow within the rocks. The slightly lower growth density of UV exposed samples to the sunlight exposed ones is explained by the fact that although fluorescent rocks do generate light, the intensity cannot match ordinary daylight, thus resulting in a slightly lower growth density.

The argument that UV exposed microbes might have used another energy source to fuel their growth, similar to a study by (Madigan and Gest, 1979), can be easily refuted because the dark controls were incubated in the same conditions without UV, and they failed to show the same percentage of growth. If an alternate chemoautotrophic pathway was present in the UV samples, it should have also been undergoing in the dark controls as well. Giving further confirmation to our findings, results for (Chlorophyll a) content for both cyanobacteria and algae when exposed to (UV- A) (Figure 5-23, Figure 5-24, and Figure 5-25) correlate with the OD readings for cellular growth measurements (Figure 5-20, Figure 5-21, Figure 5-22). Fluorescence

observed in this work resulted from the absorption of ultraviolet light by fluorite, calcite and pyrite, which led to the excitation of molecules within them, vibrational relaxation of excited state electrons to the lowest energy level, ending with emission of a longer wavelength photon (visible light), a little amount of heat also results through conversion of the excess vibrational energy (Chen *et al.*, 2003).

Shielding from harmful UV has been investigated before, studies that were done on board the international space station (ISS) showed that microbes can survive space and simulated Martian conditions if they were sufficiently shielded. Spores of *Bacillus subtilis* were able to survive for 559 days on board the European Space Agency's exposure facility (EXPOSE-E) (Wassmann *et al.*, 2012), and a study done by Bryce *et al.* (2014) has demonstrated that phototrophs carried on board the ISS have been able to survive within porous rocks while exposed to extreme space conditions for 22 months. Another study tested the survivability of both lichens and cyanobacteria in space conditions while exposed for ten days on the Biopan facility of the European Space Agency (ESA), lichens were found to be more resistant to space conditions than bacteria (de La Torre *et al.*, 2010a). It must be noted however that all of these previous studies involved testing the survivability of dried microbial cells against UV among other factors in space. This study however differs in that we use microbial living cells, not dried cells. And although we did not test the survivability of the microbes in semi-transparent rocks that are non- fluorescent, a study performed by Cockell and Stokes (2006) showed photosynthetic microbes to be shielded from harmful radiation using the semi-transparent crystals in the opaque rocks, furthermore, because the dark controls which were completely sealed to prevent UV penetration showed a lower growth rate than the UV samples. This suggests that microbes within the UV exposed ones did survive the radiation and replicated. More importantly, our results showed that microbes actually harnessed the harmful UV indirectly by utilizing the visible light generated from fluorescence. These results show that if algae and cyanobacteria can access the inside of fluorescent rocks (presumably via fissures) which are located on the surface of a given planet, they can be

protected from damaging UV light (as well as some other environmental constraints). In this way the interior of fluorescent-mineral rocks, like the ones studied here provide an ideal protective environment for photosynthetic microbes beneath the UV-baked- surface of an inhospitable environment.

The value of such a system might be questioned by arguing that normal light would already enter through the rocks and provide the necessary energy. However, it is worth noting that with the presence of fluorescent rocks, conditions for life can improve significantly, because they absorb the harmful UV more than ordinary glass or other transparent rocks, and increase the light dosage with additional visible light to the subsurface environment in addition to the transmitted sunlight. The advantages will become clearer within environments in the universe that contain high UV dosage with little white light, because photosynthetic microbes could still thrive in it, especially considering that young stars, including the sun, emitted UV levels up to 10000 times more than from the current level, while the white light of the same sun was fainter at the time (Cockell and Horneck, 2001). The work presented here shows that life can survive in such conditions without the need of a protective atmosphere made up of the oxygen necessary to form a protective ozone layer.

CHAPTER 6

6 Chapter Six: General Discussion

Many studies have attempted to investigate the theory of cometary panspermia, Hoyle and Wickramasinghe (1981a) and lithopanspermia (Wainwright *et al.*, 2009). Of particular novelty is the work explored in this thesis which is devoted to Neopanspermia (Wainwright, 2003), the view that life is continually arriving to Earth from space. The experiment verification of this idea is based on microbial sampling of the stratosphere at heights which theoretically life from Earth cannot reach, a conclusion which is based on experimental as well as theoretical considerations. Emphasis is also placed on studies of the possible presence in meteorites of fossilized, putative microbes which originated elsewhere in the cosmos. The final aim was to evaluate the survivability of bacteria in environments which had high dosage of UVC similar to the stratosphere and the conditions which are thought to have been prevailing on early Earth when no oxygen was in the atmosphere.

Previous studies which sampled the stratosphere revealed the presence of microbes in this region, some of which were isolated and identified, although others were uncultivable (Imshenetsky *et al.*, 1978, Harris *et al.*, 2002, Yang *et al.*, 2009, Smith and Team, 2015). The possibility of contamination has however, been emphasised by critics in order to discredit such results (Smith, 2013). Similarly, early findings made by us in detecting DNA from stratospheric clumps of the Indian balloon mission using DAPI and $DiOC_6$ stains (Wainwright *et al.*, 2015b) have been also argued by critics to be contaminants. However, our large scale project of conducting six stratospheric balloon launches over the course of several years is the most comprehensive effort to understand the biology of the upper stratosphere to date. When the results from the first three sampling missions were published (Wainwright *et al.*, 2015a), critics doubted the results on the basis that they needed to be repeated, which was done. Contamination is extremely unlikely to be a factor in our stratospheric samples because in the many controls that were used, no contaminants was found. Many particles were isolated from the stratosphere, most were non-biotic cosmic dust particles, but many others showed strong indications of having a biological origin. The distribution and type of the recovered biological particles is also different

between the six launches, with some of the missions producing no recovered biological entities (the second and fourth mission findings reported only cosmic dust particles), which is to be expected when doing multiple sampling trips over a long time-period. It also strongly suggests the arrival of the biological particles to be associated with meteorites incoming over certain times, e.g. coinciding with the Perseid meteor shower. The images and data from SEM and EDAX for the biological particles showed a clear distinction between them and inorganic cosmic dust particles, mainly the fact that BEs contained C, O, and N, while the dust and micrometeorites comprised mainly Al or Si. However, the conclusive proof for the recovered BEs to be biological came from the isolation and identification of DNA using WGA techniques accompanied by 16S rRNA PCR and Next- Generation sequencing, which showed the stratosphere to contain numerous microbes, some of which like *Oceanobacillus iheyensis* and *Marinithermus hydrotherm* have been found in specific and localized regions around the world. Despite the large number of microbial species identified through Single-cell amplification and Next-gen sequencing in this work, none of them have a cell size of over 5 µm despite the presence of a few which are eukaryotic organisms, this confirms previous studies of the maximum size of particles which can be lifted to over 20 km from earth (Kasten, 1968, Dehel *et al.*, 2008). Therefore, we conclude that while some of the larger BEs which we recovered are incoming from space, those smaller than 5 µm can be lifted from Earth. However, they could be incoming from space; the association of the recovered BEs with micrometeorites and the impact crater on the SEM stubs is a strong indication of an extra-terrestrial origin, with similar findings when we used copper slides. The use of neodymium magnets as a mean to attract extra-terrestrial particles produced interesting results, with many of the BEs showing rare Earth minerals when examined by EDAX. The findings are also in agreement with the studies reporting the presence of complex organic molecules in meteorites which are brought to Earth (Kvenvolden *et al.*, 1970, Engel and Macko, 1997, Ciesla and Sandford, 2012). The very recent discovery of glycine and phosphorus in the gas cloud around the comet 67P Churyumov-Gerasimenko, by the Rosetta spacecraft (Altwegg *et*

al., 2016) is another strong asset for the panspermia theory and provides additional proof that comets can carry the building blocks of life.

The question of whether a microbe can survive millions of years in "hibernation" and later regain the ability to grow and replicate when the conditions are right, was addressed in Chapter Three. Amber samples, containing insect remains were broken using a contamination-proof technique with a built-in control. Similar attempts were made to isolate microbes trapped in the fluid inclusions of halite samples. It was also shown that a wide variety of terrestrial rocks contain bacteria, and such rocks could possibly act as "protective vehicles capable of transporting bacteria from Earth to the cosmos through the process of reverse panspermia. The Archipanspermia theory was also examined by determine the presence of bacteria in manufactured materials such as bricks and cement.

Efforts to isolate microbes from the amber samples were unsuccessful; however, considering that similar attempts by others have reported finding bacteria in amber (Cano and Borucki, 1995, Wainwright *et al.*, 2009) it is clear that further such studies need to be conducted. The isolation of *B. amyloliquefaciens* from halite suggest the possibility that microbes could withstand long periods of nutrient deprivation and high NaCl concentrations while travelling through the cosmos in this material. The recovery of microbes from halite has also been reported in previous studies (Benison and Goldstein, 1999, Satterfield *et al.*, 2005). Those findings show that "shelf-life" of DNA might be longer that what has been previously been though possible (Hebsgaard *et al.*, 2005, Paéibo, 2012).

Although most meteorites burn or break up while entering our atmosphere, some fragments do reach the Earth's surface. Work reported in Chapter Four showed that two of three meteorite samples showed presumptive microfossils. The Northwest Africa 4925 meteorite sample contained filament and biofilm formations which were indigenous to the meteorite as confirmed by EDAX. Similarly, the Polonnaruwa meteorite contained large microfossil formations which did not resemble known terrestrial microbes, both meteorites showed worm-like entities similar to the ones reported by McKay

et al. (1996) in the ALH84001 meteorite. The suggested microfossils found within the Polonnaruwa meteorite were very similar to the ones reported in other studies (Wainwright *et al.*, 2013a, Wainwright *et al.*, 2013b, Wainwright *et al.*, 2013e, Wallis *et al.*, 2013, Wickramasinghe *et al.*, 2013a, Wickramasinghe *et al.*, 2013d). Presumptive microfossils were not, however, found in samples of the Carancas meteorite, although inorganic carbonate crystal bundle precipitates were observed.

One of the main arguments often used to discredit the theory of panspermia was also investigated, namely the harmful effects of UV on microbes while journeying through space, notably in comets (Horneck, 1999, Paulino-Lima *et al.*, 2010). Here, we exposed several microbes to different UV wavelengths, and found that ice and water provide relatively low protection for microbes which is in accordance with the findings of Ladanyi and Morrison (1968), however, when inorganic, insoluble particles are present in the water or ice, shielding occurs, even if the individual particles are smaller in diameter than the bacteria . Fumed silica was used for this purpose (the particles were each around 0.007 µm in diameter), the presence of solid particles in the growth media also seemed to alter the growth pattern for some microbes, which might also help to explain why bacteria clump together and thereby provide shelter for cells (located in the inside of the mass) from radiation.

Chapter Five also deals with the question of how early photosynthetic microbes survived the levels of UVC, which was considerably stronger on the surface of the early Earth than today (since there was no ozone layer) and when the sun was fainter but emitted more UV (Cockell and Horneck, 2001). We proposed a novel concept to how Cyanobacteria might have been shielded inside semi-transparent fluorescent rocks, and use visible light, generated from UV via fluorescence, for photosynthetic activity. This concept was tested and proved to be possible. This theory might help explain how early live survived the harsh conditions on Earth, and it also provides novel survivability mechanisms for microbes carried in meteorites containing an abundance of fluorescent minerals, notably calcite.

Suggestions for further study:

The findings that a wide variety of microbes can be isolated from the stratosphere prove that life can survive in this region despite the presence of harsh conditions and strong UV radiation. However, the absence of known terrestrial cells that exceed 5 µm in diameter, or their DNA, and the presence of biological entities which are brought in from space, does raises new possibilities for further investigation in the following areas:

1. Conduct survivability experiments in the stratosphere and the upper layers of the atmosphere by exposing different microbial samples with different shielding material to the ambient stratospheric environment, in a manner which expands on the concept of the E-MIST mission (Smith and Team, 2015).
2. Use low-density silica-aerogel for the collection of microbes from the stratosphere, and compare the results to the future findings of the TANPOPO – JAXA mission on the ISS (Kawaguchi *et al.*, 2016).
3. Use of the Single Cell amplification techniques for future minute samples obtained from the stratosphere and the exosphere, as well as meteorites.
4. Conduct further research into the use of fluorescent minerals as an alternative source of energy for Cyanobacteria, using a) microbial mats and b) taking dissolved oxygen measurements, and c) use photocells as a way to produce comprehensive data on the effect of harmful UV on microbes shielded behind transparent fluorescent minerals, and finally, determine the amount of light generated and made available.

References

ABREVAYA, X. C., PAULINO-LIMA, I. G., GALANTE, D., RODRIGUES, F., MAUAS, P. J., CORTÓN, E. and LAGE, C. D. A. S. 2011. Comparative survival analysis of *Deinococcus radiodurans* and the *Haloarchaea Natrialba magadii* and *Haloferax volcanii* exposed to vacuum ultraviolet irradiation. *Astrobiology,* 11**,** 1034-1040.

AHN, J. and BALASUBRAMANIAM, V. 2007. Physiological responses of Bacillus amyloliquefaciens spores to high pressure. *Journal of Microbiology and Biotechnology,* 17**,** 524.

ALHARBI, S. A., WAINWRIGHT, M., AL-HARBI, N. A., HAJOMER, S. and ALSHAMMARI, F. 2011. Evidence in support of the theory of archipanspermia. *Journal of Food, Agriculture and Environment,* 9**,** 1082-1084.

ALTSCHUL, S. F., MADDEN, T. L., SCHÄFFER, A. A., ZHANG, J., ZHANG, Z., MILLER, W. and LIPMAN, D. J. 1997. Gapped blast and psi-blast: A new generation of protein database search programs. *Nucleic Acids Research,* 25**,** 3389-3402.

ALTWEGG, K., BALSIGER, H., BAR-NUN, A., BERTHELIER, J.-J., BIELER, A., BOCHSLER, P., BRIOIS, C., CALMONTE, U., COMBI, M. R. and COTTIN, H. 2016. Prebiotic chemicals—amino acid and phosphorus—in the coma of comet 67P/Churyumov-Gerasimenko. *Science Advances,* 2**,** e1600285.

AMANN, R. I., LUDWIG, W. and SCHLEIFER, K.-H. 1995. Phylogenetic identification and in situ detection of individual microbial cells without cultivation. *Microbiological Reviews,* 59**,** 143-169.

ANDREWS, S. 2010. FastQC: a quality control tool for high throughput sequence data.

ANTAL, M. J. and GRØNLI, M. 2003. The art, science, and technology of charcoal production. *Industrial and Engineering Chemistry Research,* 42**,** 1619-1640.

ARRHENIUS, S. 1903. Die verbreitung des lebens im weltenraum. *Die Umschau,* 7**,** 481-485.

ARRHENIUS, S. 1908. *Worlds In The Making: The Evolution of The Universe*, London, Harper and brothers.

ATRIH, A. and FOSTER, S. J. 2002. Bacterial endospores the ultimate survivors. *International Dairy Journal,* 12**,** 217-223.

BADA, J. L., BIGHAM, C. and MILLER, S. L. 1994. Impact melting of frozen oceans on the early Earth: implications for the origin of life. *Proceedings of the National Academy of Sciences of the United States of America,* 91**,** 1248-50.

BASTIAN, F., ALABOUVETTE, C. and SAIZ-JIMENEZ, C. 2009. Bacteria and free-living amoeba in the Lascaux Cave. *Research in Microbiology,* 160**,** 38-40.

BAUER, H., KASPER-GIEBL, A., LÖFLUND, M., GIEBL, H., HITZENBERGER, R., ZIBUSCHKA, F. and PUXBAUM, H. 2002. The contribution of bacteria and fungal spores to the organic carbon content of cloud water, precipitation and aerosols. *Atmospheric Research,* 64**,** 109-119.

BEATTY, J. T., OVERMANN, J., LINCE, M. T., MANSKE, A. K., LANG, A. S., BLANKENSHIP, R. E., VAN DOVER, C. L., MARTINSON, T. A. and PLUMLEY, F. G. 2005. An obligately photosynthetic bacterial anaerobe from a deep-sea hydrothermal vent. *Proceedings of the National Academy of Sciences of the United States of America,* 102**,** 9306-9310.

BECQUEREL, P. 1924. La Vie Terrestre Provient-Elle d'un Autre Monde? *L'Astronomie,* 38**,** 393-417.

BENISON, K. C. and GOLDSTEIN, R. H. 1999. Permian paleoclimate data from fluid inclusions in halite. *Chemical Geology,* 154**,** 113-132.

BERKNER, L. V. and MARSHALL, L. 1965. On the origin and rise of oxygen concentration in the Earth's atmosphere. *Journal of the Atmospheric Sciences,* 22**,** 225-261.

BIANCIARDI, G., MILLER, J. D., STRAAT, P. A. and LEVIN, G. V. 2012. Complexity analysis of the Viking labeled release experiments. *International Journal Aeronautical and Space Sciences,* 13**,** 14-26.

BLUMTHALER, M., AMBACH, W. and ELLINGER, R. 1997. Increase in solar uv radiation with altitude. *Journal Of Photochemistry And Photobiology B: Biology,* 39**,** 130-134.

BOCKELÉE-MORVAN, D. 2011. An overview of comet composition. *Proceedings of the International Astronomical Union,* 7**,** 261-274.

BOROVIČKA, J. and SPURNÝ, P. 2008. The Carancas meteorite impact–Encounter with a monolithic meteoroid. *Astronomy* and *Astrophysics,* 485**,** L1-L4.

BRADLEY, J. P., HARVEY, R. P., MCSWEEN, H., GIBSON, E., THOMAS-KEPRTA, K. and VALI, H. 1997. No 'nanofossils' in martian meteorite. *Nature,* 390**,** 454-456.

BRASSEUR, G. and SOLOMON, S. 2006. *Aeronomy Of The Middle Atmosphere: Chemistry And Physics Of The Stratosphere And Mesosphere*, New York, Springer.

BRYCE, C. C., HORNECK, G., RABBOW, E., EDWARDS, H. G. and COCKELL, C. S. 2014. Impact shocked rocks as protective habitats on an anoxic early Earth. *International Journal of Astrobiology***,** 1-8.

BURCHELL, M., HARRISS, K., PRICE, M. and YOLLAND, L. 2017. Survival of fossilised diatoms and forams in hypervelocity impacts with peak shock pressures in the 1–19GPa range. *Icarus,* 290**,** 81-88.

BURCHELL, M. J., MANN, J. and BUNCH, A. W. 2004. Survival of bacteria and spores under extreme shock pressures. *Monthly Notices of the Royal Astronomical Society,* 352**,** 1273-1278.

BURTON, A. S., STERN, J. C., ELSILA, J. E., GLAVIN, D. P. and DWORKIN, J. P. 2012. Understanding prebiotic chemistry through the analysis of extraterrestrial amino acids and nucleobases in meteorites. *Chemical Society Reviews,* 41**,** 5459-5472.

CAIRNS-SMITH, A. G. 1982. *Genetic Takeover And The Mineral Origins Of Life*, Cambridge University Press Cambridge.

CAMPINS, H. and SWINDLE, T. D. 1998. Expected characteristics of cometary meteorites. *Meteoritics* and *Planetary Science,* 33**,** 1201-1211.

CANO, R. J. and BORUCKI, M. K. 1995. Revival and identification of bacterial spores in 25-to 40-million-year-old Dominican amber. *Science,* 268**,** 1060-1064.

CANUTO, V. M., LEVINE, J. S., AUGUSTSSON, T. R. and IMHOFF, C. L. 1982. UV radiation from the young Sun and oxygen and ozone levels in the prebiological palaeoatmosphere. *Nature,* 296**,** 816-820.

CARTER, N. L. and HEARD, H. C. 1970. Temperature and rate dependent deformation of halite. *American Journal of Science,* 269**,** 193-249.

CASTELLO, J. D., ROGERS, S. O., STARMER, W. T., CATRANIS, C. M., MA, L., BACHAND, G. D., ZHAO, Y. and SMITH, J. E. 1999. Detection of tomato mosaic tobamovirus RNA in ancient glacial ice. *Polar Biology,* 22**,** 207-212.

CATRANIS, C. and STARMER, W. 1991. Microorganisms entrapped in glacial ice. *Antarctic Journal of the United States,* 26**,** 234-236.

CHANG, J. C., OSSOFF, S. F., LOBE, D. C., DORFMAN, M. H., DUMAIS, C. M., QUALLS, R. G. and JOHNSON, J. D. 1985. UV inactivation of pathogenic and indicator microorganisms. *Applied and Environmental Microbiology,* 49**,** 1361-1365.

CHAPMAN, C. R. and MORRISON, D. 1994. Impacts on the Earth by asteroids and comets: assessing the hazard. *Nature,* 367**,** 33-40.

CHEN, W., WESTERHOFF, P., LEENHEER, J. A. and BOOKSH, K. 2003. Fluorescence excitation-emission matrix regional integration to quantify spectra for dissolved organic matter. *Environmental Science and Technology,* 37**,** 5701-5710.

CHISHOLM, S. W., OLSON, R. J., ZETTLER, E. R., GOERICKE, R., WATERBURY, J. B. and WELSCHMEYER, N. A. 1988. A novel free-living prochlorophyte abundant in the oceanic euphotic zone, *Nature*, 334, 340 - 343.

CHRISTNER, B. C., MORRIS, C. E., FOREMAN, C. M., CAI, R. and SANDS, D. C. 2008. Ubiquity of biological ice nucleators in snowfall. *Science,* 319**,** 1214-1214.

CHRISTNER, B. C., MOSLEY-THOMPSON, E., THOMPSON, L. G., ZAGORODNOV, V., SANDMAN, K. and REEVE, J. N. 2000. Recovery and identification of viable bacteria immured in glacial ice. *Icarus,* 144**,** 479-485.

CHYBA, C. and SAGAN, C. 1992. Endogenous production, exogenous delivery and impact-shock synthesis of organic molecules: an inventory for the origins of life.

CIESLA, F. J. and SANDFORD, S. A. 2012. Organic synthesis via irradiation and warming of ice grains in the solar nebula. *Science,* 336**,** 452-454.

CLARK, R. T. R. 1959. *Myth And Symbol In Ancient Egypt*, Thames and Hudson.

COCHRAN, A. L., LEVASSEUR-REGOURD, A.-C., CORDINER, M., HADAMCIK, E., LASUE, J., GICQUEL, A., SCHLEICHER, D. G., CHARNLEY, S. B., MUMMA, M. J. and PAGANINI, L. 2015. The composition of comets. *Space Science Reviews,* 197**,** 9-46.

COCKELL, C., KOEBERL, C. and GILMOUR, I. 2006. *Biological Processes Associated with Impact Events*, New York, Springer.

COCKELL, C. S. 1998. Biological effects of high ultraviolet radiation on early Earth—a theoretical evaluation. *Journal of Theoretical Biology,* 193**,** 717-729.

COCKELL, C. S., BRACK, A., WYNN-WILLIAMS, D. D., BAGLIONI, P., BRANDSTÄTTER, F., DEMETS, R., EDWARDS, H. G., GRONSTAL, A. L., KURAT, G. and LEE, P. 2007. Interplanetary transfer of photosynthesis: an experimental demonstration of a selective dispersal filter in planetary island biogeography. *Astrobiology,* 7**,** 1-9.

COCKELL, C. S. and HORNECK, G. 2001. The History of the UV Radiation Climate of the Earth—Theoretical and Space-based Observations. *Photochemistry and Photobiology,* 73**,** 447-451.

COCKELL, C. S. and STOKES, M. D. 2006. Hypolithic colonization of opaque rocks in the Arctic and Antarctic polar desert. *Arctic, Antarctic, and Alpine Research,* 38**,** 335-342.

COHEN, J. 1995. Getting all turned around over the origins of life on earth. *Science (New York, NY),* 267**,** 1265.

COX, M. M. and BATTISTA, J. R. 2005. *Deinococcus radiodurans*—the consummate survivor. *Nature Reviews Microbiology,* 3**,** 882-892.

CRAWFORD, R. L. 2005. Microbial diversity and its relationship to planetary protection. *Applied and Environmental Microbiology,* 71**,** 4163-4168.

CRICK, F. H. and ORGEL, L. E. 1973. Directed Panspermia. *Icarus,* 19**,** 341-346.

DE LA TORRE, R., SANCHO, L. G., HORNECK, G., RÍOS, A. D. L., WIERZCHOS, J., OLSSON-FRANCIS, K., COCKELL, C. S., RETTBERG, P., BERGER, T. and DE VERA, J.-P. P. 2010a. Survival of lichens and bacteria exposed to outer space conditions–results of the Lithopanspermia experiments. *Icarus,* 208**,** 735-748.

DE LA TORRE, R., SANCHO, L. G., HORNECK, G., RÍOS, A. D. L., WIERZCHOS, J., OLSSON-FRANCIS, K., COCKELL, C. S., RETTBERG, P., BERGER, T. and DE VERA, J.-P. P. 2010b. Survival of lichens and bacteria exposed to outer space conditions – Results of the Lithopanspermia experiments. *Icarus,* 208**,** 735-748.

DEAN, F. B., HOSONO, S., FANG, L., WU, X., FARUQI, A. F., BRAY-WARD, P., SUN, Z., ZONG, Q., DU, Y. and DU, J. 2002. Comprehensive human genome amplification using multiple displacement amplification. *Proceedings of the National Academy of Sciences,* 99**,** 5261-5266.

DEHEL, T., LORGE, F. and DICKINSON, M. 2008. Uplift of microorganisms by electric fields above thunderstorms. *Journal of Electrostatics,* 66**,** 463-466.

DELEON-RODRIGUEZ, N., LATHEM, T. L., RODRIGUEZ-R, L. M., BARAZESH, J. M., ANDERSON, B. E., BEYERSDORF, A. J., ZIEMBA, L. D., BERGIN, M., NENES, A. and KONSTANTINIDIS, K. T. 2013. Microbiome of the upper troposphere: Species composition and prevalence, effects of tropical storms, and atmospheric implications. *Proceedings of the National Academy of Sciences,* 110**,** 2575-2580.

DELLWIG, L. F. 1968. Significant features of deposition in the Hutchinson Salt, Kansas, and their interpretation. *Geological Society of America Special Papers,* 88**,** 421-428.

DENNER, E. B., MCGENITY, T. J., BUSSE, H.-J., GRANT, W. D., WANNER, G. and STAN-LOTTER, H. 1994. *Halococcus salifodinae sp*. nov., an archaeal isolate from an Austrian salt mine. *International Journal of Systematic and Evolutionary Microbiology,* 44**,** 774-780.

DETWILER, R. J. and MEHTA, P. K. 1989. Chemical and physical effects of silica fume on the mechanical behavior of concrete. *ACI Materials Journal,* 86.

EARL, D., BRADNAM, K., JOHN, J. S., DARLING, A., LIN, D., FASS, J., YU, H. O. K., BUFFALO, V., ZERBINO, D. R. and DIEKHANS, M. 2011. Assemblathon 1: a competitive assessment of de novo short read assembly methods. *Genome Research,* 21**,** 2224-2241.

ENGEL, M. H. and MACKO, S. 1997. Isotopic evidence for extraterrestrial non-racemic amino acids in the Murchison meteorite. *Nature,* 389**,** 265-268.

FIALA, G., WOESE, C. R., LANGWORTHY, T. A. & STETTER, K. O. 1990. *Flexistipes sinusarabici*, a novel genus and species of eubacteria occurring in the Atlantis II Deep brines of the Red Sea. *Archives of Microbiology,* 154**,** 120-126.

FINDLEY, K., OH, J., YANG, J., CONLAN, S., DEMING, C., MEYER, J. A., SCHOENFELD, D., NOMICOS, E., PARK, M. & SEQUENCING, N. I. S. C. C. 2013. Topographic diversity of fungal and bacterial communities in human skin. *Nature,* 498**,** 367-370.

FLORKE, O., MARTIN, B., BENDA, L., PASCHEN, S., BERGNA, H., ROBERTS, W., WELSH, W., ETTLINGER, M., KERNER, D. & KLEINSCHMIT, P. 2008. Silica, Ullmann's encyclopedia of industrial chemistry. Wiley-VCH Verlag GmbH & Co., Weinheim.

FREDRICKS, D. N. Microbial ecology of human skin in health and disease. *Journal of Investigative Dermatology Symposium Proceedings*, 2001. London, Elsevier, 167-169.

FRIEDMANN, E. I. 1982. Endolithic microorganisms in the Antarctic cold desert. *Science,* 215**,** 1045-1053.

FRITZ, J., ARTEMIEVA, N. and GRESHAKE, A. 2005. Ejection of Martian meteorites. *Meteoritics and Planetary Science,* 40**,** 1393-1411.

GALANTE, D. and ERNESTO HORVATH, J. 2007. Biological effects of gamma-ray bursts: distances for severe damage on the biota. *International Journal of Astrobiology,* 6**,** 19-26.

GASCÓN, J., OUBIÑA, A., PÉREZ-LEZAUN, A. and URMENETA, J. 1995. Sensitivity of selected bacterial species to UV radiation. *Current Microbiology,* 30**,** 177-182.

GILLON, M., TRIAUD, A. H., DEMORY, B.-O., JEHIN, E., AGOL, E., DECK, K. M., LEDERER, S. M., DE WIT, J., BURDANOV, A. and INGALLS, J. G. 2017. Seven temperate terrestrial planets around the nearby ultracool dwarf star TRAPPIST-1. *Nature,* 542**,** 456-460.

GLADMAN, B. J. and BURNS, J. A. 1996. Mars Meteorite Transfer-Simulation. *Science,* 274**,** 161-162.

GLADMAN, B. J., BURNS, J. A., DUNCAN, M., LEE, P. and LEVISON, H. F. 1996. The exchange of impact ejecta between terrestrial planets. *Science,* 271**,** 1387.

GOESMANN, F., ROSENBAUER, H., BREDEHOFT, J. H., CABANE, M., EHRENFREUND, P., GAUTIER, T., GIRI, C., KRUGER, H., LE ROY, L., MACDERMOTT, A. J., MCKENNA-LAWLOR, S., MEIERHENRICH, U. J., CARO, G. M., RAULIN, F., ROLL, R., STEELE, A., STEININGER, H., STERNBERG, R., SZOPA, C., THIEMANN, W. and ULAMEC, S. 2015.

Organic compounds on comet 67P/Churyumov-Gerasimenko revealed by COSAC mass spectrometry. *Science,* 349.

GÖTZ, D., BANTA, A., BEVERIDGE, T., RUSHDI, A., SIMONEIT, B. and REYSENBACH, A. 2002. *Persephonella marina* gen. nov., sp. nov. and *Persephonella guaymasensis sp.* nov., two novel, thermophilic, hydrogen-oxidizing microaerophiles from deep-sea hydrothermal vents. *International Journal of Systematic and Evolutionary Microbiology,* 52**,** 1349-1359.

GREENBLATT, C., DAVIS, A., CLEMENT, B., KITTS, C., COX, T. and CANO, R. J. 1999. Diversity of microorganisms isolated from amber. *Microbial ecology,* 38**,** 58-68.

GROTZINGER, J. P., SUMNER, D., KAH, L., STACK, K., GUPTA, S., EDGAR, L., RUBIN, D., LEWIS, K., SCHIEBER, J. and MANGOLD, N. 2014. A habitable fluvio-lacustrine environment at Yellowknife Bay, Gale Crater, Mars. *Science,* 343**,** 1242777.

HALDANE, J. B. S. 1929. The origin of life. *Rationalist Annual,* 148**,** 3-10.

HARDIE, L. A., LOWENSTEIN, T. K. and SPENCER, R. J. The problem of distinguishing between primary and secondary features in evaporites. Sixth international symposium on salt, 1985. Salt Institute Alexandria, 11-39.

HARRIS, G. D., ADAMS, V. D., SORENSEN, D. L. and CURTIS, M. S. 1987. Ultraviolet inactivation of selected bacteria and viruses with photoreactivation of the bacteria. *Water Research,* 21**,** 687-692.

HARRIS, M. J., WICKRAMASINGHE, N. C., LLOYD, D., NARLIKAR, J., RAJARATNAM, P., TURNER, M. P., AL-MUFTI, S., WALLIS, M. K., RAMADURAI, S. and HOYLE, F. Detection of living cells in stratospheric samples. International Symposium on Optical Science and Technology, 2002. International Society for Optics and Photonics, 4495, 192-198.

HARTMANN, D. L., HOLTON, J. R. and FU, Q. 2001. The heat balance of the tropical tropopause, cirrus, and stratospheric dehydration. *Geophysical Research Letters,* 28**,** 1969-1972.

HEBSGAARD, M. B., PHILLIPS, M. J. and WILLERSLEV, E. 2005. Geologically ancient DNA: fact or artefact? *Trends in Microbiology,* 13**,** 212-220.

HENDRICKX, L. and MERGEAY, M. 2007. From the deep sea to the stars: human life support through minimal communities. *Current Opinion in Microbiology,* 10**,** 231-237.

HENKEL, G. 1989. *The Henkel glossary of fluorescent minerals*, Fluorescent Mineral Society.

HENNING, T. 2010. Cosmic silicates. *Annual Review of Astronomy and Astrophysics,* 48**,** 21-46.

HERD, C. D., BORG, L. E., JONES, J. H. and PAPIKE, J. J. 2002. Oxygen fugacity and geochemical variations in the martian basalts: Implications for martian basalt petrogenesis and the oxidation state of the upper mantle of Mars. *Geochimica et Cosmochimica Acta,* 66**,** 2025-2036.

HEUER, H., KRSEK, M., BAKER, P., SMALLA, K. and WELLINGTON, E. 1997. Analysis of actinomycete communities by specific amplification of genes encoding 16S rRNA and gel-electrophoretic separation in denaturing gradients. *Applied and Environmental Microbiology,* 63**,** 3233-3241.

HIDA, T. 1980. *Brownian motion*, Springer.

HOMECK, G., MILEIKOWSKY, C., MELOSH, H. J., WILSON, J. W., CUCINOTTA, F. A. and GLADMAN, B. 2002a. Viable transfer of microorganisms in the solar system and beyond. *Astrobiology: The Quest for the Conditions of Life.* London, Springer.

HOMECK, G., MILEIKOWSKY, C., MELOSH, H. J., WILSON, J. W., CUCINOTTA, F. A. and GLADMAN, B. 2002b. *Viable transfer of microorganisms in the solar system and beyond*, Springer.

HOOVER, R. B. Meteorites, microfossils, and exobiology. Optical Science, Engineering and Instrumentation'97, 1997. International Society for Optics and Photonics, 115-136.

HOOVER, R. B. 2011. Fossils of cyanobacteria in CI1 carbonaceous meteorites. *Journal of Cosmology,* 16**,** 7070-7111.

HOOVER, R. B., JERMAN, G. A., ROZANOV, A. Y. and DAVIES, P. C. Biomarkers and microfossils in the Murchison, Rainbow, and Tagish Lake meteorites. Astronomical Telescopes and Instrumentation, 2003. International Society for Optics and Photonics, 15-31.

HOOVER, R. B., and ROZANOV, A. Y. Microfossils, biominerals, and chemical biomarkers in meteorites. Nato Science Series Sub Series, 2005. *Life and Behavioural Sciences* 366, 43.

HOOVER, R. B., ROZANOV, A. Y., ZHMUR, S. I. and GORLENKO, V. M. Further evidence of microfossils in carbonaceous meteorites. SPIE's International Symposium on Optical Science, Engineering, and Instrumentation, 1998. International Society for Optics and Photonics, 203-216.

HORNECK, G. 1993. Responses of *Bacillus subtilis* spores to space environment: Results from experiments in space. *Origins of Life and Evolution of the Biosphere,* 23**,** 37-52.

HORNECK, G. 1998. Exobiological experiments in Earth orbit. *Advances in Space Research,* 22**,** 317-326.

HORNECK, G. 1999. European activities in exobiology in Earth orbit: results and perspectives. *Advances in Space Research,* 23**,** 381-386.

HORNECK, G., RETTBERG, P., REITZ, G., WEHNER, J., ESCHWEILER, U., STRAUCH, K., PANITZ, C., STARKE, V. and BAUMSTARK-KHAN, C. 2001. Protection of bacterial spores in space, a contribution to the discussion on panspermia. *Origins of Life and Evolution of the Biosphere,* 31**,** 527-547.

HORNECK, G., STOFFLER, D., OTT, S., HORNEMANN, U., COCKELL, C. S., MOELLER, R., MEYER, C., DE VERA, J. P., FRITZ, J., SCHADE, S. and ARTEMIEVA, N. A. 2008. Microbial rock inhabitants survive hypervelocity impacts on Mars-like host planets: first phase of lithopanspermia experimentally tested. *Astrobiology,* 8**,** 17-44.

HOSONO, S., FARUQI, A. F., DEAN, F. B., DU, Y., SUN, Z., WU, X., DU, J., KINGSMORE, S. F., EGHOLM, M. and LASKEN, R. S. 2003. Unbiased whole-genome amplification directly from clinical samples. *Genome Research,* 13**,** 954-964.

HOYLE, F. and WICKRAMASINGHE, C. 1981a. Comets-a vehicle for panspermia. *Comets and the Origin of Life.* Springer.

HOYLE, F. and WICKRAMASINGHE, C. 1981b. Evolution from space. *Evolution from space., by Hoyle, F.; Wickramasinghe, C.. London (UK): JM Dent, 176 p.,* 1.

HOYLE, F. and WICKRAMASINGHE, C. 1985. Living comets. *Living comets.. F. Hoyle, C. Wickramasinghe. University College Cardiff Press, Cardiff, UK. 133 pp. Price£ 5.95 (1985). ISBN 0-906449-79-0.,* 1.

HUBER, H., HOHN, M. J., RACHEL, R., FUCHS, T., WIMMER, V. C. and STETTER, K. O. 2002. A new phylum of Archaea represented by a nanosized hyperthermophilic symbiont. *Nature,* 417**,** 63-67.

HULLO, M.-F., MOSZER, I., DANCHIN, A. and MARTIN-VERSTRAETE, I. 2001. CotA of *Bacillus subtilis* is a copper-dependent laccase. *Journal of Bacteriology,* 183**,** 5426-5430.

HUNTER, W. & PARKIN, D. Cosmic dust in recent deep-sea sediments. Proceedings of the Royal Society of London A: Mathematical, Physical and Engineering Sciences, 1960. The Royal Society, 382-397.

IMSHENETSKY, A., LYSENKO, S. and KAZAKOV, G. 1978. Upper boundary of the biosphere. *Applied and Environmental Microbiology,* 35**,** 1-5.

KASTEN, F. 1968. Falling speed of aerosol particles. *Journal of Applied Meteorology,* 7**,** 944-947.

KAWAGUCHI, Y., YANG, Y., KAWASHIRI, N., SHIRAISHI, K., TAKASU, M., NARUMI, I., SATOH, K., HASHIMOTO, H., NAKAGAWA, K. and TANIGAWA, Y. 2013a. The possible interplanetary transfer of microbes: Assessing the viability of *Deinococcus spp*. under the ISS environmental conditions for performing exposure experiments of microbes in the Tanpopo mission. *Origins of Life and Evolution of Biospheres,* 43**,** 411-428.

KAWAGUCHI, Y., YANG, Y., KAWASHIRI, N., SHIRAISHI, K., TAKASU, M., NARUMI, I., SATOH, K., HASHIMOTO, H., NAKAGAWA, K. and TANIGAWA, Y. 2013b. The Possible Interplanetary Transfer of Microbes: Assessing the Viability of *Deinococcus spp*. Under the ISS Environmental Conditions for Performing Exposure Experiments of Microbes in the Tanpopo Mission. *Origins of Life and Evolution of Biospheres***,** 1-18.

KAWAGUCHI, Y., YOKOBORI, S.-I., HASHIMOTO, H., YANO, H., TABATA, M., KAWAI, H. and YAMAGISHI, A. 2016. Investigation of the Interplanetary Transfer of Microbes in the Tanpopo Mission at the Exposed Facility of the International Space Station. *Astrobiology,* 16**,** 363-376.

KELLOGG, C. A. and GRIFFIN, D. W. 2006. Aerobiology and the global transport of desert dust. *Trends in Ecology and Evolution,* 21**,** 638-644.

KENKMANN, T., ARTEMIEVA, N., WÜNNEMANN, K., POELCHAU, M., ELBESHAUSEN, D. and PRADO, H. 2009. The Carancas meteorite impact crater, Peru: Geologic surveying and modeling of crater formation and atmospheric passage. *Meteoritics* and *Planetary Science,* 44**,** 985-1000.

KHODADAD, C. L., WONG, G. M., JAMES, L. M., THAKRAR, P. J., LANE, M. A., CATECHIS, J. A. and SMITH, D. J. 2017. Stratosphere Conditions Inactivate Bacterial Endospores from a Mars Spacecraft Assembly Facility. *Astrobiology*.

KLOOS, W. E. and MUSSELWHITE, M. S. 1975. Distribution and persistence of *Staphylococcus* and *Micrococcus* species and other aerobic bacteria on human skin. *Applied microbiology,* 30**,** 381-395.

KNOLL, A. H. and GROTZINGER, J. 2006. Water on Mars and the prospect of martian life. *Elements,* 2**,** 169-173.

KOZIOL, A. M. and BREARLEY, A. J. A non-biological origin for the nanophase magnetite grains in ALH84001: Experimental Results. *Lunar and Planetary Science Conference*, 2002. 1672.

KRIJT, S., BOWLING, T. J., LYONS, R. J. and CIESLA, F. J. 2017. Fast Litho-panspermia in the Habitable Zone of the TRAPPIST-1 System. *Astrophysical Journal Letters,* 839**,** L21.

KVENVOLDEN, K., LAWLESS, J., PERING, K., PETERSON, E., FLORES, J., PONNAMPERUMA, C., KAPLAN, I. and MOORE, C. 1970. Evidence for extraterrestrial amino-acids and hydrocarbons in the Murchison meteorite, 923-926.

LADANYI, P. and MORRISON, S. 1968. Ultraviolet Bactericidal Irradiation of Ice. *Applied Microbiology,* 16**,** 463-467.

LEE, N. N., FRITZ, J., FRIES, M. D., GIL, J. F., BECK, A., PELLINEN-WANNBERG, A., SCHMITZ, B., STEELE, A. and HOFMANN, B. A. 2017. The extreme biology of meteorites: Their role in understanding the origin and distribution of life on earth and in the universe. *Adaption of Microbial Life to Environmental Extremes.* Springer.

LEINERT, C. and GRÜN, E. 1990. Interplanetary dust. *Physics of the inner heliosphere I.* Springer.

LEVINE, R. and EVERS, C. 2000. The Slow Death of Spontaneous Generation. 1668-1759.

LINGAM, M. and LOEB, A. 2017. Enhanced interplanetary panspermia in the TRAPPIST-1 system. *arXiv preprint arXiv:1703.00878*.

LIPMAN, C. B. 1931. Living microörganisms in ancient rocks. *Journal of Bacteriology,* 22**,** 183.

LIU, H., ZHOU, Y., LIU, R., ZHANG, K.-Y. and LAI, R. 2009. *Bacillus solisalsi sp*. nov., a halotolerant, alkaliphilic bacterium isolated from soil around a salt lake. *International Journal of Systematic and Evolutionary Microbiology,* 59**,** 1460-1464.

LU, J., NOGI, Y. and TAKAMI, H. 2001. Oceanobacillus iheyensis gen. nov., sp. nov., a deep-sea extremely halotolerant and alkaliphilic species isolated from a depth of 1050 m on the Iheya Ridge. *FEMS microbiology letters,* 205**,** 291-297.

LUISI, P. L. 2006. *The Emergence Of Life: From Chemical Origins To Synthetic Biology*, Cambridge, Cambridge University Press.

MA, L.-J., ROGERS, S. O., CATRANIS, C. M. and STARMER, W. T. 2000. Detection and characterization of ancient fungi entrapped in glacial ice. *Mycologia***,** 286-295.

MACEDO, L. and MACHARÉ, J. 2009. The Carancas Meteorite Fall, 15 September 2007 Official INGEMMET initial report.

MADIGAN, M. T. and GEST, H. 1979. Growth of the photosynthetic bacterium Rhodopseudomonas capsulata chemoautotrophically in darkness with H2 as the energy source. *Journal of bacteriology,* 137**,** 524-530.

MALDONADO, L. A., FENICAL, W., JENSEN, P. R., KAUFFMAN, C. A., MINCER, T. J., WARD, A. C., BULL, A. T. and GOODFELLOW, M. 2005. *Salinispora arenicola gen*. nov., sp. nov. and *Salinispora tropica sp. nov*., obligate marine actinomycetes belonging to the family *Micromonosporaceae*. *International Journal of Systematic and Evolutionary Microbiology,* 55**,** 1759-1766.

MARTINS, Z., BOTTA, O., FOGEL, M. L., SEPHTON, M. A., GLAVIN, D. P., WATSON, J. S., DWORKIN, J. P., SCHWARTZ, A. W. and EHRENFREUND, P. 2008. Extraterrestrial nucleobases in the Murchison meteorite. *Earth and Planetary Science Letters,* 270**,** 130-136.

MASON, S. F. and MASON, S. F. 1991. *Chemical Evolution: Origin of the Elements, Molecules, and Living Systems*, Oxford, Clarendon Press.

MAYSON, J. H. and MORRIS, M. 2015. Life: Could it Exist on Europa? (https://www.nshss.org/media/56782/mayson.pdf) Date of access: 04 June 2017.

MCCUNE, B., GRACE, J. B. and URBAN, D. L. 2002. *Analysis of ecological communities*, MjM Software design Gleneden Beach.

MCKAY, D. S., GIBSON JR, E. K., THOMAS-KEPRTA, K. L., VALI, H., ROMANEK, C. S., CLEMETT, S. J., CHILLIER, X. D., MAECHLING, C. R. and ZARE, R. N. 1996. Search for past life on Mars: possible relict biogenic activity in Martian meteorite ALH84001. *Science,* 273**,** 16.

MEAD, R. 2010. Perseid meteor shower. *Going Down Swinging***,** 30, 129.

MEEKS, J. C. and CASTENHOLZ, R. W. 1971. Growth and photosynthesis in an extreme thermophile, *Synechococcus lividus* (Cyanophyta). *Archives of Microbiology,* 78**,** 25-41.

MILEIKOWSKY, C., CUCINOTTA, F. A., WILSON, J. W., GLADMAN, B., HORNECK, G., LINDEGREN, L., MELOSH, J., RICKMAN, H., VALTONEN, M. and ZHENG, J. Q. 2000. Natural transfer of viable microbes in space: From Mars to Earth and Earth to Mars. *Icarus,* 145**,** 391-427.

MILLER, S. L. 1953. A production of amino acids under possible primitive earth conditions. *Science,* 117**,** 528-529.

MISHRA, K. N., AAGGARWAL, A., ABDELHADI, E. and SRIVASTAVA, D. 2010. An efficient horizontal and vertical method for online dna sequence compression. *International Journal of Computer Applications,* 3**,** 39-46.

MIURA, Y. Multiple explosions during cratering at Carancas meteorite hit in Peru. Lunar and Planetary Science Conference, 2008. 2027.

MIYAMOTO-SHINOHARA, Y., SUKENOBE, J., IMAIZUMI, T. and NAKAHARA, T. 2006. Survival curves for microbial species stored by freeze-drying. *Cryobiology,* 52**,** 27-32.

MOELLER, R., HORNECK, G., RABBOW, E., REITZ, G., MEYER, C., HORNEMANN, U. and STÖFFLER, D. 2008. Role of DNA protection and repair in resistance of *Bacillus subtilis* spores to ultrahigh shock pressures simulating hypervelocity impacts. *Applied and Environmental Microbiology,* 74**,** 6682-6689.

MORITA, R. 1999. Is H2 the universal energy source for long-term survival? *Microbial Ecology,* 38**,** 307-320.

MUSHEGIAN, A. 1999. The minimal genome concept. *Current Opinion in Genetics and Development,* 9**,** 709-714.

MYERS, G. and MCCREADY, R. 1966. Bacteria can penetrate rock. *Canadian Journal of Microbiology,* 12**,** 477-484.

NAPIER, W. 2004. A mechanism for interstellar panspermia. *Monthly Notices of the Royal Astronomical Society,* 348**,** 46-51.

NARUMI, I. 2003. Unlocking radiation resistance mechanisms: still a long way to go. *TRENDS in Microbiology,* 11**,** 422-425.

NICHOLSON, W. L., FAJARDO-CAVAZOS, P., REBEIL, R., SLIEMAN, T. A., RIESENMAN, P. J., LAW, J. F. and XUE, Y. 2002. Bacterial endospores and their significance in stress resistance. *Antonie Van Leeuwenhoek,* 81**,** 27-32.

NICHOLSON, W. L., MUNAKATA, N., HORNECK, G., MELOSH, H. J. and SETLOW, P. 2000. Resistance of Bacillus endospores to extreme terrestrial and extraterrestrial environments. *Microbiology and Molecular Biology Reviews,* 64**,** 548-572.

NICHOLSON, W. L., SCHUERGER, A. C. and SETLOW, P. 2005. The solar UV environment and bacterial spore UV resistance: considerations for Earth-to-Mars transport by natural processes and human spaceflight. *Mutation Research,* 571**,** 249-64.

NIRENBERG, M. W. 1963. The genetic code.

NORTON, C. F., MCGENITY, T. J. and GRANT, W. D. 1993. Archaeal halophiles (halobacteria) from two British salt mines. *Microbiology,* 139**,** 1077-1081.

NYQUIST, L., BOGARD, D., SHIH, C.-Y., GRESHAKE, A., STÖFFLER, D. and EUGSTER, O. 2001. Ages and geologic histories of Martian meteorites. *Chronology and Evolution of Mars.* New York*,* Springer.

OEHLER, J. H. and SCHOPF, J. W. 1971. Artificial microfossils: experimental studies of permineralization of blue-green algae in silica. *Science,* 174**,** 1229-1231.

OHTOMO, Y., KAKEGAWA, T., ISHIDA, A., NAGASE, T. and ROSING, M. T. 2014. Evidence for biogenic graphite in early Archaean Isua metasedimentary rocks. *Nature Geoscience,* 7**,** 25-28.

OJHA, L., WILHELM, M. B., MURCHIE, S. L., MCEWEN, A. S., WRAY, J. J., HANLEY, J., MASSÉ, M. and CHOJNACKI, M. 2015. Spectral evidence for hydrated salts in recurring slope lineae on Mars. *Nature Geoscience,* 8**,** 829-832.

OLSSON-FRANCIS, K. and COCKELL, C. S. 2010. Experimental methods for studying microbial survival in extraterrestrial environments. *Journal of Microbiological Methods,* 80**,** 1-13.

ONSTOTT, T. C., TOBIN, K., DONG, H., DEFLAUN, M., FREDRICKSON, J. K., BAILEY, T., BROCKMAN, F. J., KIEFT, T. L., PEACOCK, A. and WHITE, D. C. Deep gold mines of South Africa: windows into the subsurface biosphere. Optical Science, Engineering and Instrumentation'97, 1997. International Society for Optics and Photonics, 344-357.

OPARIN, A. 1924. Proiskhozhedenie Zhizni. *Mosckovskii Rabochii, Moscow. Reprinted and translated in Bernal JD (1967) The Origin of Life.* London, *Weidenfeld and Nicolson*.

OPPENHEIM, A. L. 1977. *Ancient Mesopotamia: Portrait Of A Dead Civilization*, Chicago, The University of Chicago Press.

ORGANIZATION, W. H. 2002. Global Solar UV Index: A practical guide: A joint recommendation of the World Health Organization. *World Meteorological Organization, United Nations Environment Programme, and the International Commission on Non-Ionizing Radiation Protection***,** 28.

OTT, U. 1988. Noble gases in SNC meteorites: Shergotty, Nakhla, Chassigny. *Geochimica et Cosmochimica Acta,* 52**,** 1937-1948.

PACE, N. R. 2001. The universal nature of biochemistry. *Proceedings of the National Academy of Sciences,* 98**,** 805-808.

PAÉIBO, S. 2012. Amplifying ancient DNA. *PCR protocols: a guide to methods and applications***,** 159.

PALVA, I. 1982. Molecular cloning of α-amylase gene from *Bacillus amyloliquefaciens* and its expression in *B. subtilis*. *Gene,* 19**,** 81-87.

PARK, J., VREELAND, R., CHO, B., LOWENSTEIN, T., TIMOFEEFF, M. and ROSENZWEIG, W. 2009. Haloarchaeal diversity in 23, 121 and 419 MYA salts. *Geobiology,* 7**,** 515-523.

PARKINSON, C. D., LIANG, M.-C., YUNG, Y. and KIRSCHVINK, J. 2014. Habitability of Enceladus: Planetary Conditions for Life. *LPI Contributions,* 1774**,** 4094.

PAUL, N. D. and GWYNN-JONES, D. 2003. Ecological roles of solar UV radiation: towards an integrated approach. *Trends in Ecology* and *Evolution,* 18**,** 48-55.

PAULINO-LIMA, I. G., PILLING, S., JANOT-PACHECO, E., DE BRITO, A. N., BARBOSA, J. A. R. G., LEITÃO, A. C. and LAGE, C. D. A. S. 2010. Laboratory simulation of interplanetary ultraviolet radiation (broad spectrum) and its effects on Deinococcus radiodurans. *Planetary and Space Science,* 58**,** 1180-1187.

PAVLOV, A., KALININ, V., KONSTANTINOV, A. and SHELEGEDIN, V. Radioresistant Bacteria Came From Mars? EGS General Assembly Conference Abstracts, 2002. 1110.

PAVLOV, A. K., KALININ, V. L., KONSTANTINOV, A. N., SHELEGEDIN, V. N. and PAVLOV, A. A. 2006. Was Earth ever infected by martian biota? Clues from radioresistant bacteria. *Astrobiology,* 6**,** 911-918.

PETERS, T., SIMON, J., JONES, J., USUI, T., MORIWAKI, R., ECONOMOS, R., SCHMITT, A. and MCKEEGAN, K. 2015. Tracking the source of the enriched Martian meteorites in olivine-hosted melt inclusions of two depleted shergottites, Yamato 980459 and Tissint. *Earth and Planetary Science Letters,* 418**,** 91-102.

PEUCKER-EHRENBRINK, B. and RAVIZZA, G. 2000. The effects of sampling artifacts on cosmic dust flux estimates: A reevaluation of nonvolatile tracers (Os, Ir). *Geochimica et Cosmochimica Acta,* 64**,** 1965-1970.

PHILLIPS, R. W., WIEGEL, J., BERRY, C. J., FLIERMANS, C., PEACOCK, A. D., WHITE, D. C. and SHIMKETS, L. J. 2002. Kineococcus radiotolerans sp. nov., a radiation-resistant, gram-positive bacterium. *International Journal of Systematic and Evolutionary Microbiology,* 52**,** 933-938.

PIDWIRNY, M. 2006. Fundamentals of physical geography. *Date Viewed,* 19**,** 2009.

PLANE, J. M. 2012. Cosmic dust in the earth's atmosphere. *Chemical Society Reviews,* 41**,** 6507-6518.

POGODA DE LA VEGA, U., RETTBERG, P., DOUKI, T., CADET, J. and HORNECK, G. 2005. Sensitivity to polychromatic UV-radiation of strains of *Deinococcus radiodurans* differing in their DNA repair capacity. *International Journal of Radiation Biology,* 81**,** 601-11.

POINAR, G. O. 1992. *Life in amber*, Stanford University Press.

PRICE, P. B. 2007. Microbial life in glacial ice and implications for a cold origin of life. *FEMS microbiology ecology,* 59**,** 217-231.

RASTOGI, G., OSMAN, S., KUKKADAPU, R., ENGELHARD, M., VAISHAMPAYAN, P. A., ANDERSEN, G. L. and SANI, R. K. 2010. Microbial and mineralogical

characterizations of soils collected from the deep biosphere of the former Homestake gold mine, South Dakota. *Microbial Ecology,* 60**,** 539-550.

RAUF, K., HANN, A., WICKRAMASINGHE, C. and DIGREGORIO, B. E. 2011. Microstructural investigation of the Carancas meteorite. *International Journal of Astrobiology,* 10**,** 105-112.

RETTBERG, P., ESCHWEILER, U., STRAUCH, K., REITZ, G., HORNECK, G., WÄNKE, H., BRACK, A. and BARBIER, B. 2002a. Survival of microorganisms in space protected by meteorite material: Results of the experiment 'EXOBIOLOGIE' of the PERSEUS mission. *Advances in Space Research,* 30**,** 1539-1545.

RETTBERG, P., ESCHWEILER, U., STRAUCH, K., REITZ, G., HORNECK, G., WÄNKE, H., BRACK, A. and BARBIER, B. 2002b. Survival of microorganisms in space protected by meteorite material: results of the experiment 'EXOBIOLOGIE'of the PERSEUS mission. *Advances in Space Research,* 30**,** 1539-1545.

RIVKINA, E., FRIEDMANN, E., MCKAY, C. and GILICHINSKY, D. 2000. Metabolic activity of permafrost bacteria below the freezing point. *Applied and Environmental Microbiology,* 66**,** 3230-3233.

ROBBINS, M. 1983. *The collector's book of fluorescent minerals*, New York, Van Nostrand Reinhold.

ROBBINS, M. 1994. *Fluorescence: Gems and Minerals Under Ultraviolet Light*, London, Geoscience Press.

ROSALES, D., VIDAL, E., ISHITSUKA, J. and BENAVENTE, S. Geomagnetic study of carancas meteorite and its crater. Lunar and Planetary Science Conference, 2008. 1744.

SAFFARY, R., NANDAKUMAR, R., SPENCER, D., ROBB, F. T., DAVILA, J. M., SWARTZ, M., OFMAN, L., THOMAS, R. J. and DIRUGGIERO, J. 2002. Microbial survival of space vacuum and extreme ultraviolet irradiation: strain isolation and analysis during a rocket flight. *FEMS microbiology letters,* 215**,** 163-168.

SAKO, Y., NAKAGAWA, S., TAKAI, K. and HORIKOSHI, K. 2003. *Marinithermus hydrothermalis* gen. nov., sp. nov., a strictly aerobic, thermophilic bacterium from a deep-sea hydrothermal vent chimney. *International Journal of Systematic and Evolutionary Microbiology,* 53**,** 59-65.

SANKARANARAYANAN, K., TIMOFEEFF, M. N., SPATHIS, R., LOWENSTEIN, T. K. and LUM, J. K. 2011. Ancient microbes from halite fluid inclusions: optimized surface sterilization and DNA extraction. *PloS One,* 6**,** e20683.

SANTOS, P., PINHAL, I., RAINEY, F. A., EMPADINHAS, N., COSTA, J., FIELDS, B., BENSON, R., VERÍSSIMO, A. and DA COSTA, M. S. 2003. Gamma-Proteobacteria *Aquicella lusitana* gen. nov., sp. nov., and A*quicella siphonis sp*. nov. Infect Protozoa and Require Activated Charcoal for Growth in Laboratory Media. *Applied and Environmental Microbiology,* 69**,** 6533-6540.

SATTERFIELD, C. L., LOWENSTEIN, T. K., VREELAND, R. H. and ROSENZWEIG, W. D. 2005. Paleobrine temperatures, chemistries, and paleoenvironments of Silurian Salina Formation F-1 Salt, Michigan Basin, USA, from petrography and fluid inclusions in halite. *Journal of Sedimentary Research,* 75**,** 534-546.

SCHOPF, J. W. 1993. Microfossils of the Early Archean Apex chert: new evidence of the antiquity of life. *Science,* 260**,** 640-646.

SCHRAMM, D. N. and WAGONER, R. V. 1977. Element production in the early universe. *Annual Review of Nuclear Science,* 27**,** 37-74.

SCHUBERT, B. A., LOWENSTEIN, T. K., TIMOFEEFF, M. N. and PARKER, M. A. 2010. Halophilic archaea cultured from ancient halite, Death Valley, California. *Environmental Microbiology,* 12**,** 440-454.

SCHWARTZ, M. 2001. The life and works of Louis Pasteur. *Journal of Applied Microbiology,* 91**,** 597-601.

SEARS, D. W. and KRAL, T. A. 1998. Martian "microfossils" in lunar meteorites? *Meteoritics and Planetary Science,* 33**,** 791-794.

SHIVAJI, S., CHATURVEDI, P., BEGUM, Z., PINDI, P. K., MANORAMA, R., PADMANABAN, D. A., SHOUCHE, Y. S., PAWAR, S., VAISHAMPAYAN, P. and DUTT, C. 2009. *Janibacter hoylei sp.* nov., *Bacillus isronensis sp*. nov. and *Bacillus aryabhattai sp*. nov., isolated from cryotubes used for collecting air from the upper atmosphere. *International journal of systematic and evolutionary microbiology,* 59**,** 2977-2986.

SHKLOVSKII, I. S. and SAGAN, C. 1966. Intelligent life in the universe. *Intelligent life in the universe by IS Shklovskii [and] Carl Sagan. Authorized translation by Paula Fern. San Francisco: Holden-Day, 1966*.

SIMEONOV, A. and MICHAELIAN, K. 2017. Properties of cyanobacterial UV-absorbing pigments suggest their evolution was driven by optimizing photon dissipation rather than photoprotection. *arXiv preprint arXiv:1702.03588*.

SLOBODKIN, A., GAVRILOV, S., IONOV, V. and ILIYIN, V. 2015. Spore-Forming Thermophilic Bacterium within Artificial Meteorite Survives Entry into the Earth's Atmosphere on FOTON-M4 Satellite Landing Module. *PloS One,* 10**,** e0132611.

SMIL, V. 2003. *The Earth's biosphere: Evolution, dynamics, and change*, MIT Press.

SMITH, D. and TEAM, E.-M. 2015. Predicting the Response of Terrestrial Contamination on Mars with Balloon Experiments in Earth's Stratosphere. *LPI Contributions,* 1845**,** 1009.

SMITH, D. J. 2013. Microbes in the upper atmosphere and unique opportunities for astrobiology research. *Astrobiology,* 13**,** 981-990.

SMITH, D. J., GRIFFIN, D. W. and SCHUERGER, A. C. 2010. Stratospheric microbiology at 20 km over the Pacific Ocean. *Aerobiologia,* 26**,** 35-46.

SMITH, D. J., THAKRAR, P. J., BHARRAT, A. E., DOKOS, A. G., KINNEY, T. L., JAMES, L. M., LANE, M. A., KHODADAD, C. L., MAGUIRE, F. and MALONEY, P. R. 2014. A Balloon-Based Payload for Exposing Microorganisms in the Stratosphere (E-MIST). *Gravitational and Space Research,* 2.

SOMMER, R., HAIDER, T., CABAJ, A., PRIBIL, W. and LHOTSKY, M. 1998. Time dose reciprocity in UV disinfection of water. *Water Science and Technology,* 38**,** 145-150.

STAPLIN, F. L. 1962. Microfossils from the Orgueil meteorite. *Micropaleontology***,** 343-347.

SUESS, H. E. and UREY, H. C. 1956. Abundances of the elements. *Reviews of Modern Physics,* 28**,** 53.

SULLIVAN, S. W. 2013. *Optical sensors for mapping temperature and winds in the thermosphere from a CubeSat platform. All Graduate Theses and Dissertations*. 1488.

TABATA, M., KAWAGUCHI, Y., YOKOBORI, S.-I., KAWAI, H., TAKAHASHI, J.-I., YANO, H. and YAMAGISHI, A. 2011. Tanpopo cosmic dust collector: silica aerogel production and bacterial DNA contamination analysis. *Biological Sciences in Space,* 25**,** 7-12.

TAN, W. and VANLANDINGHAM, S. 1967. Electron Microscopy of Biological-like Structures in the Orgueil Carbonaceous Meteorite. *Geophysical Journal of the Royal Astronomical Society,* 12**,** 237-237.

THOMAS-KEPRTA, K. L., CLEMETT, S. J., BAZYLINSKI, D. A., KIRSCHVINK, J. L., MCKAY, D. S., WENTWORTH, S. J., VALI, H., GIBSON, E. K., MCKAY, M. F. and ROMANEK, C. S. 2001. Truncated hexa-octahedral magnetite crystals in ALH84001: presumptive biosignatures. *Proceedings of the National Academy of Sciences,* 98**,** 2164-2169.

THOMAS-KEPRTA, K. L., CLEMETT, S. J., BAZYLINSKI, D. A., KIRSCHVINK, J. L., MCKAY, D. S., WENTWORTH, S. J., VALI, H., GIBSON JR, E. K. and ROMANEK, C. S. 2002.

Magnetofossils from ancient Mars: a robust biosignature in the Martian meteorite ALH84001. *Applied and Environmental Microbiology,* 68**,** 3663-3672.

TIAN, F., TOON, O. B., PAVLOV, A. A. and DE STERCK, H. 2005. A hydrogen-rich early Earth atmosphere. *Science,* 308**,** 1014-1017.

TIMMONS, D. E., FULTON, J. D. and MITCHELL, R. B. 1966. Microorganisms of the upper atmosphere I. Instrumentation for isokinetic air sampling at altitude. *Applied Microbiology,* 14**,** 229-231.

TIPLER, F. J. 2011. Fossils of cyanobacteria in CI1 carbonaceous meteorites. *Journal of Cosmology,* 13.

TORSVIK, V. and ØVREÅS, L. 2002. Microbial diversity and function in soil: from genes to ecosystems. *Current Opinion in Microbiology,* 5**,** 240-245.

TOSCA, N. J., KNOLL, A. H. and MCLENNAN, S. M. 2008. Water activity and the challenge for life on early Mars. *Science,* 320**,** 1204-1207.

TRODAHL, H. and BUCKLEY, R. 1990. Enhanced ultraviolet transmission of Antarctic sea ice during the austral spring. *Geophysical Research Letters,* 17**,** 2177-2179.

TUCHINDA, C., SRIVANNABOON, S. and LIM, H. W. 2006. Photoprotection by window glass, automobile glass, and sunglasses. *Journal of the American Academy of Dermatology,* 54**,** 845-854.

TURAKHIA, M. H. 1986. The influence of calcium on biofilm processes, *Doctoral dissertation*, Montana State University-Bozeman, College of Engineering.

VALTONEN, M., NURMI, P., ZHENG, J.-Q., CUCINOTTA, F. A., WILSON, J. W., HORNECK, G., LINDEGREN, L., MELOSH, J., RICKMAN, H. and MILEIKOWSKY, C. 2009. Natural transfer of viable microbes in space from planets in extra-solar systems to a planet in our solar system and vice versa. *The Astrophysical Journal,* 690**,** 210.

VAN DER HEIJDEN, M. G., BARDGETT, R. D. and VAN STRAALEN, N. M. 2008. The unseen majority: soil microbes as drivers of plant diversity and productivity in terrestrial ecosystems. *Ecology letters,* 11**,** 296-310.

VERNADSKY, V. I. 1998. *The biosphere*, New York, Springer.

VREELAND, R. H. and HUVAL, J. 1991. Phenotypic characterization of halophilic bacteria from ground water sources in the United States. *General and Applied Aspects of Halophilic Microorganisms.* Springer.

VREELAND, R. H., ROSENZWEIG, W. D. and POWERS, D. W. 2000. Isolation of a 250 million-year-old halotolerant bacterium from a primary salt crystal. *Nature,* 407**,** 897-900.

WAINWRIGHT, M. 2003. A Microbiologist looks at Panspermia. *Astrophysics and Space Science,* 285**,** 563-570.

WAINWRIGHT, M. 2008. The high cold biosphere--Microscope studies on the microbiology of the stratosphere. *In Focus-Proceedings of the Royal Microscopical Society***,** 33-41.

WAINWRIGHT, M., ALHARBI, S. and WICKRAMASINGHE, N. C. 2006. How do microorganisms reach the stratosphere? *International Journal of Astrobiology,* 5**,** 13.

WAINWRIGHT, M. and ALSHAMMARI, F. 2010. The Forgotten History of Panspermia and Theories of Life From Space. *Journal of Cosmology,* 7**,** 1771-1776.

WAINWRIGHT, M., LASWD, A. and ALSHAMMARI, F. 2009. Bacteria in amber coal and clay in relation to lithopanspermia. *International Journal of Astrobiology,* 8**,** 141-143.

WAINWRIGHT, M., ROSE, C., BAKER, A., WICKRAMASINGHE, N. and OMAIRI, T. 2015a. Biological Entities Isolated from Two Stratosphere Launches-Continued Evidence for a Space Origin. *Journal of Astrobiology* and *Outreach,* 3**,** 2332-2519.1000.

WAINWRIGHT, M., ROSE, C., OMAIRI, T., BAKER, A., WICKRAMASINGHE, C. and ALSHAMMARI, F. 2014. A Presumptive Fossilized Bacterial Biofilm Occurring in a Commercially Sourced Mars Meteorite. *Journal of Astrobiology* and *Outreach,* 2**,** 2332-2519.1000.

WAINWRIGHT, M., ROSE, C. E., BAKER, A. J., BRISTON, J. and WICKRAMASINGHE, C. 2013a. Allen Hills and Schopf-like putative fossilized bacteria seen in a new type of carbonaceous meteorite. *Journal of Cosmology,* 22**,** 10198-10205.

WAINWRIGHT, M., ROSE, C. E., BAKER, A. J., BRISTON, J. and WICKRAMASINGHE, N. C. 2013b. Typical Meteoritic Worm-Like Forms Seen in the Polonnaruwa Meteorite. *Journal of Cosmology,* 22**,** 10152-10157.

WAINWRIGHT, M., ROSE, C. E., BAKER, A. J., BRISTOW, K. and WICKRAMASINGHE, N. 2013c. Isolation of biological entities from the stratosphere (22–27km). *Journal of Cosmology,* 22**,** 10189-10196.

WAINWRIGHT, M., ROSE, C. E., BAKER, A. J., BRISTOW, K. and WICKRAMASINGHE, N. C. 2013d. Isolation of a diatom frustule fragment from the lower stratosphere (22–27Km)-Evidence for a cosmic origin. *Journal of Cosmology,* 22**,** 1063-1068.

WAINWRIGHT, M., ROSE, C. E., BAKER, A. J. and WICKRAMASINGHE, N. C. 2013e. Microspherules and Presumptive Biological Entities Found Inside the Polonnaruwa Meteorite. *Journal of Cosmology,* 22**,** 10197-10202.

WAINWRIGHT, M., WICKRAMASINGHE, N., HARRIS, M. and OMAIRI, T. 2015b. Masses Staining Positive for DNA-Isolated from the Stratosphere at a Height of 41 km. *Journal of Astrobiology* and *Outreach,* 3**,** 2332-2519.1000.

WAINWRIGHT, M., WICKRAMASINGHE, N., NARLIKAR, J., RAJARATNAM, P. and PERKINS, J. 2004. Confirmation of the presence of viable but non-cultureable bacteria in the stratosphere. *International Journal of Astrobiology,* 3**,** 13-15.

WAINWRIGHT, M., WICKRAMASINGHE, N. C., NARLIKAR, J. and RAJARATNAM, P. 2003. Microorganisms cultured from stratospheric air samples obtained at 41 km. *Federation of European Microbiological Societies,* 218**,** 161-165.

WALLIS, J., MIYAKE, N., HOOVER, R. B., OLDROYD, A., WALLIS, D. H., SAMARANAYAKE, A., WICKRAMARATHNE, K., WALLIS, M., GIBSON, C. H. and WICKRAMASINGHE, N. 2013. The Polonnaruwa meteorite: oxygen isotope, crystalline and biological composition. *arXiv preprint arXiv:1303.1845*.

WALLIS, M. K., WICKRAMASINGHE, J. and WICKRAMASINGHE, N. 2009. Mars polar cap: a habitat for elementary life. *International Journal of Astrobiology,* 8**,** 117-119.

WARNER, J. R., KNOPF, P. M. and RICH, A. 1963. A multiple ribosomal structure in protein synthesis. *Proceedings of the National Academy of Sciences of the United States of America,* 49**,** 122.

WASSMANN, M., MOELLER, R., RABBOW, E., PANITZ, C., HORNECK, G., REITZ, G., DOUKI, T., CADET, J., STAN-LOTTER, H. and COCKELL, C. S. 2012. Survival of spores of the UV-resistant *Bacillus subtilis* strain MW01 after exposure to low-Earth orbit and simulated martian conditions: data from the space experiment ADAPT on EXPOSE-E. *Astrobiology,* 12**,** 498-507.

WAYNE, R. P. 1991. Chemistry of atmospheres. *Chemistry of atmospheres.*Oxford*, Clarendon Press,* 460.

WEISBURG, W. G., BARNS, S. M., PELLETIER, D. A. and LANE, D. J. 1991. 16S ribosomal DNA amplification for phylogenetic study. *Journal of Bacteriology,* 173**,** 697-703.

WEISS, B. P., KIRSCHVINK, J. L., BAUDENBACHER, F. J., VALI, H., PETERS, N. T., MACDONALD, F. A. and WIKSWO, J. P. 2000. A low temperature transfer of ALH84001 from Mars to Earth. *Science,* 290**,** 791-795.

WELKER, N. and CAMPBELL, L. L. 1967. Unrelatedness of *Bacillus amyloliquefacien*s and *Bacillus subtilis*. *Journal of Bacteriology,* 94**,** 1124-1130.

WENTWORTH, S. and GOODING, J. Carbonates in the Martian meteorite, ALH 84001: water-borne but not like the SNCs. Lunar and Planetary Science Conference, 1995. 1489.

WHITMAN, W. B., COLEMAN, D. C. and WIEBE, W. J. 1998. Prokaryotes: the unseen majority. *Proceedings of the National Academy of Sciences,* 95**,** 6578-6583.

WICKRAMASINGHE, C. and WAINWRIGHT, M. 2015. Convergence to Cometary Panspermia: Time for Disclosure. *Journal of Astrobiology* and *Outreach,* 3**,** 2332-2519.1000145.

WICKRAMASINGHE, J., WICKRAMASINGHE, N. and WALLIS, M. 2009. Liquid water and organics in Comets: implications for exobiology. *International Journal of Astrobiology,* 8**,** 281-290.

WICKRAMASINGHE, N., SAMARANAYAKE, A., WICKRAMARATHNE, K., WALLIS, D., WALLIS, M., MIYAKE, N., COULSON, S., HOOVER, R., GIBSON, C. H. and WALLIS, J. 2013a. Living Diatoms in the Polonnaruwa meteorite–Possible link to red and yellow rain. *Journal of Cosmology,* 21**,** 9797-9804.

WICKRAMASINGHE, N., WALLIS, J. and WALLIS, D. 2013b. Panspermia: Evidence from Astronomy to Meteorites. *Modern Physics Letters A,* 28**,** 1330009.

WICKRAMASINGHE, N., WALLIS, J., WALLIS, D. and SAMARANAYAKE, A. 2013c. Fossil diatoms in a new carbonaceous meteorite. *Journal of Cosmology,* 21.

WICKRAMASINGHE, N., WALLIS, J., WALLIS, D., WALLIS, M., AL-MUFTI, S., WICKRAMASINGHE, J., SAMARANAYAKE, A. and WICKRAMARATHNE, K. 2013d. On the cometary origin of the Polonnaruwa meteorite. *Journal of Cosmology,* 21**,** 38.

WICKRAMASINGHE, N. C., WAINWRIGHT, M. and WALLIS, M. 2015. Rosetta images of Comet 67P/Churyumov–Gerasimenko 2. Prospects for cometary biology. *Journal of Astrobiology and Outreach*.

WILLERSLEV, E., HANSEN, A. J., RØNN, R., BRAND, T. B., BARNES, I., WIUF, C., GILICHINSKY, D., MITCHELL, D. and COOPER, A. 2004. Long-term persistence of bacterial DNA. *Current Biology,* 14**,** R9-R10.

WOESE, C. R. 1979. A proposal concerning the origin of life on the planet earth. *Journal of Molecular Evolution,* 13**,** 95-101.

WORTH, R. J., SIGURDSSON, S. and HOUSE, C. H. 2013. Seeding life on the moons of the outer planets via lithopanspermia. *Astrobiology,* 13**,** 1155-1165.

YAMAGAMI, T., SAITO, Y., MATSUZAKA, Y., NAMIKI, M., TORIUMI, M., YOKOTA, R., HIROSAWA, H. and MATSUSHIMA, K. 2004. Development of the highest altitude balloon. *Advances in Space Research,* 33**,** 1653-1659.

YANG, Y., ITAHASHI, S., YOKOBORI, S.-I. and YAMAGISHI, A. 2008a. UV-resistant bacteria isolated from upper troposphere and lower stratosphere. *Biological Sciences in Space,* 22**,** 7.

YANG, Y., YOKOBORI, S.-I., KAWAGUCHI, J., YAMAGAMI, T., IIJIMA, I., IZUTSU, N., FUKE, H., SAITOH, Y., MATSUZAKA, S. and NAMIKI, M. 2008b. Investigation of cultivable microorganisms in the stratosphere collected by using a balloon in 2005. *JAXA Research and Development Report***,** 35-42.

YANG, Y., YOKOBORI, S.-I. and YAMAGISHI, A. 2009. Assessing panspermia hypothesis by microorganisms collected from the high altitude atmosphere. *Biological Sciences in Space,* 23**,** 151-163.

YANO, H., YAMAGISHI, A., HASHIMOTO, H., YOKOBORI, S., KEBUKAWA, Y., KAWAGUCHI, Y., KOBAYASHI, K., YABUTA, H., TABATA, M. and HIGASHIDE, M. 2015. Tanpopo: A New Micrometeoroid Capture and Astrobiology Exposure in LEO: Its First Year Operation and Post-Flight Plan. *LPI Contributions,* 1856**,** 5395.

YOON, H. S., CINIGLIA, C., WU, M., COMERON, J. M., PINTO, G., POLLIO, A. and BHATTACHARYA, D. 2006. Establishment of endolithic populations of extremophilic Cyanidiales (Rhodophyta). *BMC Evolutionary Biology,* 6**,** 78.

ZIMMERMAN, W. B., ZANDI, M., HEMAKA BANDULASENA, H., TESAŘ, V., JAMES GILMOUR, D. and YING, K. 2011. Design of an airlift loop bioreactor and pilot scales studies with fluidic oscillator induced microbubbles for growth of a microalgae *Dunaliella salina. Applied Energy,* 88**,** 3357-3369.

7 APPENDICES

Appendix A

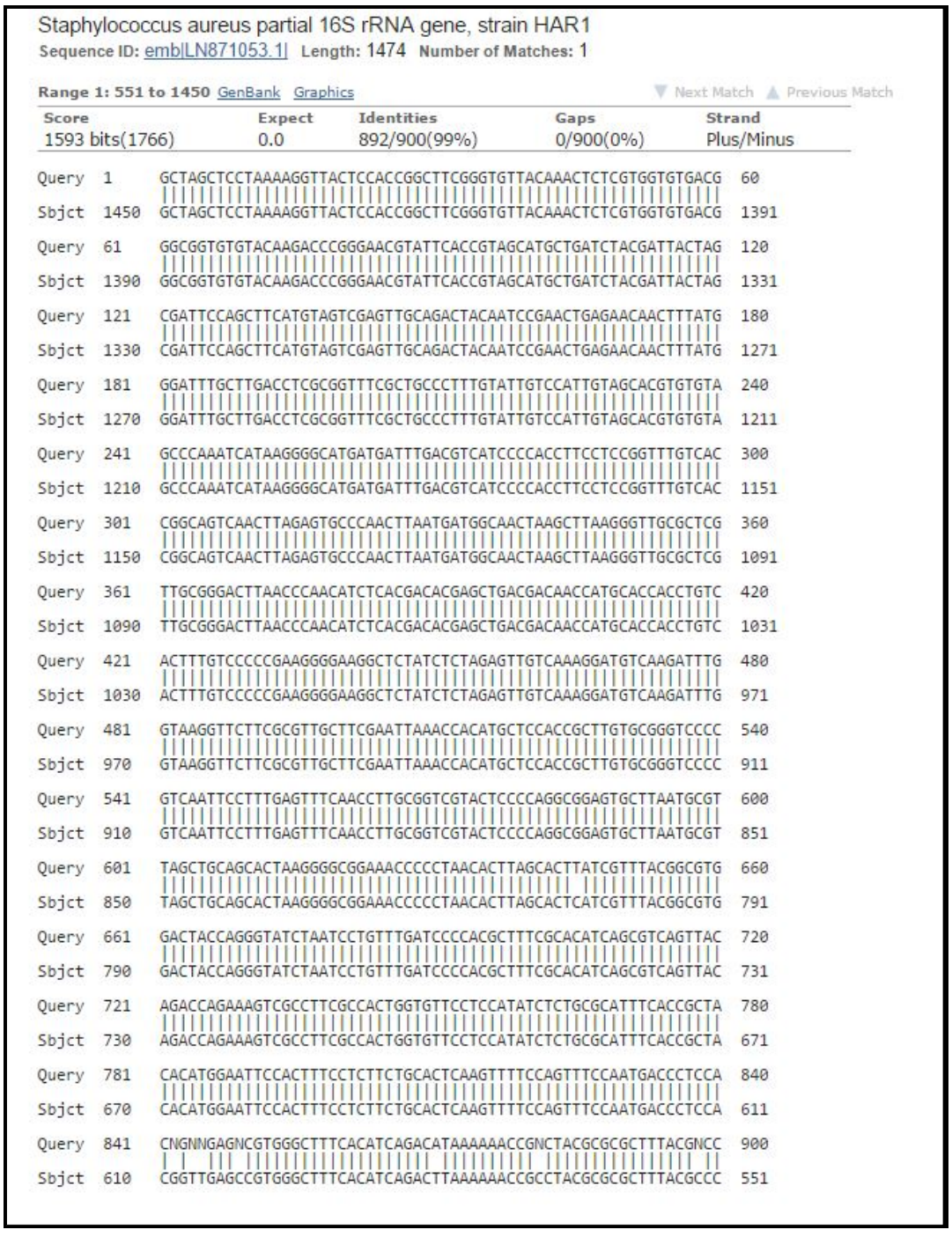

Staphylococcus aureus partial 16S rRNA gene, strain HAR1

Sequence ID: emb|LN871053.1| Length: 1474 Number of Matches: 1

Range 1: 551 to 1450 GenBank Graphics ▼ Next Match ▲ Previous Match

Score	Expect	Identities	Gaps	Strand
1593 bits(1766)	0.0	892/900(99%)	0/900(0%)	Plus/Minus

```
Query  1     GCTAGCTCCTAAAAGGTTACTCCACCGGCTTCGGGTGTTACAAACTCTCGTGGTGTGACG  60
             ||||||||||||||||||||||||||||||||||||||||||||||||||||||||||||
Sbjct  1450  GCTAGCTCCTAAAAGGTTACTCCACCGGCTTCGGGTGTTACAAACTCTCGTGGTGTGACG  1391

Query  61    GGCGGTGTGTACAAGACCCGGGAACGTATTCACCGTAGCATGCTGATCTACGATTACTAG  120
             ||||||||||||||||||||||||||||||||||||||||||||||||||||||||||||
Sbjct  1390  GGCGGTGTGTACAAGACCCGGGAACGTATTCACCGTAGCATGCTGATCTACGATTACTAG  1331

Query  121   CGATTCCAGCTTCATGTAGTCGAGTTGCAGACTACAATCCGAACTGAGAACAACTTTATG  180
             ||||||||||||||||||||||||||||||||||||||||||||||||||||||||||||
Sbjct  1330  CGATTCCAGCTTCATGTAGTCGAGTTGCAGACTACAATCCGAACTGAGAACAACTTTATG  1271

Query  181   GGATTTGCTTGACCTCGCGGTTTCGCTGCCCTTTGTATTGTCCATTGTAGCACGTGTGTA  240
             ||||||||||||||||||||||||||||||||||||||||||||||||||||||||||||
Sbjct  1270  GGATTTGCTTGACCTCGCGGTTTCGCTGCCCTTTGTATTGTCCATTGTAGCACGTGTGTA  1211

Query  241   GCCCAAATCATAAGGGGCATGATGATTTGACGTCATCCCCACCTTCCTCCGGTTTGTCAC  300
             ||||||||||||||||||||||||||||||||||||||||||||||||||||||||||||
Sbjct  1210  GCCCAAATCATAAGGGGCATGATGATTTGACGTCATCCCCACCTTCCTCCGGTTTGTCAC  1151

Query  301   CGGCAGTCAACTTAGAGTGCCCAACTTAATGATGGCAACTAAGCTTAAGGGTTGCGCTCG  360
             ||||||||||||||||||||||||||||||||||||||||||||||||||||||||||||
Sbjct  1150  CGGCAGTCAACTTAGAGTGCCCAACTTAATGATGGCAACTAAGCTTAAGGGTTGCGCTCG  1091

Query  361   TTGCGGGACTTAACCCAACATCTCACGACACGAGCTGACGACAACCATGCACCACCTGTC  420
             ||||||||||||||||||||||||||||||||||||||||||||||||||||||||||||
Sbjct  1090  TTGCGGGACTTAACCCAACATCTCACGACACGAGCTGACGACAACCATGCACCACCTGTC  1031

Query  421   ACTTTGTCCCCCGAAGGGGAAGGCTCTATCTCTAGAGTTGTCAAAGGATGTCAAGATTTG  480
             ||||||||||||||||||||||||||||||||||||||||||||||||||||||||||||
Sbjct  1030  ACTTTGTCCCCCGAAGGGGAAGGCTCTATCTCTAGAGTTGTCAAAGGATGTCAAGATTTG  971

Query  481   GTAAGGTTCTTCGCGTTGCTTCGAATTAAACCACATGCTCCACCGCTTGTGCGGGTCCCC  540
             ||||||||||||||||||||||||||||||||||||||||||||||||||||||||||||
Sbjct  970   GTAAGGTTCTTCGCGTTGCTTCGAATTAAACCACATGCTCCACCGCTTGTGCGGGTCCCC  911

Query  541   GTCAATTCCTTTGAGTTTCAACCTTGCGGTCGTACTCCCCAGGCGGAGTGCTTAATGCGT  600
             ||||||||||||||||||||||||||||||||||||||||||||||||||||||||||||
Sbjct  910   GTCAATTCCTTTGAGTTTCAACCTTGCGGTCGTACTCCCCAGGCGGAGTGCTTAATGCGT  851

Query  601   TAGCTGCAGCACTAAGGGGCGGAAACCCCCTAACACTTAGCACTTATCGTTTACGGCGTG  660
             |||||||||||||||||||||||||||||||||||||||||||||||||||||||||||||
Sbjct  850   TAGCTGCAGCACTAAGGGGCGGAAACCCCCTAACACTTAGCACTCATCGTTTACGGCGTG  791

Query  661   GACTACCAGGGTATCTAATCCTGTTTGATCCCCACGCTTTCGCACATCAGCGTCAGTTAC  720
             ||||||||||||||||||||||||||||||||||||||||||||||||||||||||||||
Sbjct  790   GACTACCAGGGTATCTAATCCTGTTTGATCCCCACGCTTTCGCACATCAGCGTCAGTTAC  731

Query  721   AGACCAGAAAGTCGCCTTCGCCACTGGTGTTCCTCCATATCTCTGCGCATTTCACCGCTA  780
             ||||||||||||||||||||||||||||||||||||||||||||||||||||||||||||
Sbjct  730   AGACCAGAAAGTCGCCTTCGCCACTGGTGTTCCTCCATATCTCTGCGCATTTCACCGCTA  671

Query  781   CACATGGAATTCCACTTTCCTCTTCTGCACTCAAGTTTTCCAGTTTCCAATGACCCTCCA  840
             ||||||||||||||||||||||||||||||||||||||||||||||||||||||||||||
Sbjct  670   CACATGGAATTCCACTTTCCTCTTCTGCACTCAAGTTTTCCAGTTTCCAATGACCCTCCA  611

Query  841   CNGNNGAGNCGTGGGCTTTCACATCAGACATAAAAAACCGNCTACGCGCGCTTTACGNCC  900
             | |  ||| |||||||||||||||||| |||||||||| |||||||||||||||| ||
Sbjct  610   CGGTTGAGCCGTGGGCTTTCACATCAGACTTAAAAAACCGCCTACGCGCGCTTTACGCCC  551
```

A1: The DNA sequence of the recovered bacterial sample (tube number 6), compared to *Staphylococcus aureus* strain, showing a 99% sequence similarity.

A2: Neighbor joining phylogenetic tree based on the 16S rRNA gene sequence, showing the phylogenetic relationship between the Fifth balloon's mission isolate (tube number 6) and other microorganisms, with a maximum sequence difference of 0.0007.

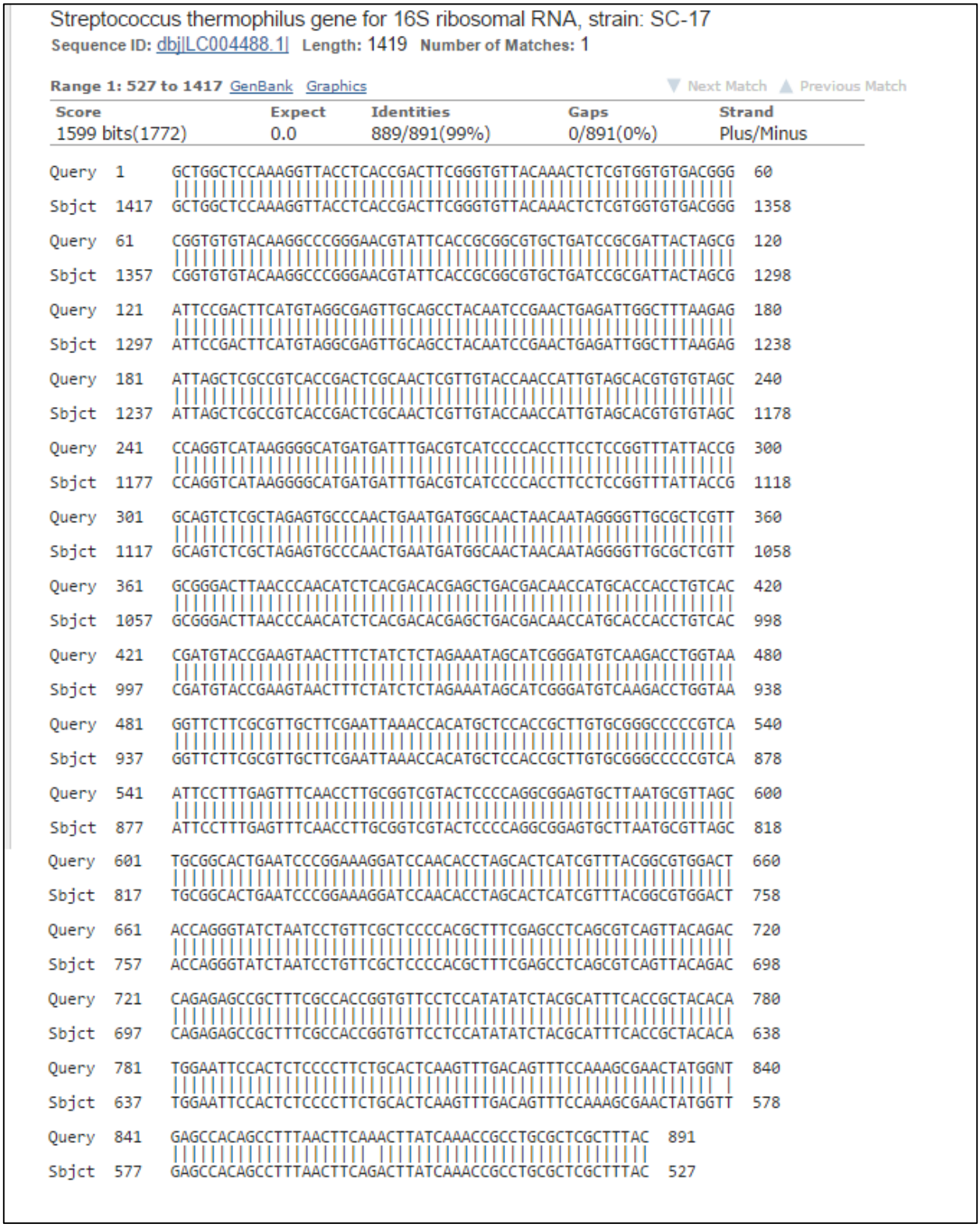

A3: The DNA sequence of the recovered bacterial sample (tube number 9), compared to *streptococcus thermophilus*, showing a 99% sequence similarity.

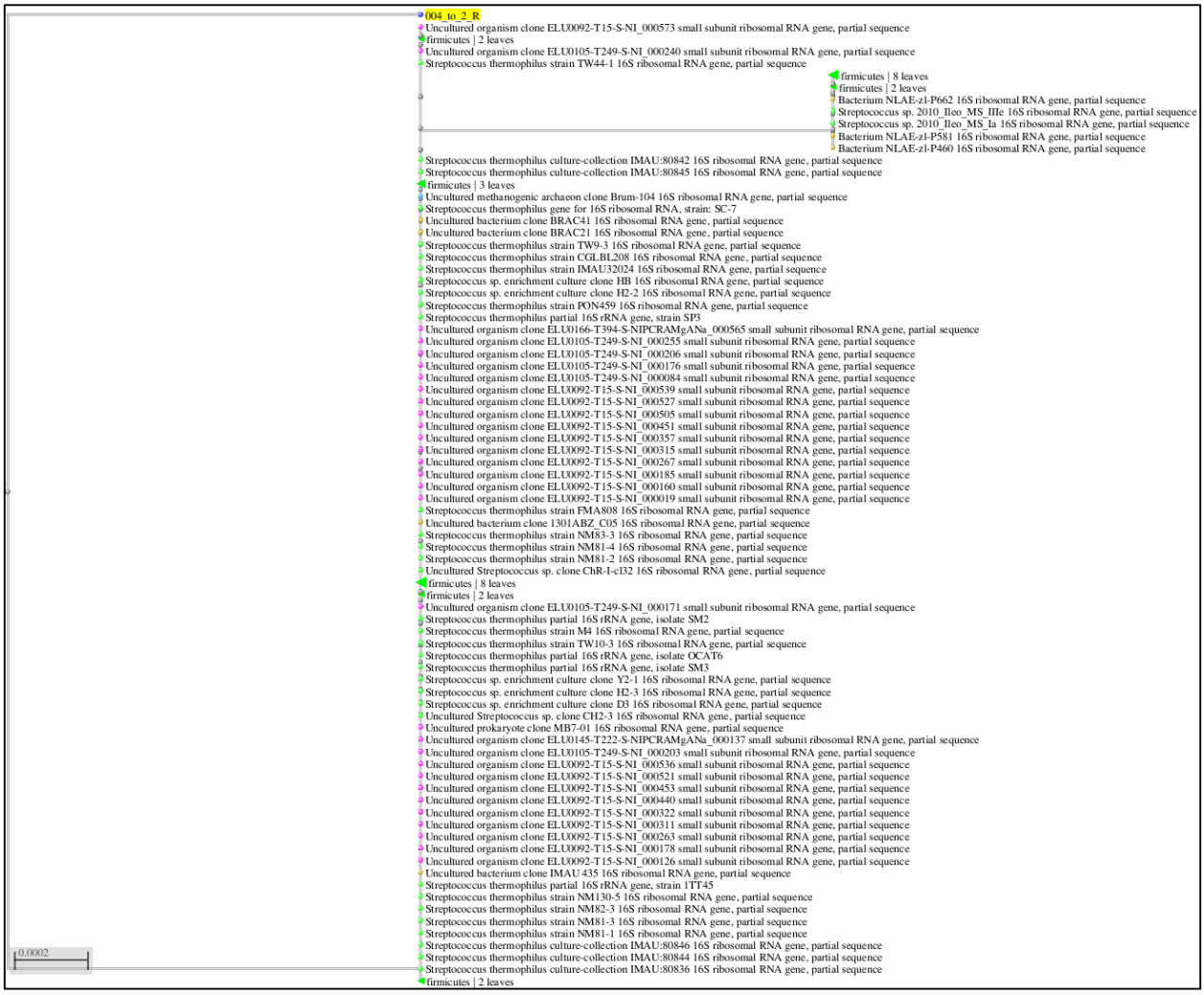

A4: Neighbour joining phylogenetic tree based on the 16S rRNA gene sequence, showing the phylogenetic relationship between the Fifth balloon's mission isolate (tube number 9) and other microorganisms, with a maximum sequence difference of 0.0002.

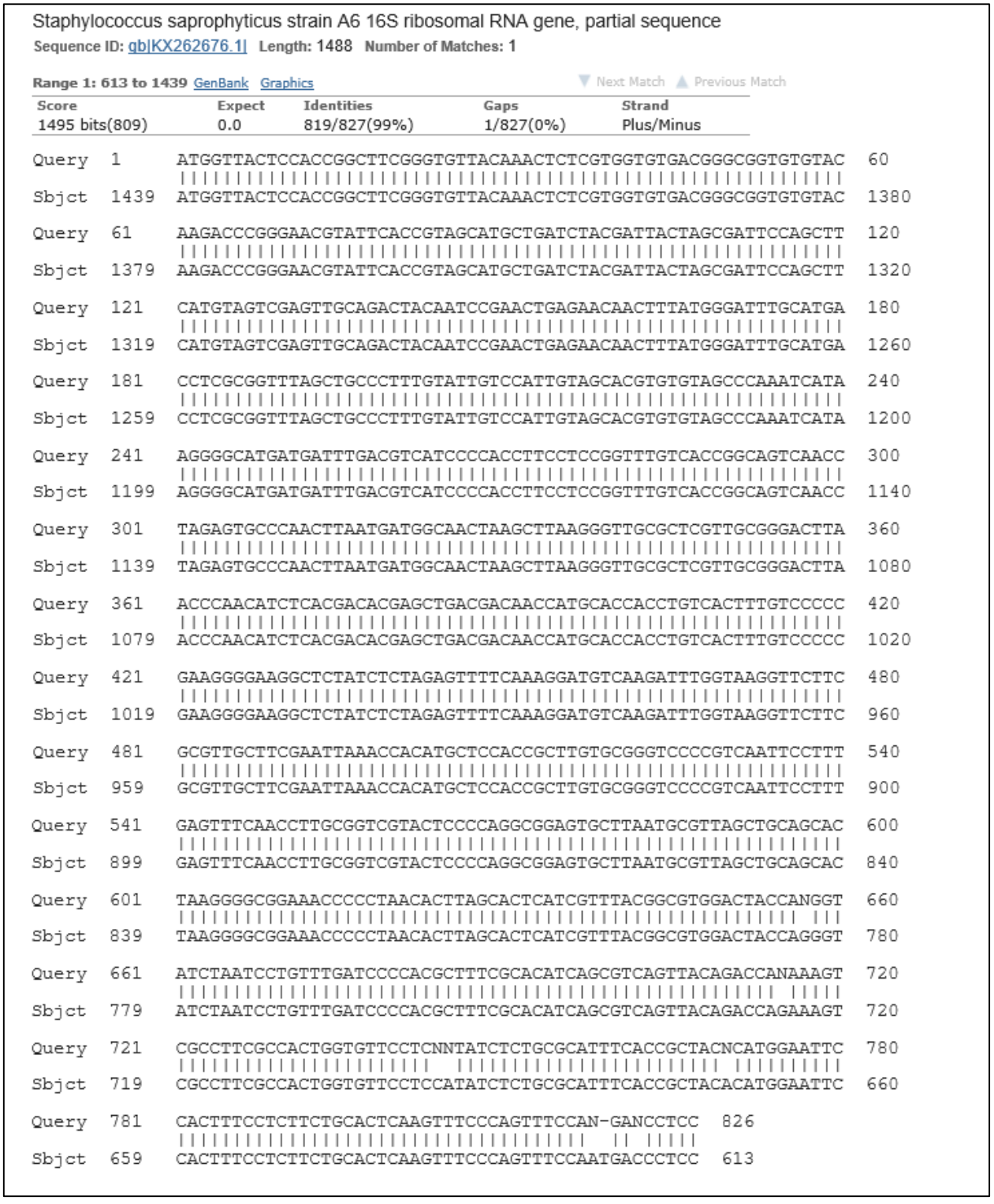

Staphylococcus saprophyticus strain A6 16S ribosomal RNA gene, partial sequence

Sequence ID: gb|KX262676.1| Length: 1488 Number of Matches: 1

Range 1: 613 to 1439 GenBank Graphics Next Match Previous Match

Score	Expect	Identities	Gaps	Strand
1495 bits(809)	0.0	819/827(99%)	1/827(0%)	Plus/Minus

```
Query  1     ATGGTTACTCCACCGGCTTCGGGTGTTACAAACTCTCGTGGTGTGACGGGCGGTGTGTAC  60
             ||||||||||||||||||||||||||||||||||||||||||||||||||||||||||||
Sbjct  1439  ATGGTTACTCCACCGGCTTCGGGTGTTACAAACTCTCGTGGTGTGACGGGCGGTGTGTAC  1380

Query  61    AAGACCCGGGAACGTATTCACCGTAGCATGCTGATCTACGATTACTAGCGATTCCAGCTT  120
             ||||||||||||||||||||||||||||||||||||||||||||||||||||||||||||
Sbjct  1379  AAGACCCGGGAACGTATTCACCGTAGCATGCTGATCTACGATTACTAGCGATTCCAGCTT  1320

Query  121   CATGTAGTCGAGTTGCAGACTACAATCCGAACTGAGAACAACTTTATGGGATTTGCATGA  180
             ||||||||||||||||||||||||||||||||||||||||||||||||||||||||||||
Sbjct  1319  CATGTAGTCGAGTTGCAGACTACAATCCGAACTGAGAACAACTTTATGGGATTTGCATGA  1260

Query  181   CCTCGCGGTTTAGCTGCCCTTTGTATTGTCCATTGTAGCACGTGTGTAGCCCAAATCATA  240
             ||||||||||||||||||||||||||||||||||||||||||||||||||||||||||||
Sbjct  1259  CCTCGCGGTTTAGCTGCCCTTTGTATTGTCCATTGTAGCACGTGTGTAGCCCAAATCATA  1200

Query  241   AGGGGCATGATGATTTGACGTCATCCCCACCTTCCTCCGGTTTGTCACCGGCAGTCAACC  300
             ||||||||||||||||||||||||||||||||||||||||||||||||||||||||||||
Sbjct  1199  AGGGGCATGATGATTTGACGTCATCCCCACCTTCCTCCGGTTTGTCACCGGCAGTCAACC  1140

Query  301   TAGAGTGCCCAACTTAATGATGGCAACTAAGCTTAAGGGTTGCGCTCGTTGCGGGACTTA  360
             ||||||||||||||||||||||||||||||||||||||||||||||||||||||||||||
Sbjct  1139  TAGAGTGCCCAACTTAATGATGGCAACTAAGCTTAAGGGTTGCGCTCGTTGCGGGACTTA  1080

Query  361   ACCCAACATCTCACGACACGAGCTGACGACAACCATGCACCACCTGTCACTTTGTCCCCC  420
             ||||||||||||||||||||||||||||||||||||||||||||||||||||||||||||
Sbjct  1079  ACCCAACATCTCACGACACGAGCTGACGACAACCATGCACCACCTGTCACTTTGTCCCCC  1020

Query  421   GAAGGGGAAGGCTCTATCTCTAGAGTTTTCAAAGGATGTCAAGATTTGGTAAGGTTCTTC  480
             ||||||||||||||||||||||||||||||||||||||||||||||||||||||||||||
Sbjct  1019  GAAGGGGAAGGCTCTATCTCTAGAGTTTTCAAAGGATGTCAAGATTTGGTAAGGTTCTTC  960

Query  481   GCGTTGCTTCGAATTAAACCACATGCTCCACCGCTTGTGCGGGTCCCCGTCAATTCCTTT  540
             ||||||||||||||||||||||||||||||||||||||||||||||||||||||||||||
Sbjct  959   GCGTTGCTTCGAATTAAACCACATGCTCCACCGCTTGTGCGGGTCCCCGTCAATTCCTTT  900

Query  541   GAGTTTCAACCTTGCGGTCGTACTCCCCAGGCGGAGTGCTTAATGCGTTAGCTGCAGCAC  600
             ||||||||||||||||||||||||||||||||||||||||||||||||||||||||||||
Sbjct  899   GAGTTTCAACCTTGCGGTCGTACTCCCCAGGCGGAGTGCTTAATGCGTTAGCTGCAGCAC  840

Query  601   TAAGGGGCGGAAACCCCCTAACACTTAGCACTCATCGTTTACGGCGTGGACTACCANGGT  660
             |||||||||||||||||||||||||||||||||||||||||||||||||||||||||| |||
Sbjct  839   TAAGGGGCGGAAACCCCCTAACACTTAGCACTCATCGTTTACGGCGTGGACTACCAGGGT  780

Query  661   ATCTAATCCTGTTTGATCCCCACGCTTTCGCACATCAGCGTCAGTTACAGACCANAAAGT  720
             |||||||||||||||||||||||||||||||||||||||||||||||||||||||| |||||
Sbjct  779   ATCTAATCCTGTTTGATCCCCACGCTTTCGCACATCAGCGTCAGTTACAGACCAGAAAGT  720

Query  721   CGCCTTCGCCACTGGTGTTCCTCNNTATCTCTGCGCATTTCACCGCTACNCATGGAATTC  780
             |||||||||||||||||||||||  |||||||||||||||||||||||| ||||||||||
Sbjct  719   CGCCTTCGCCACTGGTGTTCCTCCATATCTCTGCGCATTTCACCGCTACACATGGAATTC  660

Query  781   CACTTTCCTCTTCTGCACTCAAGTTTCCCAGTTTCCAN-GANCCTCC  826
             ||||||||||||||||||||||||||||||||||||||  || |||||
Sbjct  659   CACTTTCCTCTTCTGCACTCAAGTTTCCCAGTTTCCAATGACCCTCC  613
```

A5: The DNA sequence of the recovered bacterial sample (tube number 15), compared to *Staphylococcus saprophyticus*, showing a 99% sequence similarity.

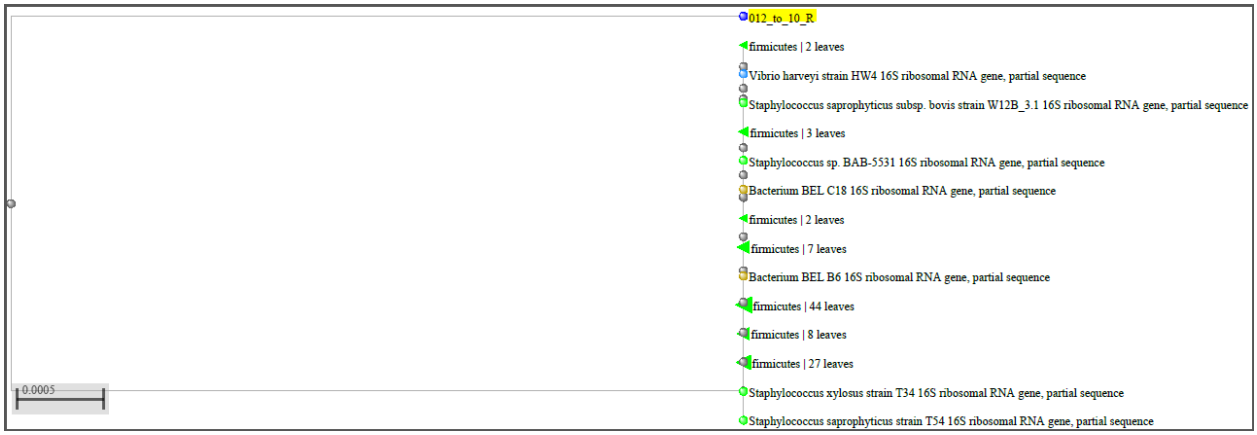

A6: Neighbour joining phylogenetic tree based on the 16S rRNA gene sequence, showing the phylogenetic relationship between the Fifth balloon's mission isolate (tube number 15) and other microorganisms, with a maximum sequence difference of 0.0005.

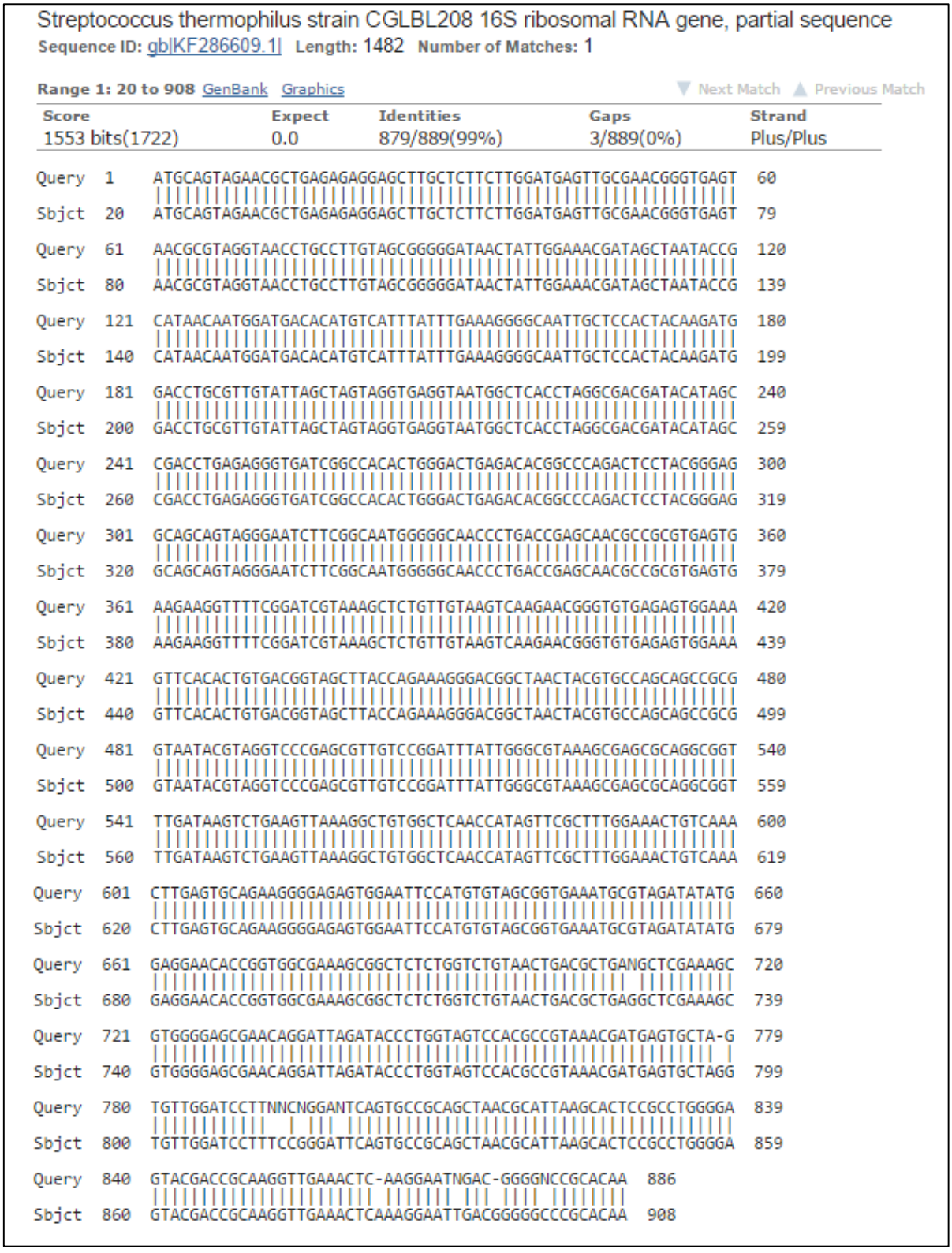

A7: The DNA sequence of the recovered bacterial sample (tube number 16), compared to *streptococcus thermophilus*, showing a 99% sequence similarity.

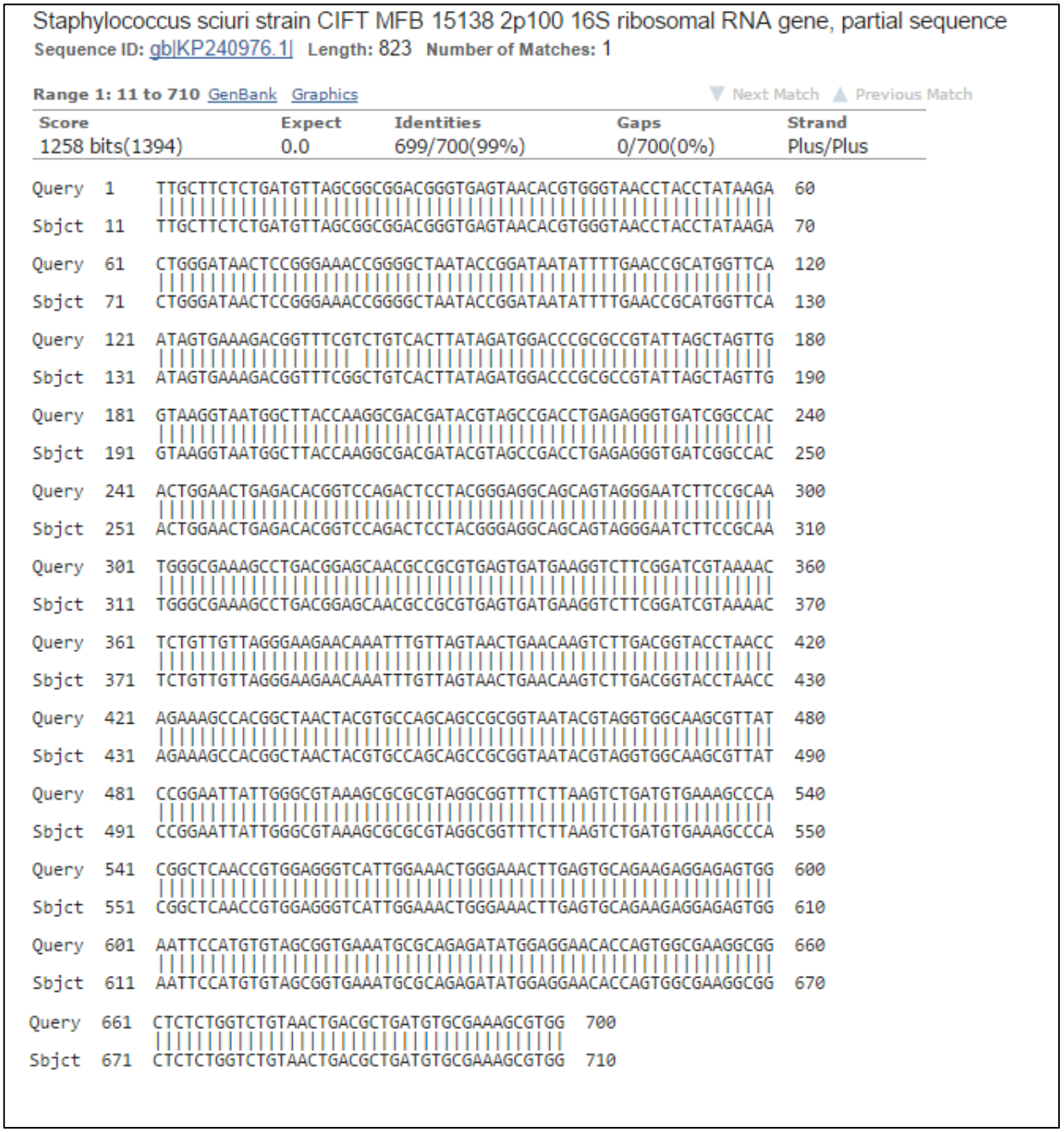

A8: The DNA sequence of the recovered bacterial sample (tube number 17), compared to *Staphylococcus sciuri*, showing a 99% sequence similarity.

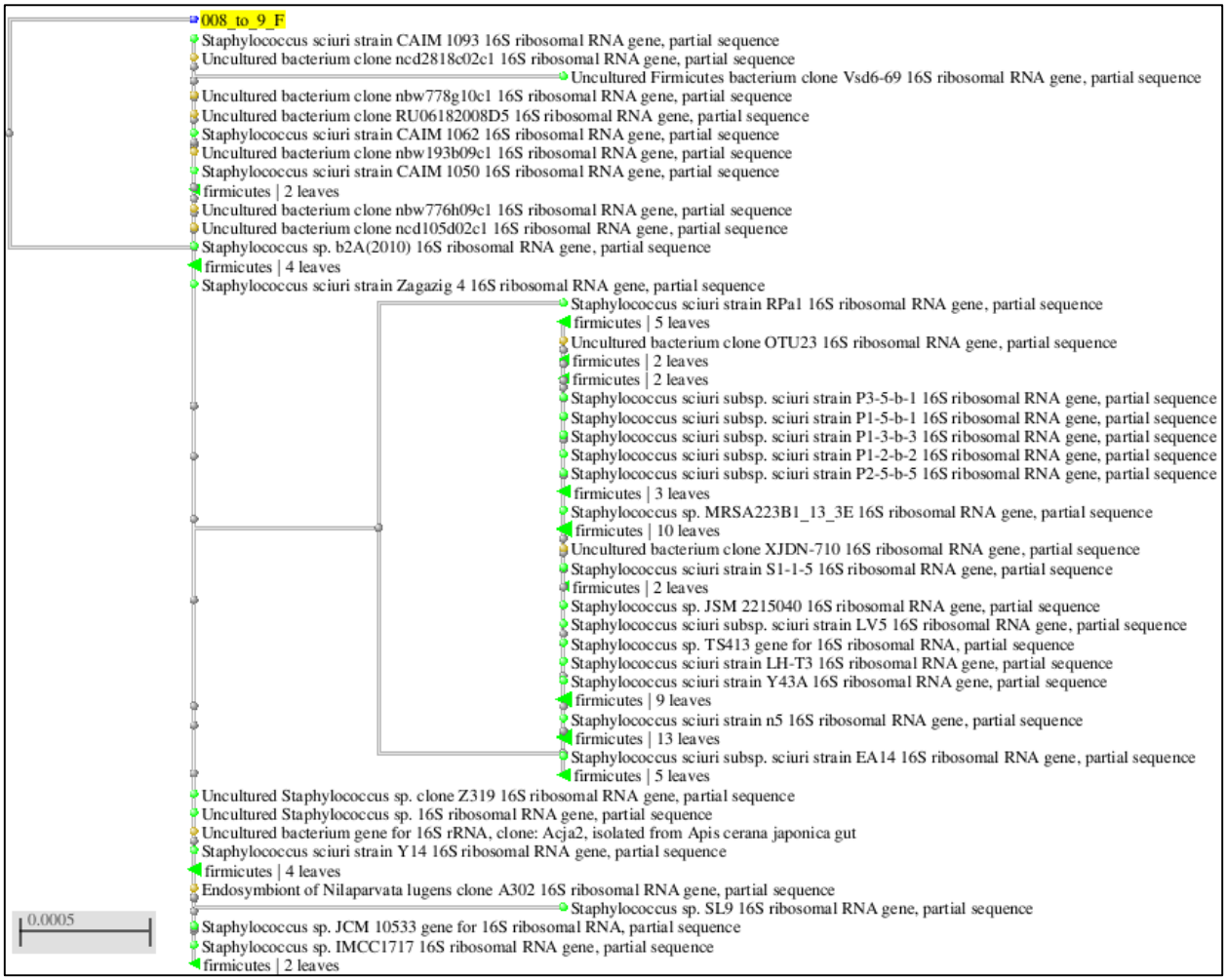

A9: Neighbour joining phylogenetic tree based on the 16S rRNA gene sequence, showing the phylogenetic relationship between the Fifth balloon's mission isolate (tube number 17) and other microorganisms, with a maximum sequence difference of 0.0005.

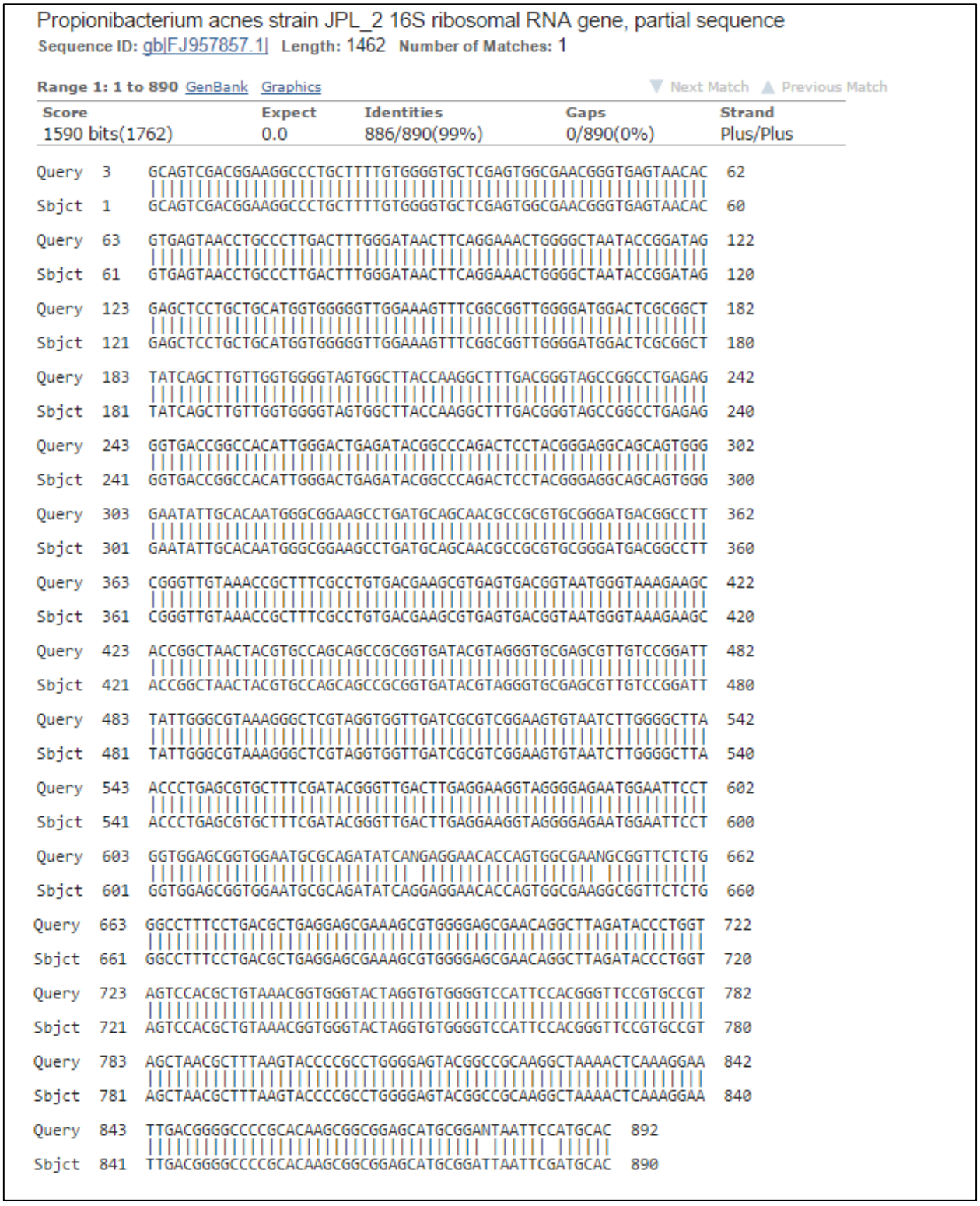

Propionibacterium acnes strain JPL_2 16S ribosomal RNA gene, partial sequence

Sequence ID: gb|FJ957857.1| Length: 1462 Number of Matches: 1

Range 1: 1 to 890 GenBank Graphics ▼ Next Match ▲ Previous Match

Score	Expect	Identities	Gaps	Strand
1590 bits(1762)	0.0	886/890(99%)	0/890(0%)	Plus/Plus

```
Query  3    GCAGTCGACGGAAGGCCCTGCTTTTGTGGGGTGCTCGAGTGGCGAACGGGTGAGTAACAC  62
            ||||||||||||||||||||||||||||||||||||||||||||||||||||||||||||||
Sbjct  1    GCAGTCGACGGAAGGCCCTGCTTTTGTGGGGTGCTCGAGTGGCGAACGGGTGAGTAACAC  60

Query  63   GTGAGTAACCTGCCCTTGACTTTGGGATAACTTCAGGAAACTGGGGCTAATACCGGATAG  122
            ||||||||||||||||||||||||||||||||||||||||||||||||||||||||||||||
Sbjct  61   GTGAGTAACCTGCCCTTGACTTTGGGATAACTTCAGGAAACTGGGGCTAATACCGGATAG  120

Query  123  GAGCTCCTGCTGCATGGTGGGGGTTGGAAAGTTTCGGCGGTTGGGGATGGACTCGCGGCT  182
            ||||||||||||||||||||||||||||||||||||||||||||||||||||||||||||||
Sbjct  121  GAGCTCCTGCTGCATGGTGGGGGTTGGAAAGTTTCGGCGGTTGGGGATGGACTCGCGGCT  180

Query  183  TATCAGCTTGTTGGTGGGGTAGTGGCTTACCAAGGCTTTGACGGGTAGCCGGCCTGAGAG  242
            ||||||||||||||||||||||||||||||||||||||||||||||||||||||||||||||
Sbjct  181  TATCAGCTTGTTGGTGGGGTAGTGGCTTACCAAGGCTTTGACGGGTAGCCGGCCTGAGAG  240

Query  243  GGTGACCGGCCACATTGGGACTGAGATACGGCCCAGACTCCTACGGGAGGCAGCAGTGGG  302
            ||||||||||||||||||||||||||||||||||||||||||||||||||||||||||||||
Sbjct  241  GGTGACCGGCCACATTGGGACTGAGATACGGCCCAGACTCCTACGGGAGGCAGCAGTGGG  300

Query  303  GAATATTGCACAATGGGCGGAAGCCTGATGCAGCAACGCCGCGTGCGGGATGACGGCCTT  362
            ||||||||||||||||||||||||||||||||||||||||||||||||||||||||||||||
Sbjct  301  GAATATTGCACAATGGGCGGAAGCCTGATGCAGCAACGCCGCGTGCGGGATGACGGCCTT  360

Query  363  CGGGTTGTAAACCGCTTTCGCCTGTGACGAAGCGTGAGTGACGGTAATGGGTAAAGAAGC  422
            ||||||||||||||||||||||||||||||||||||||||||||||||||||||||||||||
Sbjct  361  CGGGTTGTAAACCGCTTTCGCCTGTGACGAAGCGTGAGTGACGGTAATGGGTAAAGAAGC  420

Query  423  ACCGGCTAACTACGTGCCAGCAGCCGCGGTGATACGTAGGGTGCGAGCGTTGTCCGGATT  482
            ||||||||||||||||||||||||||||||||||||||||||||||||||||||||||||||
Sbjct  421  ACCGGCTAACTACGTGCCAGCAGCCGCGGTGATACGTAGGGTGCGAGCGTTGTCCGGATT  480

Query  483  TATTGGGCGTAAAGGGCTCGTAGGTGGTTGATCGCGTCGGAAGTGTAATCTTGGGGCTTA  542
            ||||||||||||||||||||||||||||||||||||||||||||||||||||||||||||||
Sbjct  481  TATTGGGCGTAAAGGGCTCGTAGGTGGTTGATCGCGTCGGAAGTGTAATCTTGGGGCTTA  540

Query  543  ACCCTGAGCGTGCTTTCGATACGGGTTGACTTGAGGAAGGTAGGGGAGAATGGAATTCCT  602
            ||||||||||||||||||||||||||||||||||||||||||||||||||||||||||||||
Sbjct  541  ACCCTGAGCGTGCTTTCGATACGGGTTGACTTGAGGAAGGTAGGGGAGAATGGAATTCCT  600

Query  603  GGTGGAGCGGTGGAATGCGCAGATATCANGAGGAACACCAGTGGCGAANGCGGTTCTCTG  662
            |||||||||||||||||||||||||||| |||||||||||||||||| ||||||||||||
Sbjct  601  GGTGGAGCGGTGGAATGCGCAGATATCAGGAGGAACACCAGTGGCGAAGGCGGTTCTCTG  660

Query  663  GGCCTTTCCTGACGCTGAGGAGCGAAAGCGTGGGGAGCGAACAGGCTTAGATACCCTGGT  722
            ||||||||||||||||||||||||||||||||||||||||||||||||||||||||||||||
Sbjct  661  GGCCTTTCCTGACGCTGAGGAGCGAAAGCGTGGGGAGCGAACAGGCTTAGATACCCTGGT  720

Query  723  AGTCCACGCTGTAAACGGTGGGTACTAGGTGTGGGGTCCATTCCACGGGTTCCGTGCCGT  782
            ||||||||||||||||||||||||||||||||||||||||||||||||||||||||||||||
Sbjct  721  AGTCCACGCTGTAAACGGTGGGTACTAGGTGTGGGGTCCATTCCACGGGTTCCGTGCCGT  780

Query  783  AGCTAACGCTTTAAGTACCCCGCCTGGGGAGTACGGCCGCAAGGCTAAAACTCAAAGGAA  842
            ||||||||||||||||||||||||||||||||||||||||||||||||||||||||||||||
Sbjct  781  AGCTAACGCTTTAAGTACCCCGCCTGGGGAGTACGGCCGCAAGGCTAAAACTCAAAGGAA  840

Query  843  TTGACGGGGCCCCGCACAAGCGGCGGAGCATGCGGANTAATTCCATGCAC  892
            |||||||||||||||||||||||||||||||||| |||||| ||||||
Sbjct  841  TTGACGGGGCCCCGCACAAGCGGCGGAGCATGCGGATTAATTCGATGCAC  890
```

A10: The DNA sequence of the recovered bacterial sample (tube number 18), compared to *Propionibacterium acnes*, showing a 99% sequence similarity.

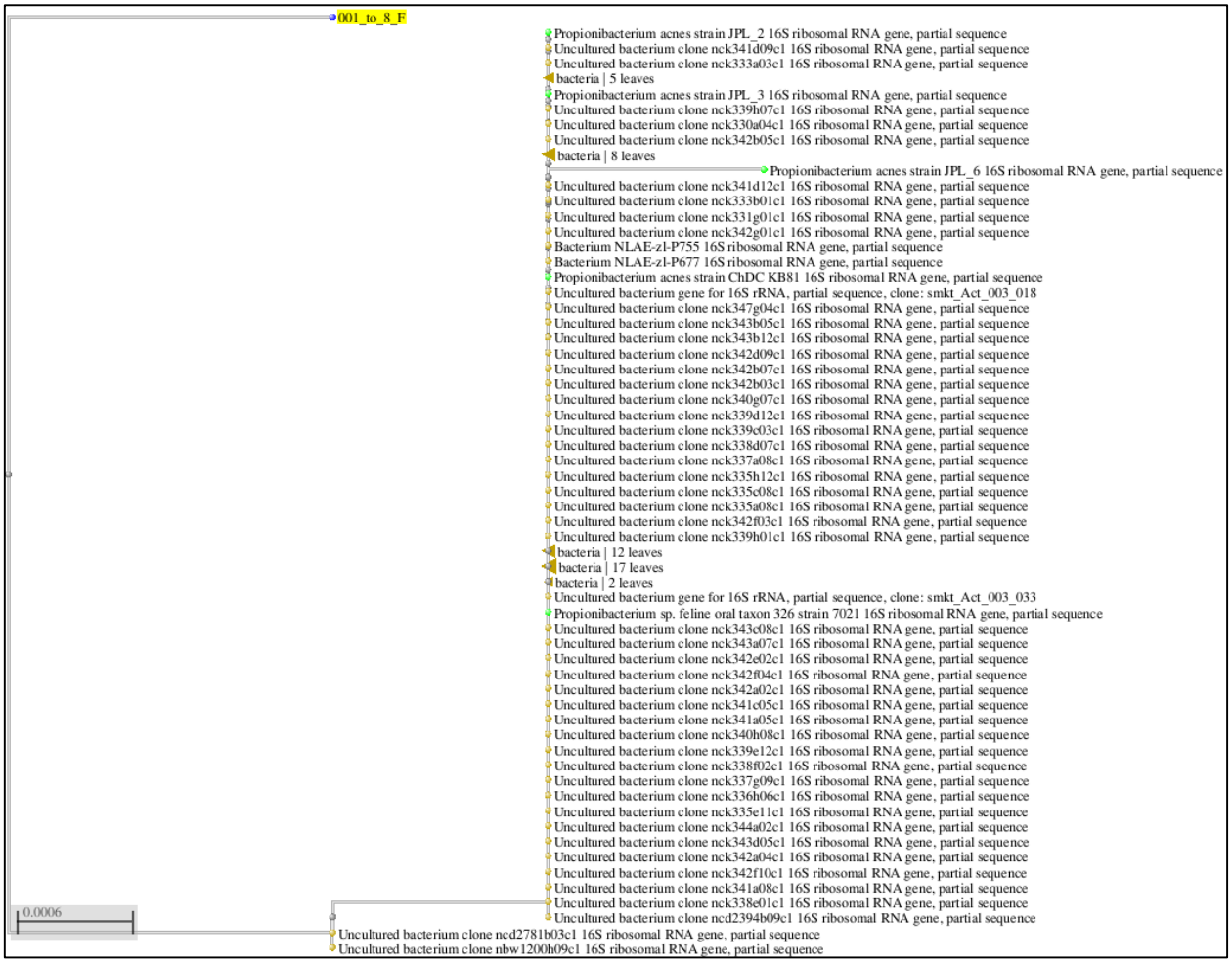

A11: Neighbour joining phylogenetic tree based on the 16S rRNA gene sequence, showing the phylogenetic relationship between the Fifth balloon's mission isolate (tube number 18) and other microorganisms, with a maximum sequence difference of 0.0006.

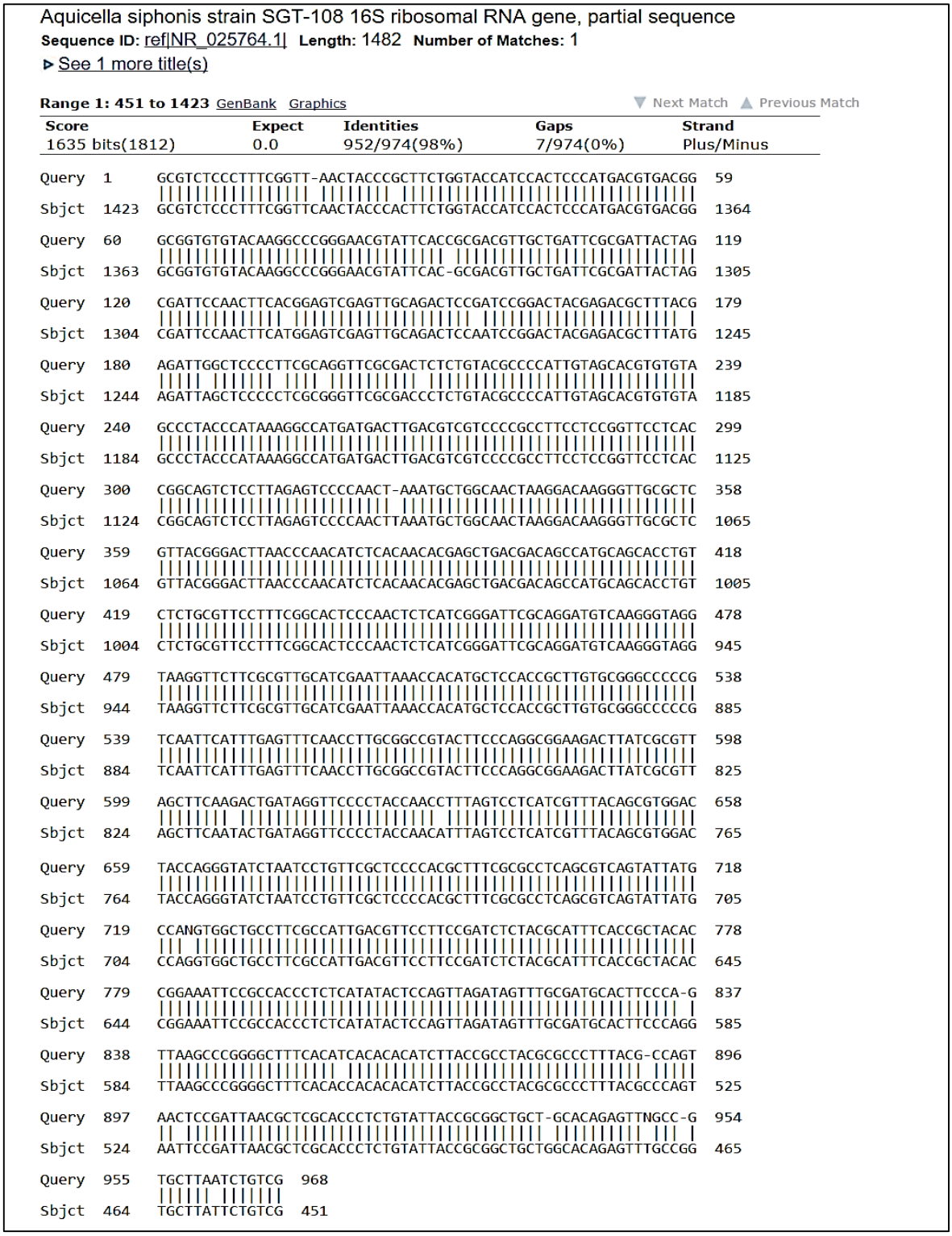

A12: The DNA sequence of the recovered bacterial sample (tube number 23), compared to *Aquicella siphonis* (Sequence ID: ref|NR_025764.1|) strain, showing a 98% sequence similarity.

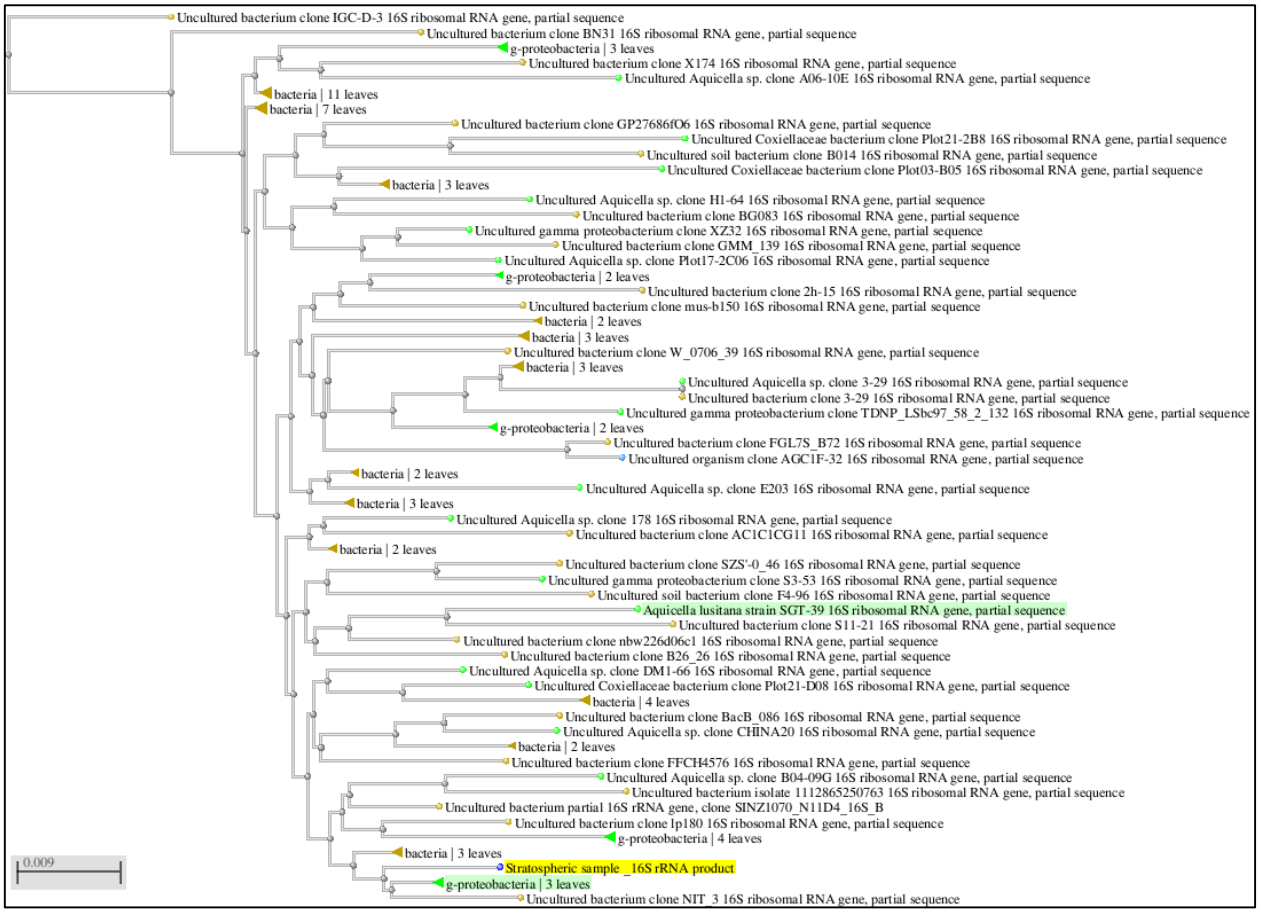

A13: Neighbour joining phylogenetic tree based on the 16S rRNA gene sequence, showing the phylogenetic relationship between our balloon's isolate (tube number 23) and other microorganisms, with a maximum sequence difference of 0.009.

Appendix B

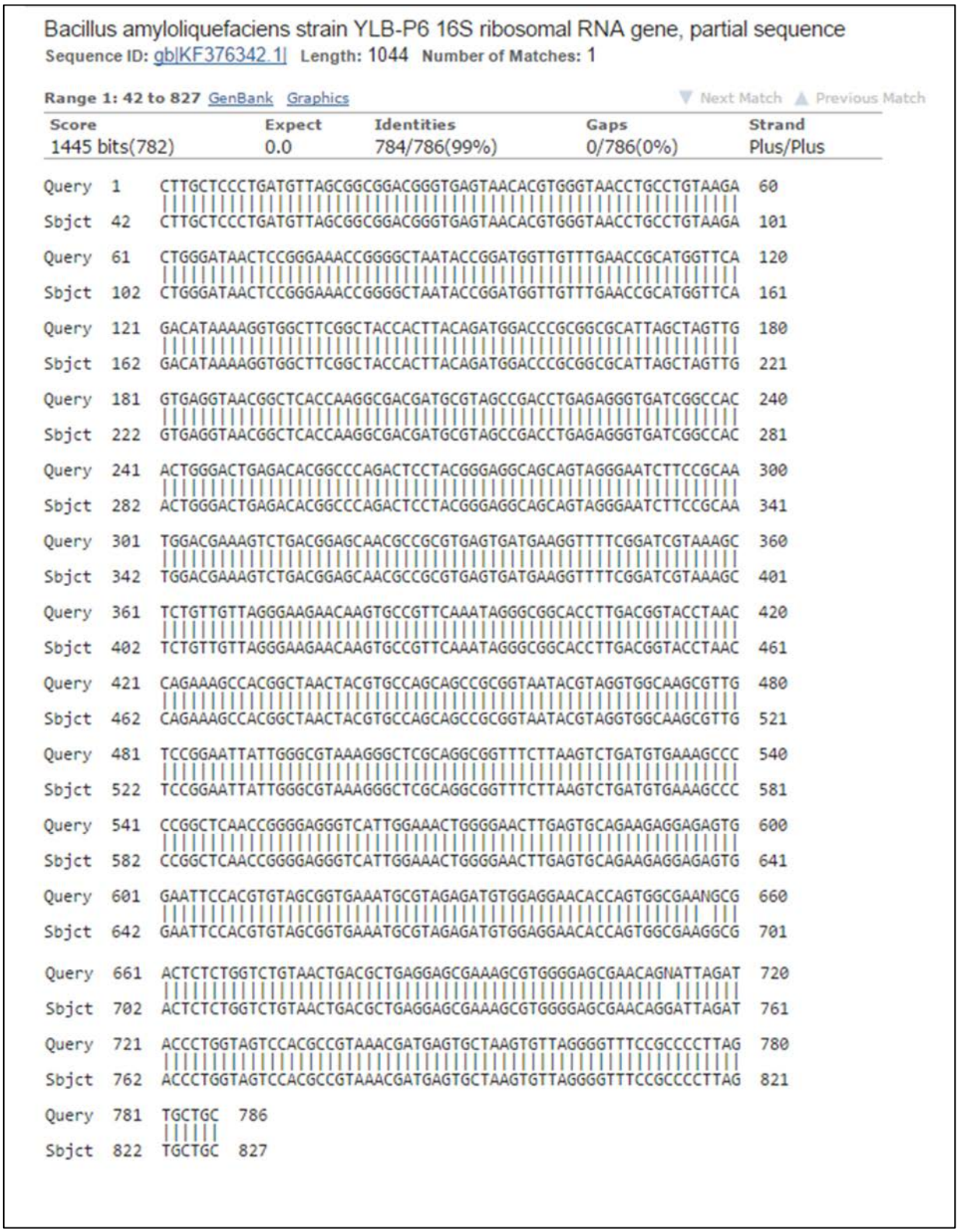

Bacillus amyloliquefaciens strain YLB-P6 16S ribosomal RNA gene, partial sequence

Sequence ID: gb|KF376342.1| Length: 1044 Number of Matches: 1

Range 1: 42 to 827 GenBank Graphics Next Match Previous Match

Score	Expect	Identities	Gaps	Strand
1445 bits(782)	0.0	784/786(99%)	0/786(0%)	Plus/Plus

```
Query  1    CTTGCTCCCTGATGTTAGCGGCGGACGGGTGAGTAACACGTGGGTAACCTGCCTGTAAGA  60
            ||||||||||||||||||||||||||||||||||||||||||||||||||||||||||||
Sbjct  42   CTTGCTCCCTGATGTTAGCGGCGGACGGGTGAGTAACACGTGGGTAACCTGCCTGTAAGA  101

Query  61   CTGGGATAACTCCGGGAAACCGGGGCTAATACCGGATGGTTGTTTGAACCGCATGGTTCA  120
            ||||||||||||||||||||||||||||||||||||||||||||||||||||||||||||
Sbjct  102  CTGGGATAACTCCGGGAAACCGGGGCTAATACCGGATGGTTGTTTGAACCGCATGGTTCA  161

Query  121  GACATAAAAGGTGGCTTCGGCTACCACTTACAGATGGACCCGCGGCGCATTAGCTAGTTG  180
            ||||||||||||||||||||||||||||||||||||||||||||||||||||||||||||
Sbjct  162  GACATAAAAGGTGGCTTCGGCTACCACTTACAGATGGACCCGCGGCGCATTAGCTAGTTG  221

Query  181  GTGAGGTAACGGCTCACCAAGGCGACGATGCGTAGCCGACCTGAGAGGGTGATCGGCCAC  240
            ||||||||||||||||||||||||||||||||||||||||||||||||||||||||||||
Sbjct  222  GTGAGGTAACGGCTCACCAAGGCGACGATGCGTAGCCGACCTGAGAGGGTGATCGGCCAC  281

Query  241  ACTGGGACTGAGACACGGCCCAGACTCCTACGGGAGGCAGCAGTAGGGAATCTTCCGCAA  300
            ||||||||||||||||||||||||||||||||||||||||||||||||||||||||||||
Sbjct  282  ACTGGGACTGAGACACGGCCCAGACTCCTACGGGAGGCAGCAGTAGGGAATCTTCCGCAA  341

Query  301  TGGACGAAAGTCTGACGGAGCAACGCCGCGTGAGTGATGAAGGTTTTCGGATCGTAAAGC  360
            ||||||||||||||||||||||||||||||||||||||||||||||||||||||||||||
Sbjct  342  TGGACGAAAGTCTGACGGAGCAACGCCGCGTGAGTGATGAAGGTTTTCGGATCGTAAAGC  401

Query  361  TCTGTTGTTAGGGAAGAACAAGTGCCGTTCAAATAGGGCGGCACCTTGACGGTACCTAAC  420
            ||||||||||||||||||||||||||||||||||||||||||||||||||||||||||||
Sbjct  402  TCTGTTGTTAGGGAAGAACAAGTGCCGTTCAAATAGGGCGGCACCTTGACGGTACCTAAC  461

Query  421  CAGAAAGCCACGGCTAACTACGTGCCAGCAGCCGCGGTAATACGTAGGTGGCAAGCGTTG  480
            ||||||||||||||||||||||||||||||||||||||||||||||||||||||||||||
Sbjct  462  CAGAAAGCCACGGCTAACTACGTGCCAGCAGCCGCGGTAATACGTAGGTGGCAAGCGTTG  521

Query  481  TCCGGAATTATTGGGCGTAAAGGGCTCGCAGGCGGTTTCTTAAGTCTGATGTGAAAGCCC  540
            ||||||||||||||||||||||||||||||||||||||||||||||||||||||||||||
Sbjct  522  TCCGGAATTATTGGGCGTAAAGGGCTCGCAGGCGGTTTCTTAAGTCTGATGTGAAAGCCC  581

Query  541  CCGGCTCAACCGGGGAGGGTCATTGGAAACTGGGGAACTTGAGTGCAGAAGAGGAGAGTG  600
            ||||||||||||||||||||||||||||||||||||||||||||||||||||||||||||
Sbjct  582  CCGGCTCAACCGGGGAGGGTCATTGGAAACTGGGGAACTTGAGTGCAGAAGAGGAGAGTG  641

Query  601  GAATTCCACGTGTAGCGGTGAAATGCGTAGAGATGTGGAGGAACACCAGTGGCGAANGCG  660
            ||||||||||||||||||||||||||||||||||||||||||||||||||||||||| |||
Sbjct  642  GAATTCCACGTGTAGCGGTGAAATGCGTAGAGATGTGGAGGAACACCAGTGGCGAAGGCG  701

Query  661  ACTCTCTGGTCTGTAACTGACGCTGAGGAGCGAAAGCGTGGGGAGCGAACAGNATTAGAT  720
            |||||||||||||||||||||||||||||||||||||||||||||||||||| |||||||
Sbjct  702  ACTCTCTGGTCTGTAACTGACGCTGAGGAGCGAAAGCGTGGGGAGCGAACAGGATTAGAT  761

Query  721  ACCCTGGTAGTCCACGCCGTAAACGATGAGTGCTAAGTGTTAGGGGTTTCCGCCCCTTAG  780
            ||||||||||||||||||||||||||||||||||||||||||||||||||||||||||||
Sbjct  762  ACCCTGGTAGTCCACGCCGTAAACGATGAGTGCTAAGTGTTAGGGGTTTCCGCCCCTTAG  821

Query  781  TGCTGC  786
            ||||||
Sbjct  822  TGCTGC  827
```

B1: The DNA sequence of the halite recovered bacterial sample, compared to Bacillus amyloliquefaciens (Sequence ID: gb|KF376342.1|) strain, showing a 99% sequence similarity.

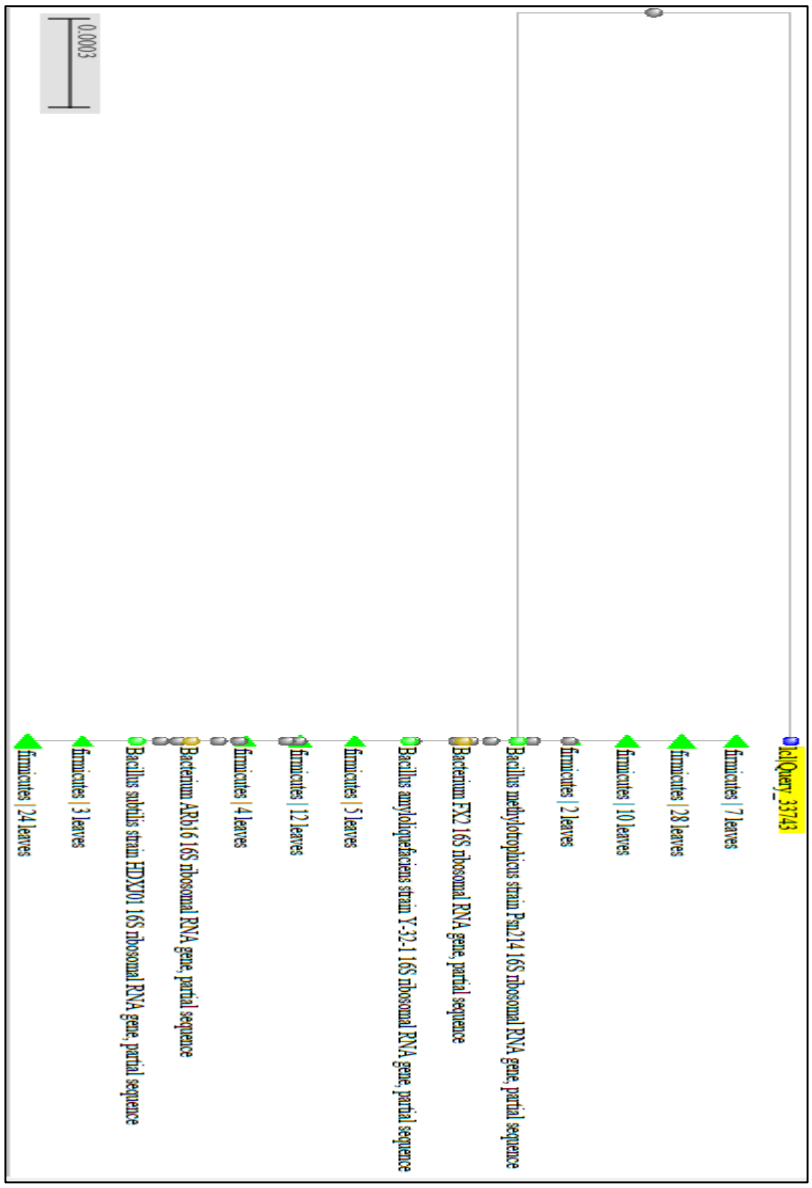

B2: Neighbour joining phylogenetic tree based on the 16S rRNA gene sequence, showing the phylogenetic relationship between our halite isolate and other microorganisms, with a maximum sequence difference of 0.003.

Appendix C

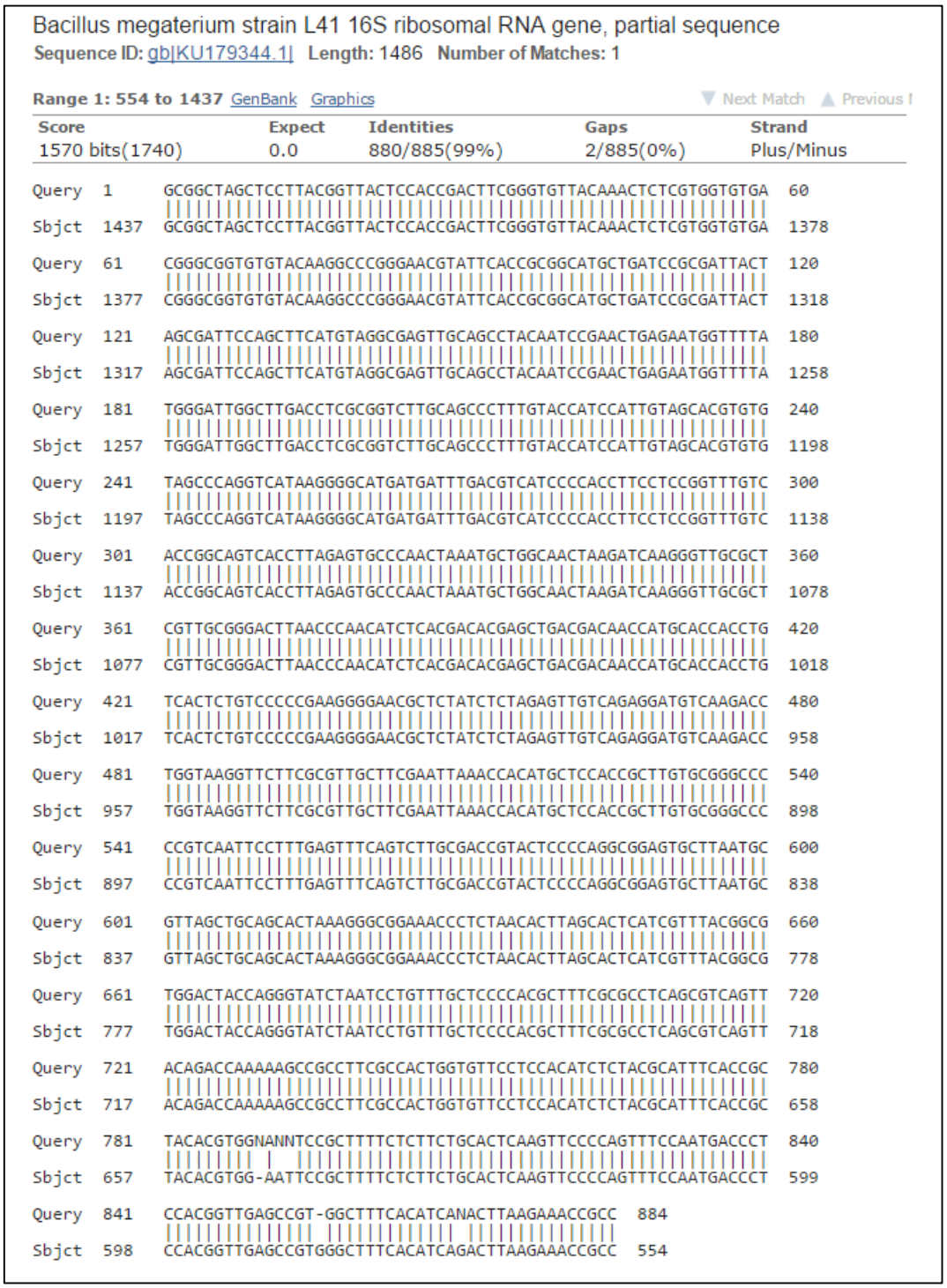

Bacillus megaterium strain L41 16S ribosomal RNA gene, partial sequence

Sequence ID: gb|KU179344.1| Length: 1486 Number of Matches: 1

Range 1: 554 to 1437 GenBank Graphics Next Match Previous I

Score	Expect	Identities	Gaps	Strand
1570 bits(1740)	0.0	880/885(99%)	2/885(0%)	Plus/Minus

```
Query  1     GCGGCTAGCTCCTTACGGTTACTCCACCGACTTCGGGTGTTACAAACTCTCGTGGTGTGA  60
             ||||||||||||||||||||||||||||||||||||||||||||||||||||||||||||
Sbjct  1437  GCGGCTAGCTCCTTACGGTTACTCCACCGACTTCGGGTGTTACAAACTCTCGTGGTGTGA  1378

Query  61    CGGGCGGTGTGTACAAGGCCCGGGAACGTATTCACCGCGGCATGCTGATCCGCGATTACT  120
             ||||||||||||||||||||||||||||||||||||||||||||||||||||||||||||
Sbjct  1377  CGGGCGGTGTGTACAAGGCCCGGGAACGTATTCACCGCGGCATGCTGATCCGCGATTACT  1318

Query  121   AGCGATTCCAGCTTCATGTAGGCGAGTTGCAGCCTACAATCCGAACTGAGAATGGTTTTA  180
             ||||||||||||||||||||||||||||||||||||||||||||||||||||||||||||
Sbjct  1317  AGCGATTCCAGCTTCATGTAGGCGAGTTGCAGCCTACAATCCGAACTGAGAATGGTTTTA  1258

Query  181   TGGGATTGGCTTGACCTCGCGGTCTTGCAGCCCTTTGTACCATCCATTGTAGCACGTGTG  240
             ||||||||||||||||||||||||||||||||||||||||||||||||||||||||||||
Sbjct  1257  TGGGATTGGCTTGACCTCGCGGTCTTGCAGCCCTTTGTACCATCCATTGTAGCACGTGTG  1198

Query  241   TAGCCCAGGTCATAAGGGGCATGATGATTTGACGTCATCCCCACCTTCCTCCGGTTTGTC  300
             ||||||||||||||||||||||||||||||||||||||||||||||||||||||||||||
Sbjct  1197  TAGCCCAGGTCATAAGGGGCATGATGATTTGACGTCATCCCCACCTTCCTCCGGTTTGTC  1138

Query  301   ACCGGCAGTCACCTTAGAGTGCCCAACTAAATGCTGGCAACTAAGATCAAGGGTTGCGCT  360
             ||||||||||||||||||||||||||||||||||||||||||||||||||||||||||||
Sbjct  1137  ACCGGCAGTCACCTTAGAGTGCCCAACTAAATGCTGGCAACTAAGATCAAGGGTTGCGCT  1078

Query  361   CGTTGCGGGACTTAACCCAACATCTCACGACACGAGCTGACGACAACCATGCACCACCTG  420
             ||||||||||||||||||||||||||||||||||||||||||||||||||||||||||||
Sbjct  1077  CGTTGCGGGACTTAACCCAACATCTCACGACACGAGCTGACGACAACCATGCACCACCTG  1018

Query  421   TCACTCTGTCCCCCGAAGGGGAACGCTCTATCTCTAGAGTTGTCAGAGGATGTCAAGACC  480
             ||||||||||||||||||||||||||||||||||||||||||||||||||||||||||||
Sbjct  1017  TCACTCTGTCCCCCGAAGGGGAACGCTCTATCTCTAGAGTTGTCAGAGGATGTCAAGACC  958

Query  481   TGGTAAGGTTCTTCGCGTTGCTTCGAATTAAACCACATGCTCCACCGCTTGTGCGGGCCC  540
             ||||||||||||||||||||||||||||||||||||||||||||||||||||||||||||
Sbjct  957   TGGTAAGGTTCTTCGCGTTGCTTCGAATTAAACCACATGCTCCACCGCTTGTGCGGGCCC  898

Query  541   CCGTCAATTCCTTTGAGTTTCAGTCTTGCGACCGTACTCCCCAGGCGGAGTGCTTAATGC  600
             ||||||||||||||||||||||||||||||||||||||||||||||||||||||||||||
Sbjct  897   CCGTCAATTCCTTTGAGTTTCAGTCTTGCGACCGTACTCCCCAGGCGGAGTGCTTAATGC  838

Query  601   GTTAGCTGCAGCACTAAAGGGCGGAAACCCTCTAACACTTAGCACTCATCGTTTACGGCG  660
             ||||||||||||||||||||||||||||||||||||||||||||||||||||||||||||
Sbjct  837   GTTAGCTGCAGCACTAAAGGGCGGAAACCCTCTAACACTTAGCACTCATCGTTTACGGCG  778

Query  661   TGGACTACCAGGGTATCTAATCCTGTTTGCTCCCCACGCTTTCGCGCCTCAGCGTCAGTT  720
             ||||||||||||||||||||||||||||||||||||||||||||||||||||||||||||
Sbjct  777   TGGACTACCAGGGTATCTAATCCTGTTTGCTCCCCACGCTTTCGCGCCTCAGCGTCAGTT  718

Query  721   ACAGACCAAAAAGCCGCCTTCGCCACTGGTGTTCCTCCACATCTCTACGCATTTCACCGC  780
             ||||||||||||||||||||||||||||||||||||||||||||||||||||||||||||
Sbjct  717   ACAGACCAAAAAGCCGCCTTCGCCACTGGTGTTCCTCCACATCTCTACGCATTTCACCGC  658

Query  781   TACACGTGGNANNTCCGCTTTTCTCTTCTGCACTCAAGTTCCCCAGTTTCCAATGACCCT  840
             ||||||||| |  ||||||||||||||||||||||||||||||||||||||||||||||
Sbjct  657   TACACGTGG-AATTCCGCTTTTCTCTTCTGCACTCAAGTTCCCCAGTTTCCAATGACCCT  599

Query  841   CCACGGTTGAGCCGT-GGCTTTCACATCANACTTAAGAAACCGCC  884
             ||||||||||||||| |||||||||||| ||||||||||||||||
Sbjct  598   CCACGGTTGAGCCGTGGGCTTTCACATCAGACTTAAGAAACCGCC  554
```

C1: The DNA sequence of the Carancas recovered sample, compared to Bacillus megaterium (Sequence ID: gb|KU179344.1|) strain, showing a 99% sequence similarity.

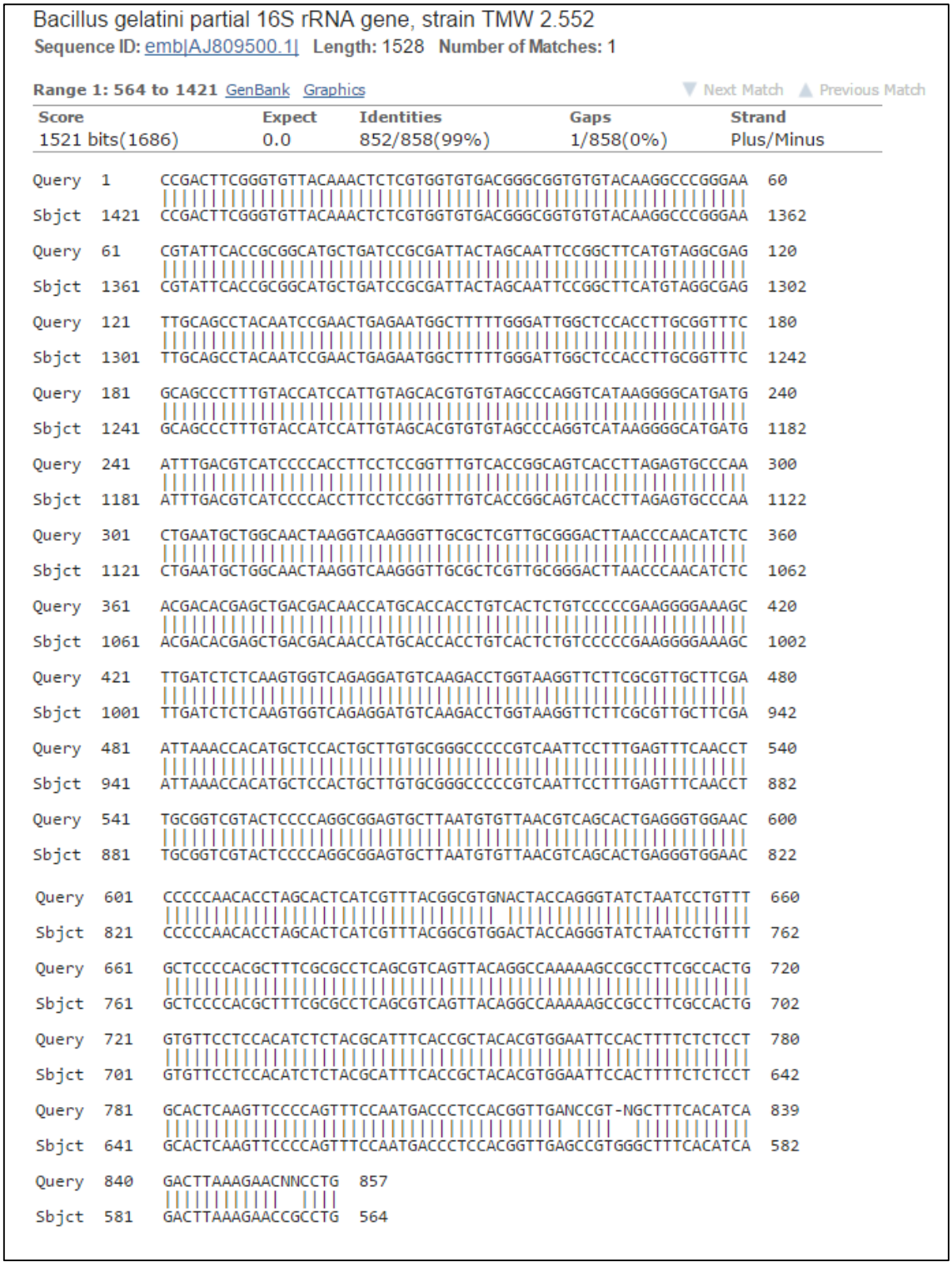

C2: The DNA sequence of the halite recovered sample, compared to Bacillus gelatini (Sequence ID: emb|AJ809500.1|) strain, showing a 99% sequence similarity.

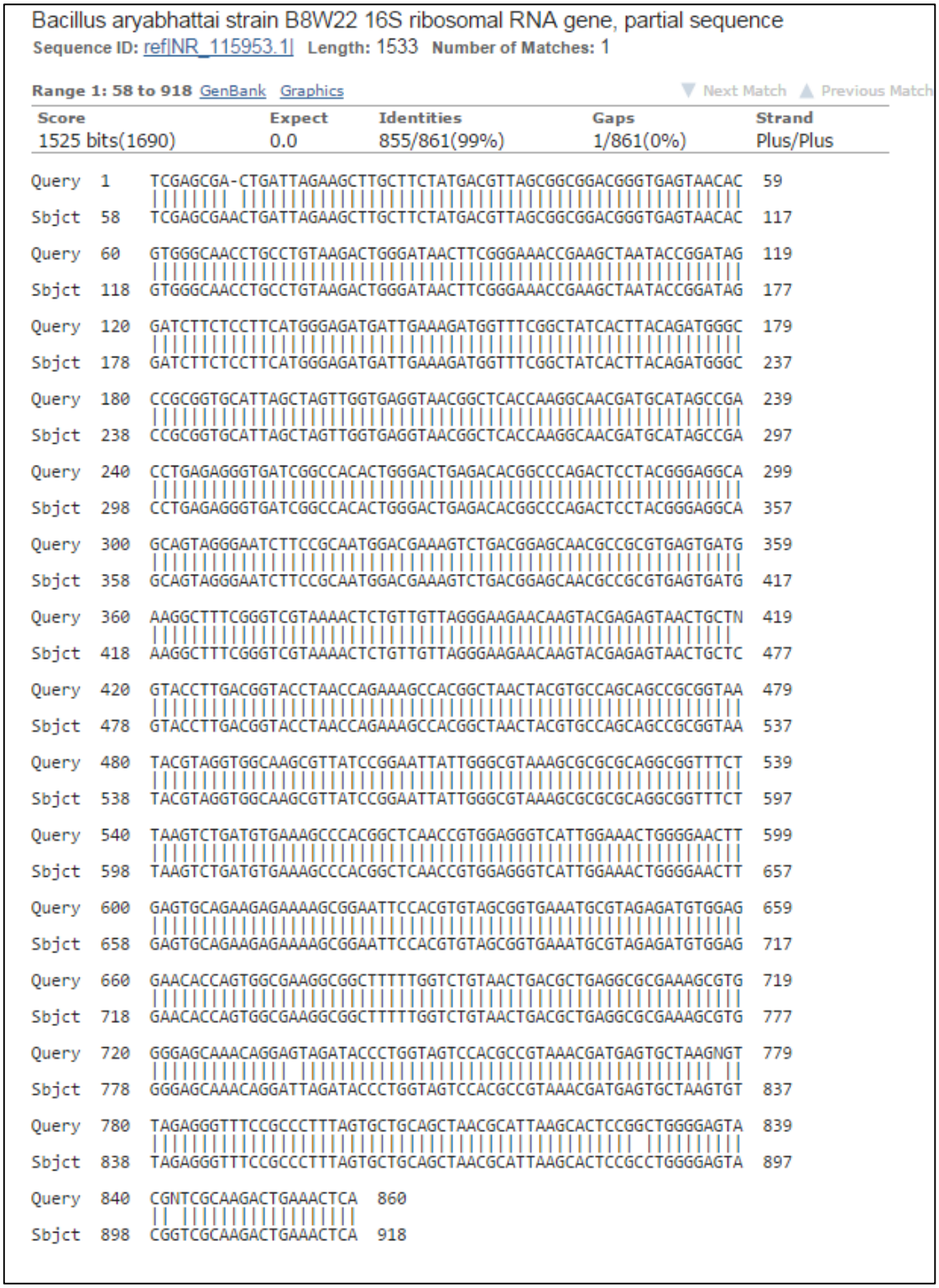

C3: The DNA sequence of the halite recovered sample, compared to Bacillus aryabhattai (Sequence ID: ref|NR_115953.1|) strain, showing a 99% sequence similarity.

Appendix D

Template Title	Sequence Count	Representative %
Staphylococcus ATCC 12228 chromosome, complete genome.	2269425	37.978%
Staphylococcus RP62A, complete genome.	2143887	35.877%
Staphylococcus subsp. aureus USA300_TCH1516 chromosome,	153458	2.568%
Staphylococcus subsp. aureus USA300_FPR3757 chromosome,	150655	2.521%
Staphylococcus JCSC1435 chromosome, complete genome.	62578	1.047%
Staphylococcus HKU09-01 chromosome, complete genome.	41882	0.701%
Staphylococcus N920143, complete genome.	41432	0.693%
Staphylococcus subsp. aureus Mu3, complete genome.	33740	0.565%
Staphylococcus subsp. aureus M013 chromosome, complete	33729	0.564%
Staphylococcus subsp. aureus Mu50 chromosome, complete	33726	0.564%
Staphylococcus subsp. aureus N315 chromosome, complete	33695	0.564%
Staphylococcus 04-02981 chromosome, complete genome.	33482	0.560%
Staphylococcus subsp. aureus JH9 chromosome, complete	33366	0.558%
Staphylococcus subsp. aureus JH1 chromosome, complete	33358	0.558%
Staphylococcus subsp. aureus MRSA252 chromosome, complete	32692	0.547%
Staphylococcus subsp. carnosus TM300 chromosome, complete	31435	0.526%
Staphylococcus subsp. saprophyticus ATCC 15305,	29561	0.495%
Staphylococcus RF122, complete genome.	25891	0.433%
Staphylococcus subsp. aureus HO 5096 0412, complete genome.	25763	0.431%
Staphylococcus subsp. aureus str. JKD6008 chromosome,	25011	0.419%
Staphylococcus HKU10-03 chromosome, complete	24602	0.412%
Staphylococcus subsp. aureus JKD6159 chromosome, complete	24395	0.408%
Staphylococcus subsp. aureus TW20, complete genome.	24289	0.406%
Staphylococcus subsp. aureus 11819-97 chromosome, complete	24034	0.402%
Staphylococcus subsp. aureus 71193 chromosome, complete	24002	0.402%
Staphylococcus subsp. aureus ST398, complete genome.	23954	0.401%
Staphylococcus subsp. aureus MW2, complete genome.	23530	0.394%
Staphylococcus subsp. aureus TCH60 chromosome, complete	23395	0.392%
Staphylococcus subsp. aureus ECT-R 2, complete genome.	23394	0.391%
Staphylococcus subsp. aureus MSHR1132, complete genome.	22896	0.383%
Staphylococcus 08BA02176 chromosome, complete genome.	22581	0.378%
Staphylococcus subsp. aureus ED133 chromosome, complete	21822	0.365%
Staphylococcus subsp. aureus NCTC 8325 chromosome, complete	21821	0.365%
Staphylococcus subsp. aureus MSSA476 chromosome, complete	21821	0.365%
Staphylococcus subsp. aureus T0131 chromosome, complete	21816	0.365%
Staphylococcus subsp. aureus str. Newman chromosome,	21794	0.365%
Staphylococcus subsp. aureus VC40 chromosome, complete	21586	0.361%
Staphylococcus ED99 chromosome, complete genome.	21556	0.361%
Staphylococcus subsp. aureus ED98, complete genome.	21550	0.361%
Staphylococcus subsp. aureus LGA251, complete genome.	21120	0.353%
Staphylococcus subsp. aureus COL chromosome, complete	20541	0.344%
Macrococcus JCSCS402, complete genome.	7189	0.120%
Bacillus WSH-002 chromosome, complete genome.	7080	0.118%
Bacillus QM B1551 chromosome, complete genome.	5551	0.093%
Bacillus DSM 319 chromosome, complete genome.	5476	0.092%
Staphylococcus subsp. aureus 11819-97 plasmid p11819-97,	4194	0.070%
Solibacillus StLB046, complete genome.	3938	0.066%
Bacillus WSH-002 plasmid WSH-002_p1, complete sequence.	3730	0.062%
Bacillus 36D1 chromosome, complete genome.	3449	0.058%
Melissococcus ATCC 35311 chromosome, complete genome.	3186	0.053%
Melissococcus DAT561 chromosome 1, complete genome.	3082	0.052%
Bacillus 42406 chromosome, complete genome.	2891	0.048%
Bacillus serovar finitimus YBT-020 chromosome,	2870	0.048%
Bacillus str. Ames chromosome, complete genome.	2839	0.048%
Bacillus QM B1551 plasmid pBM400, complete sequence.	2824	0.047%
Bacillus str. 'Ames Ancestor' chromosome, complete	2821	0.047%
Bacillus MC28 chromosome, complete genome.	2819	0.047%
Bacillus ATCC 10987 chromosome, complete genome.	2816	0.047%
Bacillus str. Sterne chromosome, complete genome.	2814	0.047%
Bacillus str. A0248, complete genome.	2813	0.047%
Bacillus Bt407 chromosome, complete genome.	2805	0.047%
Bacillus str. CDC 684 chromosome, complete genome.	2802	0.047%
Bacillus B4264 chromosome, complete genome.	2801	0.047%
Bacillus AH820 chromosome, complete genome.	2799	0.047%
Bacillus G9842 chromosome, complete genome.	2798	0.047%
Bacillus AH187 chromosome, complete genome.	2795	0.047%
Bacillus NC7401, complete genome.	2794	0.047%
Bacillus BMB171 chromosome, complete genome.	2789	0.047%
Bacillus HD-771 chromosome, complete genome.	2785	0.047%
Bacillus ATCC 14579, complete genome.	2784	0.047%
Bacillus serovar konkukian str. 97-27 chromosome,	2782	0.047%
Bacillus FRI-35 chromosome, complete genome.	2779	0.047%
Bacillus str. H9401 chromosome, complete genome.	2775	0.046%
Bacillus E33L chromosome, complete genome.	2775	0.046%
Bacillus F837/76 chromosome, complete genome.	2773	0.046%
Bacillus 03BB102, complete genome.	2768	0.046%
Bacillus serovar chinensis CT-43 chromosome, complete	2755	0.046%
Bacillus str. Al Hakam chromosome, complete genome.	2752	0.046%
Bacillus Q1 chromosome, complete genome.	2751	0.046%
Lysinibacillus C3-41 chromosome, complete genome.	2705	0.045%
Bacillus biovar anthracis str. CI chromosome, complete	2691	0.045%
Bacillus DSM 7, complete genome.	2682	0.045%
Staphylococcus ATCC 12228 plasmid pSE-12228-06,	2617	0.044%
Staphylococcus subsp. aureus USA300_FPR3757 plasmid pUSA03,	2204	0.037%
Staphylococcus subsp. saprophyticus ATCC 15305	2180	0.036%
Staphylococcus RP62A plasmid pSERP, complete sequence.	2118	0.035%
Geobacillus C56-T3 chromosome, complete genome.	2049	0.034%
Geobacillus CCB_US3_UF5 chromosome, complete	2040	0.034%
Geobacillus HTA426 chromosome, complete genome.	2033	0.034%
Geobacillus Y412MC61 chromosome, complete genome.	2032	0.034%
Geobacillus Y412MC52 chromosome, complete genome.	2020	0.034%
Staphylococcus subsp. aureus USA300_TCH1516 plasmid	1983	0.033%
Geobacillus NG80-2 chromosome, complete genome.	1927	0.032%
Staphylococcus subsp. saprophyticus ATCC 15305	1915	0.032%
Carnobacterium LMA28, complete genome.	1912	0.032%
Oceanobacillus HTE831 chromosome, complete genome.	1874	0.031%
Bacillus DSM 2522 chromosome, complete genome.	1869	0.031%
Bacillus XH7 chromosome, complete genome.	1807	0.030%
Staphylococcus subsp. aureus TW20 plasmid pTW20_1, complete	1749	0.029%
Bacillus SAFR-032 chromosome, complete genome.	1712	0.029%
Amphibacillus NBRC 15112, complete genome.	1537	0.026%
Staphylococcus subsp. aureus JH9 plasmid pSJH901, complete	1535	0.026%
Staphylococcus subsp. aureus JH1 plasmid pSJH101, complete	1529	0.026%
Staphylococcus subsp. aureus Mu50 plasmid VRSAp, complete	1501	0.025%
Staphylococcus subsp. aureus MSHR1132 plasmid pST75,	1481	0.025%
Bacillus subsp. plantarum CAU B946, complete	1476	0.025%
Bacillus KSM-K16, complete genome.	1472	0.025%
Enterococcus V583 chromosome, complete genome.	1468	0.025%
Enterococcus D32 chromosome, complete genome.	1467	0.025%
Lactobacillus subsp. sakei 23K chromosome, complete genome.	1463	0.024%
Enterococcus OG1RF chromosome, complete genome.	1460	0.024%
Staphylococcus subsp. aureus ST398 plasmid pS0385-1,	1457	0.024%
Bacillus subsp. plantarum YAU B9601-Y2, complete	1453	0.024%
Enterococcus 62 chromosome, complete genome.	1452	0.024%
Bacillus Y2 chromosome, complete genome.	1441	0.024%
Bacillus FZB42, complete genome.	1439	0.024%
Enterococcus ATCC 9790 chromosome, complete genome.	1340	0.022%
Enterococcus DO chromosome, complete genome.	1325	0.022%
Bacillus C-125 chromosome, complete genome.	1202	0.020%
Paenibacillus HPL-003 chromosome, complete genome.	1134	0.019%
Paenibacillus E681 chromosome, complete genome.	1124	0.019%
Paenibacillus SC2 chromosome, complete genome.	1045	0.017%
Bacillus DSM 13 = ATCC 14580 chromosome, complete	1037	0.017%
Carnobacterium 17-4 chromosome, complete genome.	1036	0.017%
Bacillus ATCC 14580 chromosome, complete genome.	1033	0.017%
Paenibacillus M1, complete genome.	1026	0.017%
Tetragenococcus NBRC 12172, complete genome.	999	0.017%
Bacillus MLS10 chromosome, complete genome.	945	0.016%

Bacillus KBAB4 chromosome, complete genome.	872	0.015%
Bacillus TA208 chromosome, complete genome.	870	0.015%
Bacillus LL3 chromosome, complete genome.	851	0.014%
Bacillus subsp. plantarum AS43.3, complete	830	0.014%
Bacillus NVH 391-98 chromosome, complete genome.	820	0.014%
Bacillus OF4 chromosome, complete genome.	759	0.013%
Propionibacterium 6609 chromosome, complete genome.	688	0.012%
Propionibacterium KPA171202 chromosome, complete genome.	682	0.011%
Bacillus BSn5 chromosome, complete genome.	675	0.011%
Propionibacterium 266 chromosome, complete genome.	672	0.011%
Propionibacterium C1 chromosome, complete genome.	654	0.011%
Propionibacterium SK137 chromosome, complete genome.	650	0.011%
Bacillus subsp. spizizenii TU-B-10 chromosome, complete	647	0.011%
Propionibacterium TypeIA2 P.acn17 chromosome, complete	643	0.011%
Bacillus subsp. subtilis str. 168 chromosome, complete	643	0.011%
Bacillus subsp. subtilis str. BSP1, complete genome.	640	0.011%
Propionibacterium TypeIA2 P.acn33 chromosome, complete	639	0.011%
Propionibacterium TypeIA2 P.acn31 chromosome, complete	639	0.011%
Bacillus subsp. natto BEST195, complete genome, ***	637	0.011%
Bacillus QB928 chromosome, complete genome.	635	0.011%
Bacillus subsp. subtilis str. RO-NN-1 chromosome, complete	635	0.011%
Bacillus JS chromosome, complete genome.	632	0.011%
Pediococcus ATCC BAA-344 chromosome, complete genome.	599	0.010%
Exiguobacterium AT1b chromosome, complete genome.	470	0.008%
Bacillus subsp. spizizenii str. W23 chromosome, complete	463	0.008%
Lactobacillus NRRL B-30929 chromosome, complete genome.	279	0.005%
Lactobacillus CD034 chromosome, complete genome.	272	0.005%
Halobacillus DSM 2266, complete genome.	239	0.004%
Lactobacillus CECT 5713 chromosome, complete genome.	221	0.004%
Lactobacillus UCC118 chromosome, complete genome.	217	0.004%
Exiguobacterium 255-15 chromosome, complete genome.	188	0.003%
Exiguobacterium B7 chromosome, complete genome.	188	0.003%
Propionibacterium ATCC 11828 chromosome, complete genome.	182	0.003%
Megasphaera DSM 20460, complete genome.	166	0.003%
Listeria SLCC2755 plasmid pLM1-2bUG1, complete	118	0.002%
Listeria SLCC2372 plasmid pLM1-2cUG1, complete	118	0.002%
Listeria serotype 7 str. SLCC2482 plasmid pLM7UG1,	118	0.002%
Listeria 1343576 plasmid pLM5578, complete sequence.	116	0.002%
Staphylococcus subsp. aureus ED98 plasmid pAVX, complete	112	0.002%
Streptococcus Hungary19A-6, complete genome.	105	0.002%
Streptococcus CGSP14 chromosome, complete genome.	99	0.002%
Streptococcus 670-6B chromosome, complete genome.	98	0.002%
Streptococcus ATCC 700669, complete genome.	95	0.002%
Veillonella DSM 2008 chromosome, complete genome.	89	0.001%
Staphylococcus JCSC1435 plasmid pSHaeC, complete	87	0.001%
Caldicellulosiruptor OB47 chromosome, complete genome.	80	0.001%
Clostridium 9a chromosome, complete genome.	80	0.001%
Paenibacillus 3016 chromosome, complete genome.	76	0.001%
Mycoplasma 7448 chromosome, complete genome.	68	0.001%
Caldicellulosiruptor DSM 8903 chromosome, complete	57	0.001%
Mycoplasma HF-2, complete genome.	51	0.001%
Campylobacter ATCC BAA-381, complete genome.	50	0.001%
Thermoanaerobacter ATCC 33223 chromosome, complete	47	0.001%
Thermoanaerobacter subsp. finnii Ako-1 chromosome, complete	45	0.001%
Thermoanaerobacter MB4 chromosome, complete genome.	45	0.001%
Geobacillus C56-YS93 chromosome, complete	44	0.001%
Geobacillus WCH70 chromosome, complete genome.	43	0.001%
Thermoanaerobacter Ab9 chromosome, complete genome.	43	0.001%
Thermoanaerobacterium JW/SL-YS485 chromosome,	39	0.001%
Borrelia Ly plasmid pl23, complete sequence.	39	0.001%
Thermoanaerobacterium DSM 571 chromosome,	37	0.001%
Geobacillus Y4.1MC1 chromosome, complete genome.	35	0.001%
Lactobacillus R0052 chromosome, complete genome.	33	0.001%
Desulfotomaculum DSM 771 chromosome, complete genome.	33	0.001%
Streptococcus ND03 chromosome, complete genome.	30	0.001%
Aster witches'-broom phytoplasma AYWB, complete genome.	29	0.000%
Bacillus 1942 chromosome, complete genome.	27	0.000%
Heliobacterium Ice1 chromosome, complete genome.	27	0.000%
Riemerella RA-CH-1 chromosome, complete genome.	25	0.000%
Pediococcus ATCC 25745, complete genome.	24	0.000%
Oscillatoria PCC 6304 chromosome, complete genome.	21	0.000%
Streptococcus D12 chromosome, complete genome.	21	0.000%
Riemerella ATCC 11845 = DSM 15868 chromosome,	21	0.000%
Ornithobacterium DSM 15997 chromosome, complete	21	0.000%
Kyrpidia DSM 2912 chromosome, complete genome.	19	0.000%
Lactobacillus CECT 5716 chromosome, complete genome.	19	0.000%
Thermoanaerobacter Rt8.B1 chromosome, complete genome.	19	0.000%
Candidatus mali chromosome, complete genome.	19	0.000%
Onion phytoplasma OY-M, complete genome.	19	0.000%
Lactobacillus subsp. bulgaricus ND02 chromosome,	18	0.000%
Caldicellulosiruptor DSM 6725 chromosome, complete genome.	18	0.000%
Lactobacillus TMW 1.1304 chromosome, complete	17	0.000%
Lactobacillus IFO 3956, complete genome.	17	0.000%
Lactobacillus subsp. bulgaricus 2038 chromosome,	16	0.000%
Desulfotomaculum DSM 6115 chromosome, complete genome.	16	0.000%
Lactobacillus subsp. bulgaricus ATCC 11842 chromosome,	16	0.000%
Cyanothece ATCC 51142 chromosome circular, complete sequence.	15	0.000%
Candidatus acidaminovorans.	15	0.000%
Aerococcus ACS-120-V-Col10a chromosome, complete genome.	15	0.000%
Lactococcus subsp. cremoris A76 chromosome, complete genome.	15	0.000%
Lactobacillus subsp. bulgaricus ATCC BAA-365	15	0.000%
Streptococcus ST1 chromosome, complete genome.	15	0.000%
Desulfotomaculum MI-1 chromosome, complete genome.	14	0.000%
Desulfotomaculum DSM 2154 chromosome, complete genome.	14	0.000%
Oenococcus PSU-1, complete genome.	14	0.000%
Eubacterium ATCC 27750 chromosome, complete genome.	14	0.000%
Olsenella DSM 7084 chromosome, complete genome.	14	0.000%
Alkaliphilus OhILAs chromosome, complete genome.	14	0.000%
Weissella KACC 15510 chromosome, complete genome.	13	0.000%
Atopobium DSM 20469 chromosome, complete genome.	13	0.000%
Lactobacillus subsp. plantarum ST-III chromosome,	13	0.000%
Escherichia O7:K1 str. CE10 plasmid pCE10D, complete sequence.	13	0.000%
Bacteroides YCH46 chromosome, complete genome.	13	0.000%
Secondary of Ctenarytaina eucalypti chromosome,	13	0.000%
Staphylococcus ATCC 12228 plasmid pSE-12228-02,	13	0.000%
Anoxybacillus WK1 chromosome, complete genome.	13	0.000%
Escherichia O104:H4 str. 2009EL-2050 chromosome, complete	13	0.000%
Lactobacillus JDM1, complete genome.	13	0.000%
Clostridium WM1 chromosome, complete genome.	13	0.000%
Listeria subsp. ivanovii PAM 55, complete genome.	13	0.000%
Lactobacillus WCFS1, complete genome.	13	0.000%
Listeria Finland 1998 chromosome, complete genome.	13	0.000%
Micrococcus NCTC 2665, complete genome.	13	0.000%
Clostridium DSM 519 chromosome, complete genome.	13	0.000%
Clostridium BKT015925 chromosome, complete genome.	12	0.000%
Lactococcus subsp. cremoris NZ9000 chromosome, complete	12	0.000%
Clostridium ISDg chromosome, complete genome.	12	0.000%
Listeria SLCC7179, complete genome.	12	0.000%
Dactylococcopsis PCC 8305, complete genome.	12	0.000%
Thermincola JR chromosome, complete genome.	12	0.000%
Butyrivibrio B316 chromosome 1, complete genome.	12	0.000%
Desulfosporosinus SJ4 chromosome, complete genome.	12	0.000%
Pelotomaculum SI chromosome, complete genome.	12	0.000%
Lactococcus subsp. cremoris MG1363 chromosome, complete	12	0.000%
Desulfotomaculum CO-1-SRB chromosome, complete	12	0.000%
Lactobacillus NCFM chromosome, complete genome.	11	0.000%
Clostridium DSM 5427 chromosome, complete genome.	11	0.000%
Halothece PCC 7418, complete genome.	11	0.000%
Lactococcus subsp. lactis CV56 chromosome, complete genome.	11	0.000%
Brevibacillus NBRC 100599, complete genome.	11	0.000%
Moorella ATCC 39073 chromosome, complete genome.	11	0.000%
Caldilinea DSM 14535 = NBRC 104270, complete genome.	11	0.000%

Lactobacillus DPC 6026 chromosome, complete genome.	11	0.000%
Thermodesulfobium DSM 14796 chromosome, complete genome.	11	0.000%
Coriobacterium PW2 chromosome, complete genome.	10	0.000%
Lactococcus subsp. cremoris SK11, complete genome.	10	0.000%
Lactococcus subsp. lactis Il1403 chromosome, complete	10	0.000%
Lactobacillus NCC 533, complete genome.	10	0.000%
Lactobacillus ATCC 27782 chromosome, complete genome.	10	0.000%
Listeria serovar 1/2b str. SLCC3954 chromosome, complete	10	0.000%
Listeria Clip11262, complete genome.	10	0.000%
Clostridium NT chromosome, complete genome.	10	0.000%
Listeria SLCC2376, complete genome.	10	0.000%
Listeria SLCC2378, complete genome.	10	0.000%
Lactobacillus W56, complete genome.	9	0.000%
Thermaerobacter DSM 12885 chromosome, complete genome.	9	0.000%
Alicyclobacillus subsp. acidocaldarius Tc-4-1	9	0.000%
Lactococcus subsp. lactis KF147 chromosome, complete genome.	9	0.000%
Alicyclobacillus subsp. acidocaldarius DSM 446	9	0.000%
Escherichia O104:H4 str. 2011C-3493 plasmid pG-EA11, complete	9	0.000%
Lactobacillus BD-II chromosome, complete genome.	9	0.000%
Lactobacillus BL23 chromosome, complete genome.	9	0.000%
Prochlorococcus str. MIT 9211, complete genome.	9	0.000%
Carboxydothermus Z-2901 chromosome, complete	9	0.000%
Prochlorococcus subsp. marinus str. CCMP1375 chromosome,	9	0.000%
Clostridium SY8519, complete genome.	9	0.000%
Helicobacter CIII-1, complete genome.	9	0.000%
Slackia DSM 20476 chromosome, complete genome.	9	0.000%
Lactobacillus ATCC 334 chromosome, complete genome.	9	0.000%
Eggerthella DSM 2243 chromosome, complete genome.	9	0.000%
Listeria M7 chromosome, complete genome.	9	0.000%
Butyrivibrio B316 chromosome 2, complete genome.	9	0.000%
Escherichia O104:H4 str. 2009EL-2050 plasmid pG-09EL50,	9	0.000%
Cryptobacterium DSM 15641 chromosome, complete genome.	9	0.000%
Lactobacillus LC2W chromosome, complete genome.	9	0.000%
Erysipelothrix str. Fujisawa chromosome, complete	9	0.000%
Lactobacillus str. Zhang chromosome, complete genome.	9	0.000%
Myxococcus DK 1622 chromosome, complete genome.	9	0.000%
Leuconostoc C2 chromosome, complete genome.	8	0.000%
Lactobacillus DSM 20016 chromosome, complete genome.	8	0.000%
Lactobacillus JCM 1112, complete genome.	8	0.000%
Eggerthella YY7918, complete genome.	8	0.000%
Lactobacillus SD2112 chromosome, complete genome.	8	0.000%
Listeria 08-5923, complete genome.	8	0.000%
Listeria 10403S chromosome, complete genome.	8	0.000%
Filifactor ATCC 35896 chromosome, complete genome.	8	0.000%
Mahella 50-1 BON chromosome, complete genome.	8	0.000%
Listeria EGD-e, complete genome.	8	0.000%
Cyanobium PCC 6307 chromosome, complete genome.	8	0.000%
Lactobacillus FI9785 chromosome, complete genome.	8	0.000%
Candidatus audaxviator MP104C chromosome, complete	8	0.000%
Listeria J0161 chromosome, complete genome.	8	0.000%
Flexistipes DSM 4947 chromosome, complete genome.	8	0.000%
Dehalobacter CF chromosome, complete genome.	8	0.000%
Listeria L99, complete genome.	8	0.000%
Listeria 1343576 chromosome, complete genome.	8	0.000%
Mycoplasma UAB CTIP, complete genome.	8	0.000%
Listeria HCC23 chromosome, complete genome.	8	0.000%
Listeria SLCC2372, complete genome.	8	0.000%
Dehalobacter DCA chromosome, complete genome.	8	0.000%
Acholeplasma PG-8A chromosome, complete genome.	8	0.000%
Leptospira serovar Lai str. IPAV chromosome chromosome	8	0.000%
Alkaliphilus QYMF chromosome, complete genome.	8	0.000%
Delftia SPH-1 chromosome, complete genome.	8	0.000%
Listeria Clip81459, complete genome.	8	0.000%
Eubacterium ATCC 33656, complete genome.	7	0.000%
Synechococcus CC9605, complete genome.	7	0.000%
Synechococcus WH 8102, complete genome.	7	0.000%
Thermoanaerobacterium LX-11 chromosome, complete	7	0.000%
Thermoanaerobacter X514 chromosome, complete genome.	7	0.000%
Helicobacter F16, complete genome.	7	0.000%
Acinetobacter TCDC-AB0715 chromosome, complete genome.	7	0.000%
Anaplasma HZ, complete genome.	7	0.000%
Lactobacillus ATCC 8530 chromosome, complete genome.	7	0.000%
Lactobacillus GG, complete genome.	7	0.000%
Lactobacillus GG chromosome, complete genome.	7	0.000%
Lactobacillus Lc 705 chromosome, complete genome.	7	0.000%
Leptospira serovar Hardjo-bovis JB197 chromosome	7	0.000%
Leptospira serovar Hardjo-bovis str. L550 chromosome	7	0.000%
Leptospira serovar Copenhageni str. Fiocruz L1-130	7	0.000%
Leptospira serovar Lai str. 56601 chromosome chromosome	7	0.000%
Listeria ATCC 19117, complete genome.	7	0.000%
Listeria FSL R2-561 chromosome, complete genome.	7	0.000%
Listeria L312, complete genome.	7	0.000%
Listeria serotype 7 str. SLCC2482, complete genome.	7	0.000%
Lactobacillus ATCC 33323 chromosome, complete genome.	7	0.000%
Listeria SLCC2479, complete genome.	7	0.000%
Listeria SLCC2540, complete genome.	7	0.000%
Listeria SLCC2755, complete genome.	7	0.000%
Listeria SLCC5850, complete genome.	7	0.000%
Listeria serovar 6b str. SLCC5334 chromosome, complete	7	0.000%
Mycoplasma 168 chromosome, complete genome.	7	0.000%
Desulfosporosinus DSM 13257 chromosome, complete genome.	7	0.000%
Oscillibacter Sjm18-20, complete genome.	7	0.000%
Paenibacillus JDR-2 chromosome, complete genome.	7	0.000%
Parvularcula HTCC2503 chromosome, complete genome.	7	0.000%
Rhodothermus SG0.5JP17-172 chromosome, complete genome.	7	0.000%
Shigella 2002017 plasmid pSFxv_2, complete sequence.	7	0.000%
Escherichia O104:H4 str. 2009EL-2071 plasmid pG-09EL71,	7	0.000%
Lactobacillus ATCC 367, complete genome.	7	0.000%
Helicobacter ATCC 49179 chromosome, complete genome.	6	0.000%
Ruminococcus 7 chromosome, complete genome.	6	0.000%
Desulfomonile DSM 6799 chromosome, complete genome.	6	0.000%
Cyanothece PCC 7425 chromosome, complete genome.	6	0.000%
Mycoplasma 232 chromosome, complete genome.	6	0.000%
Escherichia 'BL21-Gold(DE3)pLysS AG' chromosome, complete	6	0.000%
Haliangium DSM 14365 chromosome, complete genome.	6	0.000%
Acinetobacter ACICU chromosome, complete genome.	6	0.000%
Synechococcus CC9902 chromosome, complete genome.	6	0.000%
Methylacidiphilum V4, complete genome.	6	0.000%
Synechococcus CC9311, complete genome.	6	0.000%
Candidatus cicadicola Dsem chromosome, complete genome.	6	0.000%
Neisseria TCDC-NG08107 chromosome, complete genome.	6	0.000%
Streptococcus subsp. equisimilis AC-2713, complete	6	0.000%
Acidithiobacillus SM-1 chromosome, complete genome.	5	0.000%
Acidithiobacillus SS3 chromosome, complete genome.	5	0.000%
Acidithiobacillus ATCC 23270 chromosome, complete	5	0.000%
Acidithiobacillus ATCC 53993 chromosome, complete	5	0.000%
Micavibrio ARL-13 chromosome, complete genome.	5	0.000%
Mycoplasma PG50 chromosome, complete genome.	5	0.000%
Streptococcus JIM8777, complete genome.	5	0.000%
Paenibacillus K02 chromosome, complete genome.	5	0.000%
Cyanothece PCC 7822 chromosome, complete genome.	5	0.000%
Acinetobacter MDR-ZJ06 chromosome, complete genome.	5	0.000%
Comamonas CNB-2 chromosome, complete genome.	5	0.000%
Acinetobacter MDR-TJ chromosome, complete genome.	5	0.000%
Acinetobacter ATCC 17978 chromosome, complete genome.	5	0.000%
Paenibacillus Y412MC10 chromosome, complete genome.	5	0.000%
Acinetobacter AYE chromosome, complete genome.	5	0.000%
Desulfurivibrio AHT2 chromosome, complete genome.	5	0.000%
Sulfobacillus DSM 10332 chromosome, complete genome.	5	0.000%
Desulfosporosinus DSM 765 chromosome, complete genome.	5	0.000%
Sulfobacillus TPY chromosome, complete genome.	5	0.000%
Persephonella EX-H1 chromosome, complete genome.	5	0.000%

Synechococcus WH 7803 chromosome, complete genome.	5	0.000%
Syntrophobotulus DSM 8271 chromosome, complete genome.	5	0.000%
Syntrophothermus DSM 12680 chromosome, complete genome.	5	0.000%
Acinetobacter AB0057 chromosome, complete genome.	5	0.000%
Acinetobacter 1656-2 chromosome, complete genome.	5	0.000%
Gloeobacter PCC 7421 chromosome, complete genome.	5	0.000%
Gamma HdN1 chromosome, complete genome.	5	0.000%
Mycoplasma 99/014/6, complete genome.	5	0.000%
Mycoplasma J chromosome, complete genome.	5	0.000%
Riemerella ATCC 11845 = DSM 15868 chromosome,	5	0.000%
Roseburia A2-183 chromosome, complete genome.	5	0.000%
Acetobacterium DSM 1030 chromosome, complete genome.	5	0.000%
Thermosediminibacter DSM 16646 chromosome, complete genome.	5	0.000%
Anaerolinea UNI-1, complete genome.	5	0.000%
Candidatus australiense, complete genome.	5	0.000%
Acinetobacter TYTH-1 chromosome, complete genome.	5	0.000%
Streptococcus B6, complete genome.	5	0.000%
Streptococcus AP200 chromosome, complete genome.	5	0.000%
Mycoplasma subsp. capri LC str. 95010, complete genome.	4	0.000%
Escherichia NA114 chromosome, complete genome.	4	0.000%
Selenomonas ATCC 35185 chromosome, complete genome.	4	0.000%
Shewanella ATCC 700345 chromosome, complete genome.	4	0.000%
Desulfitobacterium Y51 chromosome, complete genome.	4	0.000%
Kocuria DC2201, complete genome.	4	0.000%
Listeria serotype 4b str. F2365 chromosome, complete	4	0.000%
Polynucleobacter subsp. asymbioticus QLW-P1DMWA-1	4	0.000%
Polynucleobacter subsp. necessarius STIR1 chromosome,	4	0.000%
Listeria 07PF0776 chromosome, complete genome.	4	0.000%
Leuconostoc JB16 chromosome, complete genome.	4	0.000%
Halothermothrix H 168 chromosome, complete genome.	4	0.000%
Alicycliphilus BC chromosome, complete genome.	4	0.000%
Pelobacter DSM 2379 chromosome, complete genome.	4	0.000%
Mycoplasma subsp. capricolum ATCC 27343 chromosome,	4	0.000%
Streptococcus S735 chromosome, complete genome.	4	0.000%
Streptococcus SS12 chromosome, complete genome.	4	0.000%
Acinetobacter PHEA-2 chromosome, complete genome.	4	0.000%
Candidatus magnifica str. Cm (Calyptogena magnifica),	4	0.000%
Mycoplasma KS1 chromosome, complete genome.	4	0.000%
Eubacterium KIST612 chromosome, complete genome.	4	0.000%
Leptothrix SP-6 chromosome, complete genome.	4	0.000%
Ilyobacter DSM 2926 plasmid pILYOP01, complete sequence.	4	0.000%
Ilyobacter DSM 2926 chromosome, complete genome.	4	0.000%
Synechococcus RCC307 chromosome, complete genome.	4	0.000%
Alicycliphilus K601 chromosome, complete genome.	4	0.000%
Delftia Cs1-4 chromosome, complete genome.	4	0.000%
Acinetobacter SDF chromosome, complete genome.	4	0.000%
Calditerrivibrio DSM 19672 chromosome, complete	4	0.000%
Paenibacillus KNP414 chromosome, complete genome.	4	0.000%
Cyanobacterium complete genome.	4	0.000%
Acinetobacter AB307-0294, complete genome.	4	0.000%
Streptococcus IS7493 chromosome, complete genome.	4	0.000%
Streptococcus CCHSS3, complete genome.	4	0.000%
Thermoanaerobacter subsp. mathranii str. A3 chromosome,	4	0.000%
Acidovorax JS42 chromosome, complete genome.	4	0.000%
Acidovorax TPSY chromosome, complete genome.	4	0.000%
Thermoanaerobacter X513 chromosome, complete genome.	4	0.000%
Mobiluncus ATCC 43063 chromosome, complete genome.	4	0.000%
Clostridium A str. Hall chromosome, complete genome.	4	0.000%
Streptococcus LMG 18311 chromosome, complete genome.	4	0.000%
Ammonifex KC4 chromosome, complete genome.	3	0.000%
Clostridium 2007855, complete genome.	3	0.000%
Clostridium ATCC 824 chromosome, complete genome.	3	0.000%
Corynebacterium YS-314 chromosome, complete genome.	3	0.000%
Escherichia W plasmid pRK2, complete sequence.	3	0.000%
Clostridiales BVAB3 str. UPII9-5 chromosome, complete	3	0.000%
Escherichia SMS-3-5 plasmid pSMS35_3, complete sequence.	3	0.000%
Mycoplasma subsp. mycoides SC str. PG1 chromosome,	3	0.000%
Erwinia Ep1/96 plasmid pEP05, complete sequence.	3	0.000%
Magnetococcus MC-1 chromosome, complete genome.	3	0.000%
Escherichia W plasmid pRK2, complete sequence.	3	0.000%
Finegoldia ATCC 29328 chromosome, complete genome.	3	0.000%
Pelobacter DSM 2380 chromosome, complete genome.	3	0.000%
Erwinia Ejp617 plasmid pJE05, complete sequence.	3	0.000%
Enterococcus Aus0004 chromosome, complete genome.	3	0.000%
Chloroflexus Y-400-fl chromosome, complete genome.	3	0.000%
Chloroflexus J-10-fl chromosome, complete genome.	3	0.000%
Chloroflexus DSM 9485 chromosome, complete genome.	3	0.000%
Streptococcus subsp. equi 4047, complete genome.	3	0.000%
Escherichia SE11 plasmid pSE11-5, complete sequence.	3	0.000%
Enterobacter subsp. cloacae ENHKU01 chromosome, complete	3	0.000%
Leptotrichia C-1013-b chromosome, complete genome.	3	0.000%
Enterobacter subsp. dissolvens SDM chromosome, complete	3	0.000%
Lactococcus Lg2, complete genome.	3	0.000%
Enterobacter subsp. cloacae ATCC 13047 chromosome, complete	3	0.000%
Lactococcus ATCC 49156, complete genome.	3	0.000%
Streptococcus 57.I chromosome, complete genome.	3	0.000%
Roseiflexus DSM 13941 chromosome, complete genome.	3	0.000%
Roseiflexus RS-1 chromosome, complete genome.	3	0.000%
Streptococcus 05ZYH33 chromosome, complete genome.	3	0.000%
Streptococcus 98HAH33, complete genome.	3	0.000%
Streptococcus A7 chromosome, complete genome.	3	0.000%
Escherichia DH1 chromosome, complete genome.	3	0.000%
Salmonella subsp. enterica serovar Newport str. SL254	3	0.000%
Sebaldella ATCC 33386 chromosome, complete genome.	3	0.000%
Streptococcus GZ1 chromosome, complete genome.	3	0.000%
Streptococcus JS14 chromosome, complete genome.	3	0.000%
Streptococcus P1/7, complete genome.	3	0.000%
Clostridium E88 chromosome, complete genome.	3	0.000%
Streptococcus SC84, complete genome.	3	0.000%
Desulfitobacterium DCB-2 chromosome, complete genome.	3	0.000%
Desulfitobacterium ATCC 51507 chromosome, complete	3	0.000%
Streptococcus CNRZ1066 chromosome, complete genome.	3	0.000%
Streptococcus JIM 8232, complete genome.	3	0.000%
Streptococcus LMD-9, complete genome.	3	0.000%
Cyanobacterium PCC 7202, complete genome.	3	0.000%
Streptococcus MN-ZLW-002 chromosome, complete genome.	3	0.000%
Cyanobacterium PCC 10605, complete genome.	3	0.000%
Mesoplasma L1 chromosome, complete genome.	3	0.000%
Dickeya Ech586 chromosome, complete genome.	3	0.000%
Escherichia str. K-12 substr. W3110, complete genome.	3	0.000%
Clostridium EA 2018 chromosome, complete genome.	3	0.000%
Escherichia str. K-12 substr. MG1655 chromosome, complete	3	0.000%
Escherichia str. K-12 substr. DH10B chromosome, complete	3	0.000%
Escherichia KO11FL plasmid pEKO1102, complete sequence.	3	0.000%
Streptococcus D9 chromosome, complete genome.	3	0.000%
Escherichia KO11FL plasmid pRK2, complete sequence.	3	0.000%
Syntrophomonas subsp. wolfei str. Goettingen chromosome,	3	0.000%
Mycoplasma ATCC 23114 chromosome, complete genome.	3	0.000%
Bacteriovorax SJ, complete genome.	3	0.000%
Escherichia DH1, complete genome.	3	0.000%
Arthrobacter Sphe3 chromosome, complete genome.	3	0.000%
Herbaspirillum SmR1 chromosome, complete genome.	3	0.000%
Escherichia BW2952 chromosome, complete genome.	3	0.000%
Mycoplasma 158L3-1, complete genome.	3	0.000%
Corynebacterium K411 chromosome, complete genome.	3	0.000%
Acinetobacter ADP1 chromosome, complete genome.	3	0.000%
Arthrobacter A6 chromosome, complete genome.	3	0.000%
Arthrobacter TC1, complete genome.	3	0.000%
Escherichia ABU 83972 plasmid pABU, complete sequence.	3	0.000%
Acidovorax AAC00-1 chromosome, complete genome.	3	0.000%
Methylocystis SC2, complete genome.	3	0.000%
Clostridium DSM 1731 chromosome, complete genome.	3	0.000%

Candidatus princeps PCVAL chromosome, complete genome.	3	0.000%
Candidatus princeps PCIT chromosome, complete genome.	3	0.000%
Enterobacter subsp. cloacae ATCC 13047 plasmid pECL_A,	3	0.000%
Streptococcus BM407 chromosome, complete genome.	3	0.000%
Salmonella subsp. enterica serovar Choleraesuis str.	2	0.000%
Helicobacter MIT 00-7128 chromosome, complete genome.	2	0.000%
Escherichia SE15, complete genome.	2	0.000%
Chromobacterium ATCC 12472 chromosome, complete genome.	2	0.000%
Selenomonas subsp. lactilytica TAM6421, complete	2	0.000%
Escherichia SMS-3-5 chromosome, complete genome.	2	0.000%
Shewanella PV-4 chromosome, complete genome.	2	0.000%
Escherichia UMN026 chromosome, complete genome.	2	0.000%
Shewanella WP3 chromosome, complete genome.	2	0.000%
Shewanella HAW-EB3 chromosome, complete genome.	2	0.000%
Shewanella ATCC 51908 chromosome, complete genome.	2	0.000%
Escherichia UTI89 chromosome, complete genome.	2	0.000%
Shigella 2002017 chromosome, complete genome.	2	0.000%
Shigella 2002017 plasmid pSFxv_3, complete sequence.	2	0.000%
Shigella 2002017 plasmid pSFxv_5, complete sequence.	2	0.000%
Shigella 2a str. 2457T, complete genome.	2	0.000%
Shigella 2a str. 301 chromosome, complete genome.	2	0.000%
Shigella 5 str. 8401 chromosome, complete genome.	2	0.000%
Shigella Ss046 plasmid pSS046_spA, complete sequence.	2	0.000%
Sideroxydans ES-1 chromosome, complete genome.	2	0.000%
Helicobacter India7 chromosome, complete genome.	2	0.000%
Escherichia str. 'clone D i14' chromosome, complete genome.	2	0.000%
Escherichia str. 'clone D i2' chromosome, complete genome.	2	0.000%
Helicobacter J99 chromosome, complete genome.	2	0.000%
Clostridium str. 13 chromosome, complete genome.	2	0.000%
Clostridium SM101 chromosome, complete genome.	2	0.000%
Collimonas Ter331 chromosome, complete genome.	2	0.000%
Corynebacterium ATCC 13032, complete genome.	2	0.000%
Corynebacterium ATCC 13032, complete genome.	2	0.000%
Corynebacterium DSM 44385 chromosome, complete	2	0.000%
Coxiella CbuG_Q212 chromosome, complete genome.	2	0.000%
Coxiella CbuK_Q154 chromosome, complete genome.	2	0.000%
Coxiella Dugway 5J108-111 chromosome, complete genome.	2	0.000%
Coxiella RSA 331 chromosome, complete genome.	2	0.000%
Coxiella RSA 493 chromosome, complete genome.	2	0.000%
Maricaulis MCS10 chromosome, complete genome.	2	0.000%
Cupriavidus N-1 chromosome 1, complete sequence.	2	0.000%
Cupriavidus LMG 19424 chromosome 1, complete sequence.	2	0.000%
Cyanothece PCC 8801 chromosome, complete genome.	2	0.000%
Janthinobacterium Marseille chromosome, complete genome.	2	0.000%
Cyanothece PCC 8802 chromosome, complete genome.	2	0.000%
Methylibium PM1 chromosome, complete genome.	2	0.000%
Deferribacter SSM1, complete genome.	2	0.000%
Methylotenera 301 chromosome, complete genome.	2	0.000%
Methylotenera JLW8 chromosome, complete genome.	2	0.000%
Francisella subsp. holarctica OSU18 chromosome, complete	2	0.000%
Kangiella DSM 16069 chromosome, complete genome.	2	0.000%
Escherichia UM146 chromosome, complete genome.	2	0.000%
Acidaminococcus RyC-MR95 chromosome, complete genome.	2	0.000%
Moraxella RH4 chromosome, complete genome.	2	0.000%
Mycoplasma PG2 chromosome, complete genome.	2	0.000%
Mycoplasma chromosome, complete genome.	2	0.000%
Gallionella ES-2 chromosome, complete genome.	2	0.000%
Mycoplasma HB0801 chromosome, complete genome.	2	0.000%
Mycoplasma Hubei-1 chromosome, complete genome.	2	0.000%
Mycoplasma PG45 chromosome, complete genome.	2	0.000%
Acidovorax subsp. avenae ATCC 19860 chromosome, complete	2	0.000%
Mycoplasma JER chromosome, complete genome.	2	0.000%
Mycoplasma M64 chromosome, complete genome.	2	0.000%
Acidovorax KKS102 chromosome, complete genome.	2	0.000%
Acinetobacter 1656-2 plasmid ABKp2, complete sequence.	2	0.000%
Acinetobacter ACICU plasmid pACICU2, complete sequence.	2	0.000%
Acinetobacter AYE plasmid p3ABAYE, complete sequence.	2	0.000%
Acinetobacter TCDC-AB0715 plasmid p2ABTCDC0715, complete	2	0.000%
Acinetobacter DR1 chromosome, complete genome.	2	0.000%
Aliivibrio LFI1238 chromosome chromosome 1, complete	2	0.000%
Lactobacillus ZW3 chromosome, complete genome.	2	0.000%
Alkalilimnicola MLHE-1 chromosome, complete genome.	2	0.000%
Ralstonia 12J chromosome 1, complete sequence.	2	0.000%
Anaerococcus DSM 20548 chromosome, complete genome.	2	0.000%
Arthrobacter Rue61a chromosome, complete genome.	2	0.000%
Azotobacter DJ chromosome, complete genome.	2	0.000%
Bacteroides P 36-108 chromosome, complete genome.	2	0.000%
Bifidobacterium ATCC 15703 chromosome, complete	2	0.000%
Desulfovibrio ND132 chromosome, complete genome.	2	0.000%
Dickeya Ech703 chromosome, complete genome.	2	0.000%
Brachyspira WA1 chromosome, complete genome.	2	0.000%
Brachyspira PWS/A chromosome, complete genome.	2	0.000%
Brachyspira DSM 12563 chromosome, complete genome.	2	0.000%
Streptococcus subsp. equisimilis ATCC 12394	2	0.000%
Streptococcus subsp. equisimilis GGS_124 chromosome 1,	2	0.000%
Streptococcus subsp. equisimilis RE378, complete	2	0.000%
Brachyspira 95/1000 chromosome, complete genome.	2	0.000%
Streptococcus subsp. zooepidemicus MGCS10565 chromosome,	2	0.000%
Streptococcus str. Challis substr. CH1 chromosome,	2	0.000%
Brachyspira B2904 chromosome, complete genome.	2	0.000%
Streptococcus Uo5, complete genome.	2	0.000%
Gemmatimonas T-27, complete genome.	2	0.000%
Buchnera str. Cc (Cinara cedri), complete genome.	2	0.000%
Buchnera (Cinara tujafilina) chromosome, complete	2	0.000%
Burkholderia BSR3 chromosome 1, complete sequence.	2	0.000%
Elusimicrobium Pei191 chromosome, complete genome.	2	0.000%
Emticicia DSM 17448 chromosome, complete genome.	2	0.000%
Campylobacter subsp. jejuni ICDCCJ07001 chromosome, complete	2	0.000%
Campylobacter subsp. jejuni PT14 chromosome, complete	2	0.000%
Erwinia Ejp617 plasmid pJE02, complete sequence.	2	0.000%
Streptococcus SK36 chromosome, complete genome.	2	0.000%
Erwinia DSM 12163 plasmid pEp5, complete sequence.	2	0.000%
Pasteurella subsp. multocida str. Pm70 chromosome,	2	0.000%
Candidatus sp. IMCC9063 chromosome, complete genome.	2	0.000%
Leptospira serovar Patoc strain 'Patoc 1 (Ames)' chromosome	2	0.000%
Leptospira serovar Patoc strain 'Patoc 1 (Paris)'	2	0.000%
Candidatus amblyommii str. GAT-30V chromosome, complete	2	0.000%
Candidatus pediculicola USDA chromosome, complete genome.	2	0.000%
Escherichia 536, complete genome.	2	0.000%
Photobacterium SS9 chromosome 1, complete genome.	2	0.000%
Photorhabdus subsp. laumondii TTO1, complete genome.	2	0.000%
Polaromonas JS666 chromosome, complete genome.	2	0.000%
Polaromonas CJ2 chromosome, complete genome.	2	0.000%
Escherichia ABU 83972 chromosome, complete genome.	2	0.000%
Streptococcus ST3 chromosome, complete genome.	2	0.000%
Escherichia APEC O1 chromosome, complete genome.	2	0.000%
Geobacter Bem chromosome, complete genome.	2	0.000%
Escherichia CFT073 chromosome, complete genome.	2	0.000%
Escherichia E24377A plasmid pETEC_6, complete sequence.	2	0.000%
Herminiimonas chromosome, complete genome.	2	0.000%
Leuconostoc LMG 18811, complete genome.	2	0.000%
Leuconostoc JB7 chromosome, complete genome.	2	0.000%
Escherichia ED1a chromosome, complete genome.	2	0.000%
Escherichia IAI39 chromosome, complete genome.	2	0.000%
Escherichia IHE3034 chromosome, complete genome.	2	0.000%
Escherichia KO11FL chromosome, complete genome.	2	0.000%
Halanaerobium chromosome, complete genome.	2	0.000%
Pseudomonas PA7 chromosome, complete genome.	2	0.000%
Pseudomonas W619 chromosome, complete genome.	2	0.000%
Psychrobacter PRwf-1 chromosome, complete genome.	2	0.000%
Ralstonia H16 chromosome 1, complete genome.	2	0.000%
Ralstonia JMP134 chromosome 1, complete sequence.	2	0.000%

Ralstonia 12D chromosome 1, complete sequence.	2	0.000%
Thermacetogenium DSM 12270 chromosome, complete genome.	2	0.000%
Escherichia LF82, complete genome.	2	0.000%
Ramlibacter TTB310 chromosome, complete genome.	2	0.000%
Renibacterium ATCC 33209 chromosome, complete genome.	2	0.000%
Rhodoferax T118 chromosome, complete genome.	2	0.000%
Haloferax ATCC 33500 chromosome, complete genome.	2	0.000%
Rhodopseudomonas TIE-1 chromosome, complete genome.	2	0.000%
Halomonas DSM 2581 chromosome, complete genome.	2	0.000%
Rickettsia str. BuV67-CWPP chromosome, complete genome.	2	0.000%
Escherichia O127:H6 str. E2348/69 plasmid pE2348-2, complete	2	0.000%
Escherichia O26:H11 str. 11368 plasmid pO26_3, complete	2	0.000%
Escherichia O55:H7 str. RM12579 plasmid p12579_4, complete	2	0.000%
Riemerella RA-GD chromosome, complete genome.	2	0.000%
Escherichia O7:K1 str. CE10 chromosome, complete genome.	2	0.000%
Escherichia O83:H1 str. NRG 857C chromosome, complete genome.	2	0.000%
Escherichia P12b chromosome, complete genome.	2	0.000%
Turneriella DSM 21527 chromosome, complete genome.	2	0.000%
Variovorax EPS chromosome, complete genome.	2	0.000%
Variovorax S110 chromosome 1, complete sequence.	2	0.000%
Rubrivivax IL144, complete genome.	2	0.000%
Verminephrobacter EF01-2 chromosome, complete genome.	2	0.000%
Verrucosispora AB-18-032 chromosome, complete genome.	2	0.000%
Vibrio LGP32 chromosome 1, complete sequence.	2	0.000%
Escherichia S88 chromosome, complete genome.	2	0.000%
Yersinia Z176003 plasmid pPCP1, complete sequence.	2	0.000%
Mycoplasma NC96_1596-4-2P chromosome, complete	1	0.000%
Mycoplasma NY01_2001.047-5-1P chromosome, complete	1	0.000%
Mycoplasma str. R(high) chromosome, complete genome.	1	0.000%
Mycoplasma str. R(low) chromosome, complete genome.	1	0.000%
Mycoplasma VA94_7994-1-7P chromosome, complete	1	0.000%
Mycoplasma WI01_2001.043-13-2P chromosome, complete	1	0.000%
Ehrlichia str. Welgevonden chromosome, complete genome.	1	0.000%
Ehrlichia str. Welgevonden, complete genome.	1	0.000%
Enterobacter EcWSU1 chromosome, complete genome.	1	0.000%
Escherichia 042, complete genome.	1	0.000%
Escherichia 55989 chromosome, complete genome.	1	0.000%
Escherichia ATCC 8739 chromosome, complete genome.	1	0.000%
Escherichia BL21(DE3) chromosome, complete genome.	1	0.000%
Mycoplasma 163K, complete genome.	1	0.000%
Escherichia BL21(DE3), complete genome.	1	0.000%
Escherichia B str. REL606 chromosome, complete genome.	1	0.000%
Escherichia E24377A chromosome, complete genome.	1	0.000%
Escherichia ETEC H10407, complete genome.	1	0.000%
Escherichia HS, complete genome.	1	0.000%
Escherichia KO11FL chromosome, complete genome.	1	0.000%
Escherichia O103:H2 str. 12009, complete genome.	1	0.000%
Neisseria 53442 chromosome, complete genome.	1	0.000%
Neisseria 8013, complete genome.	1	0.000%
Neisseria alpha14 chromosome, complete genome.	1	0.000%
Neisseria alpha710 chromosome, complete genome.	1	0.000%
Neisseria FAM18 chromosome, complete genome.	1	0.000%
Neisseria G2136 chromosome, complete genome.	1	0.000%
Neisseria H44/76 chromosome, complete genome.	1	0.000%
Neisseria M01-240149 chromosome, complete genome.	1	0.000%
Neisseria M01-240355 chromosome, complete genome.	1	0.000%
Neisseria M04-240196 chromosome, complete genome.	1	0.000%
Neisseria MC58 chromosome, complete genome.	1	0.000%
Neisseria NZ-05/33 chromosome, complete genome.	1	0.000%
Neisseria WUE 2594, complete genome.	1	0.000%
Neisseria Z2491 chromosome, complete genome.	1	0.000%
Nitrosococcus Nc4 chromosome, complete genome.	1	0.000%
Escherichia O104:H4 str. 2009EL-2071 chromosome, complete	1	0.000%
Escherichia O104:H4 str. 2011C-3493 chromosome, complete	1	0.000%
Escherichia O111:H- str. 11128, complete genome.	1	0.000%
Escherichia O127:H6 str. E2348/69 chromosome, complete genome.	1	0.000%
Escherichia O157:H7 str. Sakai plasmid pOSAK1, complete	1	0.000%
Escherichia O26:H11 str. 11368 chromosome, complete genome.	1	0.000%
Escherichia SE11 chromosome, complete genome.	1	0.000%
Escherichia UMNK88 chromosome, complete genome.	1	0.000%
Escherichia W chromosome, complete genome.	1	0.000%
Escherichia W chromosome, complete genome.	1	0.000%
Ethanoligenens YUAN-3 chromosome, complete genome.	1	0.000%
Maribacter HTCC2170 chromosome, complete genome.	1	0.000%
Fusobacterium subsp. nucleatum ATCC 25586 chromosome,	1	0.000%
Geobacter M21 chromosome, complete genome.	1	0.000%
Geobacter Rf4 chromosome, complete genome.	1	0.000%
Gluconobacter 621H chromosome, complete genome.	1	0.000%
Paludibacter WB4 chromosome, complete genome.	1	0.000%
Parabacteroides ATCC 8503 chromosome, complete genome.	1	0.000%
Helicobacter MIT 99-5656 chromosome, complete genome.	1	0.000%
Helicobacter PAGU611, complete genome.	1	0.000%
Pectobacterium subsp. carotovorum PCC21 chromosome,	1	0.000%
Helicobacter ATCC 51449 chromosome, complete genome.	1	0.000%
Helicobacter 12198 chromosome, complete genome.	1	0.000%
Helicobacter 2017 chromosome, complete genome.	1	0.000%
Helicobacter 2018 chromosome, complete genome.	1	0.000%
Helicobacter 35A chromosome, complete genome.	1	0.000%
Helicobacter 51 chromosome, complete genome.	1	0.000%
Helicobacter 83 chromosome, complete genome.	1	0.000%
Helicobacter 908 chromosome, complete genome.	1	0.000%
Phycisphaera NBRC 102666, complete genome.	1	0.000%
Helicobacter Aklavik117 chromosome, complete genome.	1	0.000%
Helicobacter Aklavik86 chromosome, complete genome.	1	0.000%
Helicobacter B38 chromosome, complete genome.	1	0.000%
Helicobacter B8 chromosome, complete genome.	1	0.000%
Helicobacter Cuz20 chromosome, complete genome.	1	0.000%
Helicobacter ELS37 chromosome, complete genome.	1	0.000%
Helicobacter F30, complete genome.	1	0.000%
Helicobacter F32, complete genome.	1	0.000%
Helicobacter F57, complete genome.	1	0.000%
Helicobacter G27 chromosome, complete genome.	1	0.000%
Helicobacter Gambia94/24 chromosome, complete genome.	1	0.000%
Helicobacter HPAG1 chromosome, complete genome.	1	0.000%
Helicobacter HUP-B14 chromosome, complete genome.	1	0.000%
Helicobacter Lithuania75 chromosome, complete genome.	1	0.000%
Helicobacter P12 chromosome, complete genome.	1	0.000%
Pseudanabaena PCC 7367 chromosome, complete genome.	1	0.000%
Pseudoalteromonas TAC125 chromosome I, complete	1	0.000%
Pseudoalteromonas SM9913 chromosome I, complete sequence.	1	0.000%
Helicobacter PeCan18 chromosome, complete genome.	1	0.000%
Pseudomonas ND6 chromosome, complete genome.	1	0.000%
Pseudomonas DOT-T1E chromosome, complete genome.	1	0.000%
Pseudomonas F1 chromosome, complete genome.	1	0.000%
Pseudomonas GB-1 chromosome, complete genome.	1	0.000%
Pseudomonas KT2440 chromosome, complete genome.	1	0.000%
Helicobacter PeCan4 chromosome, complete genome.	1	0.000%
Helicobacter Puno120 chromosome, complete genome.	1	0.000%
Helicobacter Puno135 chromosome, complete genome.	1	0.000%
Helicobacter Sat464 chromosome, complete genome.	1	0.000%
Helicobacter Shi112 chromosome, complete genome.	1	0.000%
Helicobacter Shi169 chromosome, complete genome.	1	0.000%
Helicobacter Shi417 chromosome, complete genome.	1	0.000%
Helicobacter Shi470 chromosome, complete genome.	1	0.000%
Rhizobium CIAT 652 chromosome, complete genome.	1	0.000%
Rhizobium bv. trifolii WSM2304 chromosome, complete	1	0.000%
Helicobacter SJM180 chromosome, complete genome.	1	0.000%
Helicobacter SNT49 chromosome, complete genome.	1	0.000%
Rhodopseudomonas BisB18 chromosome, complete genome.	1	0.000%
Rhodopseudomonas BisB5 chromosome, complete genome.	1	0.000%
Helicobacter 52 chromosome, complete genome.	1	0.000%
Helicobacter v225d chromosome, complete genome.	1	0.000%

Rickettsia ESF-5 chromosome, complete genome.	1	0.000%
Rickettsia str. Hartford chromosome, complete genome.	1	0.000%
Rickettsia str. Cutlack chromosome, complete genome.	1	0.000%
Rickettsia OSU 85-389 chromosome, complete genome.	1	0.000%
Rickettsia RML369-C chromosome, complete genome.	1	0.000%
Rickettsia str. CA410 chromosome, complete genome.	1	0.000%
Rickettsia str. McKiel, complete genome.	1	0.000%
Rickettsia str. Malish 7, complete genome.	1	0.000%
Rickettsia URRWXCal2 chromosome, complete genome.	1	0.000%
Rickettsia 54 chromosome, complete genome.	1	0.000%
Rickettsia YH, complete genome.	1	0.000%
Rickettsia str. AZT80 chromosome, complete genome.	1	0.000%
Rickettsia MTU5 chromosome, complete genome.	1	0.000%
Rickettsia str. Portsmouth chromosome, complete genome.	1	0.000%
Rickettsia str. Rustic, complete genome.	1	0.000%
Rickettsia str. 364D chromosome, complete genome.	1	0.000%
Helicobacter XZ274 chromosome, complete genome.	1	0.000%
Rickettsia str. Chernikova chromosome, complete genome.	1	0.000%
Rickettsia str. Dachau chromosome, complete genome.	1	0.000%
Rickettsia str. GvV257 chromosome, complete genome.	1	0.000%
Rickettsia str. Katsinyian chromosome, complete genome.	1	0.000%
Rickettsia str. Madrid E chromosome, complete genome.	1	0.000%
Rickettsia Rp22 chromosome, complete genome.	1	0.000%
Rickettsia str. RpGvF24 chromosome, complete genome.	1	0.000%
Rickettsia str. 3-7-female6-CWPP chromosome, complete	1	0.000%
Rickettsia str. Arizona chromosome, complete genome.	1	0.000%
Rickettsia str. Brazil chromosome, complete genome.	1	0.000%
Rickettsia str. Colombia chromosome, complete genome.	1	0.000%
Rickettsia str. Hauke chromosome, complete genome.	1	0.000%
Rickettsia str. Hino chromosome, complete genome.	1	0.000%
Rickettsia str. Hlp#2 chromosome, complete genome.	1	0.000%
Rickettsia str. Iowa chromosome, complete genome.	1	0.000%
Rickettsia str. 'Sheila Smith' chromosome, complete	1	0.000%
Rickettsia 13-B chromosome, complete genome.	1	0.000%
Rickettsia str. D-CWPP chromosome, complete genome.	1	0.000%
Rickettsia str. B9991CWPP chromosome, complete genome.	1	0.000%
Rickettsia str. TH1527 chromosome, complete genome.	1	0.000%
Rickettsia str. Wilmington, complete genome.	1	0.000%
Hydrogenobaculum Y04AAS1 chromosome, complete genome.	1	0.000%
Idiomarina L2TR chromosome, complete genome.	1	0.000%
Intrasporangium DSM 43043 chromosome, complete genome.	1	0.000%
Bordetella RB50 chromosome, complete genome.	1	0.000%
Jonesia DSM 20603 chromosome, complete genome.	1	0.000%
Acetohalobium DSM 5501 chromosome, complete genome.	1	0.000%
Kineococcus SRS30216 chromosome, complete genome.	1	0.000%
Kitasatospora KM-6054, complete genome.	1	0.000%
Klebsiella subsp. pneumoniae HS11286 plasmid pKPHS5,	1	0.000%
Klebsiella subsp. pneumoniae MGH 78578 plasmid pKPN6,	1	0.000%
Klebsiella subsp. pneumoniae MGH 78578 plasmid pKPN7,	1	0.000%
Sanguibacter DSM 10542 chromosome, complete genome.	1	0.000%
Acidaminococcus DSM 20731 chromosome, complete genome.	1	0.000%
Kosmotoga TBF 19.5.1, complete genome.	1	0.000%
Kribbella DSM 17836 chromosome, complete genome.	1	0.000%
Acidimicrobium DSM 10331 chromosome, complete genome.	1	0.000%
Aeromonas B565 chromosome, complete genome.	1	0.000%
Anabaena 90 chromosome chANA01, complete sequence.	1	0.000%
Arcanobacterium DSM 20595 chromosome, complete genome.	1	0.000%
Arthrobacter Re117 chromosome, complete genome.	1	0.000%
Arthrobacter FB24, complete sequence.	1	0.000%
Bifidobacterium subsp. lactis AD011 chromosome, complete	1	0.000%
Bordetella 253, complete genome.	1	0.000%
Bordetella MO149, complete genome.	1	0.000%
Bordetella 12822 chromosome, complete genome.	1	0.000%
Bordetella 18323, complete genome.	1	0.000%
Bordetella CS chromosome, complete genome.	1	0.000%
Bordetella Tohama I chromosome, complete genome.	1	0.000%
Shigella 53G plasmid B, complete sequence.	1	0.000%
Shigella Ss046 chromosome, complete genome.	1	0.000%
Bradyrhizobium USDA 6, complete genome.	1	0.000%
Shigella Ss046 plasmid pSS046_spB, complete sequence.	1	0.000%
Burkholderia BSR3 chromosome 2, complete sequence.	1	0.000%
Caldicellulosiruptor 108 chromosome, complete	1	0.000%
Caldicellulosiruptor 177R1B chromosome, complete	1	0.000%
Sphaerobacter DSM 20745 chromosome 1, complete	1	0.000%
Sphaerobacter DSM 20745 chromosome 2, complete	1	0.000%
Caldicellulosiruptor 2002 chromosome, complete	1	0.000%
Lactobacillus DPC 4571, complete genome.	1	0.000%
Lactobacillus H10 chromosome, complete genome.	1	0.000%
Caldicellulosiruptor 6A chromosome, complete genome.	1	0.000%
Caldicellulosiruptor OL chromosome, complete genome.	1	0.000%
Caldisericum AZM16c01, complete genome.	1	0.000%
Campylobacter 525.92 chromosome, complete genome.	1	0.000%
Campylobacter subsp. jejuni 81116, complete genome.	1	0.000%
Campylobacter subsp. jejuni 81-176, complete genome.	1	0.000%
Campylobacter subsp. doylei 269.97 chromosome, complete	1	0.000%
Campylobacter subsp. jejuni IA3902 chromosome, complete	1	0.000%
Campylobacter subsp. jejuni M1 chromosome, complete genome.	1	0.000%
Campylobacter subsp. jejuni NCTC 11168-BN148, complete	1	0.000%
Campylobacter subsp. jejuni NCTC 11168 = ATCC 700819	1	0.000%
Campylobacter RM1221, complete genome.	1	0.000%
Campylobacter subsp. jejuni S3 chromosome, complete genome.	1	0.000%
Campylobacter RM2100, complete genome.	1	0.000%
Candidatus thermophilum B chromosome chromosome	1	0.000%
Candidatus asiaticus str. psy62 chromosome, complete	1	0.000%
Candidatus solanacearum CLso-ZC1 chromosome, complete	1	0.000%
Candidatus mitochondrii IricVA chromosome, complete	1	0.000%
Candidatus muelleri DMIN chromosome, complete genome.	1	0.000%
Candidatus muelleri GWSS, complete genome.	1	0.000%
Candidatus okutanii HA, complete genome.	1	0.000%
Caulobacter K31 chromosome, complete genome.	1	0.000%
Cellulomonas ATCC 484 chromosome, complete genome.	1	0.000%
Cellulomonas DSM 20109 chromosome, complete genome.	1	0.000%
Chlamydia Nigg, complete genome.	1	0.000%
Chlamydia 01DC12, complete genome.	1	0.000%
Chlamydia 84/55 chromosome, complete genome.	1	0.000%
Chlamydia GR9 chromosome, complete genome.	1	0.000%
Chlamydia M56 chromosome, complete genome.	1	0.000%
Legionella 2300/99 Alcoy chromosome, complete genome.	1	0.000%
Legionella subsp. pneumophila ATCC 43290 chromosome,	1	0.000%
Legionella str. Corby chromosome, complete genome.	1	0.000%
Legionella subsp. pneumophila, complete genome.	1	0.000%
Legionella str. Lens, complete genome.	1	0.000%
Legionella subsp. pneumophila, complete genome.	1	0.000%
Legionella str. Paris, complete genome.	1	0.000%
Legionella subsp. pneumophila str. Philadelphia 1	1	0.000%
Chlamydia MN chromosome, complete genome.	1	0.000%
Chlamydia VS225 chromosome, complete genome.	1	0.000%
Chlamydia WC chromosome, complete genome.	1	0.000%
Chlamydia WS/RT/E30 chromosome, complete genome.	1	0.000%
Chlamydia 434/Bu chromosome, complete genome.	1	0.000%
Chlamydia A2497, complete genome.	1	0.000%
Chlamydia A2497 chromosome, complete genome.	1	0.000%
Chlamydia A/HAR-13, complete genome.	1	0.000%
Chlamydia B/Jali20/OT chromosome, complete genome.	1	0.000%
Chlamydia B/TZ1A828/OT chromosome, complete genome.	1	0.000%
Rhodomicrobium ATCC 17100 chromosome, complete genome.	1	0.000%
Chlamydia D-EC chromosome, complete genome.	1	0.000%
Leuconostoc KM20, complete genome.	1	0.000%
Chlamydia D-LC chromosome, complete genome.	1	0.000%
Chlamydia D/UW-3/CX, complete genome.	1	0.000%
Leuconostoc IMSNU 11154 chromosome, complete genome.	1	0.000%
Leuconostoc subsp. mesenteroides ATCC 8293	1	0.000%

Stenotrophomonas D457, complete genome.	1	0.000%
Stenotrophomonas JV3 chromosome, complete genome.	1	0.000%
Streptobacillus DSM 12112 chromosome, complete genome.	1	0.000%
Leuconostoc subsp. mesenteroides J18 chromosome,	1	0.000%
Chlamydia E/11023 chromosome, complete genome.	1	0.000%
Chlamydia E/150 chromosome, complete genome.	1	0.000%
Chlamydia E/SW3, complete genome.	1	0.000%
Chlamydia F/SW4, complete genome.	1	0.000%
Streptococcus subsp. zooepidemicus ATCC 35246 chromosome,	1	0.000%
Chlamydia F/SW5, complete genome.	1	0.000%
Streptococcus subsp. zooepidemicus, complete genome.	1	0.000%
Chlamydia G/11074 chromosome, complete genome.	1	0.000%
Streptococcus ACA-DC 198, complete genome.	1	0.000%
Chlamydia G/11222 chromosome, complete genome.	1	0.000%
Streptococcus NN2025, complete genome.	1	0.000%
Chlamydia G/9301 chromosome, complete genome.	1	0.000%
Chlamydia G/9768 chromosome, complete genome.	1	0.000%
Streptococcus 70585, complete genome.	1	0.000%
Chlamydia L2b/UCH-1/proctitis chromosome, complete	1	0.000%
Chlamydia L2c chromosome, complete genome.	1	0.000%
Chlamydia Sweden2, complete genome.	1	0.000%
Streptococcus D39 chromosome, complete genome.	1	0.000%
Streptococcus G54 chromosome, complete genome.	1	0.000%
Streptococcus gamPNI0373 chromosome, complete genome.	1	0.000%
Chlamydophila S26/3, complete genome.	1	0.000%
Streptococcus INV104, complete genome.	1	0.000%
Streptococcus INV200, complete genome.	1	0.000%
Streptococcus JJA, complete genome.	1	0.000%
Streptococcus OXC141, complete genome.	1	0.000%
Streptococcus P1031, complete genome.	1	0.000%
Streptococcus R6, complete genome.	1	0.000%
Streptococcus SPNA45, complete genome.	1	0.000%
Streptococcus ST556 chromosome, complete genome.	1	0.000%
Streptococcus Taiwan19F-14 chromosome, complete genome.	1	0.000%
Streptococcus TCH8431/19A chromosome, complete genome.	1	0.000%
Streptococcus TIGR4 chromosome, complete genome.	1	0.000%
Chlamydophila GPIC chromosome, complete genome.	1	0.000%
Streptococcus MGAS15252 chromosome, complete genome.	1	0.000%
Streptococcus NZ131 chromosome, complete genome.	1	0.000%
Chlamydophila Fe/C-56, complete genome.	1	0.000%
Chlamydophila AR39, complete genome.	1	0.000%
Chlamydophila CWL029 chromosome, complete genome.	1	0.000%
Chlamydophila J138 chromosome, complete genome.	1	0.000%
Chlamydophila LPCoLN chromosome, complete genome.	1	0.000%
Chlamydophila TW-183, complete genome.	1	0.000%
Chlamydophila 01DC11 chromosome, complete genome.	1	0.000%
Chlamydophila 02DC15 chromosome, complete genome.	1	0.000%
Chlamydophila 08DC60 chromosome, complete genome.	1	0.000%
Chlamydophila 6BC chromosome, complete genome.	1	0.000%
Chlamydophila 6BC chromosome, complete genome.	1	0.000%
Chlamydophila C19/98 chromosome, complete genome.	1	0.000%
Chlamydia CP3 chromosome, complete genome.	1	0.000%
Chlamydia NJ1 chromosome, complete genome.	1	0.000%
Chloroherpeton ATCC 35110 chromosome, complete genome.	1	0.000%
Clostridium NCIMB 8052 chromosome, complete genome.	1	0.000%
Clostridium A str. ATCC 19397 chromosome, complete	1	0.000%
Clostridium A str. ATCC 3502 chromosome, complete genome.	1	0.000%
Clostridium Ba4 str. 657 chromosome, complete genome.	1	0.000%
Clostridium B str. Eklund 17B(NRP), complete genome.	1	0.000%
Clostridium B str. Eklund 17B chromosome, complete	1	0.000%
Clostridium E3 str. Alaska E43 chromosome, complete	1	0.000%
Clostridium H04402 065, complete genome.	1	0.000%
Marinobacter HP15 chromosome, complete genome.	1	0.000%
Streptococcus 0140J chromosome, complete genome.	1	0.000%
Streptomyces A3(2) chromosome, complete genome.	1	0.000%
Streptomyces subsp. griseus NBRC 13350 chromosome, complete	1	0.000%
Marinobacter VT8 chromosome, complete genome.	1	0.000%
Marinobacter BSs20148 chromosome, complete genome.	1	0.000%
Sulfurospirillum SES-3 chromosome, complete genome.	1	0.000%
Sulfurospirillum DSM 6946 chromosome, complete genome.	1	0.000%
Sulfurovum NBC37-1 chromosome, complete genome.	1	0.000%
Symbiobacterium IAM 14863 chromosome, complete genome.	1	0.000%
Marinobacter ATCC 49840, complete genome.	1	0.000%
Clostridium 743B chromosome, complete genome.	1	0.000%
Meiothermus DSM 1279 chromosome, complete genome.	1	0.000%
Synechococcus PCC 6312 chromosome, complete genome.	1	0.000%
Synechococcus PCC 7502 chromosome, complete genome.	1	0.000%
Clostridium 630, complete genome.	1	0.000%
Clostridium M120, complete genome.	1	0.000%
Clostridium DSM 555 chromosome, complete genome.	1	0.000%
Mesorhizobium biovar biserrulae WSM1271 chromosome, complete	1	0.000%
Methanococcus SB chromosome, complete genome.	1	0.000%
Clostridium NBRC 12016, complete genome.	1	0.000%
Clostridium DSM 13528 chromosome, complete genome.	1	0.000%
Thalassobaculum L2 chromosome, complete genome.	1	0.000%
Clostridium ATCC 13124 chromosome, complete genome.	1	0.000%
Methylomicrobium chromosome, complete genome.	1	0.000%
Methylomonas MC09 chromosome, complete genome.	1	0.000%
Corynebacterium ATCC 700975, complete genome.	1	0.000%
Corynebacterium 31A chromosome, complete genome.	1	0.000%
Corynebacterium BH8 chromosome, complete genome.	1	0.000%
Corynebacterium HC02 chromosome, complete genome.	1	0.000%
Corynebacterium NCTC 13129 chromosome, complete genome.	1	0.000%
Corynebacterium PW8 chromosome, complete genome.	1	0.000%
Corynebacterium R chromosome, complete genome.	1	0.000%
Cyclocla sticus P1 chromosome, complete genome.	1	0.000%
Dehalococcoides VS chromosome, complete genome.	1	0.000%
Deinococcus DSM 21211 chromosome, complete genome.	1	0.000%
Denitrovibrio DSM 12809 chromosome, complete genome.	1	0.000%
Thermobaculum ATCC BAA-798 chromosome 1, complete	1	0.000%
Desulfotalea LSv54, complete genome.	1	0.000%
Dictyoglomus DSM 6724 chromosome, complete genome.	1	0.000%
Tropheryma TW08/27, complete genome.	1	0.000%
Tropheryma str. Twist, complete genome.	1	0.000%
Ehrlichia str. Jake chromosome, complete genome.	1	0.000%
Mycoplasma MP145 chromosome, complete genome.	1	0.000%
Ehrlichia str. Arkansas, complete genome.	1	0.000%
Ehrlichia str. Gardel, complete genome.	1	0.000%
Mycoplasma CA06_2006.052-5-2P chromosome, complete	1	0.000%
Mycoplasma str. F chromosome, complete genome.	1	0.000%
Vibrio IEC224 chromosome I, complete sequence.	1	0.000%
Mycoplasma NC06_2006.080-5-2P chromosome, complete	1	0.000%
Mycoplasma NC08_2008.031-4-3P chromosome, complete	1	0.000%
Wigglesworthia endosymbiont of Glossina brevipalpis	1	0.000%
Yersinia Angola plasmid pMT-pPCP, complete sequence.	1	0.000%
Yersinia Antiqua plasmid pPCP, complete sequence.	1	0.000%
Yersinia biovar Medievalis str. Harbin 35 plasmid pPCP,	1	0.000%
Yersinia biovar Microtus str. 91001 plasmid pPCP1, complete	1	0.000%
Yersinia CO92 plasmid pPCP1, complete sequence.	1	0.000%
Yersinia D106004 plasmid pPCY1, complete sequence.	1	0.000%
Yersinia D182038 plasmid pPCP1, complete sequence.	1	0.000%
Yersinia Nepal516 plasmid pPCP, complete sequence.	1	0.000%
Mycoplasma NC95_13295-2-2P chromosome, complete	1	0.000%
Cellvibrio ATCC 13127 chromosome, complete genome.	1	0.000%